Structural Reliability Applied To Deep Excavations
- Coupling Reliability Methods With Finite Elements -

Timo Schweckendiek [1]
Section Hydraulic and Geotechnical Engineering
Delft University of Technology

Keywords:
Structural Reliability, Probability, ProBox, Finite Elements, Plaxis, FORM, PEM, Directional Sampling, DARS, Monte Carlo Simulations, Deep Excavations, Retaining Structures

December 15^{th}, 2006

[1]Dipl.-Ing.(FH) Timo Schweckendiek email: timo@schweckendiek.net

Preface

This research was carried out as an MSc-thesis at the Section of Hydraulic Engineering at Delft University of Technology in cooperation with TNO Built Environment and Geosciences. I chose this assignment because it combined the two subjects that I enjoyed most during the MSc-study at TU Delft, probabilistics and geotechnics. The main goal was to carry out level II and level III reliability analysis using the finite element method for geotechnical structures. TNO has developed a generic tool for reliability analysis (ProBox). This had to be coupled to Plaxis, a finite element code especially suited for geotechnical analysis.

I would like to thank everybody who was involved in the work on this research. My colleagues at TNO, people from Plaxis bv and my tutors at TU Delft have always been very cooperative and supportive. I also appreciated the support by Ed Calle a lot who especially helped me in making the right choices on the way. My special thanks go to Wim Courage. He fulfilled his function as my thesis mentor in an extraordinarily dedicated manner and we had numerous extensive and fruitful discussions about the subject.

Delft, December 2006
Timo Schweckendiek

Student:
Dipl.-Ing.(FH) Timo Schweckendiek

Examination Committee:
Prof.drs.ir. J.K. Vrijling, TU Delft - Section Hydraulic Engineering
Dr.ir. P.H.A.J.M. van Gelder, TU Delft - Section Hydraulic Engineering
Dr.ir. R.B.J. Brinkgreve, TU Delft - Section GeoEngineering
Ir. E.O.F. Calle, Geodelft
Dr.ir. P.H. Waarts, TNO Built Environment and Geosciences

Delft University of Technology
Faculty of Civil Engineering and Geosciences
Section Hydraulic Engineering
Chair of Hydraulic Structures and Probabilistic Design

Summary

There is a trend in the development of safety concepts as well as in economical approaches to structural design to imply more probabilistic concepts. Recent developments were the introduction of partial safety concepts such as Load and Resistance Factor Design (semi-probabilistic) or risk based approaches like the Dutch regulations for dike safety where a certain failure probability is assigned to each dike ring based on the potential consequences of dike failure. Also Life Cycle Cost Assessment (LCCA) or maintenance strategies are based on structural reliability considerations respectively the development of the structural reliability over time.

In this thesis an attempt is made to contribute to this development by describing how structural reliability analysis can be carried out in geotechnics, a discipline that deals with large uncertainties in the properties of its most important building material - the soil. As specific subject the structural reliability of deep excavations was chosen. Several examples will demonstrate the applicability of the presented theoretical framework. Furthermore, the Finite Element Method, as state of the art structural analysis tool, will be applied for the reliability assessment.

The combination of advanced models and relatively high parameter uncertainty makes the use of reliability analysis methods in combination with the Finite Element method very attractive. It is a way of dealing with uncertainties and lack of knowledge in a rational manner and of using advanced modelling techniques at the same time.

For the reliability analysis the program *ProBox* is used. It is being developed by *TNO built Environment and Geosciences* and comprises probabilistic calculation techniques that can be applied to all kinds of models. For the Finite Element calculations the program *Plaxis 8.2* is used, a code for 2D geotechnical problems. This way level II and level III reliability analysis methods can be applied in combination with advanced structural analysis tools.

The underlying theory is explained followed by a description of the implementation of the reliability analysis coupled with FEM. Finally calculation examples and case studies demonstrate the applicability of the presented methodology. A goal is to show that fully probabilistic analysis can be carried out in this manner.

Contents

List of Symbols

A_a	anchor cross sectional area	$[mm^2]$
A_{SP}	sheet pile cross sectional area	$[mm^2]$
β	reliability index	$[-]$
c'	cohesion	$[kPa]$
$f_X(x)$	probability density function (pdf)	
γ	volumetric weight $[kN/m^3]$ or safety factor	
γ_R	material or resistance factor	
γ_S	load factor	
γ_{wet}	volumetric weight of saturated soil	$[kN/m^3]$
γ_{dry}	volumetric weight of dry soil	$[kN/m^3]$
e	sheet pile thickness	$[mm]$
Δe	sheet pile thickness loss (due to corrosion)	$[mm]$
EA	axial (compression/tension) stiffness	$[kN]$
EI	bending stiffness	$[kNm^2/m]$
$E[X]$	expectation of random variable (vector)	
F_a	anchor force	$[kN/m]$
F_N	normal force	$[kN/m]$
g	gravity constant (=9.81)	$[m/s^2]$
$\Gamma_u(V)$	variance reduction factor	$[-]$
I	moment of inertia	$[cm^4/m]$
L	sheet pile length	$[m]$
L_a	free anchor length	$[m]$
M	bending moment	[kNm] or [kNm/m]
μ	mean value	
P_f	probability of failure	
ϕ'	angle of internal friction	$[deg]$
Φ	standard normal cumulative distribution function	
R	resistance	
σ	standard deviation (in mechanical context: stress)	
σ_y	yield strength	[MPa]
σ^2	variance (or Var)	
S	load (from: solicitation)	
SP	sheet pile	(subscript)
Θ	spatial correlation length	$[m]$
W_{el}	elastic section modulus	$[cm^3/m]$
Z	limit state function	

List of Abbreviations

ARS	Adaptive Response Surface
cdf	cumulative probability distribution function
COV	coefficient of variation ($COV = \frac{\sigma}{\mu}$)
CPT	Cone Penetration Test
DARS	Directional Adaptive Response Surface Sampling
DP	Design Point
DS	Directional Sampling
FEA	Finite Element Analysis
FEM	Finite Element Method
FORM	First Order Reliability Method
FOSM	First Order Second Moment Method
HS	Hardening Soil (Model)
IS	Importance Sampling
IVS	Increased Variance Sampling
LAS	Local Average Subdivision
LHS	Latin Hypercube Sampling
LN	Lognormal Distribution
LRFD	Load and Resistance Factor Design
LS	Limit State
LSD	Limit State design
LSF	Limit State Function
LSFE	Limit State Function Evaluation
MC	Monte Carlo Sampling
MCI	Monte Carlo Importance Sampling
N	Normal Distribution
PDE	Partial Differential Equation
pdf	probability density function
PEM	Point Estimate Method
PMC	Probabilistic Model Code
pmf	probability mass function
PRNG	Pseudo Random Number Generator
QRN	Quasi-Random Numbers
RFEM	Random Finite Element Method
R	Response
RS	Response Surface
RV	Random Variables
SFEM	Stochastic Finite Element Method
SLS	Serviceability Limit State
SORM	Second Order Reliability Methods
std	standard deviation
ULS	Ultimate Limit State
u-space	Independent Standard Normal Space

Part I

Theoretical Background

Chapter 1

Introduction

1.1 General Considerations

Probabilistic concepts have made their way into safety concepts as well as into economical approaches to structural design. Recent developments are the introduction of partial safety concepts such as Load and Resistance Factor Design (semi-probabilistic) or risk based approaches like the Dutch regulations for dike safety where a certain failure probability is assigned to each dike ring based on the potential consequences of dike failure. Also Life Cycle Costing or maintenance strategies are based on structural reliability considerations respectively the development of the structural reliability over time.

Probability and reliability theory form the foundation for these concepts. Furthermore, the determination of the reliability of a structural design respectively a structure is an essential subtask within these ideas. In this thesis work an attempt is made to contribute to this development by describing how structural reliability analysis can be carried out in geotechnics. This discipline deals with large uncertainties in the properties and in the modelling of its most important building material - the soil. As specific subject the structural reliability of deep excavations was chosen, for which several examples will demonstrate the applicability of the presented theoretical framework. The Finite Element Method, as state of the art structural analysis tool, is applied for the reliability assessment.

The Finite Element Method has made complex analysis of geotechnical problems possible and has lead to more insight into the soil behavior itself. There are plenty of material models available that perform well in modelling specific material behavior aspects, such as creep, hardening/softening or stress-dependent stiffness etc. Nevertheless the model error and the modelling uncertainty, which is introduced by individual modelling choices, definitely have to be included in the considerations. The main problem is that the parameter uncertainty is usually very high due to the limited amount of soil investigation and the deficiencies of the soil investigation methods. As a consequence the use of reliability analysis methods in combination with the Finite Element method becomes very attractive. It is a way of dealing with the uncertainties in a rational manner, using advanced modelling techniques at the same time.

Current design codes are based on partial safety concepts. The load and material factors are ideally calibrated by means of probabilistic analysis. These factors might be suitable for a wide

range of typical applications, but they were certainly not defined for specific, e.g. extreme cases like very deep excavations. Reliability analysis allows us in principle to determine the reliability of any structure directly and , furthermore, the suitability of the prescribed partial safety factors can be assessed.

In this thesis reliability methods will be coupled with Finite Element analysis. It will be discussed, which information from the FEM-analyses can be used for the limit state functions in the reliability analysis to obtain appropriate information about the reliability. The realization of this coupling is one of the main goals. Furthermore, the target reliability levels of the design codes will be compared with the reliability obtained by the analyses. The uncertainties involved in the modelling process should be accounted for in an appropriate manner.

1.2 Probability and Statistics

Reliability analysis is based on the theory of probability. Elements of a system as well as the load events that might occur can be modelled as stochastic quantities. Probability theory is applied to obtain failure probabilities based on these uncertain load and strength conditions.

There are basically two ways to look at probability and statistics. One is the *frequentist* approach which deals usually with long series of similar events, the other is the *degree-of-belief* approach that treats uncertainties as the confidence one has in a certain 'state of the world'.

Uncertainties themselves can be subdivided in two basic categories. There are natural processes with a variability that is practically unforeseeable. This kind of physical randomness can be classified as *aleatory* uncertainty. On the other hand there are well defined states of the world which we are just not able to describe precisely due to lack of knowledge. This kind of is uncertainties is usually called *epistemic*. Often the first category is also referred to as *random* whereas for the second category the term *uncertain* is used.

In geotechnics we mainly deal with processes or states that are not random, but we lack the knowledge about their exact properties. The subsoil has certain properties which we are not able to measure exactly and we measure them only in discrete points. From the discrete - already uncertain - data we build averages for modelling the soil using homogeneous fields. Thus we have to deal with epistemic uncertainty and we understand the outcome of our probabilistic calculations as *degree-of-belief*. Furthermore we do not account for the natural spatial variability of the soil properties by modelling the soil continuum with homogeneous layers. The treated processes are assumed to be *time-invariant* and the expressed probabilities are therefore not to be understood as referring to any time-fraction. Variability in time is thus not subject to this research, however, it is implicitly considered in load and strength reduction assumptions.

In some situations, as for the case when spatial variability is modelled by heterogeneous fields, we assume things to be random even though one could argue that the soil state, the soil properties in a certain place, are deterministic. The randomness is in this case rather a modelling assumption that allows us to use more effective tools for estimation and inference and therefore to achieve more accurate outcomes.

1.3 Uncertainties in Geotechnical Design

Modelling and designing geotechnical structures involves three major classes of uncertainties where a designer has to make decisions when he designs the structure deterministically. In figure 1.1 [1] these decisions and their influence are illustrated by means of a decision tree[2].

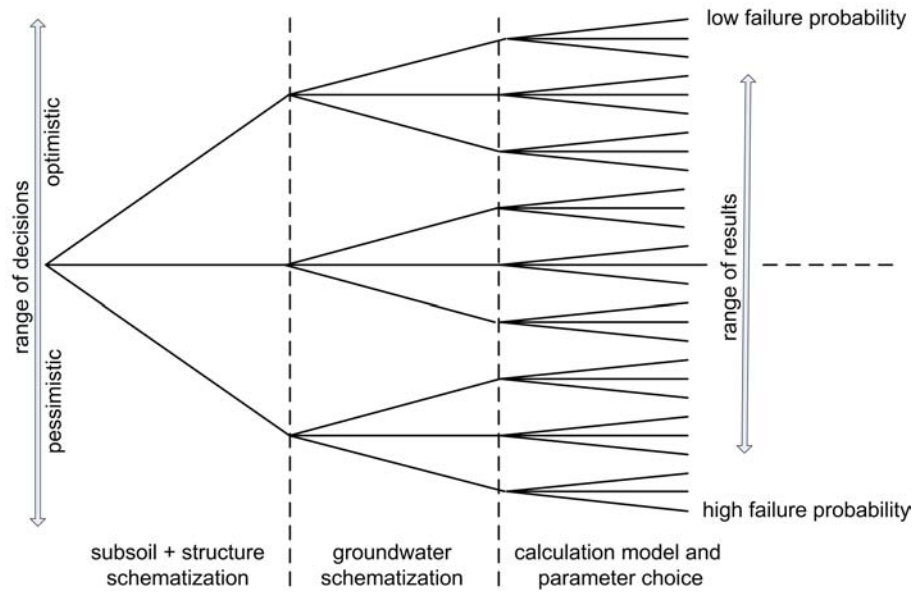

Figure 1.1: Uncertainties in Geotechnical Design

It shows that the cumulation of modelling assumptions leads to a certain outcome for the estimated failure probability as result of the design calculation. Pessimistic or conservative assumptions lead to a high calculated failure probability and an under-estimation of the reliability of the structure and vice versa.

The first of the three basic steps is the *geometry discretization* and the *subsoil characterization* using the data obtained during the site investigation. A major contribution to the uncertainty in the system response is the uncertainty in the input parameters respectively in the (soil) model parameters. The uncertainties especially in the soil parameters mainly derive from:

- Spatial variability of soil properties
- Sample disturbance for laboratory tests
- Imprecision of insitu testing methods
- Imprecisions and differences in laboratory tests and equipment

[1] thanks to Ed Calle, figure slightly modified

[2] All the decisions made in figure 1.1 could be from a continuous range of possibilities, however, here they are simplified as discrete options for sake of simplicity. The graph does not intend to show any quantitative relations or dependencies between different paths.

Geotechnical structures are usually modelled with homogeneous layers and the statistics of an ideally large number of tests are taken as characteristic for the whole layer being modelled. The influence of the intrinsic *variability of soil in space* is hereby neglected in both, *sample interpretation* and *predictive modelling*. To account for this aspect, the soil can be modelled with heterogenous fields, which is commonly achieved by random fields. In that case the *auto-correlation* in the soil properties and its length scale, commonly called *spatial correlation length*[3] θ, have to be taken into account. If homogeneous soil layers are used for modelling the subsoil, alternatively averaging effects can be accounted for depending on the correlation structure of the soil and the mechanism.

The second step is *modelling of the groundwater conditions* respectively the pore pressure field. The assumptions regarding ground water can be of large influence for calculated stability and deformations. An illustrative example for this fact are the different possibilities of pore pressure modelling for a simple excavation problem.

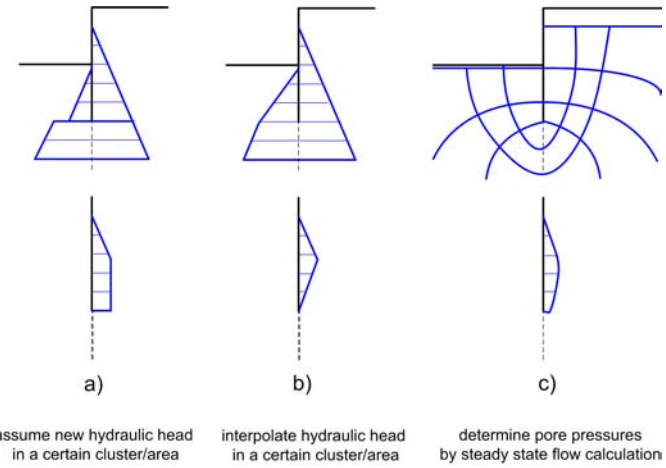

Figure 1.2: Pore Pressure Modelling for Excavations

The three examples of pore pressure models presented in figure 1.2 show that the resulting effect of the pore pressure on the retaining wall can be significantly different in magnitude as well as in distribution. In other words, the uncertainty in the system response can be to a considerable amount due to the uncertainty in groundwater conditions, even though in this example this is demonstrated by model and modelling uncertainty.

[3]The properties of two soil samples at distance larger than θ are practically statistically independent, for shorter distances they are correlated.

Finally, we make choices concerning the *constitutive models*, the calibration of parameters is performed and the model is used for predictions of the system response. Also in this phase uncertainties enter the modelling process. At first, *constitutive models* are developed in order to reproduce and predict the behavior of a material as realistically as possible. However, they never achieve this goal perfectly. This fact causes a *model error* that is difficult to quantify, but should be taken into account as an uncertainty.

Furthermore, modelling assumptions that are made for example regarding the structural members used, like plastic hinges etc, form part of the overall uncertainty. Modelling remains an imperfect description of real world behavior. This is a result of model errors and subjective choices in the modelling process.

1.4 Benefits of Uncertainty and Reliability Analysis

The stochastic analysis of uncertainties in a system's response can be used for different purposes. In the following list there are a number of categories of methods listed, each of them involving uncertainties, but all with different goals:

1. Uncertainty Analysis:
   Its aim is the description of the output distribution or at least its main characteristics, like its first central moments, based on the input uncertainties.

2. Reliability Analysis:
   The reliability of a system or process is analyzed using pre-defined failure criteria expressing unwanted events. The result is commonly expressed in terms of a reliability index or a probability of failure.

3. Risk Analysis:
   Takes furthermore into account the possible consequences of certain actions. It is therefore closely related to decision-making.

4. Probabilistic Design:
   Supports decision-making by balancing investments and risks. It includes all the previous ones extended by economically rational decision criteria.

This work mainly focuses on the first two types, especially on reliability analysis, but the results can be used and are necessary for risk analysis and risk-based design approaches for the quantification of risks. These approaches are rational concepts and should lead to more economic design.

Furthermore, for extreme structures that go beyond past experience there are no design codes or regulations where their design could be based upon. Nevertheless, their safety level has to be assessed and it has to fulfill certain requirements. Probabilistic design approaches, such as structural reliability analysis enable us to make these decisions and assessments on a solid rational basis.

1.5 Outline

In part I the relevant literature on the subject is summarized, ranging from general structural reliability theory over the use of the Finite Element Method within these concepts to the implications of the types of variability of the soil properties. Subsequently the theories of uncertainty and reliability analysis are discussed. The focus is on *structural reliability analysis* methods that are especially developed for efficiently determining the *probability of failure* of structural elements or systems.

In part II the practical implementation of the combination between reliability concepts and Finite Element Modelling is explained. The main tools that were used for this purpose are the two-dimensional finite element code *Plaxis* 8.2 (Brinkgreve et al, 2004 [6]) and the program *ProBox*, developed by TNO (Netherlands Institute for Applied Scientific Research), which is a generic tool for probabilistic analysis. The relevant features of both programs and their coupling are discussed. The main limit states are explained, also in the context of system behavior.

Part III contains simple calculation examples and a case study. The calculation examples are simple and illustrative and demonstrate the application of the proposed methodology. The case study treats an imaginary, but realistic deep excavation problem in soft soil. Ultimately conclusions and recommendations are presented.

Part IV contains the appendices.

Chapter 2

Literature Review

This literature overview resumes the recent developments in the field of reliability analysis using finite element analysis for geotechnical applications. Chapter 4 is dedicated to explaining the reliability methods themselves in detail, for which reason they are not included here.

Currently there are basically three types of approaches described in the literature that are summarized in the following sections. Further subjects like inherent soil variability will not be treated here, instead the references to the relevant literature are made in the corresponding chapters.

2.1 Reliability Analysis With Deterministic Finite Elements

This approach is based on using deterministic Finite Element Analysis (FEA) for every evaluation of the limit state function within the framework of the reliability methods (see chapter 4). Some of these methods require partial derivatives of the limit state functions (LSF) that have to be calculated numerically in this case. In this approach the soil is treated as variable in its properties, but it is still modelled with homogeneous layers. This is also sometimes called random average approach. Averaging effects of the soil properties can be important for the modelling of the variance in the soil properties. These are addressed in section 2.4.

This kind of reliability analysis using deterministic finite element analysis involves an interaction of the two analysis parts, reliability and FEA, via clearly defined interfaces. The reliability analysis determines the input for the FEA, which then delivers the output of each deterministic calculation. These outputs are used by the reliability analysis for evaluating the LSF. The reliability tool works as a 'layer around the FEA'.

Overviews of available methods and their performances are given in the PhD-thesis of Paul Waarts (2000) [45] and in the paper of Vrouwenvelder and Chryssantopoulos (2004) [44]. Waarts [45] illustrates by means of a number of examples from structural and geotechnical engineering the precision and efficiency of different reliability methods.

Waarts also uses artificial LSF with certain mathematical properties like strong non-linearity and discontinuity or degenerated LSF with e.g. two branches. His conclusions for several tested Level II and Level III methods are that FORM-ARS (First Order Reliability Method combined with Adaptive Response Surfaces perform best within the class of Level II methods. The response

surfaces smoothen the LSF and avoid thereby problems of discontinuities and non-differentiable points. FORM itself can deliver wrong answers for strongly curved or concave limit states. It only finds global minimum design points in relatively flat limit states with certainty. Its performance in terms of calculation time (number of iterations) is sensitive to the choice of the starting point which implies that performance can be improved by the applying a priori knowledge about the limit state. SORM (Second Order Reliability Method) encounters the same problems as FORM, but can give better end results for curved LSF. If the LSF is very strongly non-linear also SORM fails to deliver correct results.

The tested level III methods were Monte Carlo Sampling (MC), Monte Carlo Importance Sampling (MCI), Directional Sampling (DS) and Directional Adaptive Response Surface Sampling (DARS). While DS and MCI are sensitive to the number of dimensions, MC [1] is not and DARS seems quite insensitive for the artificial LSF tested in Waarts [45]. Level III methods do not exhibit any weaknesses when it comes to complex shaped LSF. The number of limit state function evaluations (LSFE) depends on the number of random variables and/or the failure probability. The shape of the limit state is irrelevant to the calculation effort.

For the type of problem treated in this thesis, which is a structural reliability problem, the limit states are usually non-linear and multiple limit states are involved. Therefore care has to be taken with FORM. Second order corrections by SORM or system reliability analysis might be a way to overcome these deficiencies. As long as the LSF is still relatively flat, however, FORM is very fast and especially attractive for LSFE that are expensive in terms of computation time. DARS is the option of choice when prior knowledge is absent and system behavior might be involved, since it gives very precise answers with still low number of LSFE.

Some more advanced methods are presented for example in Bucher et. al (2000) [7] and applied to problems in structural engineering. The authors propose a 'weighted radii' approximation which is a local-global approximation strategy for the response surface method (see section 4.2.4).

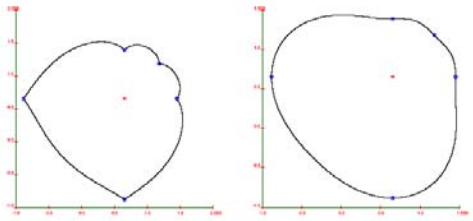

Figure 2.1: Response Surfaces for the Weighted Radii Method for (a) linear weights and (b) non-linear weights in two-dimensional u-space (from Bucher et al (2000))

Classical polynomial response surfaces have some drawbacks regarding their flexibility of assuming certain shapes and polyhedral response surfaces need a rather high number of check points for a safe domain. The authors state that most of these problems can be overcome using the 'weighted radii' approach.

In principle a number of check points in order to determine the radii are used for the response surface (RS). The weights that are given to the radii are expressed as function of the angle

[1] See appendix C for expected number of realizations in Crude Monte Carlo.

that the RS-point makes with the adjacent sampling points. Two typical response surfaces are presented in figure 2.1. For details refer to the original paper [7].

The application of reliability methods in geotechnics is extensively presented by Baecher and Christian (2003) [2]. The book contains basically four parts about general probabilistic and statistical questions, soil variability, reliability analysis and system reliability. The relevant contents from this book are elaborated in the corresponding chapters 4 and 2.4.

A number of works have been published by the Geotechnics Group from Graz University. Two of their recent PhD-theses deal with the use of finite elements in reliability analysis. Thurner (2000) [39] uses the Point Estimate Method (according to Zhou / Nowak 1988 [46]) for slope stability problems, retaining walls and tunnels for ULS and SLS criteria. As FEM tool the finite element code Plaxis (see Brinkgreve et al. 2004 [6]) has been applied. The results were produced by this particular PEM method and not checked or compared with results obtained by other methods. There are especially doubts about the suitability and accuracy of PEM for the investigated problems. PEM is explained in detail in section 4.4.3.

The second thesis dealt with an approach applying random set theory (see Peschl 2004 [30]). It gives usually upper and lower bounds of the calculated probabilities of failure and is mainly attractive, like PEM, due to the low number of calculations. The method differs considerably from classical probabilistic approaches and due to its limited precision it is not considered in this thesis any further.

For ULS-calculations several authors used a method that is implemented in Plaxis, the 'ϕ-c-reduction technique' (see Brinkgreve and Bakker 1991 [5]). The principle of this technique is to reduce the strength properties of the soil, the friction angle ϕ and the cohesion c, proportionally in small steps until the limit of equilibrium is reached. The ratio of the limit values and the start values results in a reduction factor MSF that gives an idea of the 'distance' to failure like classical safety factors. For detailed information about this technique refer to appendix F. Other authors like Lane and Griffiths (1997) [25] applied the same principle of reducing the strength properties of the soil by a common factor in various publications about slope stability analysis using FEM.

Another possibility of loading the structure until 'failure' is, in contrast to the strength-reduction in the previous method, the increase of the self weight of the structure by increasing the gravity constant g stepwise. Swan and Seo (1999) [38] apply this method for slope stability analysis in combination with an elasto-plastic constitutive model. These methods are especially suited for failure mechanisms concerning the soil body, i.e. they indicate collapse of the elements representing the soil. For mixed structures like retaining walls, however, they can give information about overall stability, which is just one failure mechanism. The correlation with and the triggering of other failure mechanisms or limit states has to be controlled in that case.

The definition of failure in the FEM calculations is a difficult subject that is not extensively discussed in the literature regarding geotechnical structures.

Oberguggenberger and Fellin (2002) [29] address the sensitivity of the reliability analysis to the choice of the input distribution function and propose alternative methods using random sets or fuzzy sets. Their conclusions are based on a foundation bearing capacity problem that they approached comparing a design value obtained with the Austrian code B4435-2 with the outcomes of a Monte Carlo simulation where the soil properties and the load were taken stochastic in the Brinch-Hansen bearing capacity formula. This comparison showed large differences

in P_f for different distribution functions of the input that were all fitted to the same data set and all passed the goodness-of-fit tests. Indeed, this is a good example for the problem that distributions can show a good fit to the data, however, the choice of distribution has still to be done carefully. More specifically, the authors found large differences for shifted distributions (three-parametric lognormal) and non-shifted distributions (two-parametric lognormal). In this case by shifting the distributions the friction angle was practically declared to be physically impossible below a certain value (shift parameter). Of course, this choice is very questionable. They also emphasize that the meaning of a calculated probability of failure cannot be a failure frequency, but rather a degree of confidence as described in the introduction part of this thesis.

2.2 Random Finite Element Methods

So far, in the first category, the soil was modelled with homogeneous layers, i.e. with random average properties. The realizations of these average properties are based on the statistics of of the samples that were taken from the area and ideally refined by regional experiences. It is questionable, if the variability that is represented by these random averages reflects also the variability along a certain failure plane respectively mechanism adequately. The answer to this question can be found by simulating the spatial variation of the soil properties by means of random fields. This technique is the basis for the *Random Finite Element Method*. In the following we give a summary of some results that can be found in the literature where this approach was applied to investigate the influence of the phenomenon of the inherent spatial variability of soil.

In the field of geotechnical engineering the works of Griffiths and Fenton are widely recognized and are based on the PhD-thesis of Fenton (1990) [12] and the book of VanMarcke (1983) [43] about procedures for the generation of random fields.

With a finite element code working with random simulated random fields they investigate the influence of spatial variability of soil on a number of geotechnical design problems. The soil strength properties are treated as random variables and the correlation pattern is modelled by an autocorrelation function using the *spatial correlation length* Θ as characteristic parameter. Their works are restricted to 2D-plane-strain problems and isotropic spatial variability.

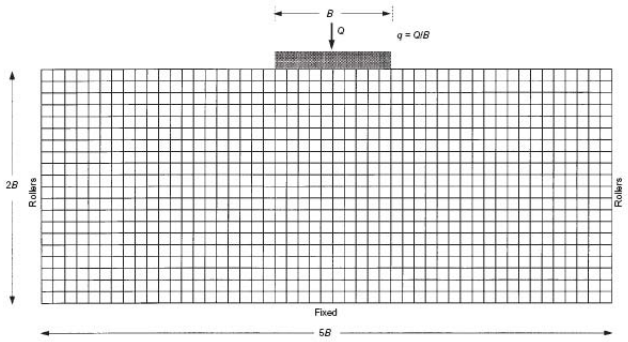

Figure 2.2: Geometrical Setup Bearing Capacity Problem from Griffiths (2001)

One of the problems treated is the bearing capacity of a foundation (Griffiths (2001) [15]).

The problem geometry is illustrated in figure 2.2. An infinitely long strip foundation of width B is loaded by a point load Q and the soil is supposed to behave undrained. An elastic-perfectly plastic stress-strain law with Tresca failure criterion is used where E and ν are held constant and c_u (undrained shear strength) is the only random variable. c_u is furthermore modelled with a lognormal distribution and therefore the value of the shear strength assigned to the i^{th} element in the random field can be described as:

$$c_{u_i} = exp(\mu_{lnc_u} + \sigma_{lnc_u} g_i) \tag{2.1}$$

,where g_i is the value of the previously generated standard normal Gaussian random field in the i^th element.

The random fields are generated via LAS (Local Average subdivision), as explained in Fenton & Vanmarcke (1990) [14]. The spatial correlation was defined by a function applied to the logarithm of c_u:

$$\rho(|\tau|) = exp(-\frac{2}{\Theta_{lnc_u}}|\tau|) \tag{2.2}$$

describing the correlation ρ between two values of c_u in points with a mutual distance τ.

In the parametric studies carried out by the authors the bearing capacity factor $N_c = \frac{Q/B}{c_u}$ that results from increasing Q until failure is compared to an N_c obtained by an analytical solution by Prandtl. The main conclusions were:

- Probably for very small values of Θ_{c_u} the response is as if it was homogeneous and that the N_c converges to the value found by Prandtl.
- For values of Θ_{c_u} of around half the foundation width B, a minimum was found for N_c. As confirmed by other studies, if the spatial correlation length is in the order of magnitude of the size of the structure, the largest influence is observed.
- The authors investigated the probability that an analytical design would give larger values for the bearing capacity than computed with the presented approach. It was concluded that for reasonable ranges of $COV(C_u)$ and Θ_{c_u} a safety factor of 3 would be necessary on the strength side to essentially eliminate this 'probability of design failure', i.e. to have a sufficiently low probability that the deterministically determined bearing capacity using homogenous soil properties exceeds the bearing capacity that is calculated using the random field approach.

Another paper of the same authors treats the active soil pressure on a retaining wall (Fenton (2005) [13]). The same approach as in the bearing capacity problem is followed by comparing an analytical solution (with the assumption of homogeneity) with the outcomes of RFEM calculations using an elastic-perfectly plastic constitutive model with Mohr-Coulomb failure criterion. This time $tan\phi'$ (friction angle) and γ (volumetric weight) were represented as log-normally distributed quantities. Therefore two Gaussian random fields have been generated, both independent and with positive correlation between the two variables. The expressions for the transformation to *x-space values* [2] and for the spatial correlation length are equivalent to

[2] x-space: all values correspond to real world units (contrary: u-space: all values are transformed to standard-normal space)

the ones from the preceding example. The setup is illustrated in figure 2.3 where also a typical calculation outcome can be contemplated.

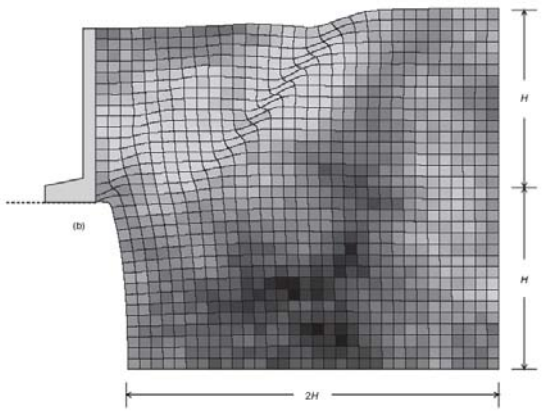

Figure 2.3: Setup and Typical Outcome Retaining Wall Problem from Fenton (2005)

Again conclusions were drawn from a number of parametric studies regarding the spatial correlation length and variation coefficients of the stochastic quantities:

- The behavior of a heterogeneous soil formation is more complex than the simple assumptions that led to the analytical formulae of Rankine (max. shear stress according to Mohr-Coulomb criterion) or Coulomb (sliding wedge moving towards the wall).
- The assumption of independence between friction angle and unit weight is conservative in this case.
- Again the effect was largest for the spatial correlation length being in the order of magnitude of the size of the structure.
- A significant difference was observed for either modelling K_0 dependent on ϕ' (spatially variable) or modelling K_0 constant according to the mean value over the whole field. In both cases totally different mechanisms are observed depending on the initial stress field.

Also in a paper about probabilistic slope analysis (Griffiths (2004)) the authors conclude that the assumption of perfect autocorrelation of the strength properties of the soil can lead to unconservative results. Especially in this example the difference between pre-defined expected failure surfaces, as is the for classical slope analysis with slip circles for example, and the FEA where the failure mechanism is automatically determined by the weakest path.

Other works published by Hicks investigate the influence of soil heterogeneity on undrained clay slope stability [17] and on a liquefaction problem [18]. In comparison to the previous papers, Hicks introduces two features in his random field approach that include more realistic soil property patterns, namely cross anisotropy of the spatial correlation length ($\Theta_{vertical} < \Theta_{horizontal}$) (see also figure 2.4) and a linear increase of the mean value of c_u over depth.

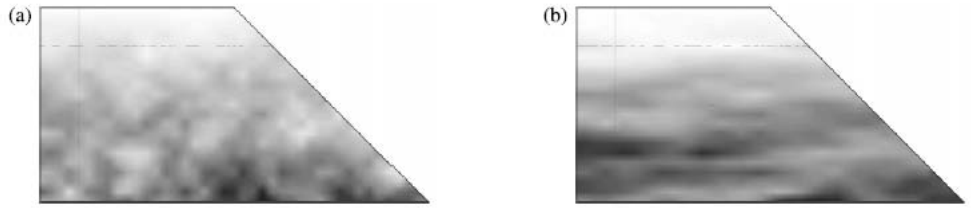

Figure 2.4: Typical Random Fields from Hicks (2002) for (a) $\Theta_h/\Theta_v = 1$ and (b) $\Theta_h/\Theta_v = 6$

In this particular case the influence of cross-anisotropy was small and the linear increase of the undrained shear strength over depth showed some influence. However, other works like by Onisiphorou (2000) show that the influence can be significant, especially if the anisotropy occurs under an angle where also the potential failure surfaces occur.

In most of the previously mentioned papers parameter studies have been carried out regarding the influence of the variation coefficients of certain parameters and also their correlation. The conclusions are usually restricted to the analysis response to these effects, not if these assumptions were realistic or reasonable. This thesis will follow similar approaches and assumptions are made for reasonable parameter ranges. The determination of appropriate statistical input is certainly subject to further research.

A drawback of the presented works is that in general it was not accounted for the influence of the third dimension. The influence of this effect is probably considerable, especially for ultimate limit state problems where the failure mechanisms are attracted by weak spots or surfaces. However, there is not much known or published about the influence of the effects of the third dimension considering random fields.

There is at least one thing that could be proven in all the presented works. The influence of soil heterogeneity is not negligible and should be accounted for by proper modelling, either directly by random fields or by using those for proper calibration of the averaging effects for the corresponding mechanisms.

2.3 Stochastic Finite Element Methods

The third and last category is the most sophisticated of this selection. Stochastic Finite Elements account for the uncertainties in the input parameters implicitly within the Finite Element calculation. A state-of-the-art report was written by Sudret and Der Kiureghian in 2000 [37]. The authors refer to the Spectral Stochastic Finite Element Method (SSFEM), which was proposed by Ghanem and Spanos (1990). In deterministic analysis a mechanical system Ω is characterized by the loading, the geometry and the material properties. These systems are usually governed by PDE (Partial Differential Equations). If there is no closed form of the solution of these PDE, the system has to be discretized and solved numerically. In FEM the geometry of Ω is replaced by a number of points $\mathbf{x} = x_1, ..., x_N$ that form the finite element mesh. The response of the system is the displacement field $\mathbf{u(x)}$ and is gathered in the displacement vector $\mathbf{U}$. The set of PDE is transformed to a set of equations $\{u^i\}_{i=1}^N$.

If a soil property is now modelled as a random field, e.g. the Young's modulus, the outcome obtained by solving the stochastic set of PDE will be a displacement random field $\mathbf{u}(x, \theta)$, where θ denotes a basic outcome in the space of all possible outcomes. The discretization procedure described previously, leads to an approximation of the response in form of a *random nodal displacement vector* $\mathbf{U}(\theta)$. The random variables $u^i(\theta)$ are determined by all possible outcomes of θ. This could be achieved by a finite set of points, e.g. by Monte Carlo strategies. However, the strength of SSFEM lies in the fact that the above mentioned random discretization can be done in a more efficient way using series expansion. Two methods are basically applied for that purpose:

- Discretization of the random field by the truncated Karhunen-Loeve expansion
- Representation of the nodal displacements $u^i(\theta)$ by its coordinates in an appropriate basis of the space of random variables, namely the *polynomial chaos*.

The authors compared the proposed method to other methods that were directly coupled to deterministic FEM-codes and found that the latter ones usually converged better and delivered results with a higher accuracy. However, they tested the performance only using one example. Therefore there could be applications where SSFEM outperforms other methods.

In this thesis this approach is not followed any further because the starting point was the coupling of two existing codes (ProBox and Plaxis) and within this frame work SSFEM is not applicable. It is however recommended to compare its performance with the results of this study in further research.

2.4 Soil Variability

There are several sources of uncertainty that pose difficulties for the proper modelling of a soil body. Furthermore, there is an interaction between the following three aspects relative to the determination of proper input statistics in a reliability approach:

- The model applied (e.g.characteristic average properties, random average properties, random fields).
- The mechanism investigated (e.g. averaging effects depend on the mechanisms).
- The types of uncertainty / variability involved (e.g. measurement uncertainty, spatial (inherent natural) variability, number of samples).

There are two information sources that give a good overview about the way soil properties have to be described for probabilistic calculations and the modelling procedures themselves:

- 'Probabilistic Model Code' [23] by the Joint Committee of Structural Safety (JCSS), section 3.7: 'Soil Properties'.
- 'Reviewing Probabilistic Soils Modelling' by Rackwitz (2000) [32].

A soil body can be described by a number of characteristics. These soil properties can be subdivided into a number of groups that are classified according to the modelling purpose:

- Bulk respectively continuum properties:
  These are physical and mechanical parameters describing the soil behavior or state parameters. They can refer to stiffness, strength, consolidation, permeability, porosity etc.
- Classification properties:
  They are used for distinguishing between soil types and support the schematization of the expected state of nature to be analyzed. Examples are color, grain size, mineral composition, liquid/plasitc limits or organic contents. If there is information about the soil type, usually also conclusions about its bulk properties can be drawn.

In this thesis work we will focus on the first type that is used for the models in the Finite Elements analysis[3], which is applied for the limit state function evaluation.

For modelling a geological formation for geotechnical purposes in a probabilistic manner we usually use statistical data in order to determine the probabilistic input. In fact, there are two basically different types of variability in our soil deposits that compose the overall variance within our sample data. We have to distinguish:

1. Local Variation or Point Variation:
   The local variations in a soil deposit derive from the fact that is is impossible to measure the properties of the deposit continuously in every point. This epistemic uncertainty can in principle be decreased by extending the soil investigation.

[3]Appendix J contains tables with typical values for soil properties and variation coefficients.

2. Spatial Variation:
   Soil is naturally spatially inhomogeneous. There are spatial fluctuations in the properties due to the geological history of the deposit. This kind of uncertainty is inherent and can be compared or modelled with a random process. Of course, we cannot influence this kind of uncertainty.

For some problems for spatial variability an averaging effect will be observed, as for settlement problems. For others like seepage problems the least conductive element is determinant. Also for this type the spatial variability is an important aspect in the assessment.

Basically there are two classes of approaches to deal with the described phenomena. The first is the *random field* approach, where the uncertainty is accounted for by a simulation, the other is the adaptation of the input statistics in a 'random average' approach accounting for the averaging effects in the analyzed mechanisms. Both are discussed briefly.

Random Fields

The influence of the spatial variability of soil can be accounted for using random field theory. The simulation of random fields is the generation of realizations of stochastic soil properties, variable (and eventually correlated) in space. Fenton and Griffiths (2005) [13] have given an indication in their paper that the soil heterogeneity has a considerable influence on the horizontal loads on retaining walls. Their conclusions have to be treated carefully, since they used a plane-strain model and 2D random fields, thereby neglecting the effect of the third dimension. There are several possibilities of taking the third dimension into account. 3D random fields could be used in combination with 3D-FEM models and it could be investigated how the spatial averaging effects the results compared to the simplified 2D plane-strain assumption.

The approach that was used by Fenton and Griffiths in several papers and several by other authors, is based on the concept of 'Local Average Subdivision'. It is described extensively in Fenton and Vanmarcke (1990) [14]. Some examples have been presented in the previous section in combination with the Random Finite Element Method (RFEM).

Spatial Averaging

In geotechnical analysis usually homogeneous soil clusters are modelled that refer to representative average quantities, i.e. a soil layer is contemplated as a homogeneous volume. The analyzed deformations, sliding surfaces, rupture zones or deformed volumes are therefore also modelled with these average quantities. If the size of such volumes or surfaces exceeds the spatial fluctuation scale of the relevant soil properties significantly, averaging effects can occur.

For example the mean value of a soil property in a large volume is the average of the mean values of its smaller subvolumes. However, the standard deviation in the large volume is smaller than the standard deviation of the averages of the subvolumes. The structure and the scale of the spatial variability have a major influence on this *Spatial Averaging* effect.

This implies that the variance within the affected volume or surface is likely to be smaller than the variance that was determined for the whole field by small sample tests like triaxial tests

or insitu tests like CPT.

A basic concept for working with spatial variability is the 'scale of fluctuation' respectively the autocorrelation length, within which a property in two contemplated points exhibits a considerable correlation. In other words, the values in two points with a relatively short mutual distance are likely to be of similar magnitude, whereas this likelihood decreases or vanishes with increasing distance. In soil the autocorrelation length is larger in horizontal direction than in vertical direction, i.e. the variability in vertical direction is higher than in horizontal direction, which is due to the geological processes that formed the soil deposits.

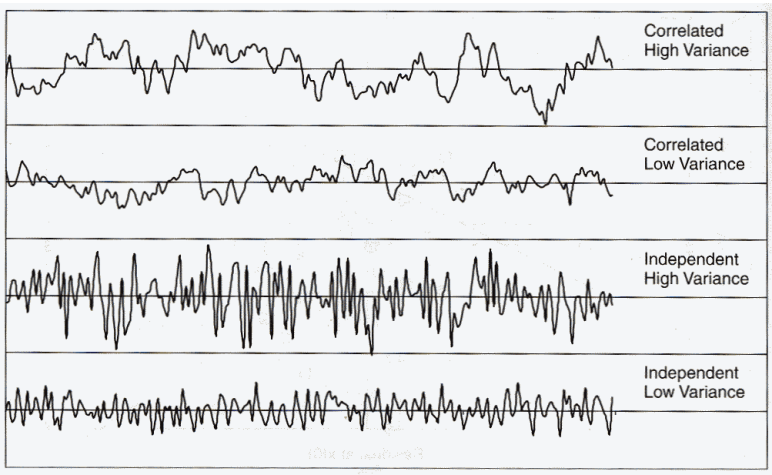

Figure 2.5: Types of Autocorrelation (see [2])

In geotechnics often average properties are determinant. For slope stability problems for example local weak spots are not sufficient to trigger failure or collapse. Stress redistribution processes play an important role for this effect from the physical point of view.

In general it can be stated that, if the characteristic or activated length, surface or volume (for example a slip surface in slope stability) is small compared to the autocorrelation length, the local variability of the soil is determinant. On the contrary, if the structural dimensions are large and the fluctuation 'wave length' is even included several times in the size of the mechanism, the average properties become more important. This also becomes obvious in figure 2.6.

To account for these effects a variance reduction factor $\Gamma_u(V)$ was defined as the ratio between σ_{u_V} (standard deviation of the average property) and σ_u (field standard deviation) and is therefore dimensionless:

$$\Gamma_u(V) = \sigma_{u_V}/\sigma_u \tag{2.3}$$

There are analytical [4] as well as numerical approaches [5] that suggest these spatial averaging effects can be in the order of 0.95 to 0.4 for typical sliding surfaces in dikes or road embankments in horizontal direction and even larger in vertical direction.

[4] see Probabilistic Model Code [23]
[5] see Vanmarcke 1977 [42]

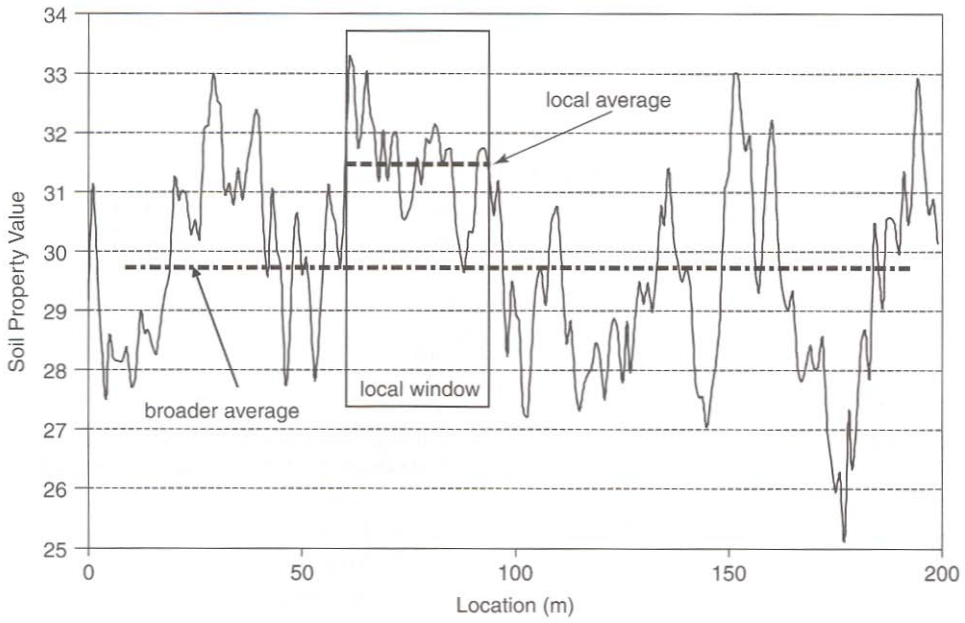

Figure 2.6: Local vs. Global Statistics (see [2])

For more detailed information one should refer to the 'Probabilistic Model Code' [23], which contains thorough elaborations on the subject.

Conclusions

For this thesis work some important consequences of this brief summary of the variability of soil in all its forms can be pointed out:

- The determination of the stochastic model input, in this case mainly the soil parameters is crucial for the results of the analysis. This input may be model dependent and also dependent on the investigated mechanisms as well as the size of the mechanisms compared to the property fluctuation scale. This should certainly be subject to further research.
- This thesis work will use the 'random average' approach. For the analysis of structures the variance reduction by averaging has to be taken into account in the model input determination.
- The next step should be to verify by means of advanced methods, if the considerations about averaging effects are reasonable. This could be achieved by means of random fields for example.

Chapter 3

Uncertainty and Sensitivity Analysis

When dealing with uncertain model input parameters, the central question is:

> How does the uncertainty in the input parameters affect the uncertainty of the model output?

To answer this question we have to propagate the uncertainties through the model (see fig. 3.1).

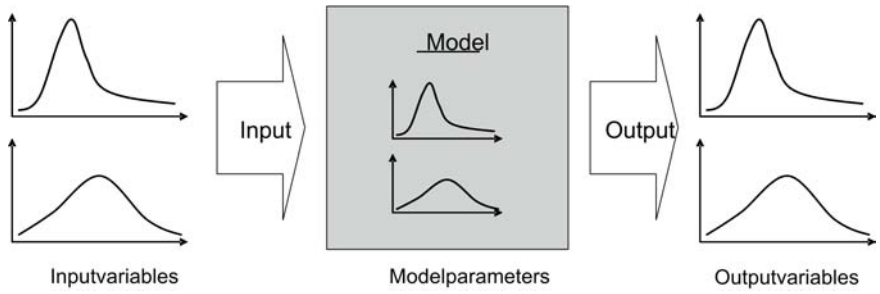

Figure 3.1: Propagation of Uncertainties Through a Model

Figure 3.1 shows that there are basically three steps in determining the uncertainty of the model output:

1. Quantification of the uncertainties in the input / model parameters in terms of probability distributions and their mutual dependence, usually by means of statistical analysis.
2. Propagation of the uncertainties through the model.
3. Evaluation of the model output uncertainties. How are they composed and what can be done to decrease them?

The focus in this work will be on the second part of the process - the propagation of uncertainties through the model. Since the outcomes of the calculations are used for determining the reliability of structures, reliability methods will be applied, which imply uncertainty modelling techniques and will be described in chapter 4.

Sensitivity analysis aims at identifying *important parameters* for the system response. This can be helpful in both, pre-processing and post-processing. Before conducting an uncertainty

or reliability analysis we normally want to filter out parameters of less significance in order to reduce the modelling respectively computational effort. After obtaining the results of an analysis, the sensitivity measures support our subsequent decisions. Usually investments are needed either for reducing specific uncertainties or for modifications of the system. Sensitivity analysis provides basic information about the expected benefits of these investments.

There are several possibilities to carry out sensitivity analysis and to express the 'importance' of a variable for the system response. We can divide them into two categories, numerical and graphical methods. The numerical methods can be subdivided into global and local sensitivity measures.

The suitability of these methods is highly dependent on the problem to be analyzed. Some are for example only suitable for (nearly) linear models, others only for monotonic behavior. As a consequence there has to be already some knowledge about the characteristics of the problem before adequate methods can be chosen.

3.1 Global Sensitivity Measures

Screening techniques are auxiliary methods for uncertainty analysis that aim to isolate the variables that contribute most to the model outcome's uncertainty. They are in fact sensitivity analysis techniques and especially suited for problems with a large number of variables. The following are some examples:

Individual Factor Variation

The simplest form of sensitivity analysis is the variation of individual factors (see e.g. Daniel, 1958 [9]). A reference calculation is carried out with nominal values for each variable. Subsequently a series of calculations is carried out where for each only one individual variable is changed once to a high extreme and another time to a low extreme value. The difference between each calculation and the reference result is called residual. According to the values of the residuals the variables can be ranked with respect to their influence on the result.

Full Factorial Design

A drawback of the Individual Factorial Variation is that it does not give any information on the interaction between individual variables. This problem can be overcome by full factorial design (see e.g. Box et al, 1978 [3]) where e.g. k possible values are assigned to each of the n variables and subsequently all n^k model evaluations are carried out. This can lead to unpractically high number of necessary calculations and is therefore not used often in this pure form. The following methods are derived from the full factorial design and need less evaluations.

Fractional Factorial Design

According the variable interactions of most interest only part of the combination scheme of the Full Factorial Design is carried out. This scheme can be designed especially for the desired output and the rest of the method remains unchanged. (see e.g. Box et al, 1978 [3])

Iterated Factorial Design

Iterated Factorial Design is another variant of Full Factorial Design, especially designed for detecting the interaction between couples of two variables and with a relatively low number of evaluations even for large numbers of variables. For details refer to Andres, 1997 [1].

Correlation Ratio

The problem of finding the most important parameters can be viewed as decomposing the variance of the output according to the input variables. We would like to assign the uncertainty of the output G that is caused by the contributions from uncertainties of the model inputs X_i $(i = 1, ..., n)$. Fixing X_i at a certain value and calculating how much the variance of G decreases, gives us an indication about the importance of X_i. Therefore we consider the following quantity:

$$Var(G|X_i = x_i^*) \tag{3.1}$$

The question is which value x_i^* should be chosen and, moreover, $Var(G|X_i = x_i^*)$ can be bigger than $Var(G)$ for nonlinear models. One possible solution would be to average over all values of X_i. Thus the following measure of importance of the variable X_i could be considered:

$$E[Var(G|X_i)] \tag{3.2}$$

where the expectation is calculated with respect to the distribution of X_i. The smaller 3.2, the more important X_i. Another useful relation in this context is:

$$E[Var(G|X_i)] + Var(E[G|X_i]) = Var(G) \tag{3.3}$$

Therefore alternatively $Var(E[G|X_i])$ can be used as importance measure and then holds that the larger $Var(E[G|X_i])$, the bigger the importance of X_i. From the above the following definition can be derived:

> Correlation ratio [1]:
> For random variables $G, X_1, ...X_n$, the correlation ratio of G with X_i is
>
> $$CR(G, X_i) = \frac{Var(E[G|X_i])}{Var(G)} \tag{3.4}$$

The correlation ratio is not symmetric ($CR(G, X) \neq CR(X, G)$).

[1] see Kurowicka (2005) [24]

The correlation ratio is an important non-directional measure of uncertainty contribution. It is always positive and does therefore not give any information about the direction of the influence. Computing correlation ratios can be difficult, because it involves a conditional expectation which is often not available in closed form. If it is possible to sample Y' from the conditional distribution $(Y|X)$ independently of Y , the following algorithm may be applied (here for two random variables):

1. Sample (x, y) from (X, Y)
2. Compute $G(x, y)$
3. Sample y' from $(Y|X = x)$ independent of $Y = y$
4. Compute $G' = G(x, y')$
5. Store $Z = G * G'$
6. Repeat steps 1 to 5

The average value of Z is an approximation for $E[E^2[G|X]]$, from which the correlation ratio may be computed as

$$\frac{E(E^2(G|X)) - E^2(G)}{\sigma_G^2} \tag{3.5}$$

If X and Y are dependent, it may be difficult to sample from $(Y|X)$.

3.2 Local Sensitivity Measures

In contrast to the previously mentioned global sensitivity measures, the local ones do only give information about the influence of a variable in a specific region. Examples for these are:

- the α-values in a FORM-calculation [2]
- Local Probabilistic Sensitivity Measure [3] etc.

In fact, for reliability analysis the local sensitivities will be more important than global ones. It cannot be ensured that all variables that are of significant influence in specific points, as e.g. the so called *design point*, are identified by the global methods. Therefore attention will mainly be paid to local sensitivity measures within the scope of this thesis.

The α-values in FORM are explained in section 4.4.1. For the other reliability methods there are ways to approximate these α and this way comparable results can be achieved in the reliability calculations.

[2] In fact these are partial correlation coefficients: $\alpha_i = \rho(Z, X_i) = \partial_i G(x*)\ \sigma_i/\sigma_G$

[3] Introduced by Cooke and Noortwijk (1998)

3.3 Graphical Sensitivity Measures

In addition to the numerical methods there are very helpful graphical tools [4] tools that especially allow us to control multi-dimensional problems, since the whole range of information can be represented at once. Examples graphical representations of sensitivity are:

- Multiple Scatter Plots
- Cobweb Plots (conditional)
- Radar Plots etc.

Cobweb and Radar Plots allow us to visualize correlations between variables and other calculated quantities. In both we can observe if for typically high/low values of one variable another variable

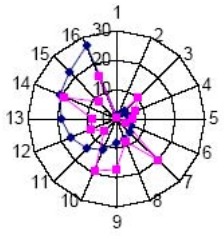

Figure 3.2: Typical Radar Plot of 16 Variables for Two Series

is also relatively high or low. Usually the ranges of the variables are normalized to this end. The Cobweb plot tool, as e.g. implemented in UNICORN [5], gives furthermore the possibility to conditionalize on a certain parameter range (normalized) of a variable. This feature is a powerful tool for visual analysis of data sets with respect to dependencies (e.g. compare figures 3.3 and 3.4).

[4] for more information refer to Kurowicka and Cooke (2005) [24]
[5] Copyright 2005 TU Delft & HKV Consultants

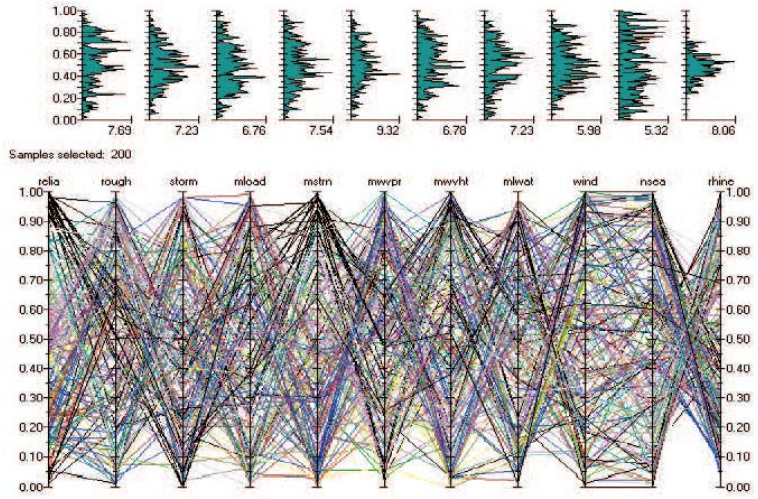

Figure 3.3: Cobweb Plot of a Dike Ring Reliability Analysis

Figure 3.3 shows the results of a MC-analysis of a dike ring reliability problem. Roughly there are already some patterns in this graph that let us assume certain correlations between the involved variables. In figure 3.4 the same data set has been conditioned on high values of reliability (the very left column). This, for example, allows us to conclude that there is a strong negative correlation with the third variable and positive correlation with the fifth one. By conditioning and changing the order of variables (columns) these patterns can be identified quite easily.

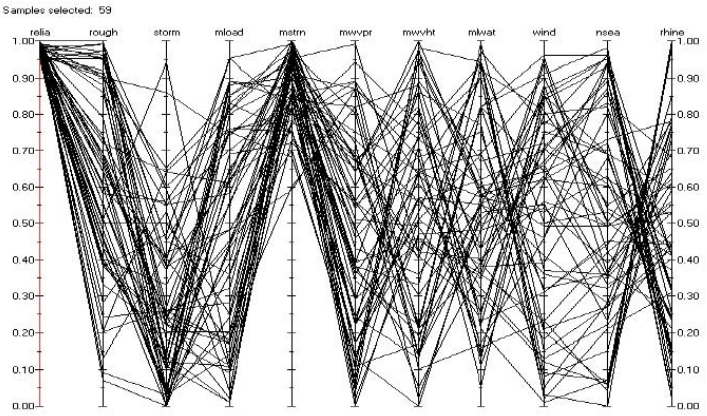

Figure 3.4: Cobweb Plot of the Same Analysis, Conditioned on High Reliability Values

(Both figures were taken from Kurowicka and Cooke (2005) [24])

Chapter 4

Structural Reliability Analysis

4.1 Basics of Structural Design Philosophies

Most engineering problems can be reduced to two basic ingredients, supply and demand or, more specific, load and resistance. The basic principle of structural design is that the resistance needs to be larger than the load:

$$R > S \tag{4.1}$$

where R is the resistance and S is the load (solicitation).

The primary task of design is to ensure that this performance criterion is ensured throughout the life time of a structure. However, most of the quantities involved on both sides of the equation are uncertain. The satisfactory performance according to the above mentioned criterion cannot be assured absolutely. Instead, a probability of satisfying the criterion is to be evaluated. This probabilistic way of assuring the performance is called *reliability*.

While reliability gives us the probability of non-failure under certain circumstances, often the alternative way is chosen by looking at the probability of failure P_f. Both these terms are complementary and their sum is therefore 1. Reliability is the probability of successful performance.

4.1.1 Overall Safety Concepts

Traditionally the problem was approached using empirical safety factors that were based on experience. It is important to notice that also safety factors cannot guarantee satisfactory performance, neither do overall safety factors allow us to treat components of the system according to their relative influence on the system performance.

Engineering design is usually an optimization problem with the two conflicting requirements of maximizing safety and minimizing cost. Whereas classical safety factor design does not give us any information about the relative importance of the parameters in this optimization problem, probabilistic design methods do provide this information and allow us to design more rationally.

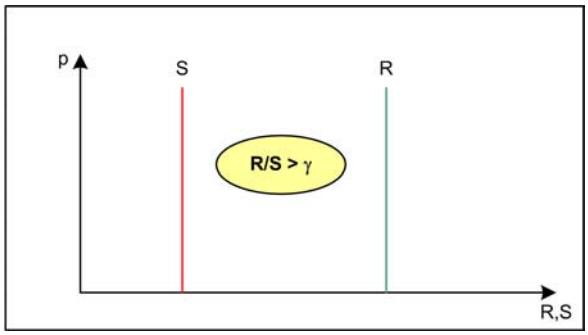

Figure 4.1: Design with Overall Safety Factors

4.1.2 Load and Resistance Factor Design

A first step towards including probabilistic concepts in design methodologies is 'Load and Resistance Factor Design' (LRFD). Instead of using overall safety factors, partial safety factors for load and resistance components of the system are used. These have to be established and calibrated beforehand by fully probabilistic calculations and they account for the typical spread (uncertainty) in the parameters and also for their relative influence on the system reliability. The calibration is carried out with the constraint of a certain reliability level that is required from the structure. LRFD allows us to design more rationally than using overall safety factors.

Referring back to the overall safety approach, the basic idea can be illustrated as shown in figure 4.1. The ratio between estimated resistance and load has to fulfill a minimum value considering 'best guesses' for both quantities according to engineering judgement (or conservative estimates alternatively):

$$R/S \geq \gamma \tag{4.2}$$

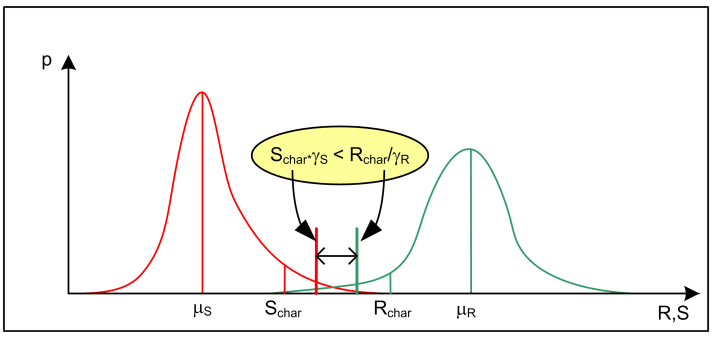

Figure 4.2: Design with Partial Safety Factors (LRFD)

When partial safety concepts like LRFD are applied, we use commonly high characteristic values for the load parameters ($S_{i,char}$) and low characteristic values for the resistance parameters ($R_{i,char}$). These characteristic values are often chosen as the 95 % (non-)exceedance values of the probability distribution of the respective parameter. In the following step the characteristic values are multiplied with the aforementioned partial safety factors ($\gamma_R, \gamma_S \geq 1$) and the

following criterion has to be satisfied for satisfactory performance (see also figure 4.2):

$$\frac{R_{char}}{\gamma_R} \geq S_{char}\gamma_S \tag{4.3}$$

As mentioned, LRFD is more rational than the use of overall safety factors. Its weakness is, however, that there is a limited set of load and material (resistance) factors and this set has to be calibrated in order to cover the majority of the cases that are likely to occur. As a consquence it cannot be guaranteed that all the designs to which the set of factors is applied result in the reliability level that was aimed for. Furthermore, a posterior check of the reliability level is not an option, otherwise one would opt for fully probabilistic design approaches anyway. The consequence is that usually it is chosen for a conservative calibration that is likely to result in sufficient reliability for the cases that could be carried out within the scope of current knowledge or the state of the art. This can lead to 'over-designed' structures for a large number of structures.

4.1.3 Probabilistic Design

The deficiencies of LRFD can be overcome by carrying out reliability analysis and thereby determining the reliability of the structural design directly. This is the approach of probabilistic design methods, which basically follow the steps mentioned earlier: uncertainty analysis, reliability analysis, risk analysis, probabilistic design. In this work the focus will be on reliability analysis and on the determination of the probability of failure P_f or its converse, the reliability (probability of satisfactory performance).

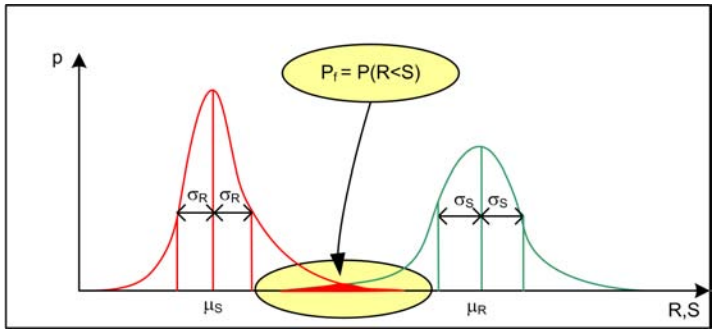

Figure 4.3: Probability of Failure as Probability of the Load Exceeding the Resistance

Probabilistic design methods are not explained at this point in detail, but in essence failure probabilities and parameter sensitivities in combination with cost considerations regarding failure (risk = probability of failure * cost associated with failure), maintenance or investments are the basic variables in this approach. Therefore reliability analysis does not only give a more rational measure of the structural safety level, but also parameters that are necessary for the rational decision making and optimization processes, namely the failure probability and the parameter sensitivities.

4.2 Overview Reliability Analysis Methods

The standard reliability problem as schematized in section 4.1.3 can be characterized as follows. A system can be in two states, the desired state and the undesired state which is complementary to the desired one. A system in the undesired state is considered as failed. The boundary of these two states is called *limit state*. Due to the uncertainties in the parameters characterizing the system we cannot predict the state of the structure with absolute certainty, but we may derive the probability of the system attaining the undesired state, the failure probability:

$$P_f = \int_{Z(x)\leq 0} f_X(x)dx \tag{4.4}$$

where $\mathbf{X}$ is the vector of random variables and $Z(\mathbf{x})$ is the limit state function for the failure mode considered. Negative values of Z correspond to failure, positive ones to satisfactory performance. In fact this a k-dimensional integration problem with k as the number of random variables.

The reliability of a structure is often expressed by the *reliability index* β instead of the failure probability:

$$\beta = -\Phi^{-1}(P_f) \tag{4.5}$$

with Φ^{-1} being the inverse of the standard normal cumulative distribution function.

The basic case for a reliability problem is the single mode failure with limit state function Z where the probability of failure can be expressed as:

$$P_f = P(Z(\mathbf{X}) < 0) \tag{4.6}$$

It is usually convenient to transform all random variables $\mathbf{X}$ to the independent standard normal space, also called ***u**-space*. If independent random variables have to be transformed to independent standard normally distributed variables we can use the simple relationship:

$$u_i = \Phi^{-1}(F_{X_i}(X_i)) \tag{4.7}$$

If the random variables are dependent, more complex transformation rules like the *Rosenblatt Transformation* (Rosenblatt (1952) [33], Hohenbichler and Rackwitz (1981) [19]) have to be applied.

The problem can now be rewritten in the form:

$$P_f = P(g(\mathbf{u}) < 0) \tag{4.8}$$

As stated before, the solution to this problem is basically the integration of the failure domain. If the problem is solved numerically this might require a large number of limit state function (LSF) evaluations, especially if the number of basic stochastic variables is high. If the LSF-evaluations are 'cheap' (low calculation time), this can still be feasible. However, if FEM-codes are used for the LSF-evaluation, the calculation time can be considerable and usually at least in the order of minutes. Therefore methods have been developed for reducing the calculation effort, usually at the cost of accuracy.

In the following methods are presented that are commonly applied for this purpose. The suitability of these methods will be investigated with respect to the particular calculation examples and the case study.

4.2.1 Level I Methods (semi-probabilistic)

Level I methods are usually applied in design codes for the verification of structures. They can also be applied to obtain rough estimates of the reliability. In level I methods previous knowledge is required about the basic random variables. It must be known, if they are of *load-type* $\partial g(\mathbf{u})/\partial u_i < 0$ or of *resistance-type* $\partial g(\mathbf{u})/\partial u_i > 0$ in the whole parameter space (**u**-domain). In this special case the reliability would be simply:

- $U = |\mathbf{u}| = \beta$ (for loads)
- $U = |\mathbf{u}| = -\beta$ (for resistances)

For an estimate of the reliability one can calculate the value of β for which $g(\mathbf{u}$ becomes zero. The estimate is conservative as long as the limit state is not strongly non-linear. One way of improving this estimate is giving weights to the different involved random variables according to their influence on the limit state function, i.e. high weights close to one for dominant and weights between zero and one to other variables. In fact, this effect is applied in the LRFD as explained before and the partial factors are calibrated in probabilistic studies.

The Level I methods are only mentioned here for sake of completeness. They are not suitable for the investigated approach due to their low accuracy and especially because previous knowledge about the influence of the random variables is required.

4.2.2 Level II Methods (fully probabilistic with approximations)

Level II methods take all the probabilistic properties of the random variables into account, but they include approximations that at the same time can be severe limitations for their use in specific problems. The following paragraphs give an overview of the basic ideas of this class of methods, its (expected) calculation effort and its advantages and limitations. The methods applied in this thesis are described more in detail in section 4.4.

First Order Reliability Method (FORM)

Hasofer and Lind (1974) [16] developed this approach that is based on the linearization of the limit state function in **u**-space. It's accuracy decreases with the degree of non-linearity of the LSF in the regions of high probability density. A severe limitation is that FORM cannot handle system behavior respectively multiple limit states. However there are possibilities to treat the limit states separately and to combine them subsequently using system reliability theory methods (see chapter 7). FORM should therefore only be used, when for a limit state is known that neither non-linearities nor system effects have a significant impact on the result.

The applied algorithms (see 4.4.1) require the determination of partial derivatives that have to be calculated numerically in case of using FEA for the LSF-evaluation. The algorithm implemented in ProBox requires $n + 1$ LSF-evaluations per iteration step. The number of iterations is dependent on the smoothness and on the degree of linearity of the LSF. For the problems considered the number of iterations needed to reach the convergence criteria should be in the range of 5 to 20. The typical number of basic random variables to be treated in the problems of this thesis will probably not exceed 20, also for reasons of interpretability of the results.

For a more detailed description of FORM see section 4.4.1.

Second Order Reliability Method (SORM)

In SORM a second-order correction is carried out to account for the non-linearity of the limit state. The success is dependent on the shape of the limit state. For non-linear, but smooth LSF it will improve the result obtained by FORM by taking into account the second derivatives of the LSF in the design point which are determined numerically. It can, however, also decrease the accuracy of the result, if the LSF exhibits a 'rough' surface and the second-order correction is based on local curvatures that do not represent the general shape of the LSF (see figure 4.10).

SORM requires the same order of magnitude of LSF-evaluations like FORM, only an extra determination of the local second derivatives. Depending on the implementation this can mean only a few extra evaluations or roughly twice the evaluations compared with FORM.

For a more detailed description of SORM see section 4.4.2.

Point Estimate Method (PEM)

The method is essentially a *weighted average method* that works with sampling points and weight factors, similar to numerical integration methods. The basic idea is to replace a given continuous *pdf* by a discrete function with the same first three central moments (mean value μ, standard deviation σ and skewness ν). The integration points and weights are chosen systematically according to the input distributions. After propagating the integration points (points in parameter space are combinations of values of the basic random variables) through the model and applying the according weights, the first two respectively three central moments of the response are approximated.

This method is an uncertainty method by definition. In order to make it applicable for reliability analysis we need more than an approximation of the central moments of the response. In fact it is necessary to make some assumptions regarding the response distribution and its parameters have to be fit to the obtained moments. Then this distribution is truncated at the value describing the limit state to obtain the probability of failure. It is obvious that this method is very sensitive to the choice of response distribution, since we are interested in the tail of the distribution (low failure probabilities).

There is a plenty of variations of the PEM in the literature and the number of LSF-evaluations varies between $2n$ and 2^n, which is an attractively low number, especially when the number of variables is low.

For a more detailed description of PEM see section 4.4.3.

4.2.3 Level III Methods (fully probabilistic)

Level III methods are characterized as fully probabilistic and exact methods, exact in the sense that no simplifying assumptions are implied. The accuracy of these methods can usually be controlled by parameters like the variance of the resulting failure probability σ_{P_f} or step sizes which also have an impact on the calculation time. The following paragraphs give an overview over the basic ideas of some methods, their (expected) calculation effort, advantages and limitations. The methods that are selected for application to the problem are described more in detail in section 4.4.

Monte Carlo (MC) Methods are based on the statistical analysis of large numbers of model outcomes, which are generated by randomly chosen values of the random variables. MC-methods generally need large number of model evaluations depending on the calculated probability of failure. In the following the basic Crude Monte Carlo as well as several other techniques are presented that offer possibilities to decrease the number of calculations.

Numerical integration (NI) techniques approximate integrals usually by following their boundaries in small steps. In contrast to Monte Carlo the number of calculations is highly dependent on the number of random variables.

Crude Monte Carlo Method

In the Crude Monte Carlo method random samples for each variable are taken and the model is evaluated using these realizations of the random variables. The samples are taken using pseudo-random number generators (PRNG) that generate uniformly distributed series of numbers that exhibit serial independence. The uniform random numbers are transformed to the according distributions by means of inversion or using other methods like e.g. the rejection method (see Madras 2002 [26]), if the respective cdf is not invertible.

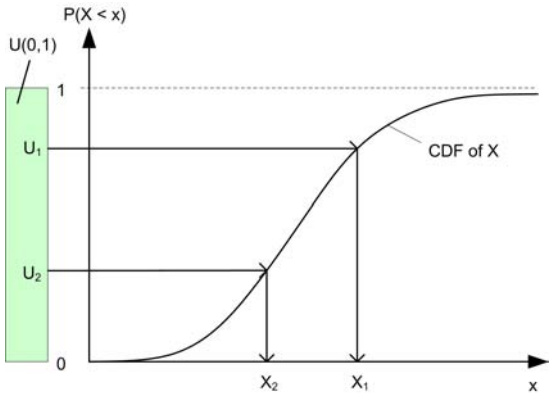

Figure 4.4: Generating Samples From a Distribution By Using Its Inverse CDF

If the model variables are independent, the samples can be taken from the marginal distributions. For dependent variables this can be the first step, but further transformations are necessary.

The obtained sample matrix

$$X = \begin{bmatrix} x_{11} & x_{12} & \dots & x_{1N} \\ x_{21} & x_{22} & \dots & x_{2N} \\ \vdots & \vdots & \ddots & \vdots \\ x_{M1} & x_{M2} & \dots & x_{MN} \end{bmatrix} \tag{4.9}$$

has to be propagated through the model. Each of the N columns represents one realization of the set of M model parameters. The N model outcomes according to these combinations can be seen as one sample of the distribution of the model outcomes. This enables us to use standard statistical techniques for the analysis of the model outcomes and its distribution as well as its central moments.

For reliability analysis it is even simpler, because basically one only has to count the number of times that a combination of parameters lead to failure and then use the following ratio for the determination of the failure probability:

$$P_f = \frac{number\ of\ calculations\ that\ lead\ to\ failure}{total\ number\ of\ calculations} \tag{4.10}$$

For Crude Monte Carlo the number of calculations is roughly inverse proportional to the failure probability. Systems with a high target reliability require a large number of calculations [1] until the P_f shows a sufficiently low variance.

Stratified Sampling

Stratified Sampling aims for a more homogeneous distribution of the samples in the sample space. To this end the sample space S is divided into non-overlapping subspaces S_i, called strata. The number of random samples taken from the subspaces S_i corresponds to the probability mass in the subspace S_i/S (the probability that a sample is located in the subspace). The sampling is carried out with distributions conditioned on the strata. This way a homogeneous distribution of the samples even with relatively low numbers of samples can be achieved with a lower probability of under-represented sample subspaces.

This method requires previous knowledge about the important sample regions to make a good choice for the subdivision into strata. The improvement compared to Crude Monte Carlo highly depends on this choice.

Quasi-Random Sampling (QRN)

Quasi-random number (QRN) sequences are presented as an alternative to pseudo-random numbers. They are generated with the purpose to cover the d-dimensional unit cube $I^d = [0, 1)^d$ more uniformly. Thus the rate of convergence is increased at the cost of serial independence (compared to PRNG). A well-known generator was developed by Sobol (1967) [36]. It is based on the concept of primitive polynomials.

[1] For an estimation method for the required number of calculations in Crude Monte Carlo see appendix C.

Discrepancy *(definition taken from [24])*
The discrepancy of a quasi-random sequence is a measure of the uniformity of the distribution of a finite number of points over the unit hypercube. Informally, a sequence of points is considered uniformly distributed in the d-dimensional unit cube $I^d = [0,1)^d$, if in the limit the fraction of points lying in any measurable set of I^d is equal to the area of that set.

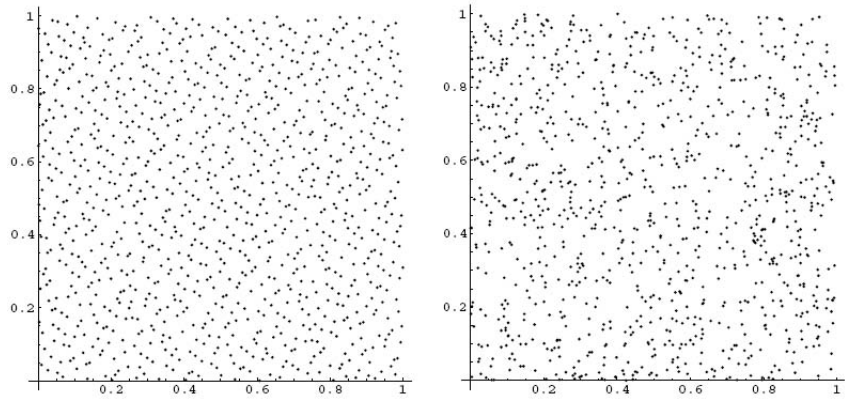

Figure 4.5: Comparison Quasi Random Sample (left) with Pseudo Random Sample (right), sample size: 1024 (from [24])

Referring to this definition, Quasi-Random Sampling is developed for decreasing the discrepancy. Usually QRN yield more efficient estimators for a specific characteristic of a distribution like in most cases the mean. They do not improve the efficiency of all estimators though, e.g. for other central moments like the variance. For the approach of counting the number of failed calculations this could mean that the estimate of the failure probability might be acceptable, but we have the practical problem of lacking the possibility to use a convergence-criterion that implies the variance of P_f.

Importance Sampling (IS)

When appropriately implemented, Importance Sampling can improve the efficiency of MC by orders of magnitude. But again, previous knowledge about the function to be sampled is indispensable and an inappropriate implementation can even decrease the efficiency by orders of magnitude. The basic idea of the method is to sample from an 'artificial' sampling distribution, which is not the one given by the actual problem and chosen beforehand. A re-weighting of the samples is carried out to get an unbiased estimate.

Suppose, we want to estimate an integral $I = \int_0^1 k(x)dx$. The Crude Monte Carlo estimator is based on the observation that $I = E(k(U))$ (with $U \sim U[0,1]$ (uniformly distributed between 0 and 1)). Therefore our sampling estimator in Crude Monte Carlo is:

$$\hat{I}_n = \frac{1}{n}\sum_{i=1}^{n} k(U_i) \tag{4.11}$$

For any pdf γ that is strictly positive on $[0,1]$ holds

$$I = \int_0^1 \frac{k(x)}{\gamma(x)}\gamma(x)dx = E\left[\frac{k(X)}{\gamma(X)}\right] \tag{4.12}$$

where X is a random variable with pdf γ. This leads us to the following estimator, which is called *importance sampling estimator based on* γ:

$$\hat{J}(\gamma)_n = \frac{1}{n}\sum_{i=1}^{n} \frac{k(X_i)}{\gamma(X_i)} \tag{4.13}$$

Equation 4.12 shows furthermore that $\hat{J}(\gamma)_n$ is an unbiased estimator for I ($E(\hat{J}(\gamma)_n) = I$).

This is the basic idea of importance sampling and it can be implemented in many different facets. Its benefit is that sampling from $\gamma(x)$ will (probably) lead to faster convergence and therefore to a smaller number of necessary calculations than for Crude Monte Carlo. Usually we lack the knowledge about even approximate shapes of the LSF and therefore importance sampling is considered to be unsuitable for the types of problem treated in this thesis.

Increased Variance Sampling (IVS)

Increased Variance sampling is a special case of Importance Sampling. It is especially suitable for reliability analysis, since the only previous knowledge that is used for conditioning the sampling pdf is that the limit state is 'far away' from the origin of the sample-space. The variance the input distribution is therefore increased. Thus more evaluations are carried out in, or close to the failure domain. This results in an over-representation of the failure-domain, but it can be corrected for the error in the way as explained for general importance sampling.

Quicker convergence can lead to a reduction of calculations compared to Crude MC. The amount of reduction is uncertain and the number of LSF-evaluations is still considered to be in the same order of magnitude as Crude Monte Carlo.

Latin Hypercube Sampling (LHS)

In Latin Hypercube Sampling (LHS) (see Iman and Helton (1988) [22]; McKay et al. (1979) [27]), which is a special case of stratified sampling, the domain of each random variable is subdivided into N disjoint intervals with equal probability mass. From each interval one sample is generated for the first variable and then these N samples are paired at random and without replacement with N samples of the second variable. The procedure is repeated for all M variables. This way the sample space is filled homogeneously and the number of samples can be reduced considerably compared to e.g. Crude Monte Carlo. It gives an unbiased estimator of the mean, however the estimator of the variance is biased, with a normally small but unknown magnitude of bias.

The method described above applies for mutually independent variables. In order to account for correlations refer to [24] for general procedures and remarks. For the specific case of Latin Hypercube Sampling Iman and Conover (1982) [21] propose the following procedure [2]:

1. Draw N LHS samples of M variables.
2. Convert these to ranks and place them in an N M matrix.
3. Draw N samples from an M-dimensional joint normal distribution with correlation matrix K.
4. Convert the normal variables to ranks.
5. Permute the columns of the LHS matrix so that the ranks in each column coincide with those of the normal matrix.
6. Unrank the LHS variables.

Again, as in the case of PEM, we obtain results referring to the distribution of the response. This approach does not lead directly to a probability of failure and further assumptions have to be made (truncated response distribution).

4.2.4 Response Surface Techniques (RS)

This family of techniques uses *response surfaces* (RS)[3], approximations of the model response instead of the model itself. It cannot be classified within the level I to III classification system, because RS can be combined with practically all the methods that have been presented so far.

Generally speaking, response surfaces are built using all kinds of interpolation methods (linear, quadratic, higher order, with/without cross-terms, splines) based on previously calculated LSF-evaluations. Some methods apply the obtained RS for the integration of the (non-)failure domain, in others like DARS they help decreasing the calculation effort by supporting the decision, if a certain parameter combination is worthwhile evaluating (see section 4.4.5).

RS are useful, especially in combination with FEM, for extrapolations into a failure domain where FEM cannot return any results due to loss of equilibrium. They also smoothen the responses, which helps the determination of partial derivatives of unstable LSF.

[2] The correlation between the random variables is accounted for via rank correlation.

[3] A general description of response surfaces is given in appendix B.

For more information over response surface techniques refer to Box and Draper (1987) [4]. Waarts (2000) [45] uses a response surface approach (see also section 4.4.5) in combination with Monte Carlo methods for reliability analysis.

4.3 Summary and Evaluation

The previously enumerated reliability methods are summarized in tables 4.1 and 4.2 evaluating the following criteria:

1. The method should be as *generic* as possible. The precision of the answer should not depend on choices that have to be made on the basis of previous knowledge about the problem.

2. The precision of the method should be controllable and within an acceptable range. Usually we can control this aspect by using the variance of the obtained results as convergence-criterion or with the step size for classical numerical integration techniques.

3. The expected calculation time must remain within acceptable limits. One crucial aspect for the choice of suitable methods is thus the required number of LSF-evaluations.

It should be stated that it is impossible to compare most of the criteria quantitatively or in an objective way. For example the accuracy of the methods can usually be controlled by certain convergence criteria (except PEM and LHS), but these are of different nature for level II methods like FORM/SORM and the methods of the Monte Carlo family. They cannot be compared directly. Also the number of calculations can only be known for PEM and LHS beforehand, for the rest of the methods only expected numbers of calculations can be given respectively orders of magnitude.

Table 4.1: Evaluation of Level II Reliability Methods (n = number of basic random variables)

Method	**Previous Knowledge**	**Accuracy**	**Calculation Effort**	**Remarks**
FORM	not required [a]	exact for Gaussian variables and linear LSF, error dependent on non-linearity of LSF	dependent on linearity LSF and number of RV, e.g. for n = 10 and 50 iterations: 1000 LSFE	algorithm does not require previous knowledge in principle, but one has to be critical with of local minima; unable to deal with system effects
SORM	same as FORM	only exact up to 2nd order-functions, error dependent on shape of LSF	same as FORM plus $2 * \sharp(RV)$ for 2nd order correction	same as FORM, the FORM-results can be either improved or made worse by the second order correction, therefore: knowledge about the shape of the LSF is necessary
PEM	assumption about response-distribution	depends highly on LSF and quality of fit of the response distribution's tail	between $2n$ and 2^n	applicability depends on the problem structure and is to be analyzed
LHS	assumption about response-distribution	depends highly on LSF and quality of fit of the response distribution's tail	$n * m$ calculations with m as the number of subintervals	resolution dependent (size of subintervals)

[a] Previous knowledge is not required for the application of the algorithm, but the problem must be suitable for the use of FORM. The suitability can e.g. be verified by the use of level III methods.

Table 4.2: Evaluation of Level III Reliability Methods (n = number of basic random variables)

Method	**Previous Knowledge**	**Accuracy**	**Calculation Effort**	**Remarks**
Crude MC	not required	required accuracy level can be controlled by convergence criteria	expected number of calculations $N > 400\left(\frac{1}{P_f} - 1\right) \approx 4,000,000$ calculations see appendix C	simple and robust
QRN	not required	required accuracy level can be controlled by convergence criteria	expected number of calculations same order of magnitude as Crude MC (from experience the max. improvements in efficiency could be up to factor 10)	results are reached quicker than with crude MC, but the estimator for the variance (and therefore the convergence criteria) is biased
IS	required	accuracy like Crude MC	the efficiency depends on the choices made for the Importance sampling method, it can be higher or lower than for Crude MC	usually the required previous knowledge is not available
IVS	not required	accuracy like Crude MC	efficiency higher than Crude MC, but amount of improvement unpredictable	could serve for accuracy checks of level II methods and system analysis
DS	not required	required accuracy level can be controlled by convergence criteria	efficiency higher than Crude MC, but amount of improvement unpredictable	well suited for accuracy checks of level II methods and system analysis
DARS	not required	required accuracy level can be controlled by convergence criteria	efficiency higher than DS, but amount of improvement unpredictable	well suited for accuracy checks of level II methods and system analysis

The ultimate answer on the question, which methods are the best for the type of analysis that is treated in this thesis, cannot be answered after this short evaluation yet. The answer is problem dependent. In the overall performance considerations one should also take into account that level III methods automatically account for system effects, i.e. the system reliability can be determined directly whereas for level II methods additional analyses have to be carried out.

For this specific research the program *ProBox* will be used, which includes FORM, SORM, Crude Monte Carlo, Numerical Integration, Directional Sampling, DARS, Increased Variance Sampling and combinations. These will be tested depending on the problem at hand. Additionally the PEM method is tested, because requires only a small number of calculations.

Furthermore, Latin Hypercube Sampling is a promising approach that should be subject to further investigation. Due to time reasons it is not treated in this thesis. The same holds for the combination of FORM with adaptive response surfaces (FORM-ARS). Since the FEM-calculations can produce non-smooth response surfaces and since there are impossible domains (equilibrium condition), ARS could be applied for mitigating these problems. For more details refer to Waarts (2000) [45].

4.4 Detailed Description of Selected Reliability Methods

In the following sections the reliability analysis methods that will be applied in combination with Finite Element Analysis are described in more detail.

4.4.1 First Order Reliability Method (FORM)

FORM stands for '*First Order Reliability Method*' where the term 'First Order' indicates that the limit state function is linearized. The linearization of the limit state is carried out in the so called '*Design Point*', which is the point on the limit state ($Z = 0$) with the highest probability density (see figure 4.6).

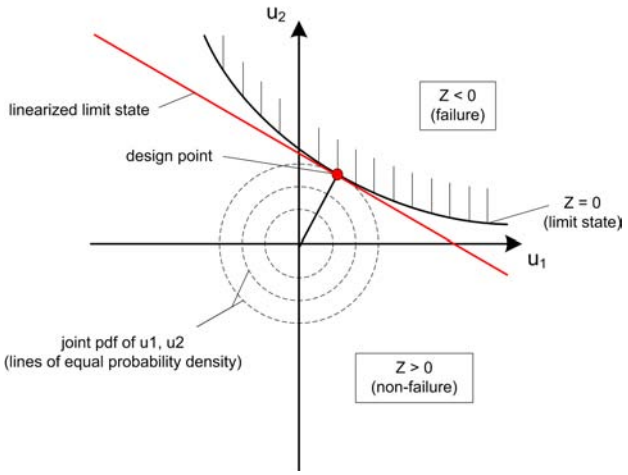

Figure 4.6: Design Point and Linearized Limit State for Two Dimensions in U-Space

First Order Second Moment Method (FOSM)

The first approaches of the first order category were the First Order Second Moment (FOSM) approaches. The original formulation by Cornell (1969) was based on two independent normally distributed variables R (strength) and S (load). Since the performance function is $Z = R - S$, failure is defined as $R - S < 0$ or $R < S$. The reliability index β then is the ratio of the mean value of Z and its standard deviation and can be expressed as:

$$\beta = \frac{\mu_Z}{\sigma_Z} = \frac{\mu_R - \mu_S}{\sqrt{\sigma_R^2 + \sigma_S^2}} \tag{4.14}$$

There are also other formulations based on Taylor expansions that can handle lognormal distributions as well and more than two random variables. However, FOSM is limited to statistically independent normally or lognormally distributed variables and it is only suitable for rough estimations of the reliability level of a structure. It is also not indifferent to the formulation of the limit state. Example given, FOSM will also not give the same results for LSF-formulations in terms of safety factors ($R/S < 1$) and in terms of margins of safety ($R - S < 0$). In a simplified numerical example this is illustrated in figure 4.7. For the same margin values, different factors of safety could be found. Due to these severe limitations it is not suitable for our purpose and we continue with more advanced first order methods.

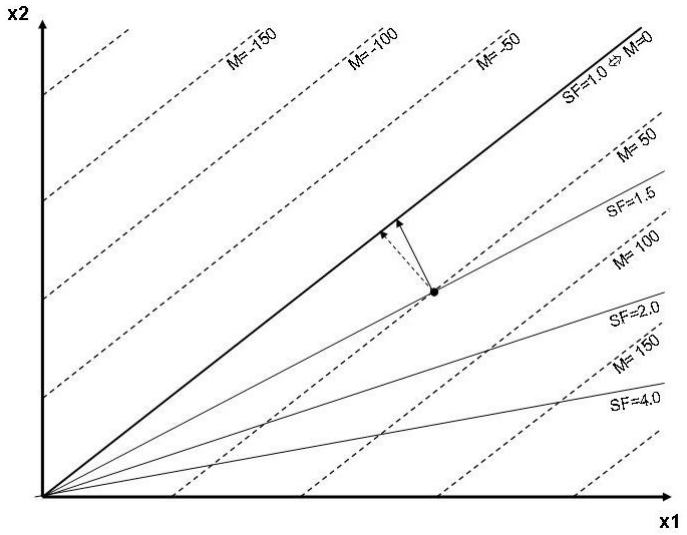

Figure 4.7: Example for Margins and Safety Factors in FOSM

Hasofer-Lind Method

This approach is probably the most wide-spread first order method and usually, when the term FORM is used, one refers to '*Hasofer-Lind*'. The random variables are transformed to equivalent standard normally distributed (Gaussian) variables and the whole procedure is carried out in **u**-space. For variables with a normal distribution this step is simply:

$$u_i = \frac{x_i - \mu_{x_i}}{\sigma_{x_i}} \tag{4.15}$$

For other types of distributions there are procedures available for carrying out this transformation. The LSF $Z(\mathbf{x})$ is rewritten in terms of **u**: $Z(\mathbf{u})$.

The FORM-algorithms require the determination of partial derivatives of the LSF with respect to **x'**. The following relation is can be used to this end:

$$dx_i/du_i = \sigma_{x_i} \tag{4.16}$$

therefore

$$\frac{\partial Z}{\partial u_i} = \frac{\partial Z}{\partial x_i} \cdot \frac{\partial x_i}{\partial u_i} = \frac{\partial Z}{\partial x_i} \cdot \sigma_{x_i} \tag{4.17}$$

The limit state function, only expressed in terms of R and S, becomes:

$$Z = R - S = \sigma_R \mathbf{u}_R - \sigma_S \mathbf{u}_S + \mu_R - \mu_S = 0 \tag{4.18}$$

Since the origin of the **u**-space is the combination of the mean[4] values of all basic random variables the distance to the failure criterion in $\mathbb{R}^d$ can be described by:

$$d = \sqrt{u_1^2 + u_1^2 + ... + u_n^2} = (\mathbf{u}^T \mathbf{u})^{1/2} \tag{4.19}$$

This distance has to be minimized in order to find the design point, β and P_f (see figure 4.6). This minimization problem can be elaborated, e.g. using a Lagrangian Multiplier Approach or a Taylor Series Approach[5]. Both lead to the same solution:

$$\beta = \frac{\mu_Z}{\sigma_Z} = -\frac{\sum u_i \cdot \left(\frac{\partial Z}{\partial u_i}\right)}{\sqrt{\sum \left(\frac{\partial Z}{\partial x_i}\right)^2}} \tag{4.20}$$

and we define the following terms which are commonly called the *influence factors* α_i:

$$\alpha_i = \frac{\left(\frac{\partial Z}{\partial u_i}\right)}{\sqrt{\sum \left(\frac{\partial Z}{\partial x_i}\right)^2}} \tag{4.21}$$

[4]To be precise it is the mean value for symmetrical and the median value for not symmetrical distributions
[5]for elaboration see e.g. Baecher (2003) [2]

In order to tackle the solution with the help of the previous equations, the *Rackwitz-algorithm* can be applied:

1. Guess values in the design point (e.g. mean values: $u_i \rightarrow u_i'^*$) [6]
2. Compute Z and α (partial derivatives) at u_i^*
3. compute the new DP[7] - approximation: $x_i^* = \mu_{x_i} - \alpha_i \sigma_{x_i} \beta$
4. Substitute the new u_i^* into Z and solve for β.
5. Re-evaluate $u_i^* = -\alpha_i \beta$.
6. Repeat steps 2 to 5 until convergence criteria are fulfilled.

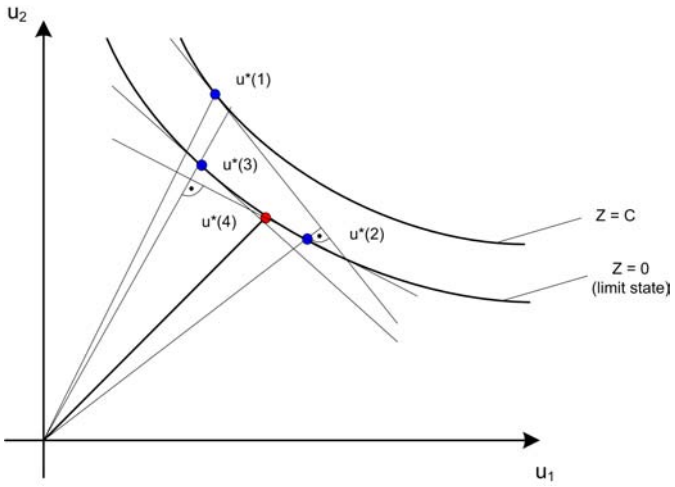

Figure 4.8: Graphical Representation of Rackwitz Algorithm (in brackets: iteration steps)

Other algorithms are available , e.g. Newton-Raphson schemes etc. The suitability of these methods is determined usually by the shape of the LSF. Some algorithms are more efficient in case of non-linearities than others. Another criterion for a good FORM-algorithm is its capability of finding a global minimum instead of local minima.

After obtaining the results of the reliability analysis, the values for the design point can be back-transformed to (original) **x**-space.

Note that FORM does not require any assumptions regarding the shape of the distribution of the failure criterion (like e.g. PEM). Its limitations are mainly that it is only accurate for linear limit state functions and that the degree of non-linearity of Z determines the magnitude of the error.

Three types of problems can occur with FORM. The algorithm might not converge or converge at a local instead of the global minimum or the accuracy is low due to the non-linearity of the limit state.

[6] The star(*) indicates a (estimated) design point value.
[7] DP = design point

4.4.2 Second Order Reliability Method (SORM)

SORM[8] starts with a FORM-calculation as described in the preceding section. The method also works in **u**-space and a second order correction is carried out in the design point determined by FORM.

The linearized form of the LSF in the design point can be given expressed as:

$$Z_{lin} = Z(\mathbf{u}^*) + \sum \alpha_i (u_i - u_i^*) = 0 + \sum \alpha_i u_i - \sum -\alpha_i^2 \beta = \beta + \sum \alpha_i u_i \tag{4.22}$$

The second derivatives of Z can be determined in the design point and with them we can develop a second order expansion of the LSF:

$$Z_{2nd} = \beta + \sum \alpha_i u_i + \frac{1}{2} \sum \sum \frac{\partial^2 Z}{\partial u_i \partial u_j} (u_i - u_i^*)(u_j - u_j^*) \tag{4.23}$$

Subsequently a rotation of the coordinate system is carried out (transform u_i to v_i), where the direction through the design point is chosen as the v_1-direction. This transformation leads to:

$$v_1^* = \beta \quad whereas \quad v_k^* = 0 \quad with\ k = 2, ..., n \tag{4.24}$$

$$\alpha_1 = 1 \quad whereas \quad \alpha_k = 0 \quad with\ k = 2, ..., n \tag{4.25}$$

For the rotated coordinate system the LSF can be rewritten to:

$$Z_{2nd} = \beta - v_1 + \frac{1}{2} \sum \sum \frac{\partial^2 Z}{\partial v_i \partial v_j} (v_i - v_i^*)(v_j - v_j^*) \tag{4.26}$$

For the two-dimensional case there are $\frac{\partial^2 Z}{\partial^2 v_1}$, $\frac{\partial^2 Z}{\partial v_1 \partial v_2} = \frac{\partial^2 Z}{\partial v_2 \partial v_1}$ and $\frac{\partial^2 Z}{\partial^2 v_2}$ as terms for the second derivatives. The last one is responsible for the curvature in the v_1-v_2-plane. Using this fact and that $v_2^* = 0$ the LSF can be rewritten as:

$$Z_{2nd} = \beta - v_1 + \frac{1}{2} \frac{\partial^2 Z}{\partial v_2^2} v_2^2 \tag{4.27}$$

Knowing the radius of the LSF R_{22} (and therefore also the curvature $\kappa = 1/R$ in the design point, we can obtain the second derivative from:

$$\frac{\partial^2 Z}{\partial v_2^2} = -\frac{1}{R_{22}} = -\kappa_{22} \tag{4.28}$$

which inserted in the LSF gives:

$$Z_{2nd} = \beta - v_1 - \frac{1}{2} \kappa_{22} v_2^2 \tag{4.29}$$

[8]The version of SORM as implemented in *ProBox* is explained. There are other versions with different approaches like the original version by Rackwitz.

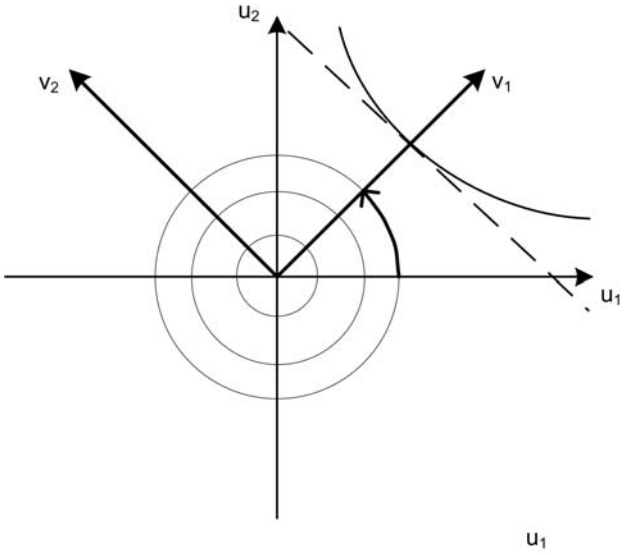

Figure 4.9: Transformation of Two-Dimensional Coordinate System in SORM

The failure probability can now be approximated by[9]:

$$P(Z_{2nd} < 0) = \frac{\Phi(-\beta)}{\sqrt{1 - \beta\kappa_{22}}} \tag{4.30}$$

The problem can also be generalized for n dimensions. To this end we can define a matrix G as:

$$G_{ij} = \frac{\partial^2 Z}{\partial v_i \partial v_j} \quad with\ i, j = 2, ..., n \tag{4.31}$$

The main curvatures (stored in the vector $\boldsymbol{\kappa}$) in $v_2, ..., v_n$-space are found by solving:

$$\|\mathbf{G} - \boldsymbol{\kappa}\boldsymbol{I}\| = 0 \quad with\ \boldsymbol{I} = unity\ matrix \tag{4.32}$$

Now the failure probability can be estimated with:

$$P_f = \Phi(-\beta) \prod_{i=2}^{n} (1 - \beta\boldsymbol{\kappa_i})^{-1/2} \tag{4.33}$$

As mentioned before, this procedure is only applicable to a limited amount of curvature. Furthermore it can lead to severe errors in case of irregularly shaped LSF when local curvatures are applied as in the example illustrated in figure 4.10. The example shows that in principle the SORM correction can decrease the accuracy of the FORM-result.

[9]The approximation is only reasonably accurate for $\beta\kappa_{22} < 0.75$.

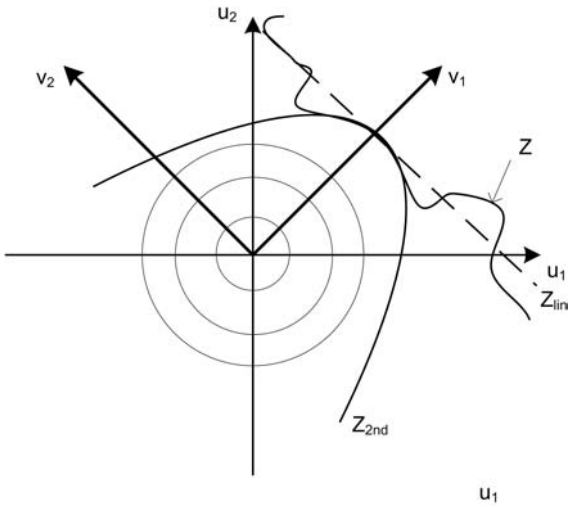

Figure 4.10: SORM Result for Arbitrary Irregular LSF

4.4.3 Point Estimate Method (PEM)

The method is essentially a *weighted average method* that works with sampling points and weighting parameters, similar to numerical integration methods. The basic idea is to replace a given continuous *pdf* by a discrete function with the same first three central moments (mean value μ, standard deviation σ and skewness ν). The original version of Rosenblueth [34] is used to illustrate the basic concept and some useful variants will be presented subsequently.

Mathematical Background

We have a set of random variables $\mathbf{X}$, e.g. soil properties, and another variable Y, which is a deterministic function of $\mathbf{X}$, $Y = g(\mathbf{X})$. This could be the factor or margin of safety or directly our limit state function. The basic question is:

> How to approximate the low-order moments of $f_Y(y)$ using only the low-order moments of $f_X(x)$ and the function $g(x)$?

The PEM-approach replaces the continuous random variable $\mathbf{X}$ by a discrete random variable whose pmf $p_X(x)$ has the same low-order moments as $f_X(x)$. Subsequently $p_X(x)$ is transformed by $Y = g(\mathbf{X})$ to another discrete function with the corresponding pmf $p_Y(y)$, whose moments are supposed to be approximations of the moments of the continuous distribution of the response Y.

The first moment of $f_X(x)$ is the mean:

$$\mu_X = \int x \cdot f_X(x) \cdot dx \tag{4.34}$$

The m^{th} order moments of $f_X(x)$ are:

$$\mu_X^m = \int (x - \mu_X)^m \cdot f_X(x) \cdot dx \tag{4.35}$$

The corresponding moments of the discrete pmf $p_X(x)$ are:

$$\mu_X^m = \sum (x - \mu_X)^m \cdot p_X(x) \tag{4.36}$$

General Formulation (Rosenblueth)

We use the following notation as introduced by Rosenblueth in his original paper in 1975:

$$E[Y^m] \approx P_+ y_+^m + P_- y_-^m \tag{4.37}$$

in which:	Y	deterministic function $Y = g(\mathbf{X})$
	$E[Y^m]$	expected value of Y raised to the power m
	y_+	value of Y evaluated in point $x_+ > \mu_x$
	y_-	value of Y evaluated in point $x_- < \mu_x$
	P_+ and P_-	weights

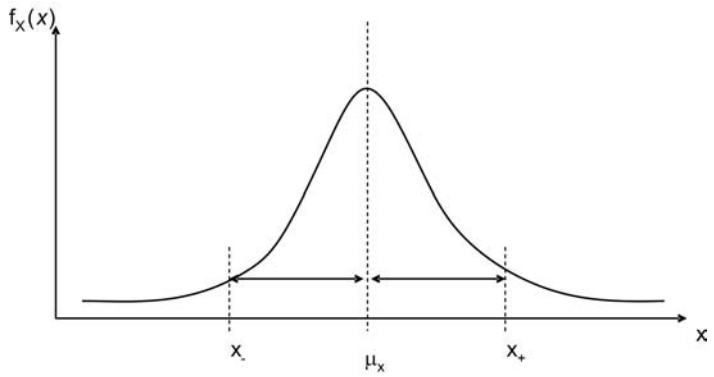

Figure 4.11: PEM for univariate case

We can distinguish three cases:

1. Y is a function of one variable; mean, std and skewness are known.
2. Y is a function of one variable whose distribution is symmetrical and approximately Gaussian.
3. Y is a function of n variables $X_1, X_2, ..., X_n$ whose distributions are symmetrical and which may be correlated.

The first two cases are special cases with significant simplifications, such as only one random variable. For the problems to be studied they will be of little use and therefore we focus on the third case whose most important simplification is that the skewness of the variables is neglected.

For each variable we choose two points, each at a distance of one standard deviation below and above the mean value. This gives a total of 2^n points[10] to be evaluated. The general form of the weights can be described with:

$$P_{s_1 s_2 \ldots s_n} = \frac{1}{2^n} \cdot \left[1 + \sum_{i=1}^{n-1} \sum_{j=i+1}^{n} (s_i)(s_j)\rho_{ij} \right] \tag{4.38}$$

where s_i is +1 for points one std above the mean and -1 for the opposite case.
The m-th moment is approximated by

$$E[Y^m] \approx \sum P_i y_i^m \tag{4.39}$$

In figure 4.12 the case of two correlated variables is illustrated.

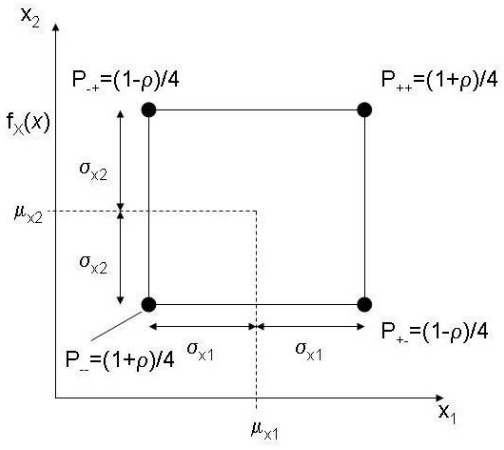

Figure 4.12: PEM for bivariate case including correlation

Analogy to Numerical Integration

Rosenblueth's method can be compared with the generalized method of numerical integration with orthogonal polynomials that applies for any probabilistic distribution of X.

Gaussian quadrature is a numerical approximation to the integral

$$I = \int g(z) \cdot f(z) \cdot dz \tag{4.40}$$

where $g(x)$ function to be evaluated
$f(x)$ weighting function

[10] A point is a parameter combination in this case.

The approximate integral is

$$I = \sum H_i \cdot g(z_i) \tag{4.41}$$

where $g(z_i)$ function evaluated in point i
H_i weight of point i (assuming $f(x)$ as normal distribution)

Rosenblueth's third case is a similar extension of the one-dimensional Gaussian quadrature points to a grid of higher dimensions. The general formulation of the point estimate method allows incorporating the effect of different probabilistic variables from different distributions, as long as their means and variances are known.

Limitations

1. For some cases two points are insufficient for estimating the moments of Y.
2. PEM should not be used for evaluating higher moments than second moment of Y.[11]
3. PEM should not be used for evaluating moments of higher order than the moments used from the input variables.
4. Should be used cautiously, when the distribution is severely changed by function g.[12]

In the literature about geotechnical problems it was mostly applied for uncorrelated variables. However, the effort to account for correlation is insignificant which is one of the attractive properties of the method.

The accuracy of the method is difficult to describe in general terms and therefore it is preferred to study its performance for several cases.

Number of Computation Points

The classical method proposed by Rosenblueth requires 2^n evaluations of the limit state function. Since the computational effort for higher numbers of variables is considerable, other methods have been developed that reduce this number to $2n$ respectively $2n + 1$ by some simplifying assumptions.

Harr's Method (1989) (skewness = 0; correlated variables)

The method of Harr makes use of the eigenvalues and eigenvectors of correlation matrix $\mathbf{K}$. One has to calculate the values of Y in $2n$ points. These points are the intersections of the eigenvectors with a hypersphere that goes through the corner points of the unit hypercube. The weight of each value is the corresponding eigenvalue divided by $2n$. The rest of the calculation corresponds to the classical approach.

[11] E.g. the case 1 procedure returns always skewness of X instead of skewness of Y
[12] E.g. normal to lognormal with functions such as $Y = e^X$

Method by Zhou and Nowak (1988) (correlated variables, marginal distributions)

The method Zhou-Nowak is applied to geotechnical problems in several publications from Graz University ([39], citeSch01). It uses $2n^2 + 1$ calculation points in **u**-space and seems for the present purpose to be the best compromise between accuracy and computational effort of the PEM-methods.

The idea is again to use numerical procedures to approximate the m^{th} moment of the response $g(\boldsymbol{X})$ to the random vector $\boldsymbol{X}$ whose exact formulation is:

$$E[g^m(\boldsymbol{X})] = \int_{-\infty}^{+\infty} ... \int_{-\infty}^{+\infty} f_X(x_1, ..., x_n) \cdot g^m(x_1, ..., x_n)\ dx_1 ... dx_n \tag{4.42}$$

Using the Gauss-Hermite formula we can approximate the m^{th} moment of g for a single standard normal variable z with the following integration formula:

$$E[g^m(Z)] = \int_{-\infty}^{+\infty} \phi(z) g^m(z)\ dz \cong \sum_{j=1}^{k} w_j g^m(z_j) \tag{4.43}$$

in which ϕ is the standard normal pdf, and z_j and w_j are the integration points, the weights of which are given in table 4.3.

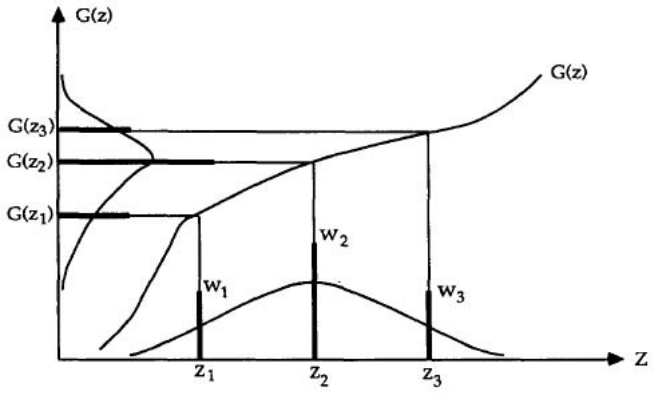

Figure 4.13: Integration with Gauss-Hermite Quadrature Using 3 Points

For a single non-normally distributed variable X the same principle applies, only the transformation from standard normal space to x-space is necessary:

$$E[g^m(X)] \cong \sum_{j=1}^{k} w_j g^m(x_j) = \sum_{j=1}^{k} w_j\ g^m(F_X^{-1}(\Phi(z_j))) \tag{4.44}$$

These approximations are exact, if g is a polynomial of maximum (k-1)th degree (k is the number of integration points).

Table 4.3: Points and Weight Factors for Integration Formulae

Number of Points k	Points z_j	Weight factors w_j
1	$z_1 = 0$	$w_1 = 0$
2	$z_1 = -1$	$w_1 = \frac{1}{2}$
	$z_2 = +1$	$w_2 = \frac{1}{2}$
3	$z_1 = -\sqrt{3}$	$w_1 = \frac{1}{6}$
	$z_2 = 0$	$w_2 = \frac{4}{6}$
	$z_3 = +\sqrt{3}$	$w_3 = \frac{1}{6}$
4	$z_1 = -\sqrt{3+\sqrt{6}}$	$w_1 = \frac{3-\sqrt{6}}{12}$
	$z_2 = -\sqrt{3-\sqrt{6}}$	$w_2 = \frac{3+\sqrt{6}}{12}$
	$z_3 = +\sqrt{3-\sqrt{6}}$	$w_3 = \frac{3+\sqrt{6}}{12}$
	$z_4 = +\sqrt{3+\sqrt{6}}$	$w_4 = \frac{3-\sqrt{6}}{12}$

Zhou and Nowak (1988) [46] describe in their paper several possibilities, also for multivariate cases, with and without known joint pdf. For the present purpose the methods for known marginal distributions are preferred in combination with the Gauss quadrature rules and the Gauss quadrature weight factors, where due to experience from the literature the integration methods using $k = 2n^2 + 1$ integration points are chosen (table 4.4):

$$E[g^m(Z_1, ..., Z_n)] \cong \sum_{j=1}^{k} w_j g^m(z_{1j}, ..., z_{nj}) \tag{4.45}$$

Table 4.4: Points and Weight Factors for $k = 2n^2 + 1$ Integration Formulae

Number of Points k	Points $(z_{1n}, z_{2n}..., z_{jn}$	Weight factors w_j
$2n^2 + 1$	$\mathbf{Z} = (0, 0, ..., 0)$	$w_j = \frac{2}{n+2}$
	$\mathbf{Z} = (\pm\sqrt{n+2}, 0, ..., 0)$ [a]	$w_j = \frac{4-n}{2(n+2)^2}$
	$\mathbf{Z} = (\pm\sqrt{\frac{n+2}{2}}, \pm\sqrt{\frac{n+2}{2}}, ..., 0)$ [a]	$w_j = \frac{1}{(n+2)^2}$

[a] all possible permutations

For a set of known marginal distributions and known correlation coefficients (correlation matrix **C**) we can follow this procedure:

1. Calculate correlation matrix $\boldsymbol{C_0}$ [13].
2. Determine $\boldsymbol{L_0}$ by Cholesky-decomposition of $\boldsymbol{C_0}$.
3. Determine the integration points in standard-normal space (see tables).
4. Calculate the correlated standard normal vectors $\boldsymbol{Y} = \boldsymbol{L_0 Z}$.
5. Perform the marginal transformation: $X_i = F^{-1}[\Phi(y_i)]$
6. Calculate the first two moments of G using formula 4.45.

For statistically independent variables, the procedure reduces to the steps 3, 5 and 6. Step 6 uses the following relations that relate to the integration formulae and known probabilistic relations:

$$\mu_X = E[g(X)] \cong \sum_{j=1}^{k} w_j g^m(x_j) \tag{4.46}$$

$$\sigma_X^2 = E[g^2(X)] - E^2[g(X)] = E[g^2(X)] - \mu_X^2 \quad with\ E[g^2(X)] \cong \sum_{j=1}^{k} w_j g^2(x_j) \tag{4.47}$$

Application in Reliability Problems

With all the described PEM-variants we haven't yet made the step to determine a reliability level. We have only obtained the characteristics of a response in terms of its first two (eventually three) central moments. One way to obtain a reliability level is to assume a distribution type and choose the parameters according to these moments. The distribution is then truncated at the limit state value.

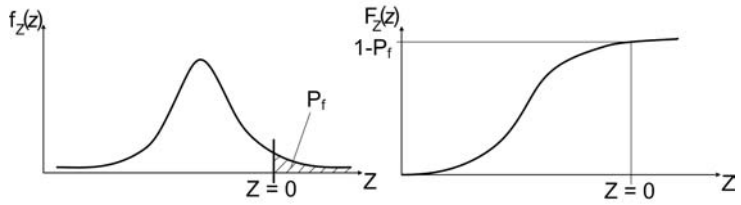

Figure 4.14: Truncated Response Distribution Obtained in PEM

This part is the most significant weakness of the use of PEM for reliability problems. The assumption of the distribution type can have a large influence on the shape of the response's tail and therefore especially in the low failure probability regions we usually operate in.

[13] Not elaborated here, for sake of simplicity we restrict ourselves in the tests to independent variables

4.4.4 Directional Sampling

Directional Sampling belongs, as indicated earlier, to the category Monte Carlo methods. It is carried out in **u**-space. That means that the random realizations of parameter combinations are taken from an n-dimensional joint normal distribution. The method follows basically these steps:

1. A mean (respectively median) value calculation in $\mathbf{u} = 0$ is carried out.
2. A point in the parameter space is generated randomly. The vector **u** is defined as the vector with the origin of the parameter space as starting point and the randomly generated point as end point.
3. This vector is scaled to a predetermined length $|u| = u_0$ (e.g. $|u| = 1$). In other words we only keep the direction of the vector as information of the random realization. An LSF-evaluation is carried out in this point.

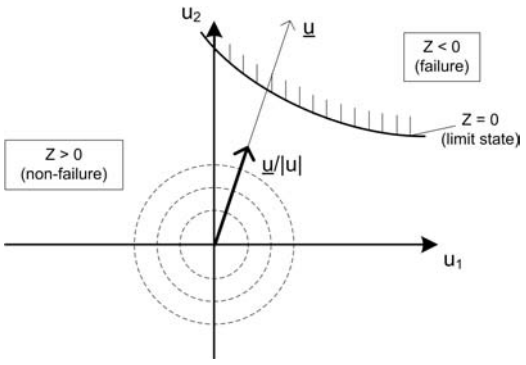

Figure 4.15: Directional Sampling for Two-Dimensional Problem (steps 1 to 3)

4. An iteration method (e.g. bisection-method or Newton-Raphson) is used to determine the scale factor λ ($\lambda \geq 0$) that corresponds to $Z = 0$ (limit state) whilst the direction of **u** is maintained[14].

[14]The accuracy of the iteration method can be controlled by an accuracy parameter ϵ.

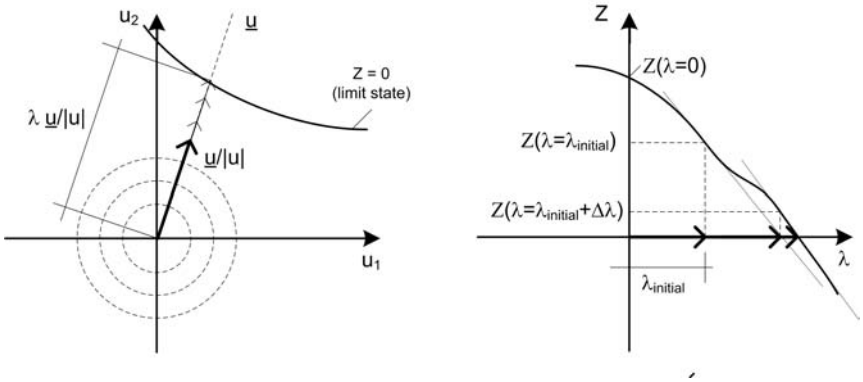

Figure 4.16: Directional Sampling for Two-Dimensional Problem (step 4)

5. $\sum_{i=1}^{n} \lambda_i^2$ is χ^2-distributed with n degrees of freedom (number of basic random variables). If λ was constant for all directions, the probability of failure could be written as:

$$P_f = 1 - \chi^2(\lambda^2, n) \tag{4.48}$$

If we have N random realizations of $\mathbf{u}$ with different results for λ, we can compose the failure probability as:

$$P_f = \frac{1}{N} \sum_{j=1}^{N} (1 - \chi^2(\lambda_j^2, n)) \tag{4.49}$$

The corresponding variance for N realizations is:

$$\sigma_{P_f}^2 = \frac{1}{N(N-1)} \sum_{j=1}^{N} (P_j - P_f)^2 \quad with\ P_j = 1 - \chi^2(\lambda_j^2, n) \tag{4.50}$$

6. The steps 1 to 5 are repeated until the convergence/stop criteria are reached, e.g. a sufficiently low variance $\sigma_{P_f}^2$ of the failure probability. Alternatively it is stopped after a maximum number of calculations.

4.4.5 DARS

DARS (Directional Adaptive Response Surface Sampling) is a combination of Directional Sampling (DS) and Adaptive Response Surface techniques (ARS). The response surfaces (see appendix B) serve in the current configuration of DARS as tool for deciding, if a directional sample is worthwhile evaluating or not, i.e. wether a direction is important. The ARS are therefore not used for integration of the safe/unsafe domain for example. The use of response surfaces is efficient, when the LSF-evaluation is expensive in terms of calculation effort. The basic principles of DS are introduced followed by the incorporation of ARS in this technique.

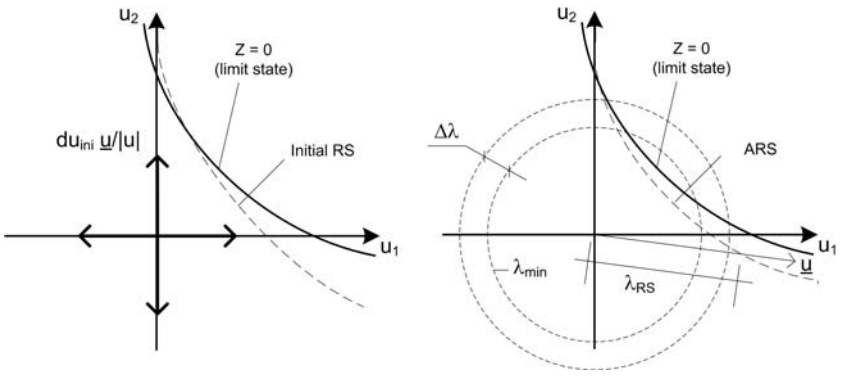

Figure 4.17: Parameters and Steps of the DARS-method

As mentioned earlier, in DARS the response surfaces serve as tool for detecting 'important' sampling regions, i.e. to decide wether a real LSF-evaluation is necessary or not. For the rest DARS follows the principles of Directional sampling:

1. Sampling along the axes of the basic random variable space. Length of the vector $u_j = du_{ini}$.
2. Fitting initial response surface[15].
3. Sample $\mathbf{u}$ as described in Directional Sampling $\rightarrow$ determine λ_1. $\lambda_{min} = \lambda_1$.
4. Update response surface fit using the new information[16].
5. Sample $\mathbf{u}$ according to Directional Sampling $\rightarrow$ determine expected $\lambda_{j,RS}$ according to ARS. If the expected $\lambda_{j,RS}$ is smaller than $\lambda_{min} + \Delta\lambda$ ($\Delta\lambda$: calculation sensitivity parameter), LSF calculations with the actual model are carried out and λ_j is determined. Otherwise the contribution of this direction is considered negligible, thus $P_j \approx 0$.
6. If $\lambda_j < \lambda_{min}$, then $\lambda_{min} = \lambda_j$.
7. Evaluate P_f and $\sigma^2_{P_f}$ as in ordinary directional Sampling.
8. Repeat steps 4 to 7 until convergence/stop criteria are reached.

The important advantage of this method is, that a relatively large number of LSF-evaluations will not have to be carried out based on the information obtained by the ARS. The performance of DARS is difficult to predict. For complex LSF, it could be that the ARS changes considerably after obtaining new information. The question arises, wether after updating the RS the previously as negligible considered points have to be re-evaluated. If there is no previous knowledge at all about the LSF, this is strongly recommendable. In ProBox this can be done optionally.

[15] In ProBox: quadratic polynomial with/without cross-terms
[16] All LSF-evaluations carried out with the actual model are used as information for updating the ARS.

Part II

Coupling of Reliability Analysis and FEM For Geotechnical Structures

Chapter 5

Problem Description and Approach

Part II of this thesis deals with the application of the reliability methods that were described in part I to geotechnical problems. The limit state function evaluations (LSFE) will be carried out with the Finite Element Analysis (FEA) software *Plaxis 8.2*, which is specifically designed for 2D plane-strain or axisymmetric analysis in geotechnics. Using FEA for this purpose implies that the limit state formulation is *implicit* and can only be solved numerically. For many of the methods described in chapter 4 the evaluation of partial derivatives is required, for which no analytical formulation is available in this approach.

5.1 Goals and Perspectives

The goal is to develop a methodology for assessing the reliability of geotechnical structures, in particular deep excavations. Non-linear and plastic soil behavior and the system behavior of the structure should be taken into account. Some of the presented reliability methods can deal with system reliability problems directly, whilst for others additional methods are to be used for combining the reliability information of singular limit states to obtain the system reliability (estimates). However, in general it will be more important to determine the failure probabilities for the mechanisms than for the complete system.

For each type of problem there are several relevant limit states, for which different constitutive models could be considered as the most suitable. As in deterministic Finite Element Analysis (FEA), the choice of constitutive models is always a compromise between modelling performance respectively accuracy and modelling effort, i.e. the effort required for obtaining sufficient information on the model parameters. The aim for the future should be to identify suitable combinations of limit state descriptions and constitutive models. In this thesis a first step is made by describing the constitutive model choice in general (see appendix F), but for the calculations an elasto-plastic soil model with Mohr-Coulomb failure criterion will be used for sake of simplicity.

This work also aims at demonstrating that reliability analysis can be carried out with reasonable effort for specific structures whose system behavior is known. Also the potential benefits of this approach over the classical design practice will be highlighted, especially by showing the differences between the target reliability in deterministic design and the calculated reliability

using the presented approach.

In recent actualizations of design codes and technical recommendations, such as relevant for our case the 'CUR 166 - Damwandconstructies'[1] it can be observed that guidelines for the use of FEA have been implemented parallel to the existing analytical or empirical calculation methods. FEA is this way more and more accepted as an alternative for SLS design and recently also for ULS calculations. The complexity of FEA required some instructions for the designer to properly model the structure and choose the corresponding parameters.

The vision is that a similar development could be initiated for reliability methods. An approach on a more general scale has been undertaken by JCSS[2] with the Probabilistic Model Code (PMC) (see [23]) that was first published on internet in 2001 and gives recommendations for modelling structural reliability problems. This kind of guidelines for reliability analysis could be introduced in the design guidelines as an alternative to the partial safety factor design (LRFD - Load and Resistance Factor Design) for those who want to refine or optimize their structure or use the reliability results in more advanced probabilistic design concepts, i.e. as a design alternative.

5.2 Approach and Structure

The *coupling of Reliability Analysis and Finite Element Analysis* requires interfaces for the communication between both. In *chapter 6* we will discuss how this was achieved for the specific combination of *ProBox* and *Plaxis*. In *appendix F* an overview is given over the most relevant *constitutive models* for soils and structural elements that are available in Plaxis and suitable for problems involving deep excavations. Furthermore, several features and aspects related to the *Finite Element Method* that are necessary or useful for application in combination with reliability analysis are presented.

An approach for determining the *(system) reliability* of deep excavations is presented in *chapter 7*. An inventory of the most relevant failure mechanisms is presented in form of a fault tree. The fault tree also illustrates the interaction and the relations between the failure mechanisms and modes. The treatment of these failure mechanisms is discussed in detail. These refer to the structural members of deep excavations as well as to the soil as part of the system. Soil has to be seen in this context as load and as resistance variable at the same time, which requires a special treatment. The formulation of *limit states* is a main aspect in this chapter.

In part III the application of the presented coupled techniques is demonstrated using *simple examples* beginning with *chapter 8*. The first example, a simple beam on two supports, is used in comparison to exact analytical solutions. The second one, the classical bearing capacity problem, deals with the description of soil shear failure. The third example is the first application to an excavation problem. The *failure mechanisms* of an excavation with a non-anchored retaining wall in homogeneous cohesionless soil are investigated.

The *case study* in chapter 9 demonstrates the applicability of the presented methodology to

[1] Dutch technical recommendation for sheet pile walls [8]
[2] Joint Committee for Structural Safety (http://www.jcss.ethz.ch/)

a realistic respectively 'real world' problem. It treats an excavation with one anchor layer in typical Dutch (soft) soil conditions. Uncertainties in the soil properties, the phreatic levels and also the corrosion of the sheet pile wall are accounted for.

Finally, in chapter 10 *conclusions* are drawn based on the results of this study and *recommendations* for future research are formulated. A short *outlook* on the short and medium term developments regarding this research concludes the report.

5.3 Limitations

The author is aware of the following limitations of this work, of which some could be subject to further research:

- The conclusions that can be drawn from this research are limited to the input that was used. The determination of proper input statistics, especially uncertainties in soil parameters are difficult to determine. The description of the input determination is not subject of this work.
- For proper reliability analysis all uncertainties have to be quantified to obtain correct results for the distribution of the system response and the failure probability. For most of the investigated problems the uncertainties are reduced to the most important basic random variables. Therefore there is an error involved that is, however, intended to be kept acceptably small.
- The quantification of the model error will not be scope of this work. For the problems investigated, proper constitutive models will be chosen based on experience in the literature. For the calculations it will either be assumed that the used models represent the real world behavior perfectly or a standard model error can be assumed to estimate its influence on the reliability. The determination of such a model error as well as eventually of a modelling error (subjective modelling choices) would have to be determined by comparison of predictions and measurements.
- The research will be limited to a number of problem configurations and case studies. Configurations substantially different to these could give different results and therefore the conclusions and recommendations cannot be applied to these directly.
- A large number of structural failures are caused by unforeseen anomalies and human error. These types of uncertainties are not taken into account.
- This work is restricted to plane-strain problems, however, the general approaches can be applied also for three dimensions.
- Models are commonly calibrated for parameter ranges that are around the expectation values. For reliability analysis we are, however, contemplating situations close to failure. The validity of the model would have to be investigated for each limit state and this type of model error would have to be quantified. This is beyond the scope of this thesis.

In fact, in this thesis work we do not go beyond the quantification of the output uncertainties and the determination of exceedance probabilities, given a certain input uncertainty. That means that we still lack model error and subjectivity considerations for the transferability to 'real world' structural behavior. In deterministic design approaches these considerations are included either in the partial safety concepts or in conservative target reliabilities. In probabilistic concepts this could be achieved by appropriate model error and 'human error' factors or alternatively by increasing the target reliabilities.

Chapter 6

Coupling Reliability Analysis and FEM

This chapter deals with the coupling of reliability analysis and Finite Element Method as adopted for this thesis work. The general aspects of such a combination are discussed as well as specific aspects that refer to the coupling of the two programs that were used for this purpose - ProBox[1] (reliability analysis) and Plaxis[2] (FEM).

6.1 The Functionality of ProBox

The software package ProBox is still under development during the work on this thesis. At present the following reliability methods are available:

- FORM / SORM
- Numerical Integration (NI)
- Crude Monte Carlo (CMC)
- Directional Sampling (DS)
- Directional Adaptive Response Surface Sampling (DARS)
- Increased Variance Sampling (IVS)

For all the methods the algorithms work with numerical differentiation or iteration methods. Thus it is not necessary to have closed-form limit state formulations neither their derivatives. This is important for the coupling with other programs that are used for the limit state function evaluation.

[1] ProBox stands for Probabilistic Tool Box and was developed by TNO Built Environment and Geosciences, Delft, The Netherlands.

[2] Plaxis Finite Element Code developed by Plaxis bv, Delft, The Netherlands.

ProBox handles 14 types of distributions amongst which the most common ones, like the Normal, Lognormal, Exponential and the Beta Distribution. Also extreme value distributions are available and self-defined empirical distributions can be defined in table form.

Correlations are accounted for via a product moment correlation. Of course, this type of correlation matrix has to be positive definite.

6.2 General Aspects of the Coupling

When a reliability tool is coupled with another software program, the reliability program carries out the whole reliability analysis and it uses the other program only for the evaluation of the limit state function. Limit state function evaluations may be necessary for the evaluation of realizations of the random variables or for perturbation or iteration methods that are involved in the numerical algorithms of the reliability methods.

Usually the influence on the routines of the evaluation program is limited. The communication of the programs is limited to modifying the input quantities for the limit state function evaluation, starting the calculation and reading the relevant output quantities.

6.3 The Coupling ProBox-Plaxis

The coupling of ProBox and Plaxis is basically establishing an interface between the two programs that is capable of exchanging the data from the input and the output parameters. It was chosen for implementing the respective routines in ProBox, i.e. ProBox has to be able to read and amend data in Plaxis files that contain material parameters, groundwater information or load definitions and to read the information of the calculation output (see fig. 6.1).

A basic Plaxis model has to be defined, e.g. using the mean values of the properties that are to be treated as stochastic quantities. ProBox can read the input and output files of this Plaxis model and make the accessible input parameters accessible. In principle one can assign statistical distributions to each quantity. Sometimes it is necessary to use more external models at the same time or to define additional relations internally (e.g. conversion rules for parameters). Subsequently the limit state function is defined based on the available model output variables and eventually on other self-defined variables. In this case this could be e.g. based on displacements, forces or stresses obtained by the Plaxis-analysis. Then after defining the reliability method, the calculation is started and ProBox enters a calculation loop.

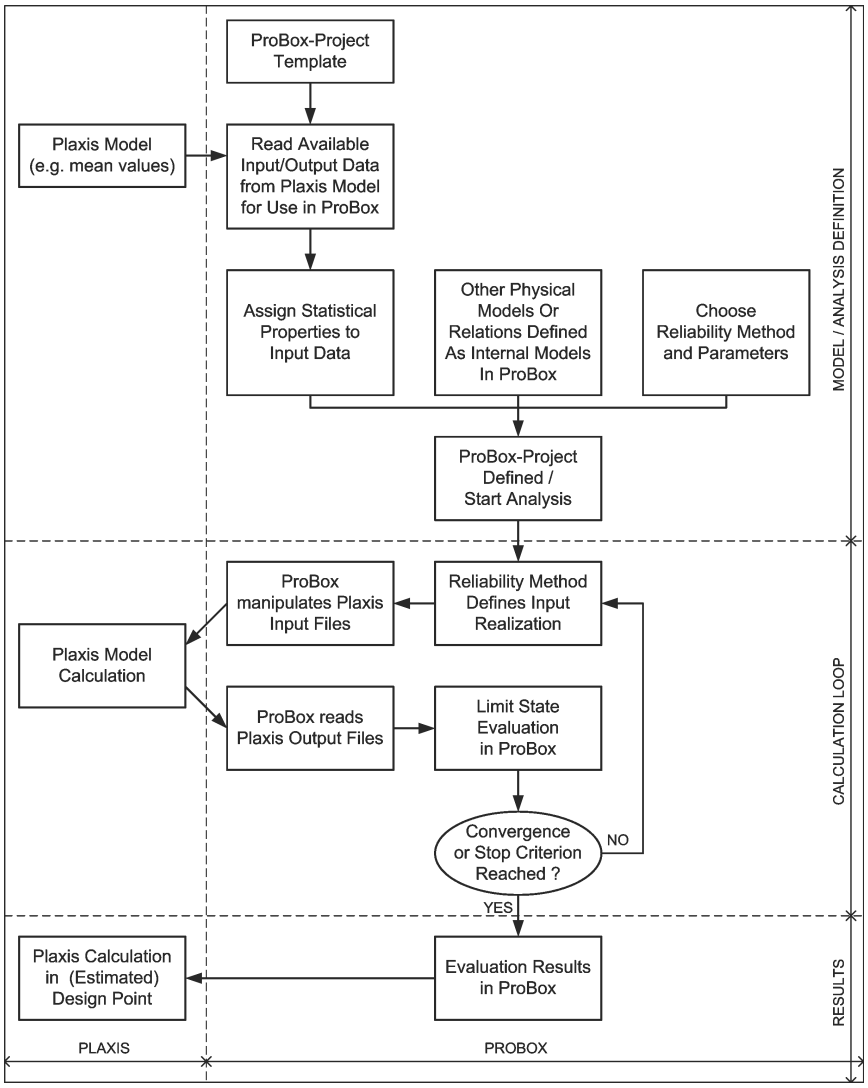

Figure 6.1: Coupling-Scheme Reliability Analysis ProBox-Plaxis

The input for each Plaxis calculation is a parameter set that is determined by the chosen reliability method. The input files are amended and the calculation is carried out. The necessary output data are extracted and the limit state function is evaluated. If the stop or convergence criterion is satisfied, the results are presented by ProBox, otherwise the new input quantities are determined and the procedure is repeated. Optionally, one can carry out a Plaxis calculation in the design point to draw conclusions about the failure mechanism(s).

The information that can be amended or read from Plaxis for the use in reliability analysis is summarized in the following sections. All this information can be either used as stochastic input, for the formulation of the limit state(s) or both.

Material Parameters

The material parameters are stored in the *.mat-files. These include the soil parameters as well as the properties of beam/plate elements[3], anchors/struts or geogrids (see table 6.1).

Table 6.1: Material Parameters In Plaxis For Use As Stochastic Variables

Category	Variable	Symbol	Unit
Soil	saturated volumetric weight	γ_{sat}	[kN/m^3]
(Mohr-Coulomb)	dry volumetric weight	γ_{unsat}	[kN/m^3]
	Young's modulus	E_{ref}	[kPa]
	Poisson ratio	ν	[-]
	angle of internal friction	ϕ'	[deg]
	cohesion	c	[kPa]
	angle of dilation	ψ	[deg]
	interface strength	R_{inter} [-]	
Plates/Beams	normal stiffness	EA	[kN/m]
	bending stiffness	EI	[kNm^2/m]
	equivalent thickness	d_{eq}	[m]
	weight	w	[kN/m^2]
	Poisson ratio	ν	[-]
	plastic bending moment	M_p	[kNm/m]
	plastic normal force	N_p	[kN/m]
Anchors	normal stiffness	EA	[kN]
	anchor spacing	a	[m]
	tensile capacity	$F_{max,tens}$	[kN]
	compressive capacity	$F_{max,comp}$	[kN]
Geogrids	normal stiffness	EA	[kN/m]
	tensile capacity	$F_{max,tens}$	[kN/m]

Load Parameters

Several load types can be handled in Plaxis and manipulated by ProBox:

- Prescribed displacements:
  Prescribed displacements for a series of nodes can be specified.

- Point Loads:
  Point loads in a 2D-plane strain environment represent line loads in the 3D-environment. The components of theses loads can be specified by their components in x- and y-direction.

- Distributed loads:
  Distributed Loads in a 2D-plane strain environment represent surface loads in the 3D-

[3]For beam/plate elements the information is stored by Plaxis in terms of properties that correspond to an equivalent rectangular cross-section. The details are explained in appendix M

environment. The components of theses loads can be specified by their components in x- and y-direction. They can be constant over their length or linearly increasing/decreasing.

Pore Pressures

The pore pressure fields can be generated in Plaxis basically in three different ways:

1. Pore pressure generation via pre-defined phreatic lines.
2. Pore pressure generation by flow-calculation.
3. User-defined pore pressures.

The generation of pore pressures is executed in the Plaxis Input module. During the automated calculations in the reliability analysis, only the Plaxis Calculation module can be used. That means that variations of the pore pressure field, e.g. for stochastically defined phreatic level, have to be carried out 'manually'. To this end a Matlab script was developed that is able to recognize the spatial coordinates of the integration points and to overwrite the pore pressure information according to a phreatic level that is defined by the reliability method in ProBox (see figure 6.2).

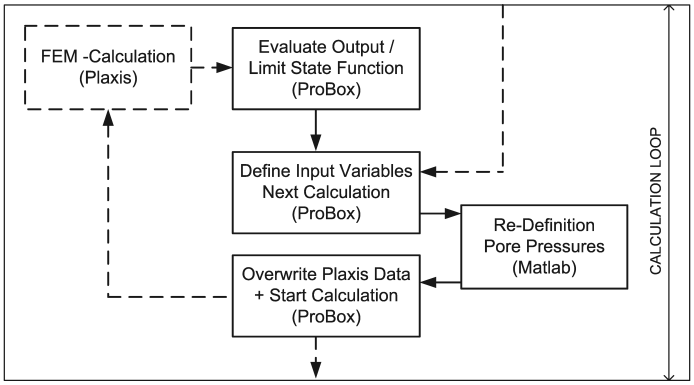

Figure 6.2: Coupling-Sub-Scheme Pore Pressure Manipulation

Note that, compared to the scheme in figure 6.1, the pore pressure field is amended before the calculation is carried out.

Calculation Information

The calculation information might be used for limit state definitions. In chapter 7.6, for example, a limit state will be defined purely on the information, if the calculation was 'successful' (equilibrium reached) or not. For more information refer to appendix F.

Nodes / Integration Points

The most important numerical results of a Finite Element analysis are the deformations of the system and the new stress state in terms of effective stresses and pore pressures. This information can be read from the calculation results in the nodes of the finite element mesh and its integration points.

The information that is stored for nodes and integration points is listed in table 6.2.

Table 6.2: Output Quantities In Nodes And Integration Points

Category	Variable	Symbol	Unit
Nodes	vertical displacements	u_y	[m]
	horizontal displacements	u_x	[m]
Integration Points	vertical normal effective stress	σ_{yy}	[kPa]
	horizontal normal effective stress	σ_{xx}	[kPa]
	out-of-plane normal effective stress	σ_{zz}	[kPa]
	shear stress	τ_{xy}	[kPa]
	active pore pressures	p	[kPa]
	excess pore pressures	p_{exc}	[kPa]
	vertical strain	ϵ_{yy}	[kPa]
	horizontal strain	ϵ_{xx}	[kPa]
	shear strain	γ_{xy}	[kPa]

Structural Elements

Plaxis uses several structural elements that can be applied for modelling typical elements of geotechnical structures. The plate elements represent the retaining walls for the presently treated excavation examples. Anchor elements can be used to represent anchors or struts and geogrids might represent the grout bodies of tie-back anchors. The internal forces/moments of these elements that are available for limit states are listed in table 6.3.

Table 6.3: Output Quantities Structural Elements

Category	Variable	Symbol	Unit
Plates/Beams	normal force	F_N	[kN/m]
	shear force	F_S	[kN/m]
	bending moment	M	[kNm/m]
Anchors	x-component normal force	$F_{a,x}$	[kN/m]
	y-component normal force	$F_{a,y}$	[kN/m]
Geogrids	x-component normal force	$F_{g,x}$	[kN/m]
	y-component normal force	$F_{g,y}$	[kN/m]

Chapter 7

Failure Mechanisms and Limit States

For structural reliability calculations a system analysis is important for defining the relevant failure modes and the setup of the analysis. In the following the relevant failure modes for typical retaining structures are identified and and their role in the system reliability is explained. Additionally it will be explained how the system reliability can be determined by either combining knowledge about the reliability of singular failure mechanisms or in a direct calculation.

7.1 System Analysis

For the system reliability analysis all the possible failure modes and mechanisms are listed up and summarized in a fault tree. Figure 7.1 on page 69 shows a fault tree that contains the most important failure modes for sheet pile supported excavations.

The unwanted top event is the failure of the retaining structure. The structure of the fault tree is similar to the one suggested in CUR 166 [8] (part II), but is slightly modified for convenience, taking the possibilities of the use of finite element analysis into account. The failure probabilities of the mechanisms indicated in green can be determined directly by reliability analysis, whereas knowing these $P_{f,i}$ the yellow ones can be deduced or approximated.

Finally, two failure probabilities have to be calculated, $P_{f,SLS}$ (failure Serviceability Limit State due to excessive displacements) and $P_{f,ULS}$ (failure Ultimate Limit State due to structural failure). Since for both there are different requirements, they will not be combined to a total failure probability. An upper limit for $P_{f,ULS}$ can be obtained by assuming that all the three contributions are uncorrelated:

$$P_{f,ULS} = P_{f,sp} + P_{f,soil} + P_{f,supp} \tag{7.1}$$

where $P_{f,sp}$ is the probability of *sheet pile failure*, $P_{f,soil}$ is the probability of *soil shear failure* and $P_{f,supp}$ is the probability of *support failure*.

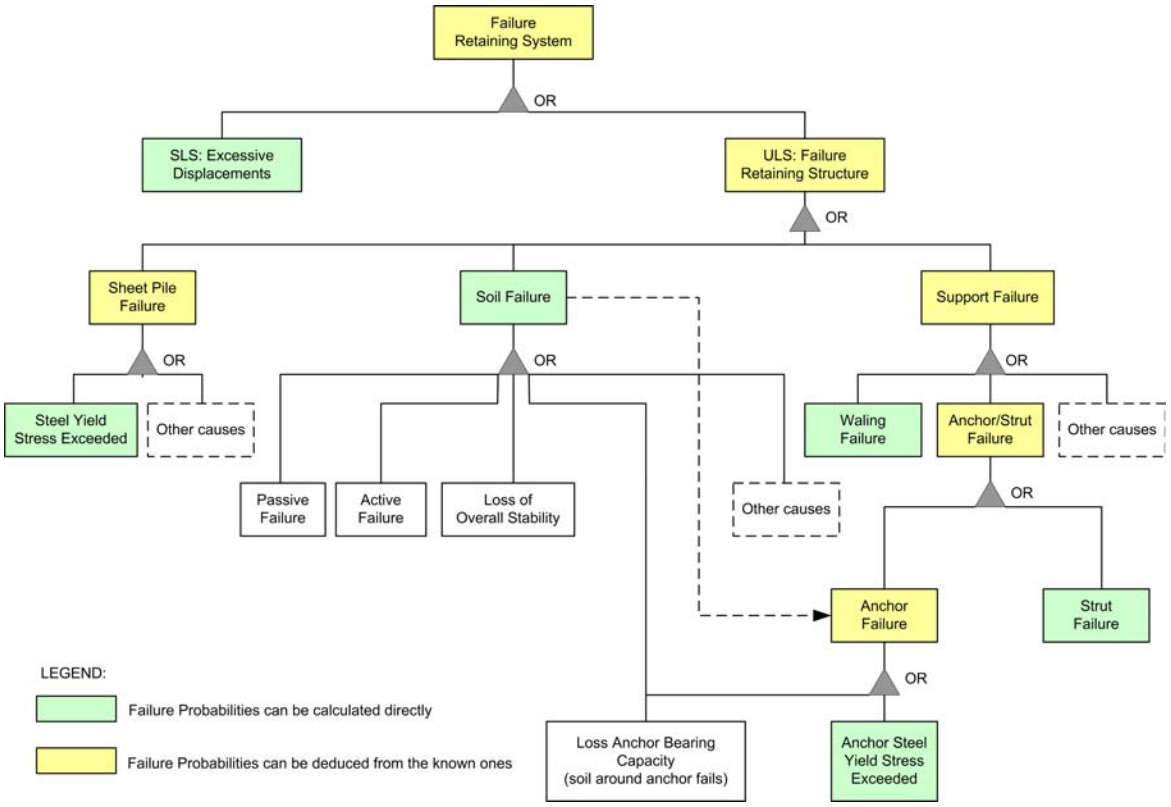

Figure 7.1: Fault-Tree for Retaining Structures using Sheet Piles

When the failure probabilities of singular failure mechanisms are known, there are methods for determining narrower lower and upper bounds or approximations of the system reliability. One method is the one introduced by 'Hohenbichler' (see appendix D) that uses the outcomes of FORM-analyses (β's and α's) for an approximation of the failure probability. Also the well known 'Ditlevsen Bounds' (see appendix E) can be applied. If all the limit states are defined at once, level III methods like DS can be applied.

7.2 Limit State Functions

This section is dedicated to the description and formulation of the limit states that are relevant for retaining structures (see chapter 7.6). The possibilities and limitations due to the the use of the coupled reliability-FEM analysis are considered.

Often the key to an efficient reliability analysis is an adequate limit state function formulation. We will distinguish between limit states for Serviceability Limit State (SLS) criteria and Ultimate Limit State (ULS) criteria. The focus in this thesis will be on ULS.

For retaining structures there are basically four classes of structural elements, as illustrated in the system fault tree in figure 7.1. For each of them the reliability respectively the probability of failure is to be determined:

- retaining walls (sheet piles, diaphragm walls etc.)
- anchors or struts
- walings
- the soil

7.2.1 What is a Limit State?

Before going into detail we will revise shortly the function respectively the definition of a limit state in the framework of reliability analysis.

Definition Limit State

> The limit state (LS) is the border between the desired state (no failure) and the undesired state (failure). The limit state itself belongs to the failure domain.

7.2.2 Limit State Function Definition

In reliability analysis Limit State Functions (LSF) are defined in order to have a mathematical expression describing the state of a mechanism or structure with respect to a limit state. We denote the limit state function as Z. It is a function of the basic random variables $\mathbf{X}$:

$$Z = f(\mathbf{X}) \tag{7.2}$$

Three cases can be distinguished:

- $Z > 0$: desired state (no failure)
- $Z = 0$: limit state
- $Z < 0$: unwanted state (failure)

As explained in chapter 4 the task of reliability analysis is to integrate the joint probability density over the failure domain ($Z < 0$) to obtain the probability of failure or its complement - the reliability.

$$P_f = \int\limits_{Z(\mathbf{X})\leq 0} f_X(x)dx \tag{7.3}$$

The techniques for solving this integration problem were discussed in detail in chapter 4. For structural reliability problems often the more illustrative description

$$Z = R - S \tag{7.4}$$

is used, where R is the resistance of a structure and S is the load. That means that failure is defined in this case as the load exceeding the resistance and in the reliability analysis the according exceedance probability is calculated.

7.3 Serviceability Limit State

The SLS (Serviceability Limit State) is checked in design calculations in order to avoid excessive deformations of a structure that could lead to the loss of functionality of the structure or indirectly cause damage to other buildings or structures.

The general formulation of this limit state, directly using the requirements that are also applicable for design calculations, would simply be to determine the exceedance probability of the maximum admissible displacements. Therefore a convenient limit state formulation would be:

$$Z = u_{adm} - u \tag{7.5}$$

where u_{adm} is the maximum admissible displacement and u is the calculated displacement. This formulation is the general form for displacement based criteria.

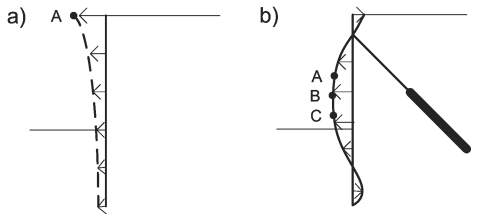

Figure 7.2: Sheet Pile Walls: a) Not Anchored b) Anchored (One Layer)

For each type of structure the determination of u requires some knowledge about the deformation behavior. Considering for example the typical sheet pile structures in figure 7.2, we know that the largest displacements for situation a) can be expected at the top of the wall in point A. So for u simply the calculated displacements in A can be used. In situation b), however, there is no point respectively node that clearly could be used as the one that determines the maximum displacements. In this case, depending on the necessary degree of accuracy one can opt for either calculating the maximum horizontal displacements of all nodes belonging to the sheet pile wall ($u = max(u_{x,i})$, where i is the node number) or, if convenient one chooses a number of relevant points like in this case A, B and C and uses the maximum calculated displacement of these ($u = max(u_{x,A}, u_{x,B}, u_{x,C})$).

In some cases the SLS-criteria are used to avoid damage to adjacent structures and to limit the influence of a construction on the surroundings. For retaining structures there are hardly any analytical relations for the effects of excavations on the surrounding soil that would allow to calculate e.g. settlements next to a sheet pile wall as a function of the distance to the wall. The Finite Element Method enables us to model these soil-structure interaction problems and therefore also damage criteria for buildings could be used directly in the coupled reliability analysis.

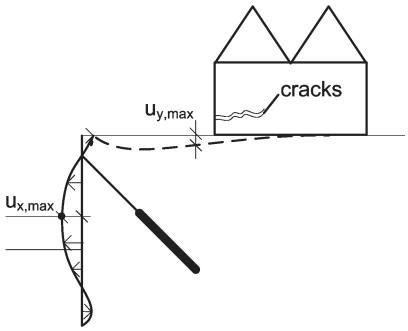

Figure 7.3: Direct Damage Criteria vs. Indirect Deformation Criteria

Figure 7.3 illustrates how the horizontal deformations of a sheet pile wall lead to settlements next to the excavation, which themselves affect an adjacent building. If the aim is to avoid damage to the building, one could consider the following criteria instead of the horizontal displacements of the retaining wall itself:

- Settlements at certain locations of the building[1].
- Stresses in the walls of the building.
- Crack widths in the walls of the building etc.

The evaluation of these criteria would require very sophisticated models and is more a question of deterministic FEM-modelling. The subject is not strictly related to reliability analysis and is therefore not treated in this thesis. It is, however, demonstrated that the use of FEM in reliability analysis has important advantages.

7.4 Ultimate Limit State for Structural Members

The Ultimate Limit State (ULS) describes structural failure respectively collapse. Convenient limit state functions will be presented for each relevant structural component.

7.4.1 Retaining Walls

Sheet Piles

The most relevant failure mode for sheet piles is the exceedance of the yield strength respectively the ultimate steel strength. Both are expressed in terms of stresses. We will focus on the description for the yield strength. The description for the ultimate strength can be developed accordingly.

[1]The critical settlements would have to be determined by a preceding damage analysis. They are thus also indirect criteria in a strict sense.

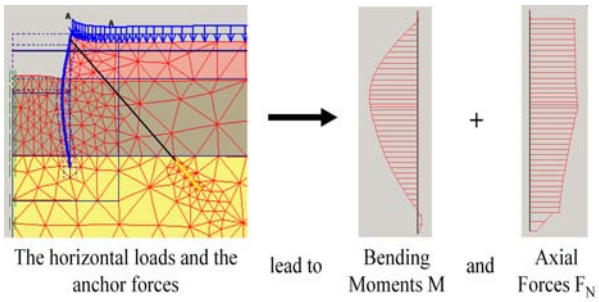

Figure 7.4: Loading of Sheet Piles

Figure 7.4 illustrates a typical loading situation for a sheet pile structure with one anchor layer. It is demonstrated by means of typical FEA-outcomes that the maximum stresses in the outer fibre of a retaining wall are composed of a bending moment and a normal force component[2]:

$$\sigma = \frac{M(z)}{W_{el}(z)} + \frac{F_n(z)}{A_{SP}(z)} \tag{7.6}$$

where W_{el} is the elastic section modulus and A_{SP} the cross-sectional area of the sheet pile.

All four quantities on the right side of the equation can be variable over depth and are therefore denoted as depth-dependent (z-direction). M and F_n can be roughly characterized as the load variables in this LSF. They are determined mainly by the soil properties. W_{el} and A_{SP} are variables representing the structural resistance. The FEM has the advantage that also second order effects are taken into account automatically, e.g. a stiffer structure will experience higher bending moments than a more flexible one. That implies that the load variables have to be determined together with the resistance variables in the same analysis and cannot be determined separately due to the mutual influence.

According to the preceding considerations the limit state function can be defined as

$$Z = \sigma_y - \sigma = \sigma_y - \left(\frac{M(z)}{W_{el}(z)} + \frac{F_n(z)}{A_{SP}(z)} \right) \tag{7.7}$$

In words, the definition of the reliability problem would be to determine the probability that the yield strength σ_y is exceeded in any point of the sheet pile wall[3]. Equation 7.7 is the general form of this definition. It can account for variations in the geometrical properties of the sheet piles over depth. That is necessary, when e.g. also corrosion of the piles is modelled in a depth-dependent manner.

[2]Vertical anchor force component reduced by interaction with soil over depth.

[3]The according Eurocodes and the CUR 166 allow the use of plastic hinges (using W_{pl}) in special cases. The limit state function can be adapted accordingly.

Usually the geometrical properties are assumed to be constant over depth. If we additionally assume the normal force contribution to the stresses to be negligible, the LSF can be reduced to

$$Z = M_d - M_{max} \tag{7.8}$$

where $M_d = W_{el} \cdot \sigma_y$ is the design moment and $M_{max} = max[M(z)]$ is the maximum calculated moment over depth. The design moment M_d is usually also available in tables by the suppliers.

Diaphragm Walls

For diaphragm walls we can use the simplified description that is also applicable for sheet piles:

$$Z = M_d - M_{max} \tag{7.9}$$

where M_d is to be determined in structural design calculations. One could also use formulations that are based on the compression strength of concrete based on concrete structural design considerations. The concrete-reinforcement interaction requires a more detailed analysis that is not treated here in detail.

7.4.2 Anchors and Struts

Anchors are loaded by their reaction to the horizontal loads on the retaining walls. An anchor can fail by failure of any of its components. We assume here that the connection between anchors and the retaining wall can be realized with little investment in a very reliable manner and thus the influence to be negligible. Also the slipping of a grout body is supposed to have a minor contribution to the failure probability and this contribution is implicitly treated in section 7.5. The focus in this section is on determining the failure probability of the steel members of anchors (tubes, bars, cables, etc.) that are loaded by traction forces (see figure 7.5).

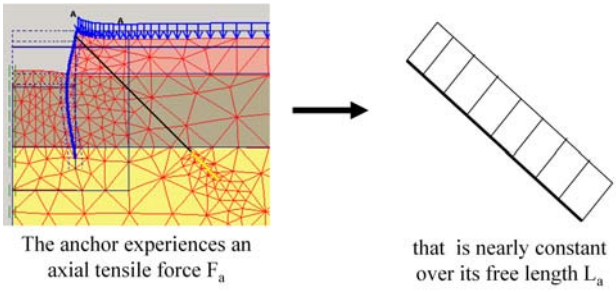

Figure 7.5: Loading of Anchors

These steel members have a certain yield or ultimate strength and can therefore be treated similarly as the sheet pile using a stress margin as limit state function:

$$Z = \sigma_y - \sigma = \sigma_y - \frac{F_a}{A_a(x,z)} \tag{7.10}$$

where F_a is the calculated anchor force and $A_a(x,z)$ is the cross sectional area of the anchor that could be spatially variable, depending on the model used.

Assuming A_a to be constant the limit state function can be reduced to:

$$Z = F_{a,d} - F_a \tag{7.11}$$

where $F_{a,d} = \sigma_y \cdot A_a$ is the design value for the anchor force.

The approach for dealing with the reliability of struts as part of the support structure is similar to the anchors. The strut force is assumed to be constant over the entire length and also in most scenarios the geometrical properties will be constant. In contrast to the anchor, the design strut force could be dominated by the buckling force instead of the maximum stresses in the steel (yield strength). For approaches to determine $F_{strut,d}$ see for example van Baars (2003) [40].

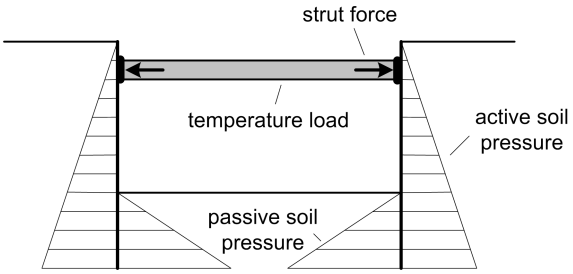

Figure 7.6: Loading of Struts

Figure 7.6 illustrates the role of a strut in the retaining system. In contrast to anchors, struts require an opposite support that is typically the opposite retaining wall. Struts are positioned horizontally and do therefore not contribute to the normal forces in the retaining wall.

Their exposure to the outside temperature and to direct sunlight combined with their limited extension in longitudinal direction lead to additional forces (temperature load). The temperature loading is difficult to account for because it is an interaction problem between the temperature induced longitudinal extension and the reaction (horizontal displacements) of the wall. A possible approach is illustrated in figure 7.7.

Then the temperature load can be approximated by:

$$\Delta F_{strut} = \frac{\alpha_T \Delta T L}{1/k + L/EA} \tag{7.12}$$

where α_T is a thermal expansion coefficient (for steel: $\alpha_T = 1.2 \cdot 10^{-5}$ $[K^{-1}]$), ΔT [K] is the temperature change and EA/L is the axial stiffness of the strut.

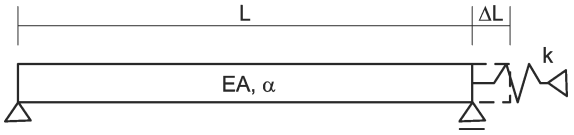

Figure 7.7: Restrained Deformation due to Temperature Differences

The determination of the spring stiffness k can be achieved by an appropriate analysis, e.g. also using FEM. Also empirical relations have been derived from measurements taking into account circumstances such as exposure to sunlight etc. Using this information, the following simplified relation can be used:

$$\Delta F_{strut} = f_T \alpha_T \Delta T L \tag{7.13}$$

where f_T is an empirical reduction factor[4]. According to Moormann [28] this factor can be reasonably assumed in a range between $0.2 \leq f_T \leq 0.4$.

The additional load can be implemented in the limit state function for struts and has therefore not to be modelled in the FEA, even though in this case the second order affects are not accounted for. A convenient limit state function would be:

$$Z = F_{strut,d} - (F_{strut} + L_{strut} \cdot f_T \alpha_T \Delta T) \tag{7.14}$$

Another possibility would be to model these temperature effects explicitly in the FEA, e.g. by introducing the additional strut force ΔF_{strut} in a second calculation loop or by prescribed displacements of the strut that simulate its elongation (in axial direction).

Temperature influences can, according to measurements carried out in recent studies (see [28]), lead to differences in the order of magnitude of 100% in the strut forces and should not be neglected. This should, however, be subject to improvements in deterministic modelling. At this stage it is solely shown that the influences can be accounted for in reliability analysis approaches.

[4]The value is usually not constant for a project and depends on the range of expected temperature differences. Also the sun exposure of the struts has an influence and low strut layers that are located in shadow areas are less influenced. These effects are neglected for the time being.

7.4.3 Walings

The waling is the element that transfers the loads from the retaining wall to the anchors or struts. The loading of walings can be schematized as a continuous beam on several supports as illustrated in figure 7.8.

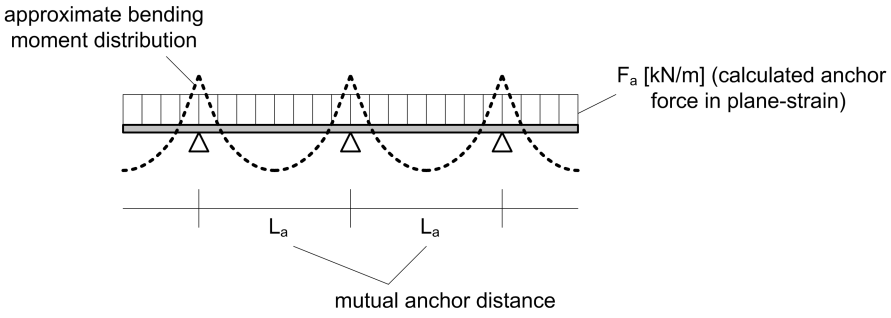

Figure 7.8: Loading of Walings

The field moment in such a beam can be approximated by:

$$M_{waling} = \frac{F_a \cdot L_a^2}{10} \tag{7.15}$$

where F_a [kN/m] is the calculated anchor force per m in z-direction.

Therefore we could formulate the limit state function as:

$$Z = M_{waling,d} - M_{waling} = M_{waling,d} - \frac{F_a \cdot L_a^2}{10} \tag{7.16}$$

where $M_{waling,d}$ is the design moment of the waling.

For a sharp design of the waling the limit state will give the same failure probability as for the anchor or strut force itself and for a conservative design the failure probability will be lower. Therefore it will normally not be necessary nor helpful to carry out this analysis. The anchor or strut failure will be the determinant mechanism.

7.5 Ultimate Limit State for Soil Shear Failure

Soil failure can usually be classified as shear failure or tension failure. There are several failure mechanisms that are related to the shear strength of the soil. Using analytical or other approximation methods (like Bishop's slip circle analysis), these can be assessed. Using FEA the 'most critical' failure mechanism is determined automatically. This is for some applications very useful, but it makes the assessment of other mechanisms impossible or at least difficult.

Some failure mechanisms for deep excavations are illustrated in figure 7.9:

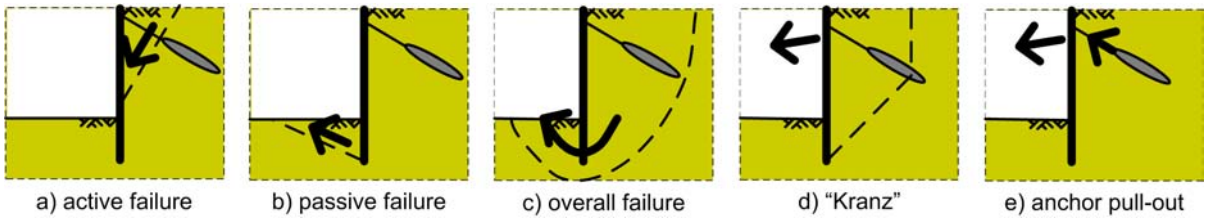

Figure 7.9: Failure Mechanisms in the Soil For Anchored Retaining Walls

Mechanism a) describes the *active failure*. Displacements of the wall towards the excavation lead to the development of active soil stresses $\sigma_{yy} = \sigma_{zz} \cdot K_a$ that are lower than the stresses in neutral position $\sigma_{yy} = \sigma_{zz} \cdot K_0$. The decrease in horizontal stresses leads at the same time to a decrease in shear strength (considering the Mohr-Coulomb failure criterion). When the shear stresses in the soil exceed the shear strength, a slip plane forms and a soil wedge collapses. The result is an increased earth pressure on the wall for which it is not designed. Furthermore, settlements next to the excavation are another undesired consequence.

In mechanism b) the passive soil resistance is exceeded by the horizontal loads. In this case the shear strength is larger due to the deformation of the wall and the horizontal stresses increase $\sigma_{yy} = \sigma_{zz} \cdot K_p$ ($K_a < K_0 < K_p$). This failure mechanism usually occurs due to a underestimation of the sheet pile length. Also a preceding active failure and the subsequent increase of the load on the wall can lead to *passive failure*.

The *overall failure*, as described in mechanism c), can occur when a slip plane occurs somewhere around the structure. The methods to check this stability are similar to slope stability analysis. Usually deeper lying weak soil layers are a potential cause of this type of failure.

Furthermore, too short anchors could cause a soil block to collapse (*'Kranz-stability'*) or the shear resistance of the soil around the anchor could be exceeded (*'anchor pull-out'*).

These failure mechanisms are certainly correlated with each other, because certain parameter combinations might trigger several of the mechanisms at once. Therefore the common failure probability would be smaller than the sum of the singular probabilities:

$$P_{f,soil} < \sum_{i=1}^{n} P_{f,i} \tag{7.17}$$

with $P_{f,soil}$ being the total failure probability for soil related mechanisms and $P_{f,i}$ being one mechanism's occurrence probability.

In the following sections it will be discussed how the total probability[5] of soil shear failure $P_{f,soil}$ can be determined and several approaches for limit state formulations will be presented. Not all of the approaches have proven to be successful, but they are mentioned in order to present the general ideas, which could be useful in similar situations and with the necessary refinements.

In all approaches the basic problem is to find a definition of failure that seems reasonable and at the same time can be quantified using the outcomes and information obtained by Finite Element Analysis.

7.5.1 Excessive Deformations

The first approach is to define structural failure, similarly to the ideas used in the SLS, by deformations that are unacceptable. Deformations respectively displacements are direct FEM-outcomes. Figure 7.10 shows some examples of displacement-based criteria that could be used to detect structural failure.

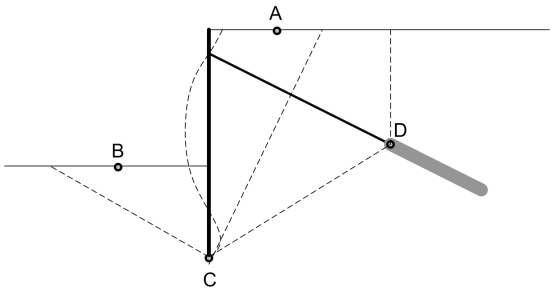

Figure 7.10: Displacement-Criteria for Structural Failure

The indicated points A, B, C and D could give a clear indication of failure. The limit state could be formulated for each point separately or 'observing' all points together:

$$Z = u_{limit} - max[|u_A|, |u_B|, |u_C|, |u_D|] \tag{7.18}$$

where the probability is calculated that the displacement of one of the selected nodes/points exceeds the limit value u_{limit}. Usually it is advantageous to define limit values for each point

[5]The separate determination of the probability for each mechanisms proved to be not feasible using FEM.

independently due to the nature of deformations that is expected. The the limit state can be rewritten as:

$$Z = min[u_{limit,A} - |u_A|, u_{limit,B} - |u_B|, u_{limit,C} - |u_C|, u_{limit,D} - |u_D|] \tag{7.19}$$

Tests with this approach exhibited several problems:

- The deformation behavior of the structure does not always show monotonous reactions of the described limit state function to monotonous changes in the soil properties. The main reason is that many of the described failure mechanisms are 'triggered' suddenly. In other words, there are no significant displacements observed before moving very close to failure. This poses problems for many iterative procedures as used e.g. in FORM or Directional Sampling.
- To obtain results in terms of nodal forces and displacements an FEM-calculation has to reach an equilibrium state. If the limit displacements are larger than the ones that can be calculated within the parameter range that leads to equilibrium, the FEA does not return results.
- A practical problem is the definition of suitable limit displacements u_{limit}. They have to be large enough to serve as failure criterion and at the same time they may not be larger than the values that can be calculated within the limits of equilibrium. This requires previous knowledge not only about the analyzed system, but also about the feasibility of calculations in FEM particularly for the analyzed problem. In some cases it could even occur that for the two conflicting requirements no suitable u_{limit} can be found.

The consequence is that even for relatively simple problems a lot of trial-and-error calculations have to be carried out, before a suitable or even feasible limit state function is defined. Furthermore, some subjectivity is included in the limit state definition. Therefore this approach is not elaborated any further in this thesis, even though for some problems it could be a good choice.

7.5.2 ϕ-C-Reduction

A method for determining a sort of safety factor that is implemented in Plaxis is the ϕ-c-reduction technique (see appendix F). This feature can also be used in reliability analysis. Again we would obtain a reliability against failure in the soil body in general, be it active, passive or overall failure. The LSF is simply:

$$Z = MSf - 1.0 \tag{7.20}$$

where MSf is the so called *Multiplier Safety Factor* obtained by the ϕ-c-reduction. A safety factor smaller than 1 ($MSF < 1$) is thus considered as failure and vice versa.

From the LSF we see that the implementation of this approach is relatively straight forward. There are, however some critical points:

- For non-linear limit states and system effects, there can be convergence problems for reliability methods with iterative procedures, especially due to the fact that the ϕ-c-reduction follows a certain path in the parameter space[6].
- The safety factor MSf can be misleading in situations where parameters, other than the soil strength properties could trigger a failure mechanism[7].
- The method can be time-consuming and the outcome can be unstable[8].

The application of this method is shown for an example in chapter 8, where it could be used successfully. The more complex problems that are treated in the case study could not be solved with this approach[9].

7.5.3 Mobilized Shear Resistance

The performance of most of the applied reliability methods depends on the failure criterion respectively the limit state function formulation. For example FORM or DS use iteration methods for determining a point on the limit state ($Z = 0$). It is therefore desirable to use a an LSF that is continuous with a monotonic and ideally linear behavior. It should give an indication for the 'distance to failure' in parameter space. The previously presented approaches did not fulfill these requirements satisfactorily.

The idea of using the mobilized shear strength can be explained from a soil mechanics point of view. Soil is a frictional material that 'fails' under *shear* or *tension* loading. One of the simplest, but still widely used yield criteria is the *Mohr-Coulomb criterion* (see appendix F). It defines the maximum shear resistance before plastic yielding occurs for any given stress state. Of course, the occurrence of plasticity is not directly failure of the structure and it will be impossible to make this indicator generic. However, for specific problem configurations, as for the retaining structures treated in this work, regions can be defined where the occurrence of plasticity and, before that, the mobilized shear resistance can be a useful indicator for the 'distance' to failure.

In fact, this approach can be seen as a classical comparison between load and strength, averaged over a pre-defined region. The difference to the classical measures is that it is based on internal loads and strength on the level of stresses in the soil continuum instead of external loads and 'overall' strength of the structure.

[6] Reduction of all soil strength properties by a common factor, see section F.2.

[7] For example the stiffness properties of the soil in deep excavations on the load side or the volumetric soil weight in uplift problems.

[8] The calculations do not always converge and the results can be dependent on the number of calculation steps.

[9] To be clear, the applicability of the 'ϕ-c-reduction' does not depend on the degree of complexity of the structure, but on other properties that should still be defined in further research.

In a plane-strain environment, the stress tensor is completely defined by:

$$\boldsymbol{\sigma} = \begin{pmatrix} \sigma_{xx} & \tau_{xy} & 0 \\ \tau_{yx} & \sigma_{yy} & 0 \\ 0 & 0 & \sigma_{zz} \end{pmatrix} \quad with\ \tau_{xy} = \tau_{yx} \tag{7.21}$$

Solving the Eigenvalue problem of this matrix we obtain:

$$\sigma_1 = \frac{\sigma_{xx} + \sigma_{yy}}{2} + \sqrt{\left(\frac{\sigma_{xx} - \sigma_{yy}}{2}\right)^2 + \tau_{xy}^2} \tag{7.22}$$

$$\sigma_2 = \sigma_{zz} \tag{7.23}$$

$$\sigma_3 = \frac{\sigma_{xx} + \sigma_{yy}}{2} - \sqrt{\left(\frac{\sigma_{xx} - \sigma_{yy}}{2}\right)^2 + \tau_{xy}^2} \tag{7.24}$$

$$\tag{7.25}$$

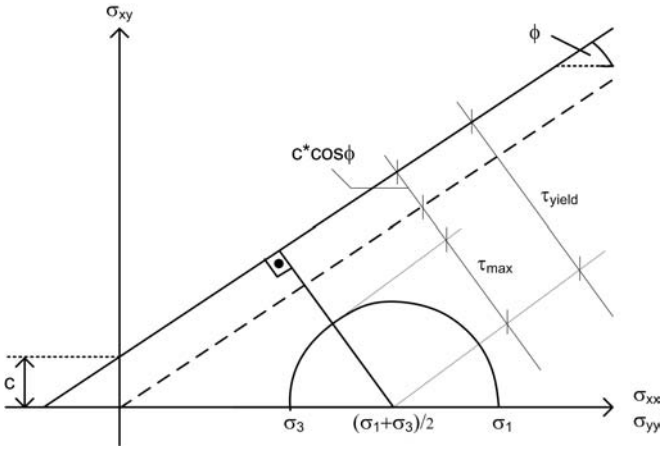

Figure 7.11: Mohr's Stress-Circle and Mohr-Coulomb Criterion

The *maximum shear stress* (radius of Mohr's Circle) is thus:

$$\tau_{max} = \sqrt{\left(\frac{\sigma_{xx} - \sigma_{yy}}{2}\right)^2 + \tau_{xy}^2} \tag{7.26}$$

And the distance of the mean stress point to the yield surface, i.e. the *shear resistance* is described by:

$$\tau_{yield} = \frac{\sigma_1 + \sigma_3}{2} \cdot sin\phi + c \cdot cos\phi = \frac{\sigma_{xx} + \sigma_{yy}}{2} \cdot sin\phi + c \cdot cos\phi \tag{7.27}$$

The *mobilized shear resistance* is thus the ratio of the two quantities[10]:

$$\tau_{mob} = \frac{\tau_{max}}{\tau_{yield}} = \frac{2\sqrt{\left(\frac{\sigma_{xx} - \sigma_{yy}}{2}\right)^2 + \tau_{xy}^2}}{(\sigma_1 + \sigma_3) \cdot sin\phi + c \cdot cos\phi} \tag{7.28}$$

[10]Attention has to be paid to the sign conventions!

The parameter τ_{mob} was presented as measure for a load-resistance ratio, i.e. an 'inverse safety factor'. It can be determined in any integration point in the soil continuum. The questions to be answered for the use this criterion are:

1. Where respectively in which integration point(s) do we have to monitor the parameter?
2. How do we combine the values of several integration points?
3. How do we determine the limit state criterion based on the monitored data?

These three problems have to be treated together and the solution applied in this thesis has been found rather by trial and error than deductive reasoning. In fact, we can only describe a procedure to find a suitable criterion, not give the LSF itself.

Coulomb's theory for **active and passive failure** of the soil also helps us to get a first idea about the according failure surfaces. In this simplified model for minimum active and maximum passive horizontal soil pressure, it is assumed that wedges are kept in equilibrium by a shear plane whose angle is $\theta_p = \frac{\pi}{4} + \frac{\phi}{2}$ for the passive wedge and $\theta_a = \frac{\pi}{4} - \frac{\phi}{2}$ for the active one (see fig. 7.12).

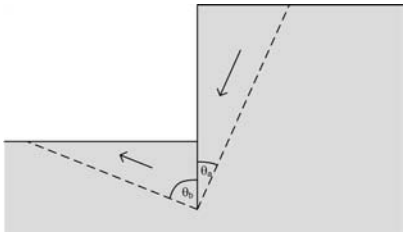

Figure 7.12: Angles of Shear Planes According To Coulomb Theory

In fact, after carrying out a 'ϕ-c-reduction' for the problem of the case study[11] in Plaxis we observe a similar behavior (see fig. 7.13).

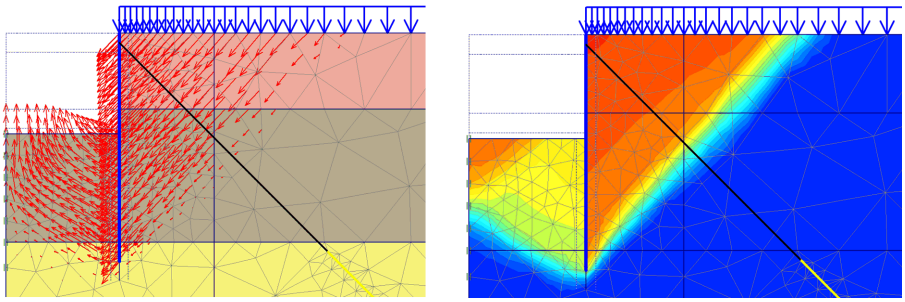

Figure 7.13: Displacement Field After ϕ-c-Reduction

[11] For a detailed description of the case study see chapter 9.

According to figure 7.13 we can expect active/passive failure as the 'most likely' failure mechanism [12]. Therefore we expect that around the clear visible shear planes the shear resistance is fully mobilized.

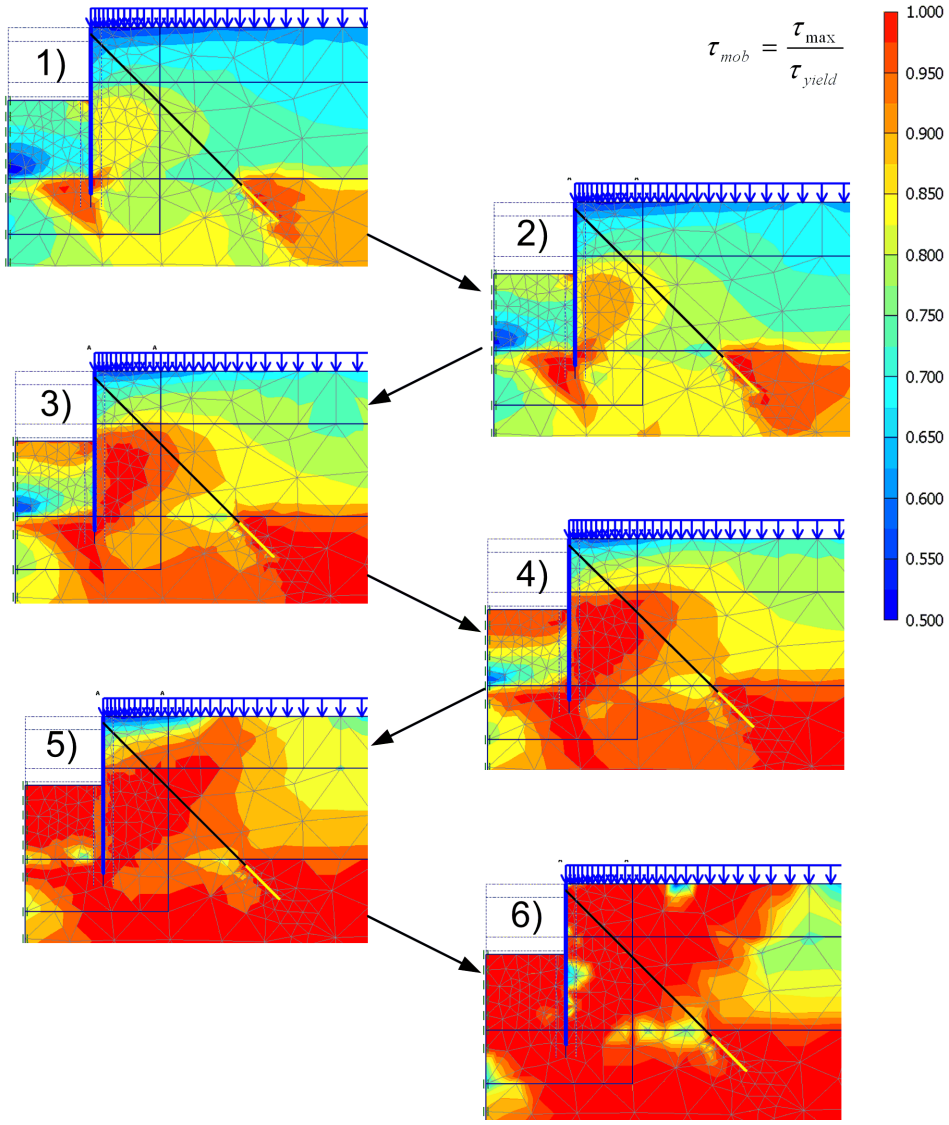

Figure 7.14: Development of Mobilized Shear Strength During ϕ-c-Reduction

Figure 7.14 illustrates the development of the mobilized shear strength around the retaining wall during a ϕ-c-reduction. The red / orange regions have a high mobilized shear strength value, or in other words less remaining shear strength. The green/yellow regions have low values of τ_{mob}. Picture 1 shows the situation in the final construction phase. Around the sheet pile wall itself we see in the sequence of pictures that an active failure mechanism is forming from

[12]The term 'most likely' is not to be interpreted in statistical sense here. It is the first mechanism that is triggered by the ϕ-c-reduction method.

the tip of the wall towards the surface under an angle that is comparable to what was defined in figure 7.12. It is also remarkable that the passive failure on the excavation side of the wall seems to follow the active failure, probably due to the increased loads on the active side.

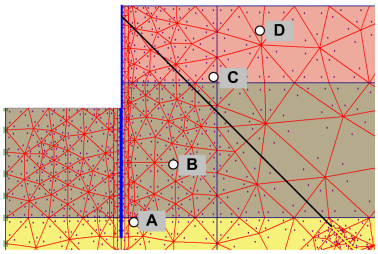

Figure 7.15: Selected Points For Mobilized Shear Strength Development

In figure 7.15 the four points A to D are indicated. These points were selected to demonstrate the development of τ_{mob} in several locations during the development of failure.

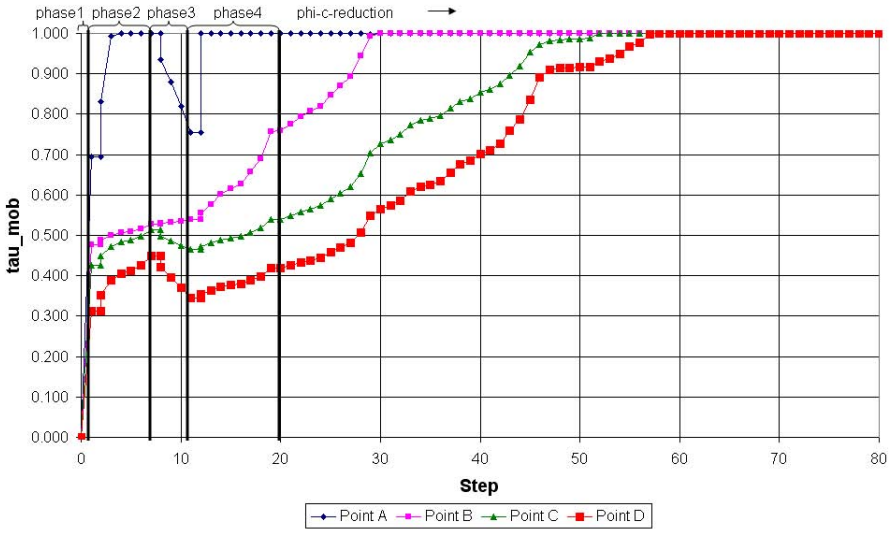

Figure 7.16: Mobilized Shear Strength During ϕ-c-Reduction

In figure 7.16 the development of τ_{mob} is shown over the calculation steps and phases[13]. The impression in figure 7.14 is confirmed that the shear resistance is mobilized from the tip of the wall towards the surface and to the right with a certain 'delay'.

[13]For detailed information see chapter 9.

We have seen the qualitative development of active / passive failure for a specific calculation example. The question remains how this information can be used in a limit state function, i.e. the **practical implementation** in the reliability analysis. Basically two variants are feasible:

1. **Single Point Observation:**
   A single point is defined for which the exceedance of a limit value $\tau_{mob,limit}$ is defined as failure. The limit state function can be formulated as:

   $$Z = \tau_{mob,limit} - \tau_{mob} \tag{7.29}$$

   where τ_{mob} is the calculated value for the mobilized shear strength in the selected point[14]. In the presented example point D could be suitable for this purpose.

2. **Cluster Observation:**
   A cluster[15] is defined for which the average value of of the mobilized shear strength $\bar{\tau}_{mob,cluster}$ is determined[16]. The exceedance of a limit value value is defined as failure and the limit state function is:

   $$Z = \tau_{mob,cluster,limit} - \bar{\tau}_{mob,cluster} \tag{7.30}$$

   where $\tau_{mob,cluster,limit}$ is the limit value for the cluster mobilized shear strength average. According to the knowledge from the analysis presented in figure 7.14 we could choose the area indicated in figure 7.17 as observed cluster for active failure.

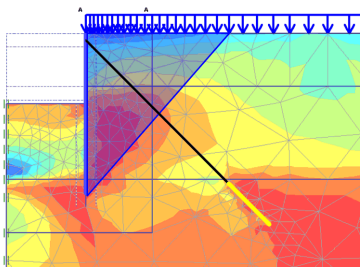

Figure 7.17: Possible Choice For Cluster Observation

We have defined an observable quantity and a way of defining the limit state function. The limit state criterion $\tau_{mob,limit}$ respectively $\tau_{mob,cluster,limit}$ is still to be determined. There might be situations, where one can be sure that the value 1 is an appropriate choice. In many cases, especially for the cluster averages however, failure might occur before the whole shear strength in the observed region is mobilized. Given that FORM can be applied to the problem in general, the scheme presented in figure 7.18 could be a solution.

[14] In case of multiple construction stages the maximum calculated value.
[15] Subset of the finite element mesh respectively the integrations points.
[16] In case of multiple construction stages the maximum calculated value.

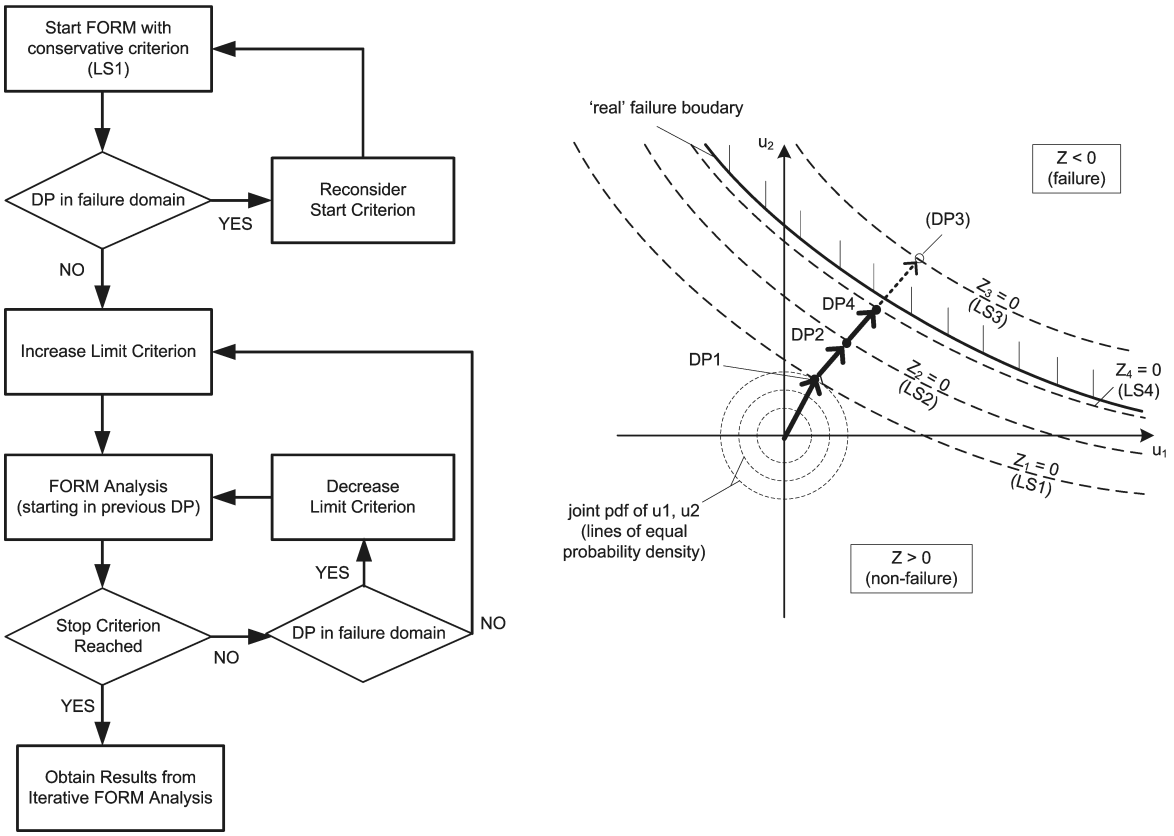

Figure 7.18: Iterative FORM Procedure For Mobilized Shear Strength Criterion

FORM can be used in an iterative way such that the limit value ($\tau_{mob,limit}$ or $\tau_{mob,cluster,limit}$) is adapted gradually according to the results of the preceding analysis. The advantage using FORM is that we do not have to carry out each analysis from the start, repeating already made calculations. Instead the starting point of an analysis can be chosen as the design point of the last successful calculation. A successful calculation is in this context, that a design point (DP) could be determined in the non-failure domain. An unsuccessful calculation would probably exhibit convergence problems, because the DP is situated in the failure domain[17].

This procedure might not give the exact solution[18] for the failure probability P_f, but it delivers a conservative estimate, because the determined design point will remain in the non-failure domain.

[17]In this case the FEA does not return results, because equilibrium is not reached in all calculation phases.
[18]Exact within the limits of linearization of the LS (FORM).

Step Plan

The described method requires previous knowledge about the problem and the limit state function cannot be defined without a thorough preceding deterministic analysis. To carry out the reliability analysis for soil shear failure with this approach, the following step plan can be followed:

1. Identify the relevant failure mechanisms (as e.g. in figure 7.9).
2. Investigate the failure development in terms of τ_{mob}.
3. Define suitable integration points or clusters for the observation of τ_{mob}.
4. Define a suitable limit state criterion (function) for the analyzed mechanisms, if necessary using an iterative procedure (as described e.g. using FORM).

Remarks

- The results of the procedure depend highly on the quality of the deterministic analysis and the identification of the relevant failure mechanisms. If other mechanisms than the expected ones play a role or the failure development is different, the results are questionable.
- For certain failure mechanisms, no results will be obtained. Before the calculation reaches the parameter space of interest, another failure mechanism can occur and no equilibrium is reached. In fact, only the failure probability of the 'most likely' mechanism can be calculated and has to be used as an estimate for $P_{f,soil}$ (lower bound).
- The procedure was discussed for active/passive failure. It can be applied also to other failure types accordingly (e.g. anchor pull-out).
- The method requires previous knowledge and certainly several attempts to obtain a reliable result. It is therefore not generic.
- In more complex problems it might be impossible to make a reasonably complete inventory of failure mechanisms. In that case a more robust and generic measure is needed. Such an approach is presented in the next section.

7.5.4 Limit Equilibrium

From the previous section can be concluded that there is a need for a robust and generic criterion for reliability analysis of soil shear failure mechanisms. In this section an approach that uses the *limit equilibrium concept* is presented. As a matter of fact this concept is also used in some deterministic approaches, e.g.:

- The earlier treated ϕ-c-reduction technique (see appendix F) uses the same criterion to determine the value MSf.
- In the CUR 166 [8] in chapter 4 (design of sheet pile walls using FEM) the criterion is used to determine wether the sheet pile wall is long enough. The practical implementation is that, if using design values all calculation phases reach equilibrium, the safety against passive failure is sufficient.

Generalizing these ideas, the following can be assumed:

- If a parameter combination / realization leads to equilibrium in all phases, the state of the structure/mechanism can be classified as *not failed* $\rightarrow Z > 0$ (non-failure domain).
- If equilibrium is not reached in one or more phases, the state of the structure/mechanism can be classified as *failed* $\rightarrow Z < 0$ (failure domain).

Using this definition, the reliability problem is the classical integration of the joint probability density of the basic random variables over the failure domain to obtain the probability of failure or vice versa:

$$P_f = \int_{Z(\mathbf{X})\leq 0} f_X(x)dx \tag{7.31}$$

Of course this problem could be solved by 'brute force' using Crude Monte Carlo. However, the calculation effort can be reduced by using more advanced techniques. The presented approach uses Directional Sampling for this purpose. The nature of the analyzed binary limit state function (the only possible results are: *failed* $\leftrightarrow$ *not failed*) required some amendments in the iterative procedure.

To understand the following description we need to define the concept of the *limit equilibrium*:

> The limit equilibrium is the hyperplane in parameter space (basic random variable space) which describes the parameters sets that are on the border of leading to a failed and a not failed FEM-calculation, where failure is defined as not reaching equilibrium and vice versa.

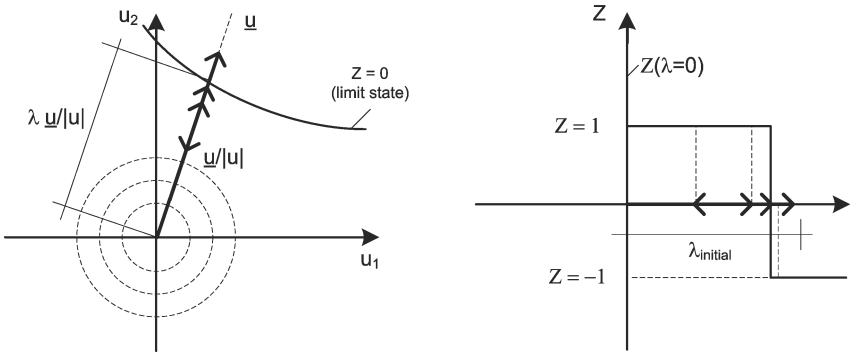

Figure 7.19: Directional Sampling For Binary Limit State Function

The application of Directional Sampling to such a binary limit state function is described in figure 7.19. In general it is advantageous to use iterative procedures that make use of the information about the gradient of the response (LSF) to determine the length λ (see section 4.4.4). In this case however, we lack information about the magnitude of the response. The only information available is whether the LSF is positive or negative. In this case, as indicated in figure 7.19 on the right-hand side, the choice was to use $Z = 1$ for not failed and $Z = -1$ for failed results. Obviously no partial derivatives can be determined from this information.

The iteration procedure for determining λ is:

1. Evaluation (FEM-calculation) in the origin of the standard normal parameter space[19] (*u-space*).

2. Evaluation in λ_{ini} (maximum length, for larger λ the contribution of the direction to the failure probability is negligible: $P_i = 1 - \chi^2(\lambda_i^2, n)) \ll P_f$).

3. If $Z = 1$, calculate the next direction. / If $Z = -1$, start iteration process using the midsection method. The precision of λ can be controlled by the number of iteration steps. The vector length λ_i that determines the parameter combination for an iteration step is determined by:

$$\lambda_j = \frac{1}{2}\left(max[\lambda_i | Z > 0 \wedge 1 \leq i \leq j-1] + min[\lambda_i | Z < 0 \wedge 1 \leq i \leq j-1]\right) \tag{7.32}$$

   (The midpoint between the maximum calculated λ_i where equilibrium was reached and the minimum λ_i that lead to failure.)

4. Calculate the next direction.

The rest of the Directional Sampling procedure is carried out in the standard manner (see 4.4.4) and thus the probability of failure can be determined. For the problems that were analyzed for this thesis, this approach proved to be more robust and reliable than the other approaches.

[19] Median Values for all basic random variables.

The advantages, limitations and other aspects of this approach are:

- The presented approach accounts for non-linearities and system effects using a level III method (Directional Sampling).
- The method is robust and not sensitive to non-linearities in the response due to its binary limit state function.
- For further use of the results in the system reliability analysis it must be considered that for level III methods like DS (no linearization) equivalent influence factors α_i are determined, the quality of which is uncertain with respect to the use in concepts such as Hohenbichler. Further research is necessary for the quality of the equivalent α_i used in first-order system reliability concepts.
- In fact, the ϕ-c-reduction technique can be seen as a special case of directional sampling. The reduction of the strength properties with a common factor MSf can be considered as one direction in parameter space. This illustrates also the considerable advantages of the presented approach. Not only the strength properties, but also stiffness parameters and volumetric weights are varied. The statistical properties of the parameters as well as correlations can be accounted for.
- It is expected that the performance of the method in terms of calculation effort can be improved considerably using the information on important and less important directions that is already available during the calculation process. Similarly to the response surface that is used in DARS (see 4.4.5), a fit-function could be used to predict the vector length λ_i as function of the direction. Due to time reasons this improvement could not be implemented during this thesis work.

7.6 System Reliability

As mentioned in section 7.1, the system reliability can be determined respectively approximated in different ways. Subsequently two suggestions are discussed.

7.6.1 System Reliability by Using First-Order Reliability Results

If the influence coefficients [20] α_{ij} and reliability indices β_i of each of the e.g. three dominant failure ($i = 1, 2, 3$) modes are known, a better estimate of $P_{f,ULS}$ can be obtained by applying the theory presented by Hochenbichler in 1983 [20][21]. Basically this method enables us to determine the failure probability of a parallel system:

$$P_f = P(Z_1 < 0 \cap Z_2 < 0) \tag{7.33}$$

This makes also the determination of serial system failure probabilities possible:

$$P_f = P(Z_1 < 0 \cup Z_2 < 0) = P(Z_1 < 0) + P(Z_2 < 0) - P(Z_1 < 0 \cap Z_2 < 0) \tag{7.34}$$

The procedure for calculating the failure probability of a serial (sub)system with two elements can be summarized as:

1. Perform reliability analysis on each mechanism i to obtain $P_{f,i}$ respectively β_i and α_{ij} (i=1,2 ; j=number of random variables).
2. Determine $P_f = P(Z_1 < 0 \cap Z_2 < 0)$ (parallel system failure probability).
3. Determine $P_f = P(Z_1 < 0 \cup Z_2 < 0) = P(Z_1 < 0) + P(Z_2 < 0) - P(Z_1 < 0 \cap Z_2 < 0)$ (serial system failure probability).
4. Determine the equivalent influence coefficients α_j^e for the (sub)system.

The last step in this calculation procedure is usually only necessary, if the equivalent influence coefficients are needed for further calculations. The calculation procedure can be applied to an arbitrary number of limit states. Then the limits are joined one by one in couples of two successively as indicated in figure 7.20.

In principle the elements can be joined in an arbitrary order, even though it is recommended to join always the two mechanisms with the highest mutual correlation (see appendix D).

[20] Remark: The definition of the influence coefficients α is only meaningful and well defined in the context of first-order (linearization) concepts. It is common practice to calculate also equivalent α-values in other reliability methods (e.g. level III). If these equivalent approximations are used, one has to be aware of the way these have been determined and the consequences for the use in the presented concept.

[21] The method of Hohenbichler is explained in detail in appendix D.

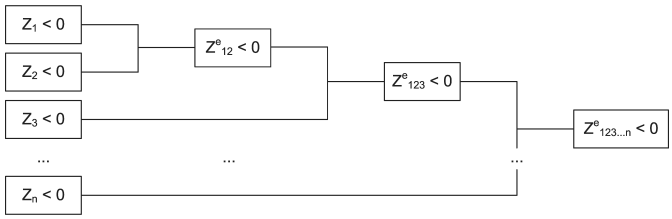

Figure 7.20: Successive Determination of System Failure Probability with Hohenbichler

7.6.2 System Reliability for Multiple Failure Mechanisms

In section 7.5.4 the use of Directional Sampling in combination with the Limit Equilibrium concept is described. In principle this method can also be applied to a problem with multiple limit states.

The analyzed system can be defined as a serial system with three major components. That means that the system failure probability is obtained by determining:

$$P_f = P(Z_1 < 0 \cup Z_2 < 0 \cup Z_3 < 0) \tag{7.35}$$

The same result can be obtained with the expression:

$$P_f = P(min[Z_1, Z_2, Z_3] < 0) \tag{7.36}$$

This fact can be used for the definition of a common limit state function that includes all three major failure criteria in one formula. The general version of this LSF would be:

$$Z = min[Z_1, Z_2, Z_3] \tag{7.37}$$

For the adapted iterative procedures presented in section 7.5.4 it is advantageous to use a binary limit state, such as:

- $Z_i = 1$ for non-failure ($Z_i > 0$)
- $Z_i = -1$ for failure ($Z_i < 0$)

If all three limit states ($i = 1, ..., 3$) are defined accordingly, it is also avoided that the iterative procedure is influenced by differences in order of magnitude of the limit state functions values.

Using the described LSF and a level III method such as Crude Monte Carlo or Directional Sampling[22] the system failure probability can be determined in a single reliability analysis.

[22]Directional Sampling can only be used with iterative procedures for the determination of λ_i that do not use the gradients of the limit state function. For more information see section 7.5.4.

Part III

Examples and Case Study

Chapter 8

Simple Calculation Examples

In this chapter the application of reliability methods to problems of structural mechanics or geotechnics using finite element methods is illustrated with a few calculation examples. We begin with a very simple example of a beam on two supports, followed by the classical Brinch-Hansen bearing capacity problem and a simple excavation with a sheet pile wall.

8.1 Example 1 - Elastic Beam On Two Supports

The first example is the classical linear elastic beam on two supports, loaded by a vertical point load acting in the center of the beam. The exceedance probability of a maximum admissible displacement u_{max} is to be determined. The results of the analytical solution are compared with results obtained using an FEM-model.

8.1.1 Geometry and Material Properties

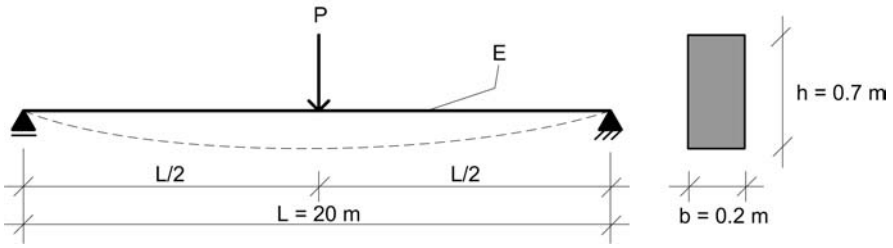

Figure 8.1: Elastic Beam On Two Supports

The spacing between the supports is $L = 20$ $[m]$. The cross sectional area of the beam is $A = 0.2 \cdot 0.7 = 0.14$ $[m^2]$ and the moment of inertia is $I = \frac{0.2 \cdot 0.7^3}{12} = 0.00572$ $[m^4]$. The load $P \sim N(100/20)$ $[kN]$ is uncertain and described with a normal distribution. The stiffness parameters for the linear elastic model are assumed to be typical concrete values. The Young's modulus $E =\sim N(30 \cdot 10^6/3 \cdot 10^6)$ $[kPa]$ is assumed to be normally distributed, whereas the Poisson's ratio is treated deterministically with $\nu = 0.15$ $[-]$.

8.1.2 Limit State

The deflections of the beam in vertical direction u_y may not exceed the admissible value u_{max}. Thus, the limit state function can be written as:

$$Z = u_{max} - u_y \tag{8.1}$$

As value for u_{max} often a fraction of the span length is handled. We arbitrarily choose $u_{max} = L/100$ as maximum deflection criterion.

The beam example is used to compare the results of different reliability methods for a problem where the exact solution is known:

$$u_y = \frac{PL^3}{48EI} \tag{8.2}$$

For some calculation methods it can make a difference, how the LSF is defined. For FORM, for example, it is advantageous to formulate the limit state as linear as possible in the most influential basic random variables. For the present problem the following expressions are equivalent:

$$Z = \frac{L}{100} - \frac{PL^3}{48EI} \;\Leftrightarrow\; Z = 0.48EI - PL^2 \tag{8.3}$$

8.1.3 Results with Analytical Solution

There are two basic random variables that are considered to be uncertain in this example, P and E. The geometry is considered deterministic. The analytical solution is also used to illustrate the efficiency of the different reliability methods.

FORM

The second formulation of the LSF in equation 8.3 has the advantage of being linear in both basic random variables. Additionally, these are normally distributed, which enables us to even find the solution with the FORM-algorithm analytically and *'by hand'* in one step:

1. Mean value calculation:
   $\mu_Z = 0.48\hat{E}I - \hat{P}L^2 = 0.48 \cdot 3E + 7 \cdot 0.00572 - 100 \cdot 20^2 = 42,368$
2. Partial derivatives:
   $\frac{\partial Z}{\partial P} = -L^2 = -400$ and $\frac{\partial Z}{\partial E} = 0.48 \cdot I = 0.00275$
3. Standard deviation of LSF:
   $\sigma_Z = \sqrt{\sum_{i=1}^{n} \left(\frac{\partial X_i^*}{\partial X_i}\sigma_{X_i}\right)^2} = \sqrt{(-400 \cdot 20)^2 + (0.00275 \cdot 3 \cdot 10^6)^2} = 11,492$
4. Reliability index: $\beta = \frac{\mu_Z}{\sigma_Z} = \frac{42,368}{11,492} \approx 3.69$
5. Probability of Failure: $P_f = \Phi^{-1}(-\beta) = \Phi^{-1}(-3.69) = 1.1 \cdot 10^{-4}$
6. Influence factors:
   $\alpha_P = \frac{\partial Z}{\partial P} \cdot \sigma_P/\sigma_Z = -0.71$
   $\alpha_E = \frac{\partial Z}{\partial E} \cdot \sigma_E/\sigma_Z = +0.70$

Considering the properties of the FORM-method (see section 4.4.1), this solution is exact and serves as reference. Evaluating the LSF in equation 8.3 in ProBox leads to the same answer, for both LSF-formulations. In terms of calculation effort the second formulation (linear in both random variables) performs better (13 LSFE for LSF type I / 7 LSFE for LSF type II).

Number of calculations (FORM) : 13

Beta : 3.691E000
P_f : 1.117E-04

	Model	Parameter	alfa	X
1	Variable	A	0.000E00	1.400E-01
2	Variable	E	7.030E-01	2.222E007
3	Variable	I	0.000E00	5.720E-03
4	Variable	L	0.000E00	2.000E001
5	Variable	P	-7.111E-01	1.525E002

	z-value
1	1.057E-01
13	-1.613E-05

Table 8.1: ProBox Results for Beam Problem with FORM

When only either P or E are treated as stochastic quantities[1], we obtain the following results:

- P stochastic: $\beta = 5.30$ (LSFE in FORM: 5 with LSF type I / 5 with LSF type II)
- E stochastic: $\beta = 5.14$ (LSFE in FORM: 11 with LSF type I / 5 with LSF type II)

Of course, the reduction of uncertainty leads to an increase in reliability. Note that the used FORM algorithm again performs better for the second formulation of the LSF.

SORM

We know beforehand that the problem is linear in the basic random variables and expect therefore no changes in the results. Table 8.2 confirms that the result is identical. The same holds, when only one variable is stochastic, either E or P.

Number of calculations (SORM) : 66

Beta : 3.691E000
P_f : 1.117E-04

	Model	Parameter	alfa	X
1	Variable	A	0.000E00	1.400E-01
2	Variable	E	7.029E-01	2.222E007
3	Variable	I	0.000E00	5.720E-03
4	Variable	L	0.000E00	2.000E001
5	Variable	P	-7.113E-01	1.525E002

	z-value
1	1.057E-01
66	-1.984E-05

Table 8.2: ProBox Results for Beam Problem with SORM

[1]The other one is treated as deterministic value. The expectation μ_X is used in this case.

PEM

The Point Estimate Method is not implemented in ProBox. A spreadsheet has been developed on basis of the variant Zhou-Nowak (see section 4.4.3). The detailed input and the results of the calculations can be found in appendix G.

It turns out that, if the LSF is a linear combination of normally distributed random variables, the assumption of a normally distributed response function leads to correct answers. This is to be expected, since the sum of normally distributed variables is always normally distributed itself. For the expression $u_y = \frac{PL^3}{48EI}$ this is not the case. The response is inverse proportional in E and therefore its distribution can only be approximated, e.g. by choosing a distribution based on goodness-of-fit tests. The results in table 8.3 show that assuming a (two-parametric) lognormal distribution does not lead to correct answers.

Table 8.3: Summary PEM Results for Example 1 (analytical solution)

		Z ∼ N		R ∼ N		R ∼ LN			
RV	LSF	β	P_f	β	P_f	β	P_f	exact β	exact P_f
P and E	1	4.60	2.1 E-6	4.60	2.1 E-6	1.28	1.0 E-1	3.69	1.1 E-4
P and E	2	3.69	1.1 E-4	—	—	—	—	3.69	1.1 E-4
P	1	5.30	5.9 E-8	5.30	5.9 E-8	1.30	9.6 E-2	5.30	5.9 E-8
P	2	5.30	5.9 E-8	—	—	—	—	5.30	5.9 E-8
E	1	10.0	3.6 E-24	n.r.	n.r.	n.r.	n.r.	5.14	1.4 E-7
E	2	5.14	1.4 E-7	—	—	—	—	5.14	1.4 E-7

Table 8.3 shows for different combinations of stochastic variables the results for the following assumptions: 1. normally distributed LSF, 2. normally distributed response and 3. lognormally distributed response. LSF 1 is the first version of the limit state function in equation 8.3, whereas LSF 2 is the second one which is linear in the random variables.

A disadvantage of PEM is that the influence factors of the random variables (α_i) are not assessed during the calculation like e.g. in FORM.

DARS

DARS calculates the correct result with about 600 LSF-evaluations for LSF 1 and about 300 LSF-evaluations for the linear versions (LSF 2).

```
Number of calculations (DARS Directional Adaptive Response Surface sampling)  : 337

Beta  :  3.693E000
P_f   :  1.108E-04

          Model        Parameter           alfa              X
 1      Variable                A       0.000E00       1.400E-01
 2      Variable                E       7.283E-01      2.193E007
 3      Variable                I       0.000E00       5.720E-03
 4      Variable                L       0.000E00       2.000E001
 5      Variable                P      -6.852E-01      1.506E002
```

Table 8.4: ProBox Results for Beam Problem with DARS (LSF2)

Crude MC

For Crude Monte Carlo we apply the convergence criterion that the variation coefficient of P_f must be smaller than 10%. We can use the following formula for estimating the necessary number of samples (see [45]):

$$N > \frac{1}{COV(P_f)^2}\left(\frac{1}{P_f} - 1\right) \tag{8.4}$$

For the given situation our number of realizations should thus be larger than $9.1E+5$, thus about 1 million. The number of calculations after which we reach this criterion in the simulations varies considerably, but is in the expected order of magnitude. It should be noted that also the approximations[2] for α_i used in ProBox are close to the exact values.

Number of calculations (Crude Monte Carlo) : 885015

Beta : 3.688E000
P_f : 1.130E-04

	Model	Parameter	alfa	X
1	Variable	A	0.000E00	1.400E-01
2	Variable	E	6.929E-01	2.233E007
3	Variable	I	0.000E00	5.720E-03
4	Variable	L	0.000E00	2.000E001
5	Variable	P	-7.210E-01	1.532E002

Table 8.5: ProBox Results for Beam Problem with Crude MC

DS

Directional Sampling gives the correct answer within the same accuracy criteria as for Crude MC within a range of about 1000 to 2000 LSFE-evaluations. The efficiency is thus more than a factor 500 higher than Crude MC for this example.

Number of calculations (Directional Sampling) : 1536

Beta : 3.668E000
P_f : 1.221E-04

	Model	Parameter	alfa	X
1	Variable	A	0.000E00	1.400E-01
2	Variable	E	7.210E-01	2.207E007
3	Variable	I	0.000E00	5.720E-03
4	Variable	L	0.000E00	2.000E001
5	Variable	P	-6.927E-01	1.508E002

Table 8.6: ProBox Results for Beam Problem with DS

[2]The influence coefficients α_i are in principle strictly connected to the linearization principles in FORM. Their magnitude is, however, very useful for e.g optimization tasks. Therefore it is common to determine 'equivalent' influence factors also from the results of other reliability methods. For the Monte-Carlo methods presented in this work, the design point is always defined as the point on $Z = 0$ with the highest probability density. The α_i are determined assuming that the limit state is orthogonal to the vector between the origin of the parameter space and the design point.

IVS

The performance of Increased Variance Sampling depends highly on the factor with which the variance is increased. In this example a factor 3 was applied. The number of LSF-evaluations is in the range of about 15,000 to 20,000. The improvement in efficiency compared to Crude MC is about a factor 50.

Number of calculations (Increased Variance) : 16693

Beta : 3.674E000
P_f : 1.194E-04

	Model	Parameter	alfa	X
1	Variable	A	0.000E00	1.400E-01
2	Variable	E	7.384E-01	2.186E007
3	Variable	I	0.000E00	5.720E-03
4	Variable	L	0.000E00	2.000E001
5	Variable	P	-6.744E-01	1.496E002

Table 8.7: ProBox Results for Beam Problem with IVS

8.1.4 Results with Finite Element Analysis

Since the programme Plaxis is developed for geotechnical applications, it does not handle one-dimensional problems and for the simple beam a work-around in a 2d-plane strain environment was used. Due to these modelling aspects the results were not 100% equal to the ones found with the analytical solution, but within acceptable limits.

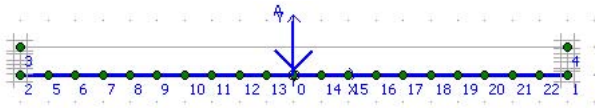

Figure 8.2: Plaxis Model For Beam On Two Supports

Naturally we expect the results obtained with the help of Finite Element Analysis (FEA) to be congruent with the ones from the analytical solution (within reasonable limits of accuracy). Nevertheless we have to deal with an *implicit limit state formulation* now. Each evaluation is the result of a *black box* calculation and derivatives or roots can only be determined numerically. The following calculations illustrate that in general handling of implicit limit states is feasible with the coupling between ProBox and Plaxis and are carried out treating P and E as stochastic variables.

FORM / SORM

FORM and SORM both return the correct solution (considering the systematic model error). Both need more LSFE compared to the analytical formula.

Number of calculations (FORM) : 13

Beta : 3.793E000
P_f : 7.439E-05

	Model	Parameter	alfa	X
1	plaxis	Fy A239 phasel	7.037E-01	-7.669E002
2	plaxis	G beam	7.105E-01	9.526E006

	z-value
1	1.104E-01
13	-3.472E-05

Table 8.8: ProBox Results for Beam Problem with FORM using FEM

PEM

The PEM calculations are not repeated with the FEM model. The results would be exactly the same as for the first version of the LSF in the analytical section, since the method is not altered. At this point it becomes obvious that one of the disadvantages for PEM in combination with implicit limit state functions like FEA is that we do not know how a variable influences the results and we cannot use tricks like re-formulating the LSF as in the explicit case. Therefore the tested version of PEM would not even be suitable for the simple beam problem.

DARS

DARS also finds the 'correct' solution and seems to be indifferent to small scale numerical instabilities.

Number of calculations (DARS Directional Adaptive Response Surface sampling) : 723

Beta : 3.802E000
P_f : 7.166E-05

	Model	Parameter	alfa	X
1	plaxis	Fy A239 phasel	6.995E-01	-7.660E002
2	plaxis	G beam	7.144E-01	9.498E006

	z-value
1	1.047E-01
723	-3.752E-04

Table 8.9: ProBox Results for Beam Problem with DARS using FEA

The reliability methods with lower efficiency are not calculated using the finite element model due to time restrictions. Consider that even for a LSFE time (basically the duration of the Plaxis calculation) of 10 seconds, a Monte Carlo Simulation with one million LSFE would take more than 115 days!

8.1.5 Conclusions

From the first simple beam example the following conclusions can be drawn:

1. Analytical Solution:

   - For explicit analytical expressions it is worthwhile to transform the limit state function in a way that it is as close to linear as possible in the basic random variables. Some of the reliability methods perform significantly better this way (especially FORM, SORM).
   - The Point Estimate Method even exhibits erroneous results for LSF that are non-linearly dependent on the basic variables. A possible improvement could be the use of the third central moment (skewness) in order to achieve a better fit of the response distribution using for example a three-parametric log-normal distribution for improving the tail fit.
   - DARS gives the correct answer, but it is not as efficient as the level II methods for this simple example.
   - Crude Monte Carlo needs a high number of LSF-evaluations to reach the convergence criterion $COV(P_f) = 0.1$. For problems with low failure probabilities it is not attractive in combination with sophisticated models (e.g. FEM) due to the excessive calculation effort.
   - The efficiency of Crude MC or IVS might be less sensitive for changes in the type of problem or the number of random variables, but even for this simple problem and a typical value of P_f they need too many LSF-evaluations. DS is more efficient and the use of response surfaces in DARS even improves the efficiency.

2. Finite Element Analysis:

   - Crude Monte Carlo is already too time consuming for this type of problem, where one LSF-evaluation takes about 10 sec.
   - FORM and SORM perform efficiently on this type of simple problem.
   - PEM exhibits problems especially with implicit LSF as described above.
   - DARS has proven to find the correct answer with high efficiency considering that it is a level III method. It will be increasingly attractive for more irregular or non-linear problems.

8.2 Example 2 - Foundation Bearing Capacity

This example treats the classical Brinch-Hansen bearing capacity problem. It is not directly related to deep excavations, but it gives insight into the presented limit state formulations to cope with soil shear failure. The bearing capacity that is calculated with the analytical Brinch-Hansen formula is compared with the reliability results obtained by an FEM model.

Geometry and Material Properties

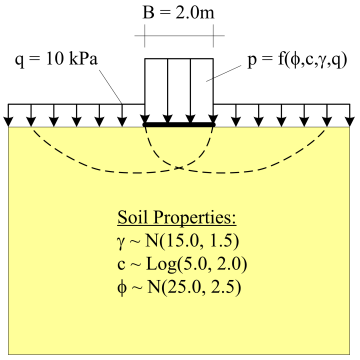

Figure 8.3: Calculation Example: Foundation Bearing Capacity

8.2.1 The Brinch-Hansen Formula

For infinitely long strip foundations an approximation of the bearing capacity p was developed by Brinch-Hansen. It is an extension of a more general version by Prandtl. The version presented here accounts for the friction angle ϕ, the cohesion c, the volumetric weight of the soil γ and a uniform surcharge load q as well as for the width of the foundation strip B.

$$p = cN_c + qN_q + \frac{1}{2}\gamma B N_\gamma \tag{8.5}$$

The dimensionless coefficients N_c, N_q and N_γ are defined as:

$$N_q = \frac{1 + sin\phi}{1 - sin\phi} e^{\pi tan\phi} \tag{8.6}$$

$$N_c = (N_q - 1)cot\phi \tag{8.7}$$

$$N_\gamma = 2(N_q - 1)tan\phi \tag{8.8}$$

That means that for any realization of the soil properties ϕ, c and γ a unique solution for the bearing capacity p can be determined (within the physically possible parameter ranges).

Given the distributions of the soil properties in figure 8.3 and using a safety factor of $\gamma_m = 1.25$ for the strength properties of the soil we obtain results for the expected, characteristic (95 %-limits) and design value with the Brinch-Hansen formula (see table 8.10).

Table 8.10: Deterministic Results With Brinch-Hansen

Mean Values							—	
ϕ [deg]	c [kPa]	γ [kN/m^3]	q [kPa]	B [m]	N_q [-]	N_c [-]	N_γ [-]	p **[kPa]**
25	5	15	10.0	2.0	10.66	20.72	9.01	**345.5**
95% - Values							—	
ϕ [deg]	c [kPa]	γ [kN/m^3]	q [kPa]	B [m]	N_q [-]	N_c [-]	N_γ [-]	p **[kPa]**
20.88	2.46	12.53	10.0	2.0	6.98	15.69	4.56	**165.6**
Design Values							—	
ϕ [deg]	c [kPa]	γ [kN/m^3]	q [kPa]	B [m]	N_q [-]	N_c [-]	N_γ [-]	p **[kPa]**
16.97	1.97	12.53	10.0	2.0	4.76	12.31	2.29	**100.5**

We see that the use of characteristic values and material factors lowers the bearing capacity value nearly by a factor 3.5. We investigate the exceedance probability of the calculated design value, given the uncertainty in the soil parameters. The results for different reliability methods are summarized in table 8.11.

Table 8.11: Reliability Results With Brinch-Hansen

FORM	β	P_f	α_ϕ	α_c	α_γ	LSF-evaluations
	3.95	$3.9 \cdot 10^{-5}$	0.92	0.38	0.06	20
SORM	β	P_f	α_ϕ	α_c	α_γ	LSF-evaluations
	4.23	$1.2 \cdot 10^{-5}$	0.92	0.38	0.06	38
DS	β	P_f	α_ϕ	α_c	α_γ	LSF-evaluations
	4.02	$2.8 \cdot 10^{-5}$	0.92	0.38	0.06	1,610
DARS	β	P_f	α_ϕ	α_c	α_γ	LSF-evaluations
	3.89	$5.0 \cdot 10^{-5}$	0.92	0.38	0.09	379
Crude MC	β	P_f	α_ϕ	α_c	α_γ	LSF-evaluations
	3.89	$5.0 \cdot 10^{-5}$	0.81	0.55	0.19	100,000

We can conclude that the safety concept, as assumed for this case with characteristic values and material factor on the soil strength properties, would lead to acceptably low failure probabilities. FORM performs well on this apparently almost linear limit state. In this configuration the friction angle ϕ is the most influential parameter.

The results of the Crude Monte Carlo analysis are represented in a histogram in figure 8.4.

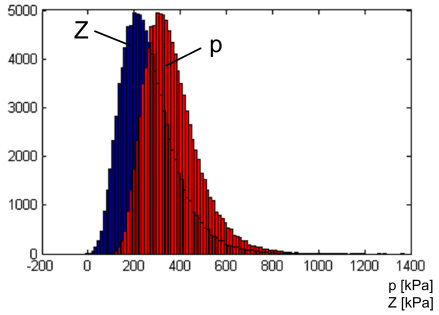

Figure 8.4: Histogram Crude Monte Carlo Realizations p and Z

The limit state function was $Z = p - 100.5$ and therefore the histogram of the Z-values is only shifted horizontally relative to the histogram of p. Only 5 values were smaller than the design bearing capacity[3].

8.2.2 Reliability Analysis With FEM-model

A main subjective of this thesis work is the reliability analysis using FEM. Therefore we will try to evaluate the same bearing capacity problem using a Finite Element Model for the limit state function evaluation. Some of the methods for dealing with this kind of soil shear failure that were discussed in section 7.5 are applied to this example.

The finite element model uses a distributed load to simulate the foundation pressure and a elasto-plastic continuum with Mohr-Coulomb failure criterion representing the soil (similar to figure 8.3). The calculation phases are:

1. Gravity loading.
2. Activation of surcharge load: $q = 10kPa$.
3. Activation of foundation strip load (unit stress).
4. Increase of load using a Load Multiplier 'MLoad'.

In the last phase either the maximum bearing capacity for a parameter realization can be determined by stepwise increasing the load until failure or the load is set to a predefined value (e.g. design value) and it is checked, whether this load is borne by the soil or not. The choice for either method depends on the limit state that is applied.

[3]The Monte Carlo analysis had not converged after the 100000 calculations for a required variation coefficient on the failure probability of 1%.

Deterministic Calculations

The same deterministic calculations as for Brinch-Hansen were carried out with the FEM-model and the results are summarized in table 8.12.

Table 8.12: Deterministic Results With FEM-Model

Mean Values				—	
ϕ [deg]	c [kPa]	γ [kN/m^3]	q [kPa]	B [m]	p **[kPa]**
25	5	15	10.0	2.0	**300.7**
95% - Values				—	
ϕ [deg]	c [kPa]	γ [kN/m^3]	q [kPa]	B [m]	p **[kPa]**
20.88	2.46	12.53	10.0	2.0	**151.7**
Design Values				—	
ϕ [deg]	c [kPa]	γ [kN/m^3]	q [kPa]	B [m]	p **[kPa]**
16.97	1.97	12.53	10.0	2.0	**98.6**

The results show differences up to approximately 20 % with respect to the Brinch Hansen formula. However, for low strength values the results show less differences. The fit around the design value is quite good and therefore we can expect comparable outcomes for the reliability analysis.

Load Multipliers

In this example the simplest and probably most efficient way to determine the probability that the bearing capacity is lower than the design value is to determine the calculated bearing capacity by means of the load multiplier MLoad. The limit state can in this case be formulated as:

$$Z = p - p_d \tag{8.9}$$

where p is the calculated and $p_d = 100.5kPa$ the design bearing capacity obtained by the Brinch-Hansen formula.

The results for this approach are summarized in table 8.13.

Table 8.13: Reliability Results With Load Multiplier

FORM	β	P_f	α_ϕ	α_c	α_γ	LSF-evaluations
	3.75	$9.0 \cdot 10^{-5}$	0.84	0.54	≈ 0.00	20
DARS	β	P_f	α_ϕ	α_c	α_γ	LSF-evaluations
	3.86	$5.8 \cdot 10^{-5}$	0.84	0.54	0.04	1,248

The reliability indices obtained with the finite element model show good agreement with the ones determined with Brinch-Hansen. The influence factors indicate a slight shift from the friction angle towards the cohesion. The soil weight is not very important in the design point. These results will serve as benchmark for the other methods.

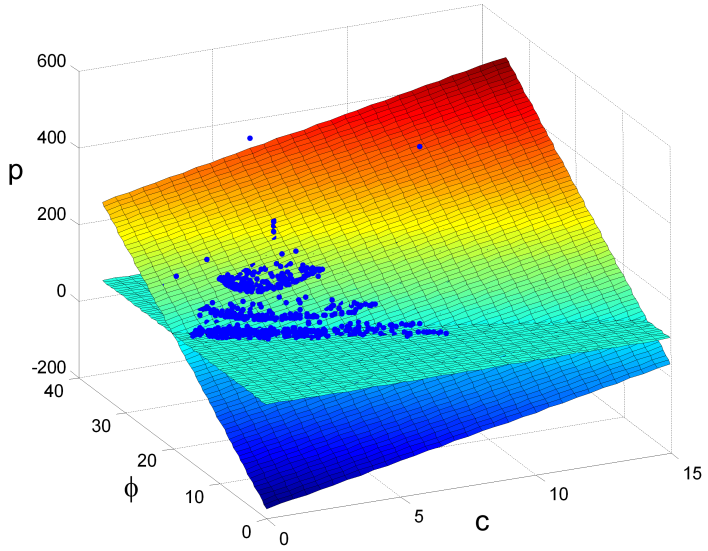

Figure 8.5: Representation of DARS Results

Figure 8.5 shows the results of the DARS analysis. The calculated bearing capacities p are plotted as *blue dots* over the two dominant parameters ϕ and c. The diagonal plane is a two-dimensional fit (by regression analysis) that shows reasonable agreement with the response. Thus, the limit state is almost linear. The horizontal plane represents the design bearing capacity $p_d = 100.5$ [kPa]. DARS was sampling almost exclusively in the important regions and many points are situated around the intersection of the planes ($Z = 0$).

Remark: Unfortunately this approach is not applicable to the deep excavation problems, since the load in that case is generated by the soil and cannot simply be controlled by a load multiplier.

ϕ-c-Reduction

In order to use the ϕ-c-reduction the following limit state function is applied (see section 7.5):

$$Z = MSf - 1 \tag{8.10}$$

A deterministic calculation with the expected values leads to $MSf = 1.69$ and therefore to $Z = 0.69$. A FORM analysis lead to the results summarized in table 8.14.

Table 8.14: Reliability Results With ϕ-c-Reduction

FORM	β	P_f	α_ϕ	α_c	α_γ	LSF-evaluations
	3.76	$8.6 \cdot 10^{-5}$	0.80	0.59	0.11	24

The analysis performed very well with respect to the reference results. The ϕ-c-Reduction seems well suited for this type of problem. In fact, the soil strength parameters are clearly the dominant variables. It is questionable, if this approach is applicable for the excavation problems treated in this thesis, where other parameters such as the volumetric weight and stiffness might play a more important role.

Figure 8.6 shows the development of MSf over the calculation steps in the design point of the FORM analysis.

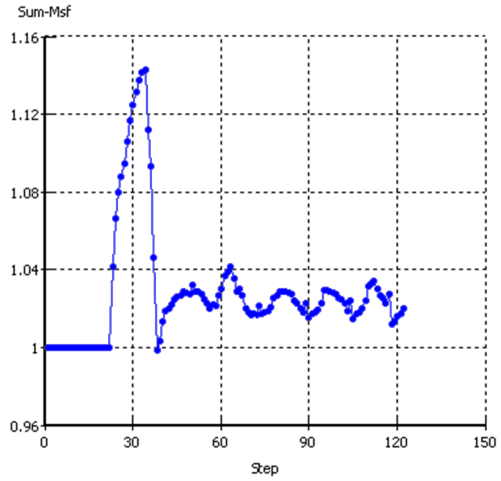

Figure 8.6: MSf vs. Steps

Ideally the value $MSf = 1$ should be found. At the end of the calculation, indeed, MSf converges to roughly one. The question is, if the preceding peak doesn't represent the actual bearing capacity. At least it can be stated that the approach is conservative, if the ϕ-c-reduction behaves this way in the given problem. However, the fluctuations after the peak can represent a problem for automatized calculations.

In figure 8.7 the DARS results were filtered and only the results close to the limit state ($p < 102$ [kPa]) are displayed. In both subfigures the ellipses approximate the lines of equal probability. In subfigure a) the path respectively direction of the ϕ-c-reduction is illustrated and also the solution (design point) that should be found by FORM is indicated. In subfigure b) the blue dots represent the filtered DARS-results and the arrows indicate the Directional Sampling scheme. The results show that the limit state is almost linear, as indicated by the red line. In this case the level III method confirms that the use of FORM is reasonable in this case. It is, however, also obvious that for non-linear limit states Directional Sampling or DARS are more appropriate. The path followed by the ϕ-c-reduction is not necessarily the one that leads to the most probable failure mechanism, which is proven in this figure. Consequently the common idea that 'a ϕ-c-reduction leads to the most probable failure mechanism' is wrong, at least speaking in terms of probability theory.

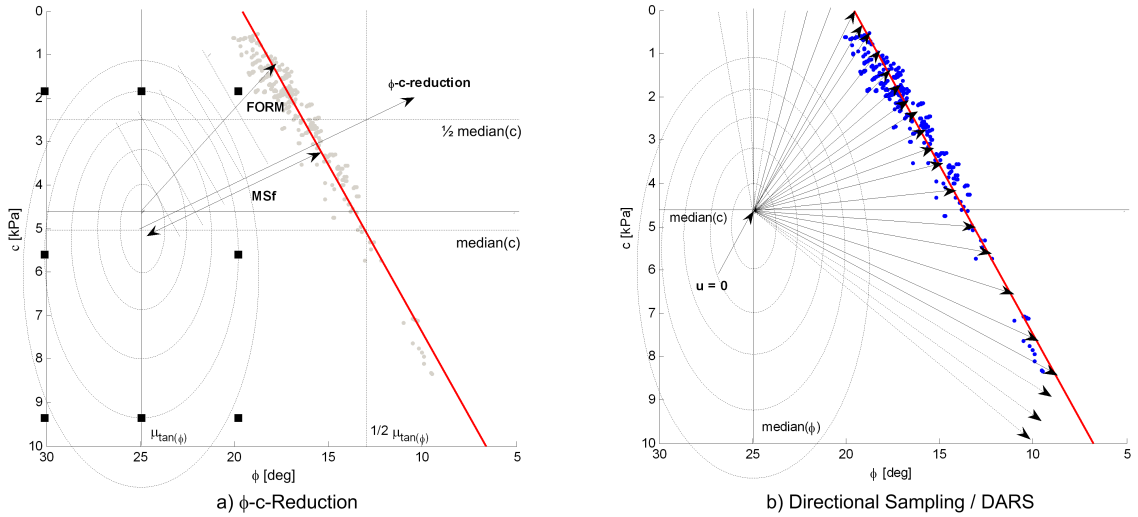

Figure 8.7: ϕ-c-Reduction / FORM (a) vs. Directional Sampling / DARS (b)

Limit Equilibrium

At last also the limit equilibrium approach is tested for the bearing capacity problem. Remember that the definition of the limit state function was:

- Z = 1, if all calculation phases reach equilibrium.
- Z = -1, otherwise.

That means that in the last calculation phase the design load is activated and it is checked if the bearing capacity is sufficient or not. This approach is not as elegant as the previous ones, because is neglects all the information that is available after the FEM-analysis except the information about equilibrium. On the other hand it is very robust and it is expected to be useful for cases where the previous methods are not applicable.

The results of the analysis are summarized in table 8.15.

Table 8.15: Reliability Results With Limit Equilibrium Approach

DS(modified)	β	P_f	α_ϕ	α_c	α_γ	LSF-evaluations
	3.97	$3.7 \cdot 10^{-5}$	0.81	0.57	-0.13	1,896

In figure 8.8 the end points of the vectors that were determined by the analysis are indicated by the blue points. The problem was 3-dimensional, but the volumetric soil weight γ did not show a considerable influence. Therefore only the ϕ-c-plane is displayed in real parameter space (x-space) and in uncorrelated standard normal space (u-space). The red dots represent the expected values respectively the determined design point. The dotted red lines indicate an approximated limit state. It can be seen that the limit state is reasonably linear in the regions

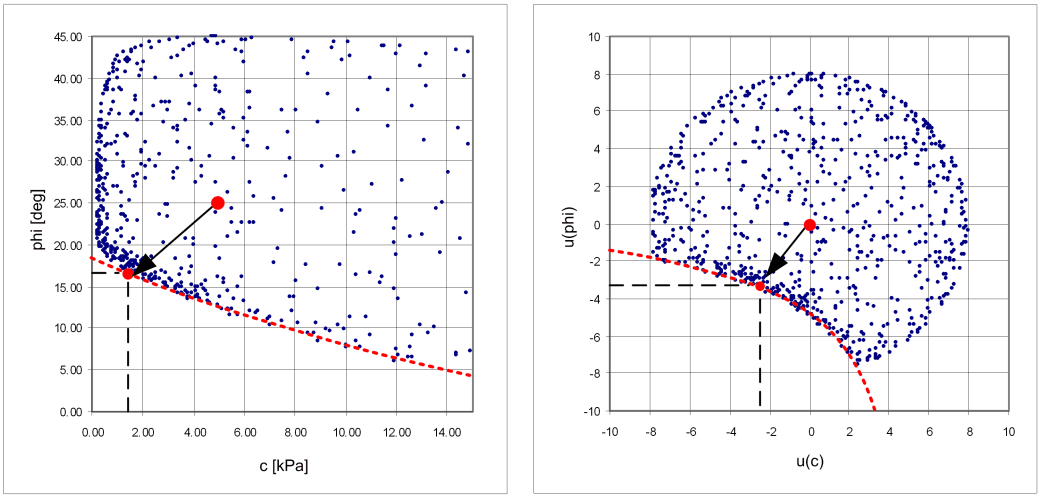

Figure 8.8: DS-Results Limit Equilibrium Approach in X-Space (left) and U-Space(right)

of high probability density, whereas is shows non-linear behavior for the less-likely parameter combinations. If the analysis was only carried out for the two displayed parameters, only dots at the margins should be observed, but since also γ was involved we observe dots also inside these limits. They are projections on the displayed plane.

The limit equilibrium approach yields basically the same results as the other methods. For more complex problems it could be a suitable alternative.

8.2.3 Conclusions

The bearing capacity problem served as test for methods to determine the probability of soil shear failure. The following conclusions can be drawn from the obtained results:

- The nature of the problem allowed us to use the load multiplier for the reliability analysis successfully. Unfortunately, this approach can only be used as a reference for the other attempts, since it is not applicable to retaining structures.
- The ϕ-c-reduction performed well. The applicability to problems, where also other parameters than the soil strength are influential, is questionable.
- The limit equilibrium approach is a robust method that has shown to yield 'correct' results, at least in the given example. It is expected to be a good option for more complex problems.
- There was a good agreement between the results of the Brinch-Hansen formula and the FEM-model in terms of reliability, even though for higher values of soil strength there was a difference up to 20% in the deterministic results.

8.3 Example 3 - Sheet Pile Wall Without Support

This example is a deep excavation in sand with a sheet pile retaining wall. It is illustrated how reliability methods can be applied in combination with FEM (Plaxis) to limit states that are typical for deep excavations respectively retaining structures. The example properties, soil parameters as well as structural dimensions, are chosen arbitrarily.

Geometry and Material Properties

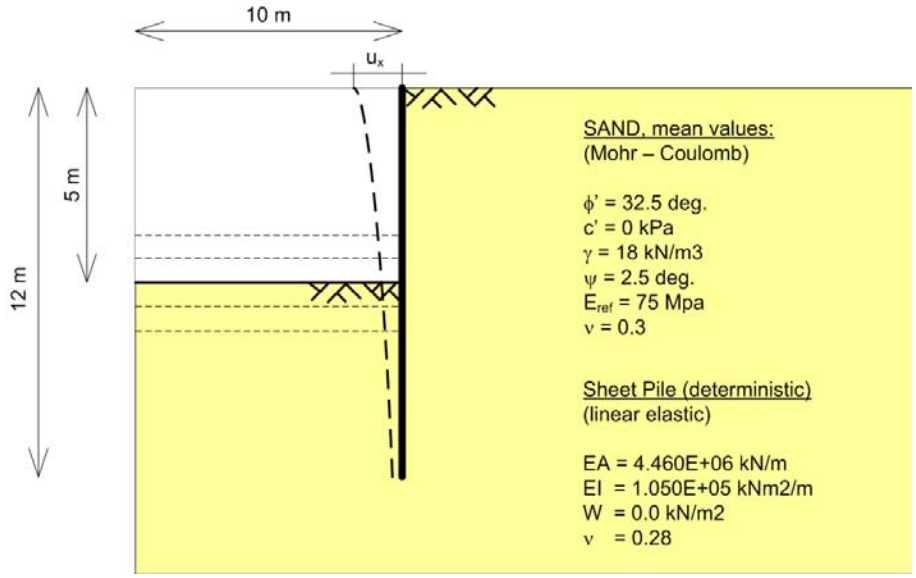

Figure 8.9: Calculation Example: Sheet Pile Wall (Without Anchors)

Construction Stages

An excavation of 5.0 m depth is executed using a sheet pile wall without anchors or bottom support in a homogeneous soil layer with uncertain 'average' properties. Neither groundwater nor external loads are present.

The calculation sequence is:

1. Gravity loading of the soil including the 'wished in place' sheet pile.
2. Excavation until final level (-5.00m).

Variable		Distribution	Mean	Std	COV
E_{ref}	[kPa]	normal	75,000	15,000	25 %
R_{inter}	[-]	normal	0.5	0.1	20 %
ϕ'	[deg]	lognormal	32.5	3.25	10 %
W_{unsat}	[kN/m3]	normal	18	0.9	5 %
ν	[-]	normal	0.3	0.03	10 %
ψ	[deg]	normal	3.25	0.16	5 %

Table 8.16: Basic Random Variables Example 3

A set of reasonable variation coefficients $COV(X_i)$ is applied in combination with the mean values μ_{X_i} given in table 8.16.

The parameters used for the sheet pile wall correspond to a *Larssen 24* profile and are treated deterministically, i.e. uncertainties in the strength properties of the structure are neglected.

The following aspects will be subject to investigation in this example:

- Local sensitivity to the soil/model parameters
- Reliability against failure in the soil in general
- Reliability against yielding of the Sheet Pile Wall
- Reliability against excessive deformations
- Dependence of the displacement criterion on β
- Influence of the coefficient of variation of $sin(\phi)$
- Influence of interface strength (R_{inter}) on the reliability index

We consider unacceptable states of the structural system as failure, like e.g. excessive deformations or plastic yielding of structural members. Some of the investigated mechanisms do not directly lead to a collapse of the system and the system would exhibit some residual strength, even though it is already considered as failed. Considerations about residual strength are especially of interest for systems that might still fulfill their primary function after 'failing'. An example are water retaining structures like dikes. A dike might still retain the water after partial failure of the inner slope. In the present example, however, we consider residual strength to be irrelevant. The functional requirements of the structure are expressed by the limit states and, if they are not fulfilled, this is considered as failure.

8.3.1 Displacement Top of the Sheet Pile Wall

The maximum horizontal displacement of the considered sheet pile will clearly occur at the top. Typically values like 1% of the retaining height or $10cm$ are chosen as admissible deformations. Using the calculated u_x at the top of the wall the LSF is:

$$Z = u_{x,adm} - u_x \tag{8.11}$$

A FORM-analysis with $u_{x,adm} = 10cm$ gives us an idea about the influence coefficients α_i:

Number of calculations (FORM) : 71

Beta : 2.326E000
P_f : 1.002E-02

	Model	Parameter	alfa	X
1	Variable	COVE	0.000E00	2.500E-01
2	Variable	COVRinter	0.000E00	2.000E-01
3	Variable	COVWunsat	0.000E00	5.000E-02
4	Variable	COVnu	0.000E00	2.000E-01
5	Variable	COVphi	0.000E00	1.000E-01
6	Variable	COVsinpsi	0.000E00	5.000E-02
7	Variable	Eref_sand	8.764E-02	7.194E004
8	Variable	maxUx	0.000E00	1.000E-01
9	Variable	nu_sand	1.180E-01	2.835E-01
10	Variable	phi_sand	9.435E-01	2.537E001
11	plaxis	Rinter sand	2.586E-01	4.398E-01
12	plaxis	Sinpsi sand	1.050E-02	4.357E-02
13	plaxis	Wunsat sand	-1.453E-01	1.830E001

Table 8.17: Results Reliability and Sensitivity Analysis for Example 2 with FORM

From the results of this initial sensitivity analysis it can be concluded that the friction angle ϕ' of the sand is by far the most influential parameter in this example with $\alpha_\phi \approx 0.94$. The other parameters are only of marginal influence for the reliability index ($\beta = 2.33$). To illustrate the sensitivity of the reliability index to the reduction of uncertainty, the number of random variables is reduced. Only the two most influential parameters, ϕ and R_{inter} (see section F.2), are treated stochastically and the other parameters assume their mean values. The reliability index increased only slightly to a value of $\beta = 2.35$. Even only considering ϕ' as uncertain we obtain $\beta = 2.47$. The deformation of the wall seems thus to be dominated by ϕ'.

Parametric Study on the influence of $COV(\phi)$

As a consequence of the large influence of ϕ' on the deformations, changing the amount of uncertainty in this parameter is expected to have a considerable impact on the reliability. In order to verify this a parametric study has been carried out for different values of $COV\phi'$ ranging from 2.5 % to 12.5% in steps of 2.5 %. The results are shown in figure 8.10.

The results confirm that the reliability level decreases considerably with an increasing uncertainty in the dominant input parameter ϕ. It is remarkable that within this reasonably realistic range of the variation coefficient of 5 % to 12.5 % there are differences in the calculated failure probability of a factor $1,000$.

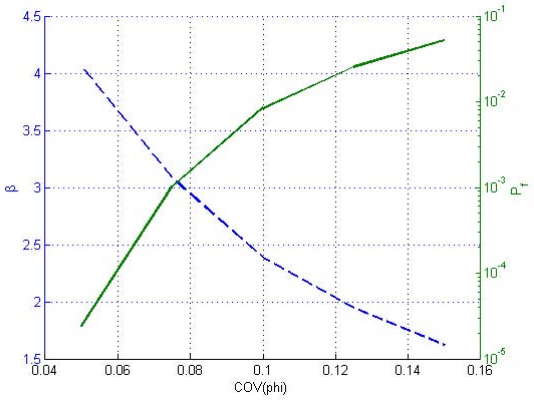

Figure 8.10: Reliability Index and Failure Probability for Varying $COV(\phi)$

Parametric Study on the influence of $u_{x,max}$ (LS-criterion)

The influence of $u_{x,max}$ is investigated by a parametric study where we combine different values of $u_{x,max}$ with two different values of $COV(sin(\phi)$ (for comparison with $COV(\phi)$ see appendix O). The reliability index β increases nearly linearly with the limit state criterion, whereas the failure probability decreases almost logarithmically:

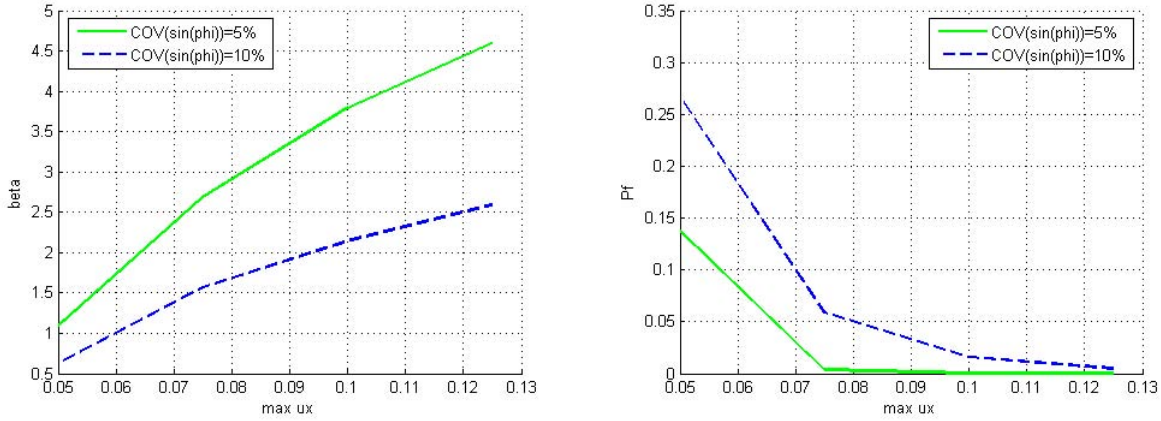

(a) Beta as function of $u_{x,max}$

(b) P_f as function of $u_{x,max}$

Figure 8.11: Beta and P_f as function of $u_{x,max}$

The influence coefficients α_i are reasonably constant over the whole contemplated range of limit state deformations. There is one outlier for 40 mm, but this calculation did not converge with FORM (it is very close to the mean value calculation).

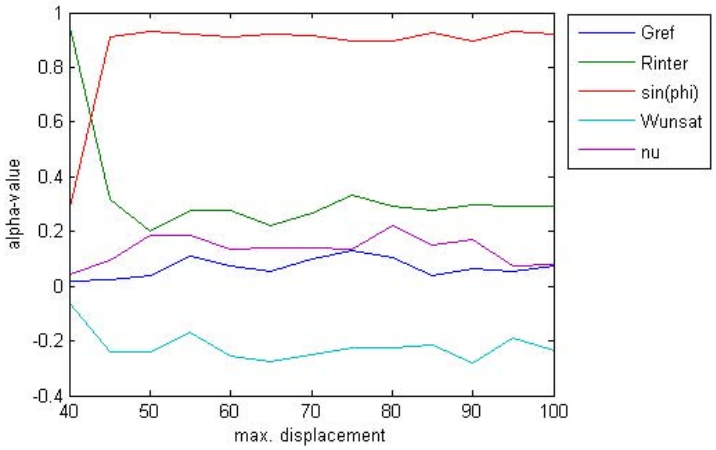

Figure 8.12: α-values as function of the LSF-criterion

It can be concluded that the three parameters of main influence on the problem are the angle of internal friction ϕ, the volumetric soil weight W_{unsat} and the interface strength ratio R_{inter}, even for the whole investigated range of admissible displacements. The uncertainty of the stiffness parameters G_{ref} respectively E_{ref} and ν can therefore be neglected and treated as deterministic quantity (expectation or a conservative estimate).

Parametric Study on the influence of R_{inter}

The FEM-model of the problem comprises interface elements (see appendix F) between the retaining structure and the surrounding soil. Even though this modelling feature is often applied and parameter values have to be chosen, like in this example the interface strength R_{inter}, there is not much information available. The interface strength is neither a soil property nor a property of the sheet pile steel. It is rather an interaction parameter between the two, for which values based on experience are applied, because it is difficult to determine. Nevertheless it is an uncertain parameter. The following parametric study gives an impression of its influence on the results.

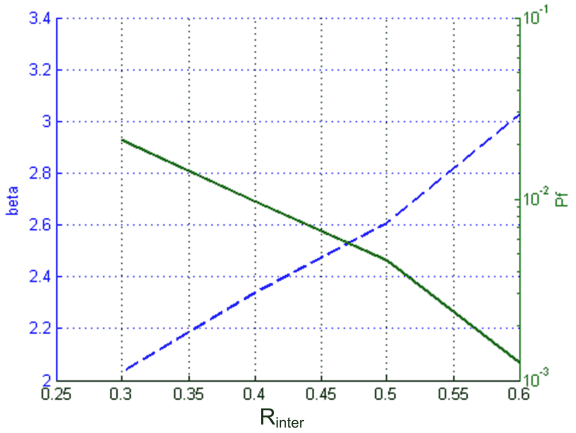

Figure 8.13: Beta and Pf as function of R_{inter}

In contrast to the fact that there is little attention paid to the properties of the interface strength in the literature, there is a considerable effect of this parameter on the results, at least for this non-anchored retaining wall. Therefore it is suggested to treat this variable as stochastic quantity in the calculations of sheet pile structures, unless it can be shown that its influence is negligible for the problem at hand, e.g. by means of sensitivity analysis.

8.3.2 Exceedance of the Yield Strength in the Sheet Pile

The horizontal load on the sheet pile wall causes it to bend and thereby also a bending moment is generated. Also normal forces can occur, especially if inclined anchors are involved. The stresses in the steel should ideally not exceed the yield strength in order to remain in the elastic domain. For a non-anchored structure the contribution of normal stresses is negligible. Therefore we contemplate only the generated bending moments in this example.

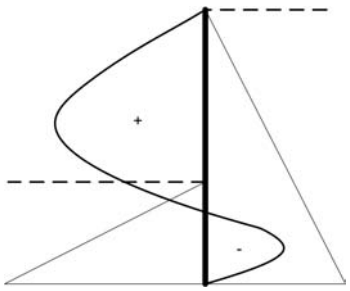

Figure 8.14: Bending Moments in a Non-Anchored Retaining Wall

From the FEM-analysis an absolute maximum value of the bending moment M_{max} is obtained. For the limit state formulation the maximum admissible moment M_d follows from the relation:

$$\sigma = \frac{M}{W} \leftrightarrow M = \sigma W \tag{8.12}$$

with the deterministic design values $\sigma_{y,d}$ and W_{el}. There fore the LSF could be:

$$Z = M_d - M_{max} = \sigma_{y,d} \cdot W_{el} - M_{max} \tag{8.13}$$

Sensitivity Analysis

We start again with a sensitivity analysis by means of FORM. The limit state criterion is arbitrarily chosen as being $M_{adm} = 500\ kNm/m$ and the LSF is simplified to:

$$Z = 500 - M_{max} \quad [kNm/m] \tag{8.14}$$

The results of this sensitivity analysis show that there are dominant and less dominant influence variables. As can be seen from table 8.18 again the stiffness parameters and the dilation angle are of minor influence. The friction angle ϕ seems to be the dominant variable, whilst R_{inter} and γ_{unsat} represent a minor contribution to the uncertainty. This is not surprising, since a linear-elastic model is used for the sheet pile itself and therefore the maximum displacements and the maximum bending moments should also be linearly related. The α_i should thus also be comparable.

Number of calculations (FORM) : 106

Beta : 3.851E000
P_f : 5.878E-05

	Model	Parameter	alfa	X
1	Variable	COVE	0.000E00	2.500E-01
2	Variable	COVRinter	0.000E00	2.000E-01
3	Variable	COVWunsat	0.000E00	5.000E-02
4	Variable	COVnu	0.000E00	1.000E-01
5	Variable	COVphi	0.000E00	1.000E-01
6	Variable	COVsinpsi	0.000E00	5.000E-02
7	Variable	Eref_sand	-1.949E-02	7.613E004
8	Variable	maxM	0.000E00	5.000E002
9	Variable	nu_sand	-2.137E-02	3.025E-01
10	Variable	phi_sand	9.738E-01	2.031E001
11	plaxis	Rinter sand	1.392E-01	4.464E-01
12	plaxis	Sinpsi sand	-2.143E-02	4.380E-02
13	plaxis	Wunsat sand	-1.763E-01	1.861E001

Table 8.18: Results FORM Sensitivity Analysis for Maximum Bending Moments

Reduction Of Uncertainty By Reducing Random Variables

The less important variables E, ν and ψ are treated as deterministic variables with their expectations in order to see how this decrease of input uncertainty affects the reliability index.

Number of calculations (DARS Directional Adaptive Response Surface sampling) : 425

Beta : 3.887E000
P_f : 5.075E-05

	Model	Parameter	alfa	X
1	Variable	A_sp	0.000E00	2.230E002
2	Variable	COVE	0.000E00	2.500E-01
3	Variable	COVRinter	0.000E00	2.000E-01
4	Variable	COVWunsat	0.000E00	5.000E-02
5	Variable	COVnu	0.000E00	1.000E-01
6	Variable	COVphi	0.000E00	1.000E-01
7	Variable	COVsinpsi	0.000E00	5.000E-02
8	Variable	Eref_sand	0.000E00	7.500E004
9	Variable	I_sp	0.000E00	5.250E004
10	Variable	maxM	0.000E00	5.000E002
11	Variable	nu_sand	0.000E00	3.000E-01
12	Variable	phi_sand	9.710E-01	2.023E001
13	plaxis	G SheetPile	0.000E00	3.440E006
14	plaxis	Rinter sand	2.295E-01	4.108E-01
15	plaxis	Sinpsi sand	0.000E00	4.362E-02
16	plaxis	Wunsat sand	-7.854E-02	1.827E001
17	plaxis	d SheetPile	0.000E00	5.315E-01

Table 8.19: Results Maximum Bending Moments for Reduced Uncertainty

The reliability is increased from $\beta = 3.85$ to $\beta = 3.89$ and the low influence of these variables is confirmed. A calculation reducing the input uncertainty to only the uncertainty in the friction angle ϕ results in a reliability index of $\beta = 4.14$.

Parametric Study On M_{max} (Limit State Criterion)

The limit state criterion M_{max} is varied in a parametric study between 300 kNm/m and 550 kNm/m to investigate the influence on the failure probability and on the influence of the variables.

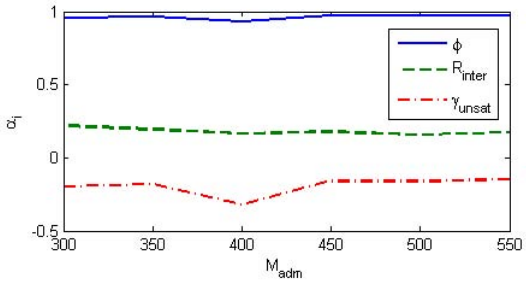

Figure 8.15: Influence Factors for Varying M_{adm}

The influence of the three mort important variables is nearly constant over the whole range of limit state criteria. The strength parameter ϕ' clearly dominates the problem.

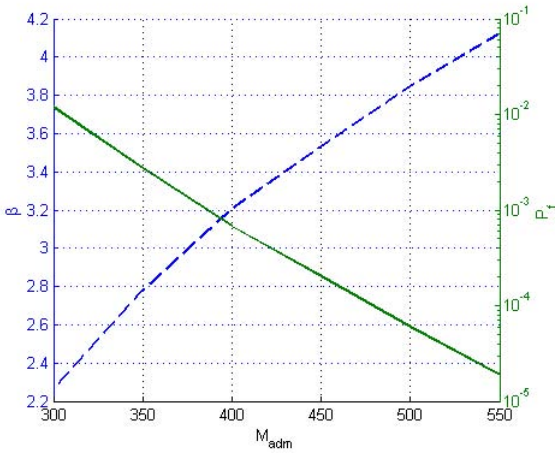

Figure 8.16: Failure Probability for Varying M_{adm}

The failure probability P_f decreases almost linearly with increasing M_{adm} in the contemplated range. This fact can be used for design considerations, such as the choice the sheet pile type.

Influence of R_{inter}

For this limit state the influence of R_{inter} was assessed by a parametric study on the calculated bending moment.

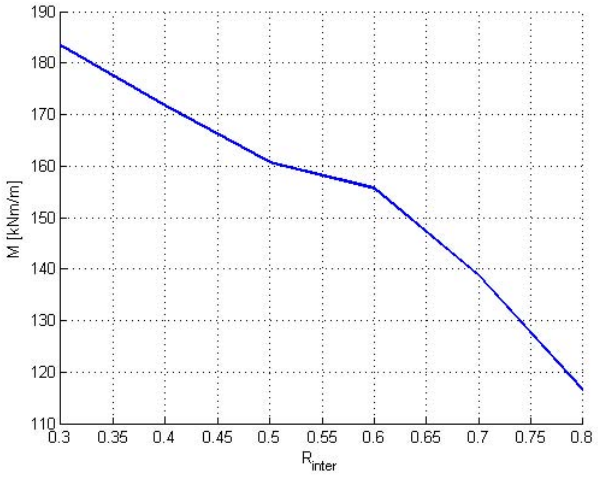

Figure 8.17: Influence of R_{inter} on the Calculated M

From the presented results we can conclude that the influence is considerable and it can be expected that the influence in the reliability is similar as for the deformation criterion[4].

8.3.3 Soil Shear Failure

For this simple example only the ϕ-c-reduction was applied for determining the soil shear failure. It is the simplest approach and leads to results for this problem. The limit state function is defined according to chapter 7:

$$Z = MSf - 1.0 \tag{8.15}$$

The results were obtained using DARS. FORM showed convergence problems. The influence factors α_i in methods other than FORM are, as explained earlier, approximations and their quality depends on the shape of the LS and the approximation method. Therefore the results of this sensitivity analysis (see table 8.20) have to be treated carefully.

Based on the influences found in the sensitivity analysis, the variable set treated as stochastic is reduced to the friction angle. The reliability changes only slightly to $\beta = 4.11$. The problem is clearly dominated by the strength and the other uncertainties in the parameters contribute only in a negligible way.

[4]These calculations could not be carried out due to time restrictions.

Number of calculations (DARS Directional Adaptive Response Surface sampling) : 358

Beta : 4.056E000
P_f : 2.500E-05

	Model	Parameter	alfa	X
1	Variable	COVE	0.000E00	2.500E-01
2	Variable	COVRinter	0.000E00	2.000E-01
3	Variable	COVWunsat	0.000E00	5.000E-02
4	Variable	COVnu	0.000E00	1.000E-01
5	Variable	COVphi	0.000E00	1.000E-01
6	Variable	COVsinpsi	0.000E00	5.000E-02
7	Variable	Eref_sand	-6.318E-02	7.864E004
8	Variable	mincphi	0.000E00	1.000E000
9	Variable	nu_sand	1.119E-01	2.860E-01
10	Variable	phi_sand	9.860E-01	1.926E001
11	plaxis	Rinter sand	-4.331E-02	5.165E-01
12	plaxis	Sinpsi sand	-1.732E-02	4.375E-02
13	plaxis	Wunsat sand	-8.933E-02	1.833E001

Table 8.20: Results DARS for Soil Failure (Sensitivity Analysis)

8.3.4 Conclusions

The results obtained for the sensitivity and reliability analyses carried out on this example lead to the following conclusions that are, of course, only applicable to similar problems of non-anchored walls in homogeneous, cohesionless soil and to the given set of variation coefficients $COV(X_i)$:

- The deformation of the sheet pile wall and the bending moments are dominated by the strength of the soil, thus, in this case only by the friction angle ϕ'.
- If we accept an accuracy of the reliability index of $\epsilon_\beta = 1\%$, it is sufficient to consider the variables ϕ', R_{inter} and γ_{unsat} as random variables. For the other variables deterministic conservative estimates can be used.
- The influence of the interface strength (R_{inter}) is, even though usually not much attention is paid to it, considerable. Further investigation should be carried out to assess this quantity and the existing recommendations about its application should be refined.
- The ϕ-c-reduction proved to be very convenient method for determining the common failure probability of actually several failure mechanisms in this example. However, simple methods, like FORM, were hardly applicable for this kind of problem and more advanced methods like DARS had to be applied due to the apparently unstable limit state function[5].

[5]Some deterministic studies revealed that the MSf that is obtained by ϕ-c-reduction lead to slightly instable results. E.g. for small decreases of the strength sometimes small increases of the MSf were observed, whereas the trend within a broader range was the expected 'monotonic' decrease of the MSF for monotonically decreasing strength properties.

Chapter 9

Case Study 1 - Anchored Retaining Wall

This case study illustrates the application of the methodology that was described in the preceding chapters to an imaginary but realistic situation. The experiences with the calculation methods presented are discussed and conclusions and recommendations will be given.

9.1 Case Description

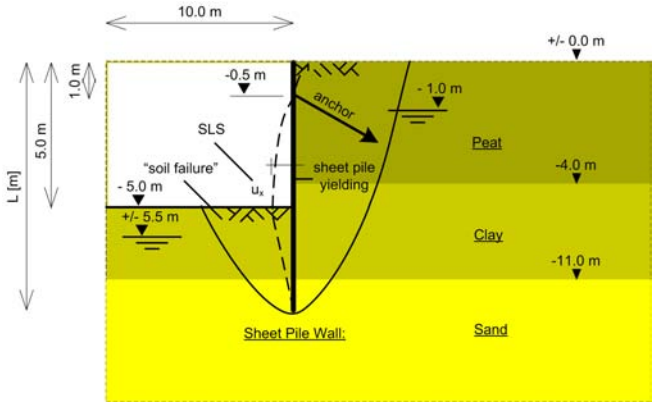

Figure 9.1: Example Properties - Anchored Retaining Wall In Layered Soil

The example is an anchored sheet pile wall in layered soil. Groundwater is present and the resulting pore pressure field is treated deterministically in first instance. We assume the structure to be homogeneous in the third dimension, representing a railway tunnel for example. Therefore a plane-strain model is applied. The soil layers are modelled using random average quantities, for which the statistics respectively the variation coefficients are chosen arbitrarily, but in a realistic range. As explained in section 2.4, in a real situation this approach would demand to account for averaging effects in the soil variability. We suppose that the used statistics already include these effects. It is, however, emphasized that the determination of the input statistics

is a crucial part of the reliability analysis, even though it was not scope of this research.

A deterministic design (see section 9.1.3) of the retaining wall was made based on the recommendations given in the CUR 166 [8] (chapter 4: *Eindige Elementenmethode*). The reliability analysis is carried out for the Ultimate Limit State (ULS).

9.1.1 Parameters

The geometrical properties and the groundwater level are indicated in figure 9.1. The soil properties are taken from *NEN6740-table 1*[1] and summarized in table 9.2. Only the properties for the use of an elastic-plastic model with Mohr-Coulomb yield criterion are presented. *NEN6740-table 1* gives *characteristic values* and indications for the variation coefficients that should be handled for each property. From these data, assuming the characteristic values to be 95 %-quantiles and the variables to be normally distributed, we can calculate the corresponding first two central moments (see appendix K):

$$\mu_x = \frac{q_{\hat{p}}}{1 + \Phi^{-1}\{P(X \leq q_{\hat{p}})\} \cdot COV(X)} \tag{9.1}$$

$$\sigma_x = \mu_x \cdot COV(X) \tag{9.2}$$

The distribution types[2] that were chosen for the soil parameters in the reliability analysis are based on knowledge about the physically possible ranges.[3]. The distributions of all parameters were chosen as indicated in table 9.1.

Table 9.1: Soil Parameter Distributions

For all layers:			
Parameter	Symbol	Distribution / Relation	Unit
Saturated volumetric weight	γ_{sat}	Normal (μ, σ)	$[kN/m^3]$
Unsaturated volumetric weight	γ_{dry}	$\gamma_{\text{dry}} = \gamma_{\text{sat}} - 1$	$[kN/m^3]$
Cohesion	c	Lognormal (μ, σ, 0)	$[kPa]$
Friction angle	ϕ'	Beta (μ, σ, 0, 45)	$[^o]$
Dilatation angle	ψ	$\psi = \phi - 30^o$	$[^o]$
Young's modulus	E	Lognormal (μ, σ, 0)	$[kN/m^2]$
Poisson ratio	ν	Beta (μ, σ, 0.0, 0.5)	[-]
Interface Strength	R_{inter}	Beta (μ, σ, 0.0, 1.0)	[-]

The stochastic values for ν, ψ and R_{inter} are best guesses with respect to their uncertainty. There is hardly any data available on these quantities. The sand as base layer has been calculated with characteristic values. Only for soil failure mechanisms the friction angle of sand was considered stochastic.

[1] Dutch code for geotechnical structures (see appendix I).

[2] Also stability aspects of the calculation process played a role in the choice of the distribution types.

[3] It is theoretically inconsistent to determine the moments of the distribution assuming a Normal Distribution whilst for the calculations other distribution types are applied. In this case this was done for sake of comparability and the error implied is negligible.

Table 9.2: Soil parameters Calculation Example

PEAT, medium						
Name	Symbol	95%-Quantile	COV	Mean	STD	Unit
Saturated volumetric weight	γ_{sat}	12	5%	13.1	0.65	$[kN/m^3]$
Cohesion	c	5	20%	7.5	1.5	$[kPa]$
Friction angle	ϕ'	15	10%	23.9	2.39	$[^o]$
Dilatation angle	ψ	0	0	0	0	$[^o]$
Young's modulus	E	500	25%	850	212	$[kN/m^2]$
Poisson ratio	ν	n.a.	10%	0.35	0.035	[-]
Interface Strength	R_{inter}	n.a.	20%	0.6	0.12	[-]
CLAY, medium						
Name	Symbol	95%-Quantile	COV	Mean	STD	Unit
Saturated volumetric weight	γ_{sat}	17	5%	18.5	0.93	$[kN/m^3]$
Cohesion	c	10	20%	14.9	2.98	$[kPa]$
Friction angle	ϕ'	17.5	10%	20.9	2.09	$[^o]$
Dilatation angle	ψ	0	0	0	0	$[^o]$
Young's modulus	E	2000	25%	3400	850	$[kN/m^2]$
Poisson ratio	ν	n.a.	10%	0.35	0.035	[-]
Interface Strength	R_{inter}	n.a.	20%	0.6	0.12	[-]
SAND, dense						
Name	Symbol	95%-Quantile	COV	Mean	STD	Unit
Saturated volumetric weight	γ_{sat}	19	5%	-	-	$[kN/m^3]$
Cohesion	c	0	20%	-	-	$[kPa]$
Friction angle	ϕ'	35	10%	35	3.5	$[^o]$
Dilatation angle	ψ	5	n.a.	-	-	$[^o]$
Young's modulus	E	125,000	25%	-	-	$[kN/m^2]$
Poisson ratio	ν	0.35	n.a.	0.35	-	[-]
Interface Strength	R_{inter}	n.a.	n.a.	1.0	-	[-]

9.1.2 Finite Element Model

The structure has been modelled with the Finite Element code Plaxis 8.2 (2D, plane-strain). The model and the automatically generated mesh (refined around the excavation area and grout body) are presented in figure 9.2.

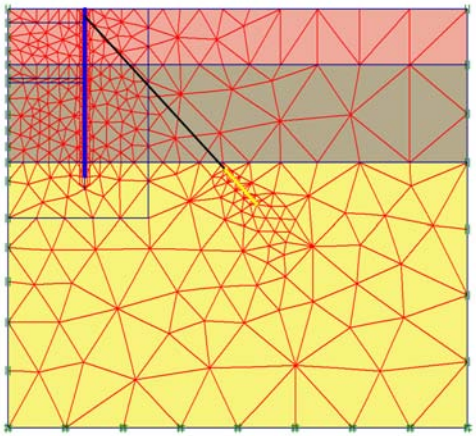

Figure 9.2: FEM-model and Mesh for Case 1

The sheet pile has been modelled with standard plate elements and the free anchor length with node-to-node anchor elements using the parameters as indicated in table 9.4 and with a Young's modulus for steel of $E = 210$ $[GPa]$. The grout bodies were modelled by geogrid elements using typical values for grout stiffness. The influence of these elements is expected to be small and the anchors are modelled in a way that the grout bodies do not considerably influence the other limit states. The slipping of the grout body is a difficult modelling issue and should be subject to further research in deterministic FEM-modelling.

9.1.3 Deterministic Design

The design of the retaining wall is based on the step plan of the CUR 166[4] respectively on the recommendations for design with the Finite Element method (chapter 4 of CUR 166).

Basic Assumptions

The structure is classified as 'safety class II' and the geometrical properties are summarized in figure 9.1.

The characteristic soil properties are taken from NEN 6740 - table 1 (see also table 9.2) for the soil types:

1. Peat, medium
2. Clay, medium
3. Sand, dense

The mean groundwater level on the right side is at $-2.0m$. The first excavation level is $-1.00m$ and the anchor layer is situated at a level of $-0.5m$. The anchors are installed under an angle of 45, their grout bodies have a length of $5m$ and these begin from a level of about $1.00m$ below the layer boundary between clay and sand. The anchors will are prestressed with $80kN/m$. The final excavation is taken to a level of $-5.00m$ and the groundwater level in the pit is lowered to $-5.50m$ below the surface level. A profile AZ 18 is chosen as sheet pile.

Design Values

The design values for the soil parameters[5] are summarized in table 9.3:

The bending stiffness and axial stiffness EI and EA of the wall and the anchor stiffness EA_a are the expected values:

$$\begin{aligned} EI &= 4.473E+04 \ kNm^2/m \\ EA &= 3.129E+06 \ kN/m \\ EA_a &= 5.880E+04 \ kN \end{aligned}$$

The surcharge load on the surface amounts 10 kPa with a width of 10 m next to the excavation. The uncertainties in the excavation level are accounted for by an increase of 30 cm:

$$D_d = \mu_D + 0.30 = 5.30 \ m$$

The design values for the water levels were determined by assumed variations in the water levels and the according safety factors:

$$\begin{aligned} GWL_{d,exc} &= \mu(GWL_{exc}) - \gamma \cdot \sigma(GWL_{exc}) = -5.50 - 1.7 \cdot 0.20 = -5.84 \ m \\ GWL_{d,load} &= \mu(GWL_{load}) + \gamma \cdot \sigma(GWL_{load}) = -2.00 + 0.85 \cdot 0.50 = -1.57 \ m \end{aligned}$$

These values are applied in the critical last excavation phase.

[4]Dutch Technical Recommendation: CUR 166 - Damwandconstructies, 4e druk, 2005

[5]Scheme B was chosen, thus only design values for the stiffness parameters are applied and a ϕ-c-reduction is used for representative values.

Table 9.3: Soil parameters Calculation Example

PEAT, medium				
Name	Symbol	Rep. Value	Design Value	Unit
Saturated volumetric weight	γ_{sat}	12	n.a.	$[kN/m^3]$
Cohesion	c	5	n.a.	$[kPa]$
Friction angle	ϕ'	15	n.a.	$[^o]$
Dilatation angle	ψ	0	0	$[^o]$
Young's modulus	E	500	385	$[kN/m^2]$
Poisson ratio	ν	0.35	n.a.	[-]
Interface Strength	R_{inter}	0.6	n.a.	[-]
CLAY, medium				
Name	Symbol	Rep. Value	Low/High Design Value	Unit
Saturated volumetric weight	γ_{sat}	17	n.a.	$[kN/m^3]$
Cohesion	c	10	n.a.	$[kPa]$
Friction angle	ϕ'	17.5	n.a.	$[^o]$
Dilatation angle	ψ	0	0	$[^o]$
Young's modulus	E	2,000	1,540	$[kN/m^2]$
Poisson ratio	ν	0.35	n.a.	[-]
Interface Strength	R_{inter}	0.6	n.a.	[-]
SAND, dense				
Name	Symbol	Rep. Value	Low/High Design Value	Unit
Saturated volumetric weight	γ_{sat}	19	n.a.	$[kN/m^3]$
Cohesion	c	0	n.a.	$[kPa]$
Friction angle	ϕ'	35	n.a.	$[^o]$
Dilatation angle	ψ	5	n.a.	$[^o]$
Young's modulus	E	125,000	96,150	$[kN/m^2]$
Poisson ratio	ν	0.3	n.a.	[-]
Interface Strength	R_{inter}	0.6	n.a.	[-]

Construction Stages

The construction is modelled in 5 stages:

1. Gravity Loading. (Generation of Initial Stresses)
2. Excavation to $-1.00m$ and activation of the load of $10kPa$.
3. Installation of the anchor layer and prestressing of the anchors with $80kN/m$.
4. Excavation to $-5.00m$ (final depth).
5. (Determination MSf by ϕ-c-reduction.)

Determination Sheet Pile Length

The sheet pile length is sufficient, if the ϕ-c-reduction gives a value larger than $1,15$. This could be achieved for sheet pile lengths of about $8.00m$, however it turned out that its vertical displacements are unacceptable. Therefore the pile tip level is taken to $1.00m$ into the firm sand layer, which leads to a total length $L = 12.00m$. This configuration leads to $MSf = 1.61$.

$$MSf = 1.61 > 1.15$$

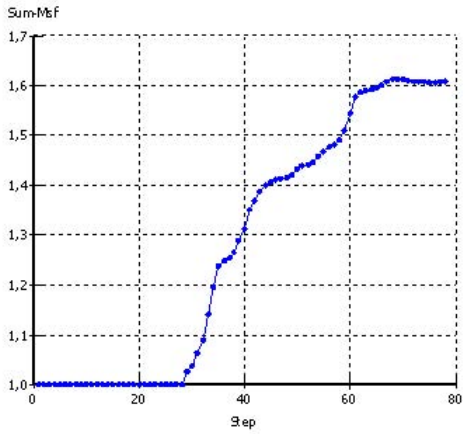

Figure 9.3: Results Phi-C-Reduction (Low Soil Stiffness Design Values)

Bending Moment

The maximum moment is to be taken at a value of $MSf = 1.15$ that is reached in step 33 according to figure 9.3. However, in this case the non-reduced strength parameters (final construction stage) in combination with the low design values for the soil stiffness lead to the highest bending moment in the sheet pile of $M = 392.5kN/m$.

$$M_{s,d} = 392.5 < 423 = M_{r,d} \quad [kNm/m]$$

→ chosen profile: AZ18 with $M_{r,d} = 423$ $[kNm/m]$

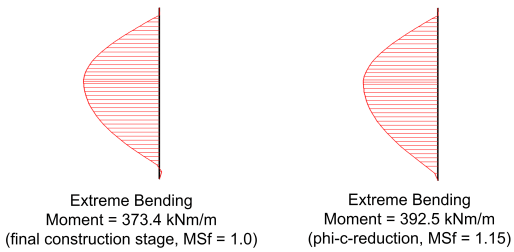

Figure 9.4: Bending Moments Deterministic Design

Anchor Force

The highest anchor force was observed for an $MSf = 1.15$ in combination with the low design values for the soil stiffness: $F_{A,max} = 193.2kN/m * 3.00m = 579.6kN$.

$$F_{s,a,st,d} = 1.25 * F_{a,max} = 724.5 < 880 = F_{r,a,st,d} \quad [kN]$$

→ chosen anchor configuration: 4-strand-anchor with cross sectional area $Aa = 560mm^2$ and a design anchor capacity $F_{r,a,st,d} = 880$ $[kN]$ each at a mutual distance of $a = 3.00m$, steel quality: S355 ($\sigma_y = 355MPa$).

Waling

The waling type is determined by the bending moment that is generated by the line load of the sheet pile wall at anchor level (see section 7.4.3):

$$M_{s,w,d} = \frac{1}{8} F_{s,w,d} \cdot a = \frac{1}{8} \cdot 1.1 \cdot 724.5 \cdot 3.00 = 298.9 < 361.9 = M_{r,w,d} \quad [kNm]$$

→ chosen profile: 2*UPE300 with $M_{r,d} = 361.9$ $[kNm/m]$ (S355)

Overall Stability

The overall stability was implicitely checked in the ϕ-c-reduction with the result:

$$MSf = 1.61 > 1.15$$

Uplift / Piping

Piping is not likely to occur due to the thick clay layer. The vertical equilibrium between the sand and the clay layer is given by:

$$\frac{17\ kN/m^3 \cdot 5.7\ m}{(-1.57m - 5.84m) \cdot 10\ kN/m^3} = \frac{99.28kPa}{42.7kPa} = 2.3 >> 1.1$$

→ sufficient safety against uplift

Serviceability Limit State

For the displacements of the sheet pile wall it may be assumed that the a calculation with characteristic values gives a conservative estimate. In this case the maximum horizontal displacements were:

$$u_{x,max} = 0.046 < 0.05 = \frac{1}{100} 5.00 = \frac{1}{100} D = u_{x,adm}$$

→ The arbitrarily chosen displacements criterion of $u_{x,adm} = D/100$ is fulfilled.

The outcomes of the calculations, i.e. the structural design parameters, are summarized in table 9.4.

Table 9.4: Parameters of Structural Members

SHEET PILES			
Property	Symbol	Value	Unit
type	-	AZ 18	$[-]$
length	L	12	$[m]$
elastic section modulus	W_{el}	1,800	$[cm^3/m]$
moment of inertia	I	34,200	$[cm^4/m]$
cross sectional area	A	150	$[mm^2]$
sheet pile thickness	e	9.5	$[mm]$
mass	m	118	$[kg/m^2]$
yield stress	σ_y	240	$[MPa]$
ANCHORS			
Property	Symbol	Value	Unit
type	-	4-strand cable anchor	$[-]$
free length	L_a	15.5	$[m]$
bond length	$L_a, bond$	6.0	$[m]$
angle	δ	45	$[deg]$
anchor cross sectional area	A_a	560	$[mm^2]$
yield stress	σ_y	1,570	$[MPa]$
mutual anchor distance	d_a	3.0	$[m]$
WALING			
Property	Symbol	Value	Unit
Type	-	2 x U 300	$[-]$
elastic section modulus	$W_{el,w}$	521.5	$[cm^3]$
moment of inertia	I_w	7,823	$[cm^4]$
yield stress	σ_y	355	$[MPa]$

In the following sections the results of the reliability calculations will be presented. Three variants are discussed:

1. Assessment of the reliability of the relevant limit states based on the deterministic design. Stochastic soil properties, deterministic structural parameters, deterministic pore pressures (design values for the phreatic levels, see section 9.1.3).

2. As 1, including stochastic pore pressures (normally distributed phreatic levels).

3. As 1, including uncertainties in the structural resistance due to corrosion.

9.2 Variant 1 - Stochastic Soil Properties

The reliability analysis is carried out with random soil properties, such that for most of the limit states the load is treated stochastically whereas the resistance is treated deterministically using nominal values. Of course, the soil properties influence both, the load and the resistance side, especially in case of soil shear failure.

The limit states are analyzed according to the descriptions in chapter 7. The results are combined to a system reliability respectively system failure probability.

9.2.1 Mean Value Calculation

For the following structural reliability calculations, statistical distributions will be used to describe the uncertainty in the relevant parameters. So far, the results of the deterministic design calculations included some 'bias' in form of conservatism that was introduced by statistical considerations (characteristic values), load and material factors (partial safety factors). Before starting the probabilistic calculations that are to a certain extent 'black box' processes, it is important to carry out some deterministic calculations and eventually a sensitivity analysis to get better insight into the problem. Some relevant results of the mean value calculation are presented. These respresent the expected behaviour of the structure (mean value = expectation).

Deformations

Whilst phase 1 creates only artificial deformations during the gravity loading[6], in phase 2 the top of the sheet pile wall deforms towards the excavation due to the decrease of support and the activation of the surcharge load. These deformations are partially reversed by the anchor pretension in the third phase. The largest deformations occur in the final excavation stage (phase 4) where a typical deformation pattern of an anchored wall is observed[7].

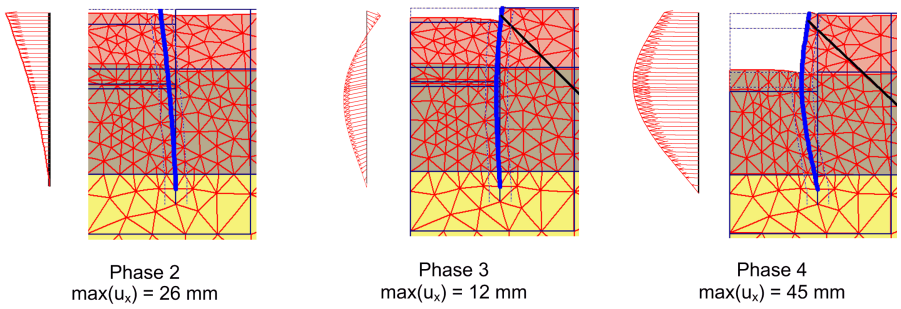

Figure 9.5: Deformations in Mean Value Calculation

[6]The displacements from the gravity loading phase are set to zero before starting the next phase.

[7]Note that almost no clamping occurs due to the small embedment depth in the firm sand layer. Possibly the design could be optimized by lowering the bending moment through applying a larger embedment depth.

The focus in this work is on the Ultimate Limit State. The Mohr-Coulomb model is used for the calculations which is commonly accepted for this purpose and should give conservative answers. It is however not very suitable for analyzing the soil deformations, like in this case the heave of the bottom of the excavation or the settlements behind the retaining wall[8].

The deformations that would occur due to the 'most likely' soil shear failure mechanism can be illustrated by carrying out a ϕ-c- reduction. Figure 9.6 shows that an active / passive failure mechanism occurs where the wall practically turns around the anchored point.

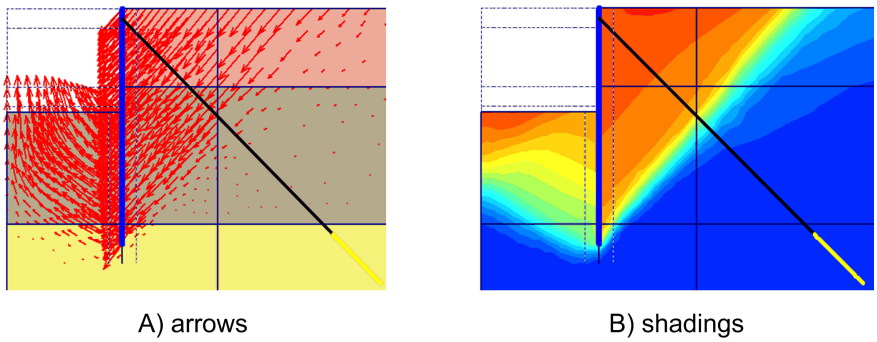

Figure 9.6: Deformations After ϕ-c-Reduction (mean values)

Anchor Forces

The anchors are installed and prestressed in phase 3 and therefore their prestress level of 80 kN/m is automatically the anchor force in this phase. In phase 4 the anchor force increases. For the mean values they increase to $F_a = 157.9kN/m$.

Bending Moments

By far, the largest bending moments are observed in the final excavation (phase 4). This bending moment will also be decisive for the respective limit state.

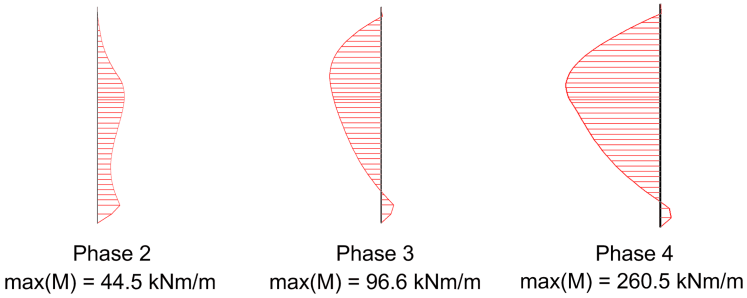

Figure 9.7: Bending Moments in Mean Value Calculation

[8]The settlements can even be obtained with the opposite sign, i.e. heave instead of settlements.

Shear Forces

The shear forces are not used in the following calculations, since their magnitudes show to be small compared to the bending moments, which are determinant for the sheet pile design. For sake of completeness, the shear force diagrams for phases 2 to 4 are shown in figure 9.8.

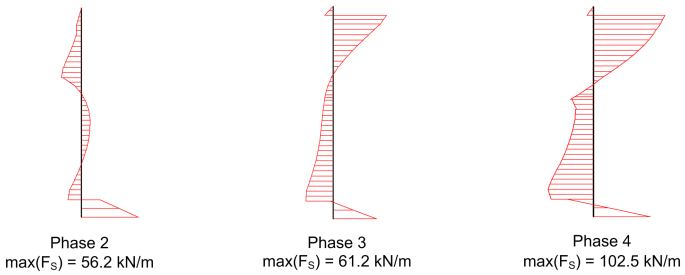

Figure 9.8: Shear Forces in Mean Value Calculation

Normal Forces

The normal forces F_N contribute to the maximum stresses in the outer fibre of the sheet pile. Therefore is interesting to see that in the expected situation high (almost maximum) values of the normal forces coincide with the maximum bending moments with respect to the depth-level.

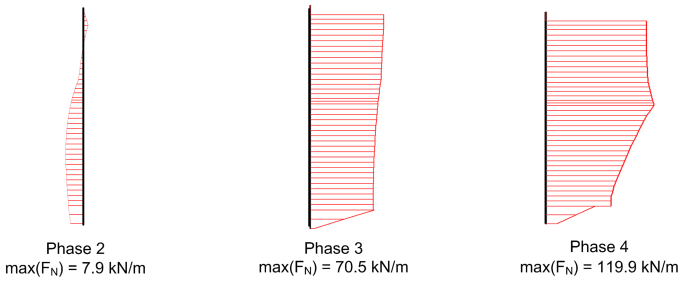

Figure 9.9: Normal Forces in Mean Value Calculation

Effective Stresses

The effective stress field is shown in figure 9.10 (A) and one can see (the crosses indicate the direction and magnitude of principle effective stresses) the passive soil behaviour on the excavation side ($\frac{\sigma_{xx}}{\sigma_{yy}} \gg 1$), whereas the oppsosite side shows an active behaviour ($\frac{\sigma_{xx}}{\sigma_{yy}} \ll 1$). The mobilized shear strength can be used for the soil shear failure limit state as discussed in section 7.5. In the clay layer on the right side of the wall, an arching effect is observed.

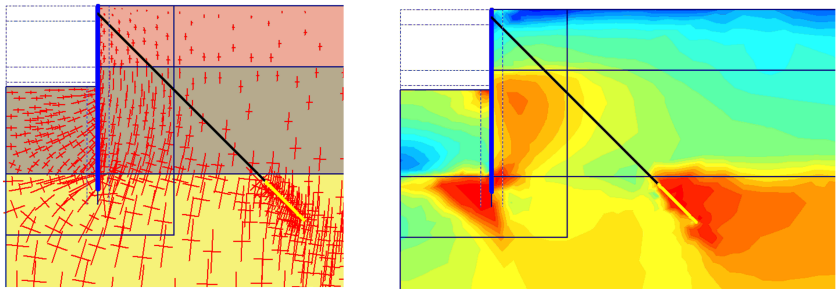

Figure 9.10: Effective Stresses in Mean Value Calculation

9.2.2 Limit State: Sheet Pile Failure

In this section we consider the strength properties of the structural members, here the sheet pile, to be deterministic constants. Therefore the general formulation of the limit state (see section 7.4.1) could be reduced[9] to:

$$Z = M_d - M_{max} \tag{9.3}$$

For sake of comparability with other calculations, where the strength properties will be varied or treated as stochastic quantities, the more general form is applied here:

$$Z = \sigma_y - \left(\frac{max[M(z)]}{W_{el}} + \frac{max[F_N(z)]}{A_{sp}} \right) \tag{9.4}$$

where σ_y is the nominal steel yield strength, $max[M(z)]$ is the maximum calculated moment over depth, W_{el} is the elastic section modulus of the sheet pile (for AZ18: $W_{el} = 1,800 cm^3/m$), $max[F_N(z)]$ is the maximum calculated normal force and A_{sp} (for AZ18: $A_{sp} = 150 cm^3/m$) cross sectional area of the sheet pile pile. This approach is conservative in the sense that $max[M(z)]$ and $max[F_N(z)]$ are combined, i.e. they are assumed to coincide with resp4ect to location.

The results are summarized in table 9.5 and figure 9.11.

[9] Additionally it is assumed that the normal force contribution to the stresses in the wall is negligible.

Number of calculations (FORM) : 99

Beta : 4.207E000
P_f : 1.293E-05

	Model	Parameter	alfa	X
1	Variable	Asp	0.000E00	1.500E002
2	Variable	E_clay	8.782E-01	1.328E003
3	Variable	E_peat	1.138E-01	7.332E002
4	Variable	Isp	0.000E00	3.420E004
5	Variable	Wel	0.000E00	1.800E003
6	Variable	gamma_sat_clay	-3.703E-02	1.864E001
7	Variable	gamma_sat_peat	-1.742E-01	1.358E001
8	Variable	nu_clay	-3.195E-01	3.959E-01
9	Variable	nu_peat	1.067E-01	3.354E-01
10	Variable	phi_clay	3.678E-02	2.048E001
11	Variable	phi_peat	-3.365E-05	2.378E001
12	Variable	phi_sand	6.448E-02	3.390E001
13	plaxis	Cref clay	7.851E-02	1.369E001
14	plaxis	Cref peat	-1.886E-03	7.366E000
15	plaxis	Rinter clay	2.427E-01	4.736E-01
16	plaxis	Rinter peat	-6.505E-03	6.078E-01
17	Variable	sig_y	0.000E00	2.400E002

Table 9.5: Reliability Results Sheet Pile Failure

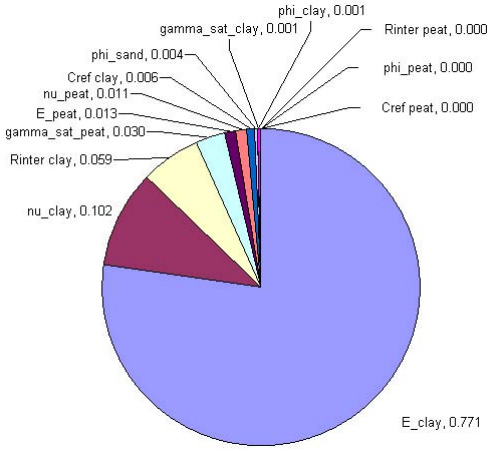

Figure 9.11: Influence Factors α_i^2 Sheet Pile Failure

The calculations were carried out with FORM[10]. The influence coefficients indicate that this limit state is dominated by the (shear) stiffness of the clay layer (remember: $G = \frac{E}{2(1+\nu)}$). Furthermore, it seems that the stiffness of the peat and its unit weight as well as the interface strength between clay and the sheet pile have influence, whilst the rest of the variables could be negligible. It can be concluded that the problem is still in the elastic domain. In case of predominantly plastic behavior we should obtain that the strength properties of the soil become more important.

Figure 9.12 gives a possible explanation for the results. Apparently the lower stiffness of the clay layer in the design point has lead to a descreased arching effect and thereby the horizontal load on the wall was increased.

[10] An analysis with DARS (level III) with comparable results confirmed the applicability of FORM for this limit state (see appendix L).

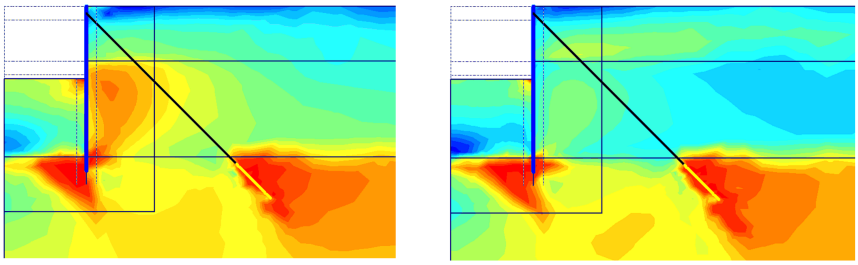

Figure 9.12: Normal Forces in Mean Value Calculation

The calculations were repeated using only the 5 most influential random variables to investigete the effect of reducing the number of random variables. The results are summarized in table 9.6.

Number of calculations (FORM) : 37

Beta : 4.379E000
P_f : 5.970E-06

	Model	Parameter	alfa	X
1	Variable	Asp	0.000E00	1.500E002
2	Variable	E_clay	9.060E-01	1.242E003
3	Variable	E_peat	1.002E-01	7.405E002
4	Variable	Isp	0.000E00	3.420E004
5	Variable	Wel	0.000E00	1.800E003
6	Variable	gamma_sat_clay	0.000E00	1.850E001
7	Variable	gamma_sat_peat	-1.862E-01	1.363E001
8	Variable	nu_clay	-3.531E-01	4.019E-01
9	Variable	nu_peat	9.906E-02	3.359E-01
10	Variable	phi_clay	0.000E00	2.090E001
11	Variable	phi_peat	0.000E00	2.390E001
12	Variable	phi_sand	0.000E00	3.500E001
13	plaxis	Cref clay	0.000E00	1.490E001
14	plaxis	Cref peat	0.000E00	7.500E000
15	plaxis	Rinter clay	0.000E00	6.000E-01
16	plaxis	Rinter peat	0.000E00	6.000E-01
17	Variable	sig_y	0.000E00	2.400E002

Table 9.6: Reliability Results Sheet Pile Failure with Reduced Parameter Set

The reliability index changes slightly from $\beta = 4.2$ to $\beta = 4.4$ (roughly a factor 2 in P_f). The relative influences do not change significantly (the absolute influence coefficients increase due to a normalization procedure to $\sum \alpha_i = 1$). Another calculation with only E_{clay} and ν_{clay} as random variables gave $\beta = 4.5$.

It is remarkable that the stiffness of the soil is dominant for the contemplated realistic problem. In design practice much attention is paid to the strength parameters. This result suggests to invest more effort into a proper determination of the stiffness properties as well.

9.2.3 Limit State: Support Failure

For the support reliability we will have to determine two failure probabilities, the anchor and the waling. The crucial part is the determination of the anchor failure probability. The load on the waling is proportional to the anchor force. The waling can also be designed deterministically, if we determine the anchor reliability by calculating the exceedance probability for a certain admissible anchor force. Then the failure probability of the waling must automatically be lower (given that only uncertainties in the loads are considered).

To this end we reduce the general formulation of the limit state (see section 7.4.2) to:

$$Z = F_{a,d} - F_a \tag{9.5}$$

where $F_{a,d} = 1570\ MPa \cdot 420\ mm^2/3\ m = 220\ [kN/m]$ is the design anchor force per m sheet pile wall (in z-direction) and $F_a\ [kN/m]$ is the calculated anchor force.
The results are summarized in table 9.7 and figure 9.13.

Number of calculations (FORM) : 99

Beta : 5.645E000
P_f : 8.273E-09

	Model	Parameter	alfa	X
1	Variable	Aa	0.000E00	4.200E002
2	Variable	E_clay	8.286E-01	1.043E003
3	Variable	E_peat	1.352E-01	6.837E002
4	Variable	La	0.000E00	3.000E000
5	Variable	gamma_sat_clay	-3.494E-02	1.868E001
6	Variable	gamma_sat_peat	-3.101E-01	1.424E001
7	Variable	nu_clay	-2.878E-01	4.042E-01
8	Variable	nu_peat	-2.474E-01	3.975E-01
9	Variable	phi_clay	1.859E-02	2.058E001
10	Variable	phi_peat	-7.212E-07	2.378E001
11	Variable	phi_sand	4.187E-02	3.401E001
12	plaxis	Cref clay	5.579E-02	1.373E001
13	plaxis	Cref peat	-2.385E-03	7.374E000
14	plaxis	Rinter clay	2.200E-01	4.454E-01
15	plaxis	Rinter peat	2.113E-03	6.029E-01
16	Variable	sig_y	0.000E00	1.570E003

Table 9.7: Reliability Results Anchor Failure

The calculations were carried out with FORM[11] and the results regarding the influence of the stochastic variables are comparable to the previous limit state. Again the problem is still in the elastic domain and the stiffness parameters of the soft soil layers are the most influential ones. This is not surprising, since the nature of the loads that generate high anchor forces as well as high bending moments in the sheet pile is the same, namely the horizontal load on the sheet pile.

[11] An analysis with DARS (level III) with comparable results confirmed the applicability of FORM for this limit state (see appendix L).

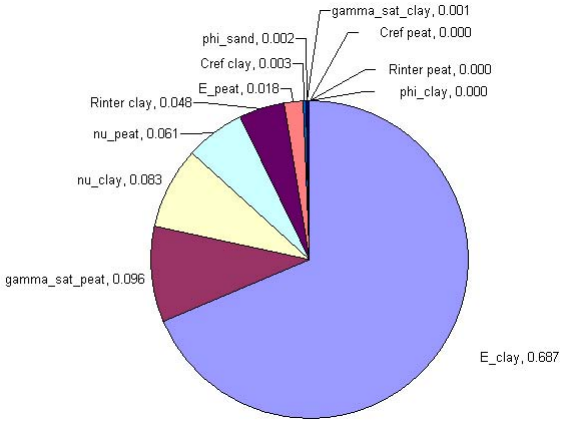

Figure 9.13: Influence Factors α_i^2 Anchor Failure

Repeating the calculations using only the 6 most influential random variables for investigating the effect of reducing the number of random variables leads to the results summarized in table 9.8.

Number of calculations (FORM) : 50

Beta : 5.672E000
P_f : 7.080E-09

	Model	Parameter	alfa	X
1	Variable	Aa	0.000E00	4.200E002
2	Variable	E_clay	8.191E-01	1.051E003
3	Variable	E_peat	1.599E-01	6.600E002
4	Variable	La	0.000E00	3.000E000
5	Variable	gamma_sat_clay	0.000E00	1.850E001
6	Variable	gamma_sat_peat	-2.984E-01	1.420E001
7	Variable	nu_clay	-3.112E-01	4.082E-01
8	Variable	nu_peat	-2.435E-01	3.970E-01
9	Variable	phi_clay	0.000E00	2.090E001
10	Variable	phi_peat	0.000E00	2.390E001
11	Variable	phi_sand	0.000E00	3.500E001
12	plaxis	Cref clay	0.000E00	1.490E001
13	plaxis	Cref peat	0.000E00	7.500E000
14	plaxis	Rinter clay	2.414E-01	4.293E-01
15	plaxis	Rinter peat	0.000E00	6.000E-01
16	Variable	sig_y	0.000E00	1.570E003

Table 9.8: Reliability Results Anchor Failure with Reduced Parameter Set

The reliability index changes slightly from $\beta = 5.65$ to $\beta = 5.67$. The relative influences do not change significantly. Another calculation with only E_{clay} and ν_{clay} as random variables gave $\beta = 6.52$. This illustrates the effect of increasing reliability for uncertainty reduction, but also that for this limit state the stiffness of the clay layer was not as dominant as for the sheet pile itself.

9.2.4 Limit State: Soil Shear Failure

The calculations for this limit state were carried out using the *limit equilibrium* methodology explained in section 7.5. The limit state is thus:

- $Z = 1$, if equilibrium is reached in all calculation phases.
- $Z = -1$, otherwise.

As explained the directional sampling method was applied for this type of limit state definition. The results are summarized in table 9.9 and figure 9.14.

Number of calculations (Directional Sampling) : 1653

Beta : 3.360E000
P_f : 3.900E-04

	Model	Parameter	alfa	X
1	Variable	Asp	0.000E00	1.500E002
2	Variable	E_clay	3.344E-01	2.501E003
3	Variable	E_peat	3.724E-01	6.065E002
4	Variable	Isp	0.000E00	3.420E004
5	Variable	Wel	0.000E00	1.800E003
6	Variable	gamma_sat_clay	6.283E-01	1.654E001
7	Variable	gamma_sat_peat	1.141E-01	1.285E001
8	Variable	nu_clay	-1.254E-02	3.531E-01
9	Variable	nu_peat	6.861E-02	3.433E-01
10	Variable	phi_clay	2.302E-01	1.925E001
11	Variable	phi_peat	4.292E-02	2.344E001
12	Variable	phi_sand	2.967E-01	3.153E001
13	plaxis	Cref clay	9.473E-02	1.372E001
14	plaxis	Cref peat	-2.887E-01	8.912E000
15	plaxis	Rinter clay	-1.091E-01	6.496E-01
16	plaxis	Rinter peat	-1.831E-01	6.793E-01
17	Variable	sig_y	0.000E00	2.400E002

Table 9.9: Reliability Results Soil Shear Failure

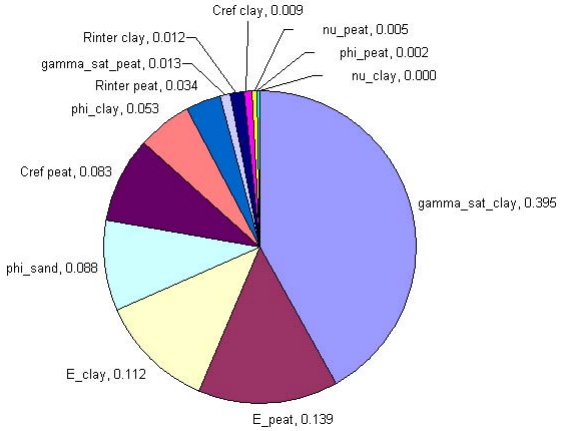

Figure 9.14: Influence Factors α_i^2 Soil Shear Failure

It should be mentioned that the influence coefficients that are obtained in Directional Sampling are based on approximating assumptions[12].

[12]The point on the limit state with the highest probability density is assumed to be the design point. The influence factors are determined, as if a linearization was carried out in this point.

9.2.5 System Failure

As discussed in chapter 7.6, two methods are applied to calculate the system failure probability, one that works by combining FORM-results and the other by carrying out one calculation that includes all relevant limit states at once.

Method 'Hohenbichler'

Using the Hohenbichler approach FORM results can be defined using the outcomes for β_i of the limit states Z_i (with $i = 1, ..., m$) and the (common) influence coefficients α_{ij} (with $j = 1, ..., n$). An important step is the determination of the correlation between the limit states. The measure that is used here is the correlation coefficient that is determined in the following way.

$$\rho = \sum_{j=1}^{n} \alpha_{1j}\alpha_{2j} \tag{9.6}$$

Since the product of these coefficients is small, the contribution of relatively small α_{ij} will be negligible. Therefore only the α_{ij} where at least one of the couple $(\alpha_{1j}, \alpha_{2j})$ is larger than 0.1 are taken into account. This also deals with the fact that for the different limit states not all variables have been treated stochastically. By assuming the respective α to be zero, thus unimportant, we can still carry out the analysis.

This way the relevant reliability analysis results can be reduced to table 9.10.

Table 9.10: Data for System Reliability Analysis

	Limit State:	1) Sheet Pile	2) Anchor	3) Soil
	Method:	FORM	FORM	DS
	β	4.38	5.67	3.36
	P_f	5.07 E-6	7.08 E-9	3.90 E-4
	α_{ij}			
1	E_{clay}	0.906	0.812	0.344
2	E_{peat}	0.100	0.160	0.372
3	$\gamma_{sat,clay}$	0.000	0.000	0.628
4	$\gamma_{sat,peat}$	-0.186	-0.298	0.114
5	ν_{clay}	-0.353	-0.311	0.000
6	ν_{peat}	-0.100	-0.244	0.000
7	ϕ_{clay}	0.000	0.000	0.230
8	ϕ_{sand}	0.000	0.000	0.297
9	c_{peat}	0.000	0.000	-0.289
10	$R_{inter,clay}$	0.000	0.241	-0.109
11	$R_{inter,peat}$	0.000	0.000	-0.183

Using equation 9.6 we obtain for the mutual correlation between the limit states the following correlation coefficients:

Table 9.11: Correlation Coefficients

$\rho_{1,2}$	$\rho_{1,3}$	$\rho_{2,3}$
0.947	0.328	0.281

What can be seen from the correlation coefficients, is that the sheet pile and the anchor limit state seem to fail under the same load conditions, which results in the high value of $\rho_{1,2}$.

Since the differences in the failure probabilities are large, it is not worth to carry out the rest of the calculation procedure. The upper bound for the system failure probability is

$$P_f = P_{f,1} + P_{f,2} + P_{f,3} = 5.07 \cdot 10^{-6} + 7.08 \cdot 10^{-9} + 3.90 \cdot 10^{-4} = 3.95 \cdot 10^{-4}$$

which is very close to β_3, which is the lower bound and also leads to a $\beta = 3.36$.

Directional Sampling with Combined Limit States

According to the ideas presented in chapter 7.6 also a calculation with all the three limit states in combination has been carried out. The previously described adapted Directional Sampling method was applied for this purpose. The according limit state function was:

$$Z = min[\{limitcheck\}, \{\sigma_{y,sp} - \left(\frac{M}{W_{el}} + \frac{F_N}{A_s p}\right)\}, \{\sigma_{y,a} - fracF_a A_a\}] \tag{9.7}$$

where *limitcheck* is 1, if all calculation phases reached equilibrium and -1 otherwise.

This calculation leads to $\beta = 3.34$, which is basically the same result as in the previous paragraph. Unfortunately with this combination of relevant failure probabilities the added value of this calculation method could not be demonstrated.

9.3 Variant 2 - Stochastic Pore Pressures

In contrast to the first variant, the phreatic levels on both sides are not assumed in their design values, but rather as stochastic quantities. For both sides a mean level, a standard deviation and a normal distribution are assumed. The aim is to demonstrate the impact of accounting for the uncertainties in the groundwater levels in a probabilistic manner instead of using deterministic design values. The calculations were carried out for sheet pile and anchor reliability[13].

9.3.1 Probabilistic Treatment of Phreatic Levels

In the deterministic calculations the water levels were treated deterministically. In phases 1-3, the general phreatic line was situated at $pl1 = -1.57m$, which resulted from the assumed distribution $pl1 \sim N(-2.0, 0.5)[m]$ and the safety considerations in the CUR 166 [8]. In the final excavation phase 4 (steady state) the phreatic level on the excavation side was lowered to $pl1 = -5.84m$. The underlying distribution was $pl2 \sim N(-5.5, 0.2)[m]$. A cluster on the excavation side assumed this level $pl2$ on its top boundary and $pl1$ at the lower boudary, whereas the values in between were interpolated[14].

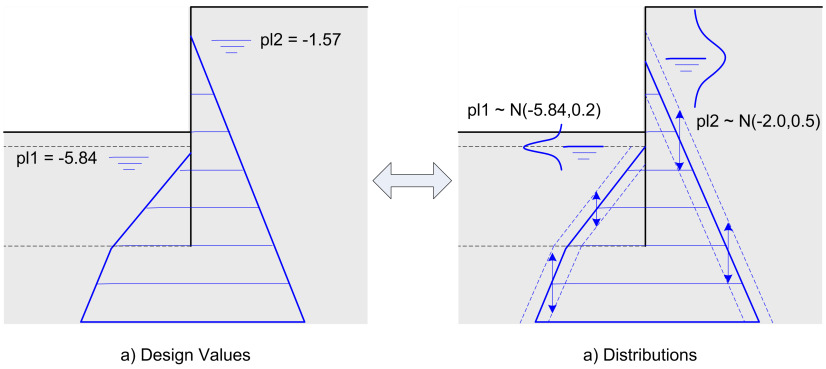

Figure 9.15: Deterministic (a) vs. Stochatic Pore Pressure Treatment (b)

In this variant of the case study the general pore pressure generation principle (two phreatic lines, interpolation cluster) is applied using the stochastic properties of the phreatic lines. That means that, according to the reliability method used, a realization of phreatic lines $pl1$ and $pl2$ is sent to a Matlab-routine that manipulates the pore pressure field before the Finite Element calculation is carried out (see section 6.3).

[13] Due to the high calculation effort for the soil shear failure limit state using Directional Sampling, these results could not be included here, but the impact should certainly be investigated.

[14] This way a jump of the pore pressures at the tip if the sheet pile is avoided.

9.3.2 Limit State: Sheet Pile Failure

Initially the results of a sensitivity study are presented and subsequently the effects of this manner of taking the uncertainties in the phreatic lines into account are discussed.

Sensitivity Study

For estimating the impact of the phreatic levels on the given problem configuration, several deterministic combinations of $pl1$ and $pl2$ were assessed. The results are listed in table 9.12 and illsutrated in figure 9.16. Note that the combination ($pl1 = -5.5m$ / $pl2 = -2.0m$) is the mean value calculation.

Table 9.12: Bending Moments for Different Combinations of Phreatic Lines

[kNm/m]	$pl2 = -3.0m$	$pl2 = -2.5m$	$pl2 = -2.0m$	$pl2 = -1.5m$	$pl2 = -1.0m$
$pl1 = -5.9m$	241.7	249.0	256.1	262.2	268.8
$pl1 = -5.7m$	240.2	247.3	254.2	260.2	267.0
$pl1 = -5.5m$	238.2	245.7	252.5	258.1	265.0
$pl1 = -5.3m$	235.9	243.7	250.3	256.3	262.8

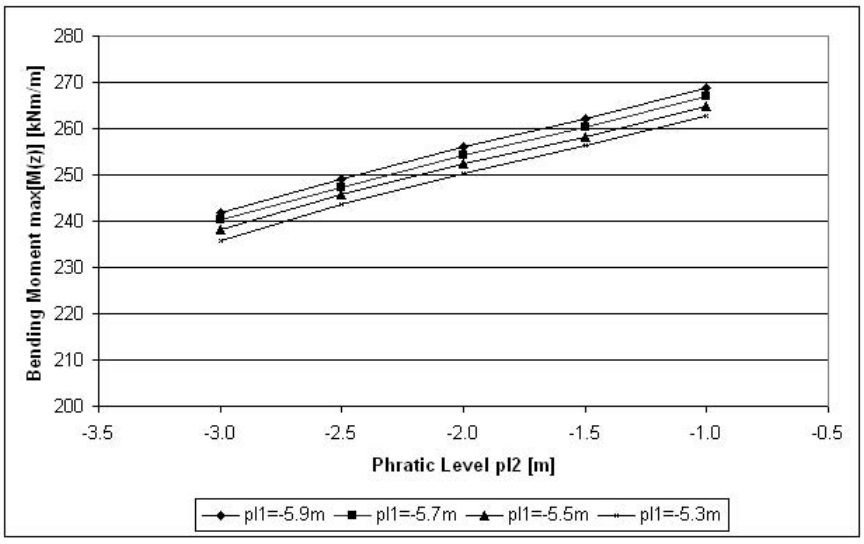

Figure 9.16: Bending Moments for Different Combinations of Phreatic Lines

Note that the chosen step size for the variation of this sensitivity study is one standard deviation for each variable. The larger variance in $pl2$ leads to larger effects on the maximum bending moments. However, based on the impact that was found by these results, it can be expected that there is only a small effect of the uncertainty in the water levels on the reliability for this limit state.

Comparison with Design Values

A reliability calculation was carried out using the earlier mentioned basic assumptions for the distributions of the phreatic levels. The results are summarized in table 9.13 and figure 9.17.

Number of calculations (FORM) : 57

Beta : 4.469E000
P_f : 3.941E-06

	Model	Parameter	alfa	X
1	Variable	Asp	0.000E00	1.500E002
2	Variable	E_clay	8.721E-01	1.263E003
3	Variable	E_peat	1.130E-01	7.285E002
4	Variable	Isp	0.000E00	3.420E004
5	Variable	Wel	0.000E00	1.800E003
6	Variable	gamma_sat_clay	0.000E00	1.850E001
7	Variable	gamma_sat_peat	-1.837E-01	1.363E001
8	matlab	pl1	1.223E-01	-5.664E000
9	matlab	pl2	-2.618E-01	-1.415E000
10	Variable	nu_clay	-3.112E-01	3.973E-01
11	Variable	nu_peat	1.118E-01	3.335E-01
12	Variable	phi_clay	0.000E00	2.090E001
13	Variable	phi_peat	0.000E00	2.390E001
14	Variable	phi_sand	0.000E00	3.500E001
15	plaxis	Cref clay	0.000E00	1.490E001
16	plaxis	Cref peat	0.000E00	7.500E000
17	plaxis	Rinter clay	0.000E00	6.000E-01
18	plaxis	Rinter peat	0.000E00	6.000E-01
19	Variable	sig_y	0.000E00	2.400E002

Table 9.13: Reliability Results Stochastic Phreatic Levels

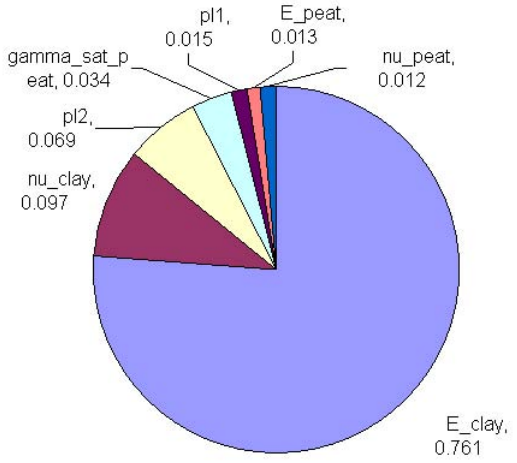

Figure 9.17: Influence Factors α_i^2 Stochastic Phreatic Levels

We can conclude that the assumptions for the design water levels were conservative in this case. The stochastic treatment of the phreatic levels lead to a higher reliability ($\beta = 4.47$ compared to $\beta = 4.21$).

The influence factors reflect that the uncertainty in both phreatic lines contributes to the response uncertainty. The smaller uncertainty on the excavation side is reflected in a smaller influence factor. The stiffness of the clay layer remains the dominant variable.

Influence of Amount of Uncertainty in the Phreatic Levels

In order to investigate the influence of the amount of variability in the groundwater heads, a parametric study has been carried out with several combinations of the standard deviations σ_{pl1} and σ_{pl2}. The results are summarized in table 9.14 and figure 9.18.

Table 9.14: Sheet Pile Reliability for Combinations of Standard Deviations of Phreatic Lines

β (P_f)	$\sigma_{pl2} = 0.3m$	$\sigma_{pl2} = 0.5m$	$\sigma_{pl2} = 0.7m$
$\sigma_{pl1} = 0.1m$	4.57 (2.42E-06)	4.49 (3.57E-06)	4.38 (5.99E-06)
$\sigma_{pl1} = 0.2m$	4.57 (2.49E-06)	4.48 (3.68E-06)	4.36 (6.48E-06)
$\sigma_{pl1} = 0.3m$	4.53 (2.94E-06)	4.47 (3.94E-06)	4.35 (6.71E-06)
$\sigma_{pl1} = 0.4m$	4.53 (3.01E-06)	4.45 (4.32E-06)	4.33 (7.37E-06)

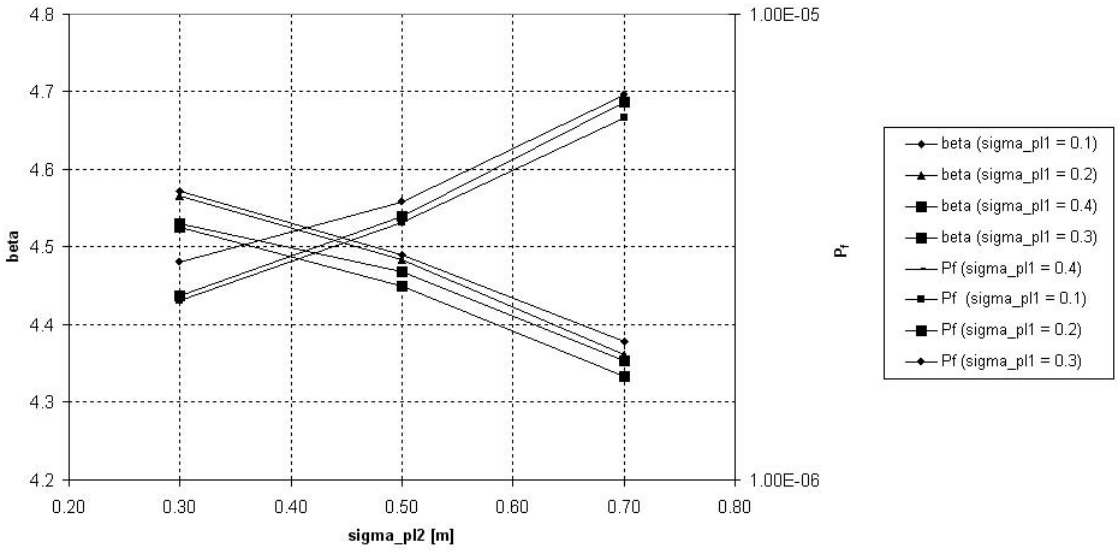

Figure 9.18: Reliability with Varying Uncertainty in Phreatic Levels

This parametric study confirms what is expected according to the sensitivity study. The impact of the phreatic levels within reasonable ranges of variability of the phreatic lines is relatively small. It is however remarkable that the calculation results are as expected in a sense that for in increasing uncertainty in the groundwater levels also a decrease in reliability was found and vice versa, even for small changes. That provides some trust in stability of the applied calculation methods.

9.3.3 Limit State: Anchor Failure

For this limit state the same analysis as for the sheet pile is carried out. Initially the results of a sensitivity study are presented and subsequently the effects of this manner of taking the uncertainties in the phreatic lines into account are discussed.

Sensitivity Study

For estimating the impact of the phreatic levels on the given problem configuration, several deterministic combinations of $pl1$ and $pl2$ were assessed. The results are listed in table 9.15 and illsutrated in figure 9.19. Note that the combination ($pl1 = -5.5m$ / $pl2 = -2.0m$) is the mean value calculation.

Table 9.15: Anchor Forces for Different Combinations of Phreatic Lines

[kN/m]	$pl2 = -3.0m$	$pl2 = -2.5m$	$pl2 = -2.0m$	$pl2 = -1.5m$	$pl2 = -1.0m$
$pl1 = -5.9m$	138.3	143.3	149.0	155.2	162.8
$pl1 = -5.7m$	137.9	142.8	148.4	154.7	162.2
$pl1 = -5.5m$	137.3	142.3	147.9	154.2	161.6
$pl1 = -5.3m$	136.8	141.8	147.3	153.5	160.9

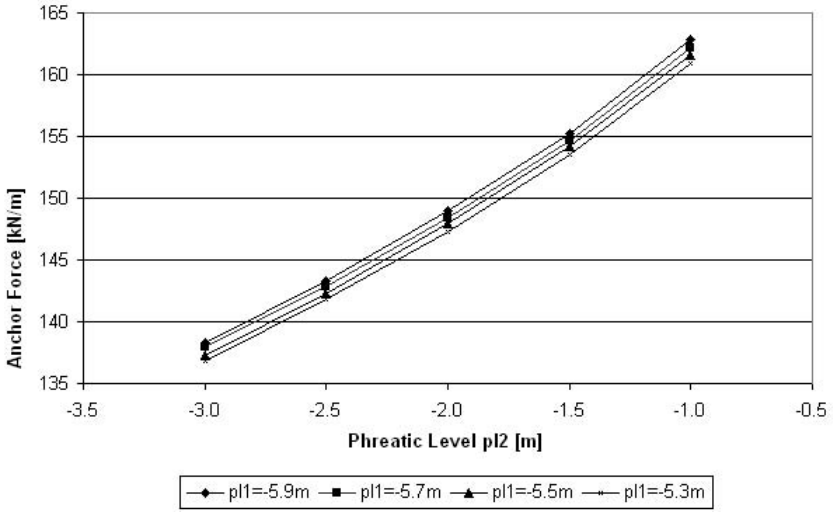

Figure 9.19: Anchor Forces for Different Combinations of Phreatic Lines

Qualitatively the same impact as for the bending moments is also found for the anchors. Larger differences in phreatic levels lead to higher horizontal loads on the wall, which themselve lead to higher anchor forces.

Comparison with Design Values

A reliability calculation was carried out using the earlier mentioned basic assumptions for the distributions of the phreatic levels. The results are summarized in table 9.16 and figure 9.20.

Number of calculations (FORM) : 46

Beta : 5.105E000
P_f : 1.658E-07

	Model	Parameter	alfa	X
1	Variable	Aa	0.000E00	4.200E002
2	Variable	E_clay	6.739E-01	1.414E003
3	Variable	E_peat	1.054E-01	7.226E002
4	Variable	La	0.000E00	3.000E000
5	Variable	gamma_sat_clay	0.000E00	1.850E001
6	Variable	gamma_sat_peat	-1.843E-01	1.371E001
7	matlab	pl1	5.657E-02	-5.558E000
8	matlab	pl2	-6.794E-01	-2.658E-01
9	Variable	nu_clay	-1.066E-01	3.704E-01
10	Variable	nu_peat	-5.680E-02	3.618E-01
11	Variable	phi_clay	0.000E00	2.090E001
12	Variable	phi_peat	0.000E00	2.390E001
13	Variable	phi_sand	0.000E00	3.500E001
14	plaxis	Cref clay	0.000E00	1.490E001
15	plaxis	Cref peat	0.000E00	7.500E000
16	plaxis	Rinter clay	1.460E-01	5.091E-01
17	plaxis	Rinter peat	0.000E00	6.000E-01
18	Variable	sig_y	0.000E00	1.570E003
19	Variable	stdpl1	0.000E00	2.000E-01
20	Variable	stdpl2	0.000E00	5.000E-01

Table 9.16: Reliability Results Stochastic Phreatic Levels

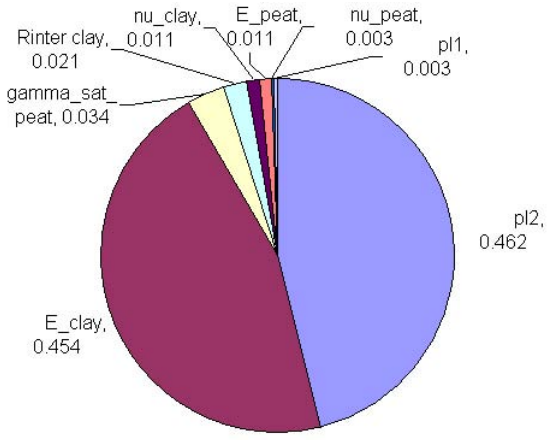

Figure 9.20: Influence Factors α_i^2 Stochastic Phreatic Levels

In contrast to the previous limit state, for the anchor forces we find a lower reliability with the probabilistic treatment of the phreatic lines ($\beta = 5.11$) than for the design groundwater levels ($\beta = 5.67$). Nevertheless, the value fulfills the target reliability of $\beta = 3.4$.

The influence of the phreatic level on the load side turns out to be as important as the stiffness of the clay layer (Young's modulus Eclay) in this case.

Influence of Amount of Uncertainty in the Phreatic Levels

In order to investigate the influence of the amount of variability in the groundwater heads, a parametric study has been carried out with several combinations of the standard deviations σ_{pl1} and σ_{pl2}. The results are summarized in table 9.17 and figure 9.21.

Table 9.17: Anchor Reliability for Combinations of Standard Deviations of Phreatic Lines

β (P_f)	$\sigma_{pl2} = 0.3m$	$\sigma_{pl2} = 0.5m$	$\sigma_{pl2} = 0.7m$
$\sigma_{pl1} = 0.1m$	5.83 (2.84E-09)	5.12 (1.57E-07)	4.29 (8.90E-06)
$\sigma_{pl1} = 0.2m$	5.81 (3.15E-09)	5.11 (1.66E-07)	4.29 (9.09E-06)
$\sigma_{pl1} = 0.3m$	5.78 (3.82E-09)	5.09 (1.76E-07)	4.28 (9.23E-06)
$\sigma_{pl1} = 0.4m$	5.79 (3.49E-09)	5.08 (1.85E-07)	4.28 (9.58E-06)

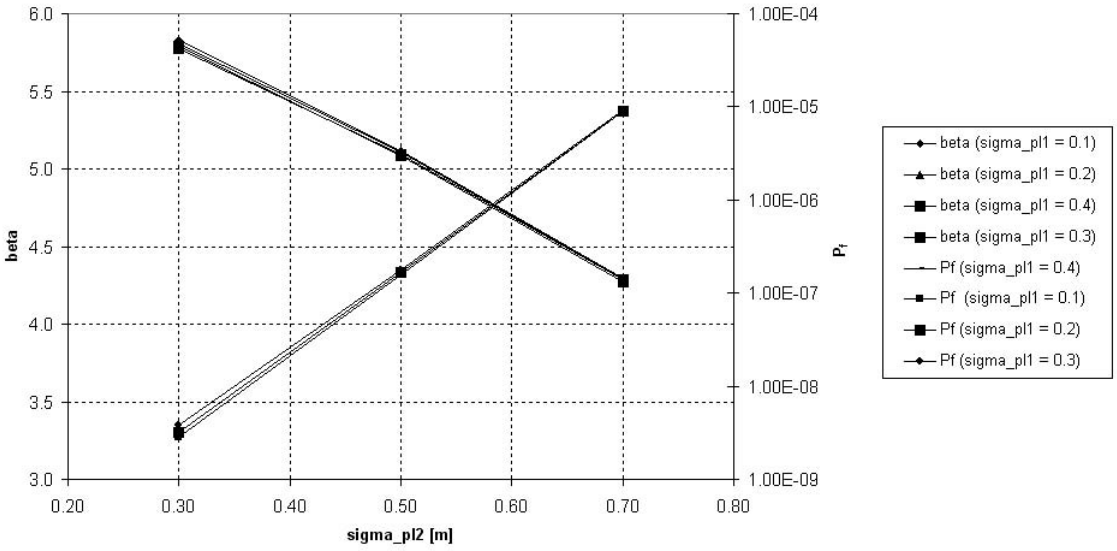

Figure 9.21: Reliability with Varying Uncertainties in Phreatic Levels

The impact of the phreatic levels within reasonable ranges of uncertainty is larger for the anchor limit state compared to the sheet pile limit state (which is mainly due to the bending moments). In terms of failure probabilities we can observe differences in the order of a factor of 10^3 within the investigated reasonable ranges of uncertainty.

It is also remarkable that in this case $pl2$ (load side) is significantly more dominant than $pl1$ (excavation side). An intuitive explanation could be that the anchor forces are dominated by the total horizontal load in the upper part on the wall, whereas for the bending moment, the pressure difference over the whole depth is determinant, where balancing elements like the passive earth pressure are present.

9.4 Variant 3 - Stochastic Corrosion Allowance

The uncertainties in the material properties of structural members applied in this case study are usually small and it is not worthwhile include them in the probabilistic analysis. The strength reduction over time, e.g. due to corrosion, however, can have a considerable impact on the reliability of the structure. Furthermore, the magnitude of this strength reduction is uncertain. Therefore the effects of stochastic corrosion on the reliability of the structural elements (sheet piles and anchors) are investigated.

For the calculations several assumptions were made with respect to the corrosion rate. A reference period of 100 years is contemplated. For this period the following distributions were assumed for the corrosion rates, based on the characteristic values from EC3 and assumptions for the mean values (see table 9.18).

Table 9.18: Corrosion Rates in [mm/m2/100 year]

	Distribution	μ	σ	shift	95%-value
Peat	Lognormal	2.0	0.67	0.0	3.25
Clay	Lognormal	0.6	0.32	0.0	1.20

Within the respective soil layers the corrosion is assumed to be homogeneous.

9.4.1 Limit State: Sheet Pile Failure

The general idea of the limit state function that is applied for including the strength reduction in the reliability analysis is illustrated in figure 9.22.

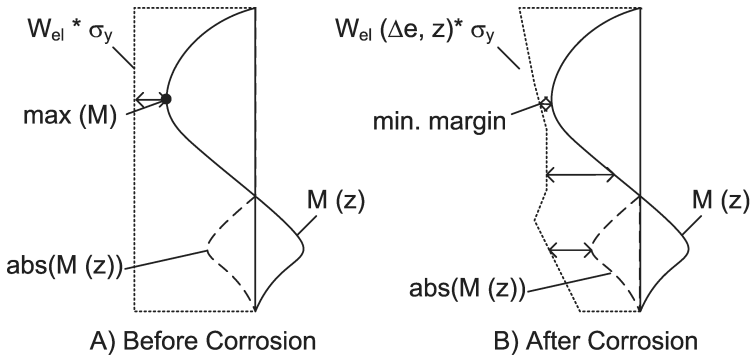

Figure 9.22: The Effect of Corrosion on the Moment Capacity of a Sheet Pile

After installation of the sheet pile, assuming that there are no relevant geometrical imperfections in the profile, the moment capacity $M_d = W_{el} \cdot \sigma_y$ is constant over depth. Therefore it was sufficient to consider the maximum (absolute) bending moment that was calculated over the whole depth in the previous calculations. When corrosion is included, we have to determine rather the minimum margin between strength (in form of M_d) and load M over depth, that does not necessarily coincide with the position of the maximum bending moment. That is because

the strength has become a function of depth. $W_{el}(\Delta e, z)$ is a geometrical property of the sheet pile profile that is influenced by corrosion. Δe, the thickness loss, can itself be a function of depth and therefore also $W_{el}(\Delta e, z)$ becomes a function of depth. The same is applicable for the cross sectional area A_{SP} that contributes to the stresses in the outer fibre together with the normal force F_N.

Due to this reason we apply the limit state function in its general form as discussed in section 7.4.1, extended by the thickness loss Δe:

$$Z = \sigma_y - \sigma = \sigma_y - \left(\frac{M(z)}{W_{el}(\Delta e, z)} + \frac{F_n(z)}{A_{SP}(\Delta e, z)} \right) \tag{9.8}$$

The corrosion assumptions simplify the problem basically to two zones, the peat and the clay layer, but we do not know beforehand where the maximum bending moment will occur. The discretization over depth to find the minimum value of the limit state function over depth is carried out in a Matlab-subroutine.

For the reduction of the geometrical properties by corrosion the following relations were used:

- For the cross sectional area an initial thickness e and intial cross sectional area $A_{SP,0}$ are reduced by Δe:

$$A_{SP}(\Delta e, z) = A_{SP,0} \frac{e - \Delta e}{e} \tag{9.9}$$

- The decrease of the elastic section modulus W_{el} [cm3/m] is nearly linearly dependent on the thickness loss Δe [mm] according to Houyoughes (2000):

$$W_{el} = W_{el,0} - 160 \cdot \Delta e \tag{9.10}$$

A calculation with the preceding assumptions for this calculation example with an AZ18 sheet pile profile gave the results that are presented in table 9.19.

Number of calculations (FORM) : 46

Beta : 1.981E000
P_f : 2.379E-02

	Model	Parameter	alfa	X
1	Variable	Asp_ini	0.000E00	1.500E002
2	Variable	E_clay	5.003E-01	2.584E003
3	Variable	E_peat	9.439E-02	7.877E002
4	Variable	Isp	0.000E00	3.420E004
5	Variable	Wel_ini	0.000E00	1.800E003
6	Variable	delta_t	-8.294E-01	3.241E000
7	Variable	e_ini	0.000E00	9.500E000
8	Variable	gamma_sat_clay	0.000E00	1.850E001
9	Variable	gamma_sat_peat	-8.459E-02	1.321E001
10	Variable	nu_clay	-1.839E-01	3.643E-01
11	Variable	nu_peat	1.091E-01	3.439E-01
12	Variable	phi_clay	0.000E00	2.090E001
13	Variable	phi_peat	0.000E00	2.390E001
14	Variable	phi_sand	0.000E00	3.500E001
15	plaxis	Cref clay	0.000E00	1.490E001
16	plaxis	Cref peat	0.000E00	7.500E000
17	plaxis	Rinter clay	0.000E00	6.000E-01
18	plaxis	Rinter peat	0.000E00	6.000E-01
19	Variable	sig_y	0.000E00	2.400E002

Table 9.19: Reliability Results Natural Corrosion with AZ18

The structure does not fulfill the requirements using these corrosion assumptions anymore. In order to find a profile for which the target reliability of $\beta = 3.4$ can be achieved, a parametric

study on the section modulus has been carried out[15]. The results are summarized in figure 9.23. The results indicate that at least an AZ25 profile is necessary to fulfill the requirements. A calculation using this AZ25 profile resulted in the outcomes in table 9.20.

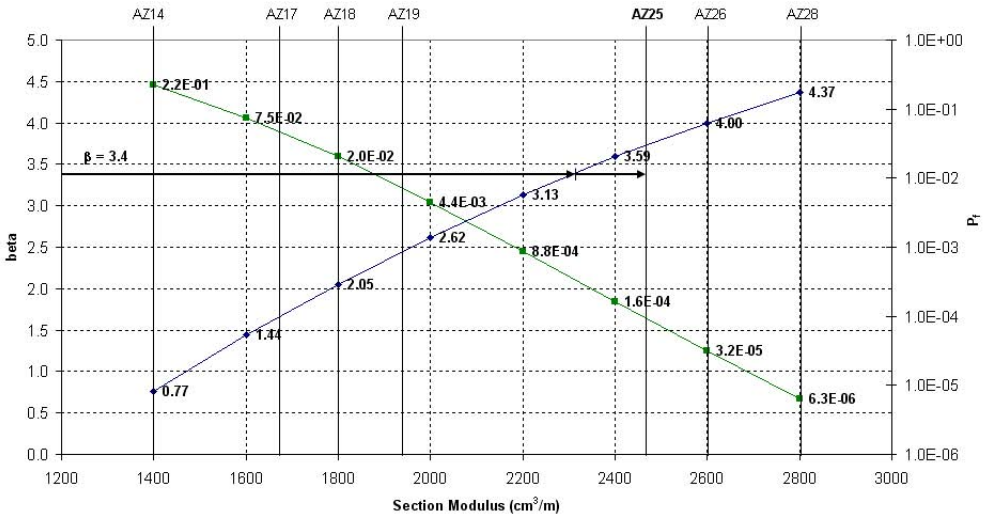

Figure 9.23: Reliability As Function of Sheet Pile Type (section modulus)

Number of calculations (FORM) : 51

Beta : 3.713E000
P_f : 1.023E-04

	Model	Parameter	alfa	X
1	Variable	Asp_ini	0.000E00	1.850E002
2	Variable	E_clay	4.077E-01	2.272E003
3	Variable	E_peat	4.642E-02	7.905E002
4	Variable	Isp	0.000E00	5.225E004
5	Variable	La	0.000E00	3.000E000
6	Variable	Wel_ini	0.000E00	2.455E003
7	Variable	delta_t	-8.928E-01	5.591E000
8	Variable	e_ini	0.000E00	1.200E001
9	Variable	gamma_sat_clay	0.000E00	1.850E001
10	Variable	gamma_sat_peat	-6.333E-02	1.325E001
11	Variable	nu_clay	-1.481E-01	3.706E-01
12	Variable	nu_peat	9.292E-02	3.392E-01
13	Variable	phi_clay	0.000E00	2.090E001
14	Variable	phi_peat	0.000E00	2.390E001
15	Variable	phi_sand	0.000E00	3.500E001
16	plaxis	Cref clay	0.000E00	1.490E001
17	plaxis	Cref peat	0.000E00	7.500E000
18	plaxis	Rinter clay	0.000E00	6.000E-01
19	plaxis	Rinter peat	0.000E00	6.000E-01
20	Variable	sig_y	0.000E00	2.400E002

Table 9.20: Reliability Results Natural Corrosion with AZ25

[15]The moment of inertia and the cross sectional area are in nearly a linear relation with the section modulus and could for these calculations be expressed as functions of W_{el} in order to automize the calculations. See also appendix N.

We can compare the corrosion allowance that was calculated by means of reliability analysis to what is suggested in the Arcelor Piling Handbook. Figure 9.24 from this book shows us that with a required profile AZ18 and 3.25 mm thickness loss a profile AZ25 is suggested to account properly for corrosion. This is consistent with the reliability analysis results.

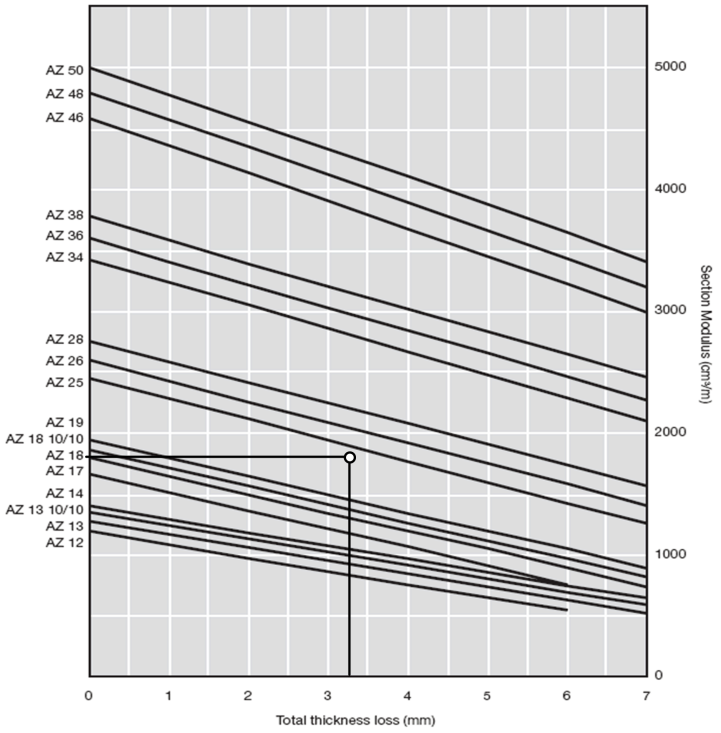

Figure 9.24: Deterministic Corrosion Allowance (Arcelor Piling Handbook)

9.4.2 Limit State: Anchor Failure

As for the sheet pile wall, also for anchors corrosion can cause an important strength reduction. The anchors considered so far have high quality steel tendons that are usually protected against corrosion by means of isolation and therefore the corrosion is negligible, given that the isolation is not damaged. Therefore, to create a realistic case, the anchors were replaced by injection anchors[16] that are only protected by a grout layer due to the installation process. The protective function of this layer is neglected in this case for illustrative puposes.

Since the anchor type is different to the one used in the preceding sections, a reliability assessment without corrosion influence is carried out first for sake of comparability. The anchor specifications are presented in table 9.21.

Table 9.21: Anchor Specifications

Property	Quantity	Unit
outer diameter	70	[mm]
inner diameter	50	[mm]
wall thickness	10	[mm]
cross sectional area	1,885	[mm^2]
steel type	S355	[-]
yield strength	355	[MPa]

The limit state used for this calculation is as described in section 7.4.2, using the initial cross sectional area $A_{a,0}$.

$$Z = \sigma_y - \sigma = \sigma_y - \frac{F_a}{A_{a,0}} \tag{9.11}$$

The results are presented in table 9.22.

Number of calculations (FORM) : 43

Beta : 5.463E000
P_f : 2.343E-08

	Model	Parameter	alfa	X
1	Variable	Aa0	0.000E00	1.885E003
2	Variable	Dout0	0.000E00	1.000E002
3	Variable	E_clay	8.292E-01	1.081E003
4	Variable	E_peat	1.649E-01	6.610E002
5	Variable	La	0.000E00	3.000E000
6	Variable	deltaR	0.000E00	2.000E000
7	Variable	gamma_sat_clay	0.000E00	1.850E001
8	Variable	gamma_sat_peat	-2.870E-01	1.412E001
9	Variable	nu_clay	-2.986E-01	4.044E-01
10	Variable	nu_peat	-2.260E-01	3.926E-01
11	Variable	phi_clay	0.000E00	2.090E001
12	Variable	phi_peat	0.000E00	2.390E001
13	Variable	phi_sand	0.000E00	3.500E001
14	plaxis	Cref clay	0.000E00	1.490E001
15	plaxis	Cref peat	0.000E00	7.500E000
16	plaxis	Rinter clay	2.502E-01	4.295E-01
17	plaxis	Rinter peat	0.000E00	6.000E-01
18	Variable	sig_y	0.000E00	3.550E002

Table 9.22: Reliability Results No Corrosion with Anchor (70/50)

[16]In Dutch: schroef-injectie-ankers.

For the next calculation the same corrosion assumtions as in the previous section are assumed. For the strength reduction we consider an initial geometry with inner and outer diameter (D_{inner} and $D_{outer,0}$ of the tubular anchor element, leading to an intial cross-sectional area $A_{a,0}$. The inner diameter is kept constant and the outer diameter is reduced by the thickness loss ($D_{outer} = D_{outer,0} - 2 \cdot \Delta t$). That leads to the reduced cross sectional area A_a. In combination with the yield strength the limit state fuction is in this case the following.

$$Z = \sigma_y - \sigma = \sigma_y - \frac{F_a}{A_a} \tag{9.12}$$

Since the anchor force is assumed constant over length A_a has to be determined using the thickness loss in the peat leayer Δt_{peat}, which has the higher value and is therefore determinant.

A calculation with the initial anchor configuration and including the corrosion as decribed leads to the results in table 9.23.

Number of calculations (FORM) : 33

Beta : 2.337E000
P_f : 9.717E-03

	Model	Parameter	alfa	X
1	Variable	Aa0	0.000E00	1.885E003
2	Variable	Dout0	0.000E00	1.000E002
3	Variable	E_clay	2.456E-01	2.864E003
4	Variable	E_peat	4.238E-02	8.049E002
5	Variable	La	0.000E00	3.000E000
6	Variable	deltaR	-9.574E-01	1.622E000
7	Variable	gamma_sat_clay	0.000E00	1.850E001
8	Variable	gamma_sat_peat	-7.754E-02	1.322E001
9	Variable	nu_clay	-7.081E-02	3.574E-01
10	Variable	nu_peat	-8.019E-02	3.582E-01
11	Variable	phi_clay	0.000E00	2.090E001
12	Variable	phi_peat	0.000E00	2.390E001
13	Variable	phi_sand	0.000E00	3.500E001
14	plaxis	Cref clay	0.000E00	1.490E001
15	plaxis	Cref peat	0.000E00	7.500E000
16	plaxis	Rinter clay	6.146E-02	5.862E-01
17	plaxis	Rinter peat	0.000E00	6.000E-01
18	Variable	sig_y	0.000E00	3.550E002

Table 9.23: Reliability Results Incl. Corrosion with Anchor (70/50)

Even though the anchor was over-designed, the target reliability is not reached anymore. In order to find an anchor configuration that fulfills the requirements a parametric study on the effect of varying the anchor cross-sectional area on the reliability was carried out. From figure 9.25 it can be concluded that at least about 2,300 mm^2 are required.

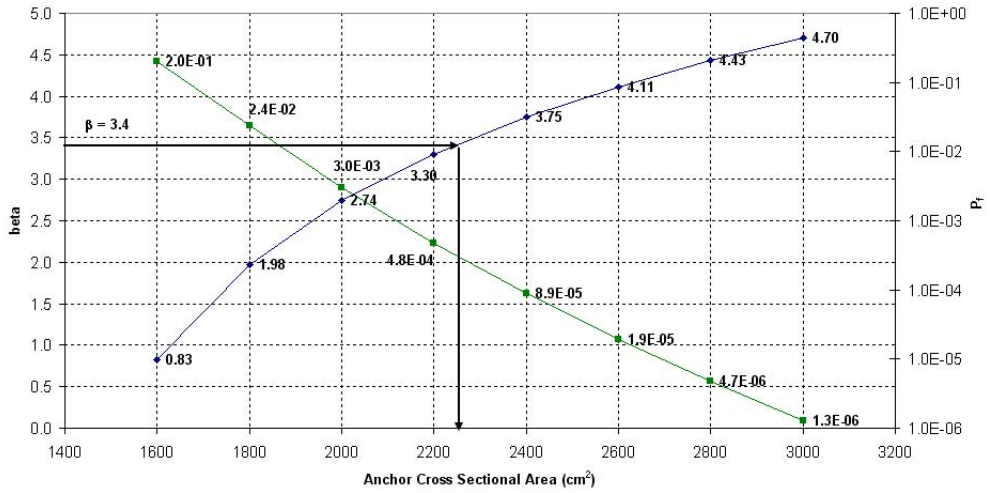

Figure 9.25: Reliability As Function of Anchor Cross Sectional Area

An extra calcuation was carried out to determine the reliability for an anchor with $A_{a,0} = 2300$ mm^2 (see figure 9.24). An assumtion was that all configurations had an initial outer diameter of 100 mm and variable thickness.

Number of calculations (FORM) : 49

Beta : 3.537E000
P_f : 2.024E-04

	Model	Parameter	alfa	X
1	Variable	Aa0	0.000E00	2.300E003
2	Variable	Dout0	0.000E00	1.000E002
3	Variable	E_clay	1.379E-01	2.925E003
4	Variable	E_peat	2.493E-02	8.071E002
5	Variable	La	0.000E00	3.000E000
6	Variable	deltaR	-9.873E-01	3.038E000
7	Variable	gamma_sat_clay	0.000E00	1.850E001
8	Variable	gamma_sat_peat	-4.098E-02	1.319E001
9	Variable	nu_clay	-3.367E-02	3.558E-01
10	Variable	nu_peat	-3.972E-02	3.566E-01
11	Variable	phi_clay	0.000E00	2.090E001
12	Variable	phi_peat	0.000E00	2.390E001
13	Variable	phi_sand	0.000E00	3.500E001
14	plaxis	Cref clay	0.000E00	1.490E001
15	plaxis	Cref peat	0.000E00	7.500E000
16	plaxis	Rinter clay	3.353E-02	5.894E-01
17	plaxis	Rinter peat	0.000E00	6.000E-01
18	Variable	sig_y	0.000E00	3.550E002

Table 9.24: Reliability Results Incl. Corrosion with $A_{a,0} = 2300$ mm^2

This anchor configuration would fulfill the requirements.

It should be noted that for this kind of anchors it is not common practice to take corrosion into account in the design considerations. As mentioned earlier, the anchor is protected by a grout layer due to the installation procedure. In this sense the assumptions made represent an unrealistic or over-conservative scenario and therefore no conclusions for the current design practice should be drawn. The idea was rather to show that the presented method is also applicable to anchors or struts, if required.

9.5 Limitations

The following limitations are to be considered with respect to the conclusions that can be derived from the preceding results:

- The parameter derivation of the soil properties was based on the variation coefficients from NEN6740 - table 1. It is not clear, if these values refer to local variability or the observed variance in average quantities or even another approach. That implies that it is not clear, if averaging effects are included and to which degree this would be the case. Therefore all conclusions are restricted to these assumtions in the input parameters.

- The stochastic quantities were treated as uncorrelated. This does certainly not represent reality. Correlations between the random variables can be used in the proposed methodology easily and the correlation structure is already implemented. It was, however, the aim of this research to show the feasibility of the proposed method. This deficiency has to be kept in mind when judging the conclusions.

- The Mohr-Coulomb model was used in all calculations. It is well known that the loads on the structure are usually over-estimated with this model. But since the deterministic design was carried out with the same model, the outcomes can be compared. In uncertainty and reliability analysis in any case the modelling uncertainties remain. They can be accounted for by e.g. a model factor. For sake of comparability that was not handled here.

- The uncertainties in the phreatic levels can only account for the input uncertainty. The modelling uncertainty is expected to be considerable in this case.

- The corrosion assumptions are simplified and the conclusions are limited to the assumed corrosion model. These assumptions, at least for the anchors, can be considered as very conservative.

9.6 Conclusions and Recommendations

The following conclusions and recommendations can be derived from outcomes of the first case study:

- It was demonstrated that it is feasible to carry out a reliability analysis for a realistic deep excavation problem. The limit states where the soil represents mainly the load on the structure could reasonably be treated with level II (FORM) methods. The soil shear failure is more difficult to control. The limit equilibrium approach presented a robust measure for this purpose. It might, however, be advantageous to keep on searching for better approaches to determine the respective failure probabilities.

- The load on the sheet pile wall is dominated by the uncertainty in the stiffness of the weak top layers in this example, especially by the clay layer. Usually not much attention is paid to the stiffness properties of the soil in the common design procedures. Many analytical methods do not even include these properties. However, if critical load levels for the structural members are reached, before the mobilized shear strength of the soil

reaches critical values, the problem is an elastic one, whilst most of the analytical methods are based on plasticity respectively limit equilibrium approaches.

- The system reliability assessment can probably be improved by using narrower bound approaches (Ditlevsen-bounds) or estimates like the Hohenbichler method, if the probabilities of failure of the components have the same order of magnitude. In the present case the results unfortunately did not give the opportunity to demonstrate this.
- The stochastic treatment of the pore pressure field was restricted to a modelling approach using hydrostatic pore pressures (and interpolations). In some cases this approach might not be sufficient and a flow calculation has to be carried out. It should be investigated how also the input of the flow calculations can be treated in a probabilistic manner.
- The impact of the uncertainty in the phreatic levels is considerable, especially in case of the anchors. For the bending moments respectively the sheet pile limit state the design values as determined based on the suggestions in the CUR 166 [8] were conservative. For the anchors the probabilistic treatment resulted even in a lower reliability as determined with the design values.
- For the corrosion of sheet pile walls it could be shown that the deterministic design rules lead to the same sheet pile choice as the reliability analysis suggested.
- The impact of anchor corrosion on the reliability was significant. That emphasizes the need for quality control and appropriate installation procedures in order to guarantee the nesessary corrosion protection.

Remark: *The conclusions are based on the results of this case study with its geometry and set of material parameters and variation coefficients. Changes in the geometry, the material parameters or the variation coefficients could lead to different results. The generalization of these conclusions is therefore to be treated carefully.*

Chapter 10

Conclusions and Recommendations

Based on the results and insight obtained in this thesis work the following main conclusions[1] can be drawn respectively recommendations can be given:

- The advances in structural reliability analysis have made a large variety of methods available. The applicability and efficiency of these methods depends on the problem that is analyzed and on the models that are used. Continuous work is done to further improve the efficiency of these methods. On the other hand information about the application of these procedures to real-world or realistic problems is rare. This work can contribute to making probabilistic respectively reliability analysis more accessible. It was demonstrated that the calculation effort for this kind of analysis does not necessarily have to be extremely high. Especially, when previous knowledge about the characteristics of the problem is available, much more efficient methods can be applied within an acceptable trade-off in terms of accuracy.

- The focus in this study was on a proper reliability analysis making use of realistic modelling of the soil and the structure with the Finite Element Method. The analysis of structural elements, like the retaining wall or the supports in deep excavations, where the soil basically represents the load, can be carried out in an efficient way, using either level II or level III methods. The information obtained by such reliability analyses is very useful for further use in probabilistic design concepts.

- The soil shear failure mechanisms are still difficult to assess with the information that is available in an FEM-analysis. Several attempts have been presented. These approaches performed reasonably well for simple problems, but exhibited weaknesses for realistic structures like in the case study. The problem does not occur only in probabilistic analysis, but also in deterministic calculations. E.g. the results of the ϕ-c-reduction can deliver results that require interpretation as shown in the bearing capacity example. The only method that proved to be robust and to deliver reliable results was the limit equilibrium approach. This approach is not very elegant, because it does not use practically any information of the FEM-analysis except the fact, whether the calculation reached equilibrium or not. On the other hand it is very generic and does in principle not require any previous knowledge

[1] More specific conclusions were presented in the respective chapters.

about the problem. The limit state of soil shear failure and its treatment should certainly be subject to further research.

- The influence coefficients obtained by the reliability analysis are a very useful information. They give further insight into the problem and allow us to distinguish important from less important or even negligible variables. This information can be used e.g. for optimization. In many cases it even helps us to achieve a better understanding of the physical problem itself. E.g. in the case study it could be shown that the problem is dominated by the elastic stiffness parameters for some limit states.

- The elastic stiffness parameters can be of major influence for limit states, not only the strength parameters of the soil. This holds especially for limit states, for which the soil represents the load on a retaining structure. The determination of the corresponding parameters should therefore be carried out properly.

- In the case study a deterministic structural design was based on a partial safety concept with a certain target reliability. Using the proposed methodology the actual reliability level could be compared with this target value. Also the suitability of the partial safety factors can be assessed using this approach. That means also that the method is especially suitable for the calibration of load and material factors in partial safety concepts, when FEM is used for the structural design.

- Uncertainties in the soil properties, the phreatic levels and the strength parameters of the structural members (corrosion) could be successfully accounted for . These cover a major part of the overall uncertainties. Geometrical uncertainties were not considered yet. Their impact might be considerable, e.g. the thickness of extremely soft layers. These geometrical uncertainties in the geology as well as in the structural geometry, e.g. due to imperfections in the execution, should be considered in further research.

- For real-life structures the quality of a reliability analysis will highly depend on the input statistics. These are difficult to determine due to differences in local and global variations, averaging effects, low sample numbers etc. In this study the focus was on adequately propagating these uncertainties through the model, regardless of their magnitude. It is strongly recommended to investigate the proper determination of the input parameter statistics in further research.

- Especially when a high number of random variables is involved, the level II methods like FORM/SORM or PEM reach their limits of applicability. The experience with calculations for this thesis has shown that For these cases methods like Directional Sampling or DARS are more suitable and more stable.

- Besides the methods that were used and evaluated in this thesis, Latin Hypercube Sampling is a promising method that could be worthwhile implementing in ProBox. Multiple limit states can be assessed on the same set of FEM evaluations and it requires considerably less calculations than Crude Monte Carlo. It has some drawbacks like the uncertainties in the choice of a response distribution, the impact of which must be investigated when judging about its applicability.

- A random average approach was applied for modelling the soil. This approach does not account for its inherent spatial variability. Only 2D-plane-strain models were used, therefore all sorts of 3D-effects are neglected. The ideal situation would be to account for both aspects by 3D-random field modelling. Whenever the computational capacities are sufficient, also this approach should be used to analyze the effects of natural spatial variability of soil properties.
- As mentioned earlier, model error and 'human error' have not been taken into account, which is certainly necessary for the determination of the reliability of a real structure. However, this allowed us to compare the results directly with the target reliability that was assumed in the deterministic design of the structure. At least in case of the CUR 166, the model error was not included in the calibration in the material factors and therefore the results achieved by purely accounting for parameter uncertainty correspond directly to the target reliability. In almost all the calculated cases the target reliability was fulfilled or was even considerably higher. On one hand that provides confidence in the current safety regulations, on the other hand it shows that there is an optimization and economic potential using the reliability methods within probabilistic or risk-based design concepts.

Outlook

The applicability of reliability analysis concepts using Finite Elements has been demonstrated in this study. In the Civil Engineering world these concepts could be used implemented in existing probabilistic design concepts. It is just a matter of time that the computational capacities allow us to carry out fully probabilistic analysis on almost any kind of problem. With the increasing application of these techniques also the databases and determination methods for the input statistics will be improved. Until then, the methods have to be improved in efficiency and especially their application has to be described appropriately.

The Finite Element Method itself was a tool only used by the scientific community in the beginning. By increasing its efficiency, its capacities and especially its user-friendliness it was made accessible for a wide range of professional groups, also for the design practice. Reliability analysis, or in general probabilistic techniques, might undergo a similar development. In principle the methods are already there and now it is the time to improve the accessibility and the user-friendliness. The generic probabilistic toolbox *ProBox* is an excellent example.

Of course, these ideas are not only applicable to geotechnical or structural engineering projects. They can be used for any kind of problem where uncertainties in the input or model parameters affect the result of an analysis. These problems could be of economical, financial, chemical nature etc. This very rational manner of treating uncertainties will certainly find its way into many of these disciplines.

Bibliography

[1] Andres, T.H. Sampling methods and sensitivity analysis for large parameter sets. *Journal of Statistical Computation and Simulation*, 1997.

[2] Baecher, G.B. and Christian, J.T. *Reliability and Statistics in Geotechnical Engineering*. Wiley, West Sussex, England, 2003.

[3] Box, G.E.P. *Statistics for Experimenters - an Introduction to Design, Data Analysis and Model Building*. Wiley, New York, USA, 1978.

[4] Box, G.E.P. and Draper, N.R. *Empirical Model Building and Respose Surfaces*. Wiley, NY, USA, 1987.

[5] Brinkgreve, R.B.J. and Bakker, H.L. Non-linear finite element analysis of safety factors. *Computer Methods and Advances in Geotechnics*, 1991.

[6] Brinkgreve, R.B.J. and Broere, W. *Plaxis Finite Element Code, Version 8.2*. Plaxis bv, Delft, The Netherlands, 2004.

[7] Bucher, C. et al. Advanced analyisis of structural reliability using commercial fe-codes. *European congress on Computational Methods in Applied Sciences and engineering*, 2000.

[8] CUR 166. Damwandconstructies. Technical Recommendation, 4e herziene uitgave 2005, The Netherlands, 2005.

[9] Daniel, C. On varying one factor at a time. *Biometrics*, vol. 14:pp. 430 – 431, 1958.

[10] Ditlevsen, O. Narrow bounds for structural systems. *Journal of Structural Mechanics, ASCE*, 1(4):453–472, 1979.

[11] Fellin, W. et al. *Analyzing Uncertainty in Civil Engineering*. Springer, Heidelberg, Germany, 2005.

[12] Fenton, G.A. *Simulation and Analysis of Random Fields*. PhD thesis, Princeton University, 1990.

[13] Fenton, G.A., Griffiths, D.V., and Williams, M.B. Reliability of traditional retaining wall design. *Geotechnique*, 55(1):55–62, 2005.

[14] Fenton, G.A. and Vanmarcke, E.H. Simulation of random fields via local average subdivision. *Journal of Engineering Mechanics*, 116:1733–1749, 1990.

[15] Griffiths, D.V. and Fenton, G.A. Bearing capacity of spatially random soil: the undrained clay prandtl problem revisited. *Geotechnique*, 51(4):351–359, 2001.

[16] Hasofer, A.M. and Lind, N.C. An exact and invariant first-order reliability format. *Journal of the Engineering Mechanics Division, ASCE*, 100(1):111–121, 1974.

[17] Hicks, M.A. et al. Influence of heterogeneity on undrained clay slope stability. *Journal of Engineering Geology and Hydrogeology*, 35:41–49, 2002.

[18] Hicks, M.A. et al. Stochastic evaluation of static liquefaction in a predominantly dilative sand fill. *Geotechnique*, 55(2), 2005.

[19] Hohenbichler, M. and Rackwitz, R. Non-normal dependent vectors in structural safety. *Journal of Eng. Mech. Div. ASCE*, 107(6):1227–1238, 1981.

[20] Hohenbichler, M. and Rackwitz, R. First-order concepts in system reliability. *Journal of Structural Safety*, (1):177–188, 1983.

[21] Iman, R. and Conover, W. A distribution-free approach to inducing rank correlation among input variables. *Communications in Statistics-Simulation and Computation*, 11(3):pp. 311 – 334, 1982.

[22] Iman, R. and Helton, J. Investigation of uncertainty and sensitivity analysis techniques for computer models. *Risk Analysis*, 8:pp. 71, 1988.

[23] Joint Committee on Structural Safety JCSS. Probabilistic model code. Technical recommendation,, Zuerich, 2001.

[24] Kurowicka, D. and Cooke, R. *Uncertainty Analysis with High Dimensional Dependence Modelling (Lecture Notes)*. Delft Institute of Applied Mathematics, Delft University of Technology, 2005.

[25] Lane, P.A. and Griffiths, D.V. Finite element slope analysis - why are engineers still drawing circles? In *Proc. 6th Int. Symp. Numerical Models in Geomechanics*, pages 589–594, Montreal, 1997.

[26] Madras, N. *Lectures on Monte Carlo Methods*. American Mathematical Society, Providence, Rhode Island, USA, 2002.

[27] McKay, M., Beckman, R., and Conover, W. A comparison of three methods for selecting values of input variables in the analysis of output from a computer code. *Technometrics*, 21(2):pp. 239 – 245, 1979.

[28] Moormann, Ch. and Katzenbach, R. Experimentelle und rechnerische untersuchungen zum tragverhalten rumlicher aussteifungssysteme von tiefen baugruben. *Bauingenieur*, 9:373–386, 2006.

[29] Oberguggenberger, M. and Fellin, W. From probability to fuzzy sets: The struggle for meaning in geotechnical risk assessment. In *Int. Conf. on Probabilistics in Geotechnics*, 2002.

[30] G.M. Peschl. *Reliability Analyses in Geotechnics with the Random Set Finite Element Method*. PhD thesis, Graz University of Technology, 2004.

[31] Plaxis bv, Delft, The Netherlands. *Plaxis Version 8 - Material Models Manual*, 8.2 edition, 2004.

[32] Rackwitz, R. Reviewing probabilistic soils modeling. *Computers and Geotechnics*, 26:199–233, 2000.

[33] Rosenblatt, M. Remarks on a multivariate transformation. *The Annals of Mathematical Statistics*, 23:470–472, 1952.

[34] Rosenblueth, E. Point estimates for probability moments. *Applied Mathematic Modelling*, 5:3812–3814, 1975.

[35] Schweiger, H.F. et al. Reliability analysis in geotechnics with deterministic finite elements. *The International Journal of Geomechanics*, 1(4):389–413, 2001.

[36] Sobol, I. The distribution of points in a cube and the approximate evaluation of integrals. *USSR Computational Mathematics and Physics*, 7(4):pp. 86 – 112, 1967.

[37] Sudret, B. and Der Kiureghian, A. *Stochastic Finite Element Methods and Reliability*. PhD thesis, University of California, Berkeley, 2000.

[38] Swan, C.C. and Seo, Y.-K. Limit analyis of earthen slopes using dual continuum/fem approaches. *Numerical and Analytical Methods in Geomechanics*, 23(10):1359–1371, 1999.

[39] R. Thurner. *Probabilistische Untersuchungen in der Geotechnik mittels deterministischer Finite Elemente-Methode*. PhD thesis, Graz University of Technology, 2000.

[40] van Baars, S. *Manual for Structural Hydraulic Engineering*. TU Delft, Delft, The Netherlands, january edition, 2003.

[41] van Gelder, P.H.A.J.M. *Statistical Methods for the Risk-Based Design of Civil Structures*. PhD thesis, Delft University of Technology, The Netherlands, 2000.

[42] Vanmarcke, E.H. Probabilistic modeling of soil profiles. *ASCE Journal of the Geotechnical Engineering Division*, 103:GT11, 1977.

[43] Vanmarcke, E.H. *Random Fields: Analysis and Synthesis*. M.I.T. Press, Cambridge, 1983.

[44] Vrouwenvelder, A. and Chryssantopoulos, M. The structural reliability analysis toolbox. In *2nd ASRANet International Colloquium*, Barcelona, Spain, July 2004.

[45] Waarts, P.H. *Structural Reliability using Finite Element Methods*. PhD thesis, Delft University of Technology, The Netherlands, 2000.

[46] Zhou, J. and Nowak, A.S. Integration formulas to evaluate functions of random variables. *Structural Safety*, 5:267–284, 1988.

Part IV

Appendices

Appendix A

Distribution Types

There is a large number of probability distributions available. This thesis focuses on the uncertainties in material parameters and groundwater levels. Therefore a selection has been made of the distributions that are used for that purpose most frequently in the literature and these are presented subsequently.

If the uncertainties in the loads are considered, extreme value distributions are more suitable for many types of loads that occur in extreme events, like e.g. extreme water levels, wind speeds of river discharges.

A.1 Normal Distribution

The *Normal Distribution* or *Gaussian Distribution* has several advantageous properties, especially for analytical work, and is therefore widely used for the description of uncertainty in parameters. It is defined by its first two central moments.

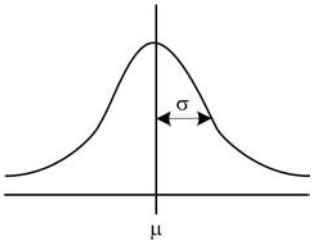

Figure A.1: Probability Density Plot of Standard Normal Distribution

Parameters and Central Moments

The parameters of the Normal Distribution are its central moments:

- μ (mean value)
- σ (standard deviation)

Probability Density Function (pdf)

$$f_X(x) = \frac{1}{\sigma\sqrt{2\pi}} e^{-\frac{1}{2}\left(\frac{x-\mu}{\sigma}\right)^2} \; ; \quad -\infty \leq x \leq +\infty \tag{A.1}$$

Cumulative Distribution Function (cdf)

$$F_X(x) = \int_{-\infty}^{x} \frac{1}{\sigma\sqrt{2\pi}} e^{-\frac{1}{2}\left(\frac{x-\mu}{\sigma}\right)^2} dx \; ; \quad -\infty \leq x \leq +\infty \tag{A.2}$$

Relevant Properties

The Normal Distribution is

- symmetrical (skewness $\xi = 0$).
- not restricted to non-negative values.
- more conservative for strength-properties than the Lognormal Distribution.

A.2 Lognormal Distribution

The Lognormal Distribution is applied when for example negative values are physically impossible or when empirical distributions of data sets exhibit a significant skewness that should not be neglected.

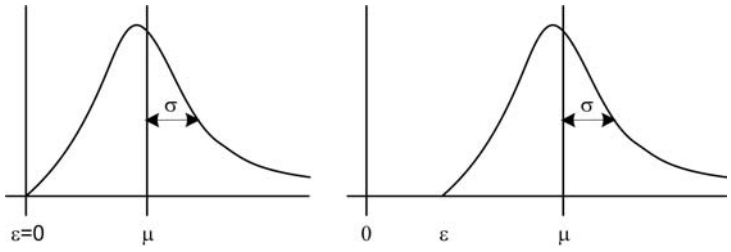

Figure A.2: Probability Density Plot of Lognormal Distribution (left: two-parametric, right: shifted or three-parametric)

Parameters and Central Moments

The parameters of the two-parametric Lognormal Distribution expressed in terms of its central moments and vice versa:

$$\lambda = ln(\mu) - \frac{1}{2} ln\left(\frac{\sigma^2}{\mu^2} + 1\right) \qquad \zeta = \sqrt{ln\left(\frac{\sigma^2}{\mu^2} + 1\right)} \tag{A.3}$$

$$\mu = e^{\left(\lambda + \frac{\zeta^2}{2}\right)} \qquad \sigma = \left(e^{\zeta^2} - 1\right) e^{2\lambda + \zeta^2} \tag{A.4}$$

(The three-parametric Lognormal Distribution is shifted 'horizontally' by ϵ.)

Probability Density Function (pdf)

$$f_X(x) = \frac{1}{(x-\epsilon)\zeta\sqrt{2\pi}} e^{-\frac{1}{2}\left(\frac{ln(x-\epsilon)-\lambda}{\zeta}\right)^2} \; ; \quad \epsilon \leq x \leq +\infty \tag{A.5}$$

Cumulative Distribution Function (cdf)

$$F_X(x) = \int_{-\infty}^{x} \frac{1}{(x-\epsilon)\zeta\sqrt{2\pi}} e^{-\frac{1}{2}\left(\frac{ln(x-\epsilon)-\lambda}{\zeta}\right)^2} dx \; ; \quad \epsilon \leq x \leq +\infty \tag{A.6}$$

Relevant Properties

The Lognormal Distribution is

- strictly non-negative (for $\epsilon \geq 0$).
- fatter in the tail than the normal distribution (conservative for load-parameters).

A.3 Uniform Distribution

The Uniform Distribution gives equal occurrence probability to any value in a specified range.

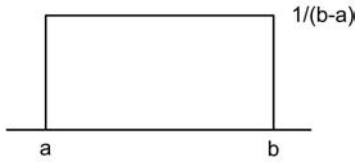

Figure A.3: Probability Density Plot of Uniform Distribution

Parameters and Central Moments

The parameters of the Uniform Distribution expressed in terms of its central moments and vice versa:

$$a = \mu - \sqrt{3}\sigma \qquad b = \mu + \sqrt{3}\sigma \tag{A.7}$$

$$\mu = \frac{a+b}{2} \qquad \sigma = \frac{b-a}{\sqrt{12}} \tag{A.8}$$

Probability Density Function (pdf)

$$f_X(x) = \frac{1}{b-a} \; ; \quad a \leq x \leq b \tag{A.9}$$

Cumulative Distribution Function (cdf)

$$F_X(x) = \frac{x-a}{b-a} \; ; \quad a \leq x \leq b \tag{A.10}$$

A.4 Beta Distribution

The Beta Distribution in its classical form is only valid between the limits $0 \leq x \leq 1$. The variant presented is scaled to the limits $a \leq x \leq b$.

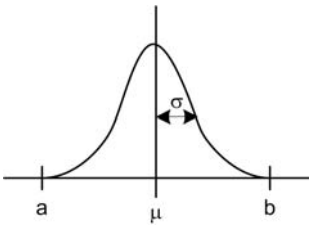

Figure A.4: Probability Density Plot of Beta Distribution

Parameters and Central Moments

The parameters of the Beta Distribution expressed in terms of its central moments and vice versa:

$$r = t \cdot \frac{\mu - a}{b - a} \Big/ \left(1 - \frac{\mu - a}{b - a}\right) \qquad t = \frac{\mu - a}{b - a}\left[\left(\frac{b - \mu}{\sigma}\right)^2 + 1\right] - 1 \tag{A.11}$$

$$\mu = a + (b - a)\frac{r}{r + t} \qquad \sigma = (b - a)\sqrt{\frac{rt}{(r + t)^2(r + t + 1)}} \tag{A.12}$$

Probability Density Function (pdf)

$$f_X(x) = \frac{\left(\frac{x-a}{b-a}\right)^{r-1}\left(1 - \frac{x-a}{b-a}\right)^{t-1}}{(b - a)B(r, t)} \;; \quad a \leq x \leq b \tag{A.13}$$

where B(r,t) is the *beta-function* applied to the parameters r and t.

Cumulative Distribution Function (cdf)

$$f_X(x) = \frac{B\left(\frac{x-a}{b-a}, r, t\right)}{B(r, t)} \;; \quad a \leq x \leq b \tag{A.14}$$

where $B\left(\frac{x-a}{b-a}, r, t\right)$ is the *incomplete beta-function.*

Relevant Properties

The Beta Distribution has some very advantageous properties, especially for simulation purposes.

- The major advantage is that the range of realizations can be restricted to values within the limits $a \leq x \leq b$. This way ill-posed problems can be avoided. In many cases the choice of these limits can be justified by physically possible limits.
- The parameters of the beta distributions can be adjusted to fit quite well to Normal and Lognormal Distributions.
- If the limits are equidistant to the mean value, the distribution is symmetric, if not, it is skewed.

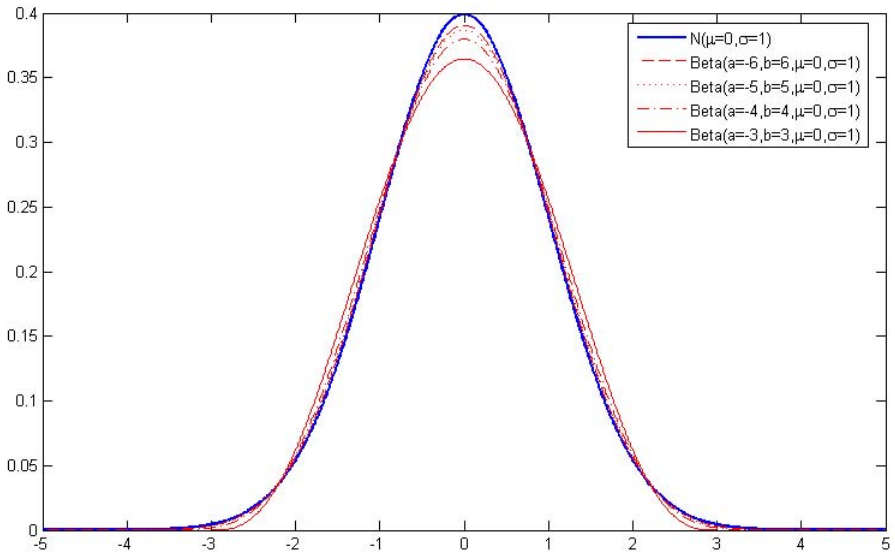

Figure A.5: Beta PDF with different limits compared to Normal PDF

If the adjusted Beta Distribution should for any reason be as similar as possible to a normal distribution with the same first two moments, the limits should be set equidistant (symmetry) and as far as possible from the mean. From figure A.5 the improving fit can be seen clearly.

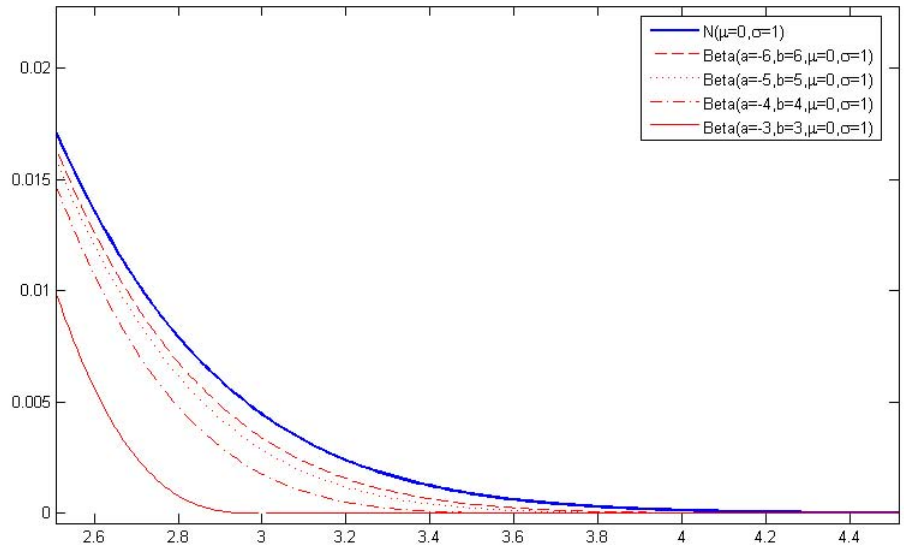

Figure A.6: Tail of Beta PDF with different limits compared to Normal PDF

Figure A.6 shows furthermore the quality of fit in the region that is usually of interest for structural reliability problems (about 3 to 4 standard deviations from the mean). Whether the choice for a distance from the mean is appropriate can in many cases only be checked after carrying out the analysis when a design value is known. This design value should not be too close to the 'physically impossible' or 'very unlikely' domain.

Appendix B

Response Surfaces (RS)

A response surface $\hat{g}(\mathbf{x})$ is an approximation of the function $g(\mathbf{x})$ that might not be known in explicit form. A polynomial closed-form expression is fit through a number of points $\hat{g}(x_i)$ that are obtained by deterministic evaluations. A commonly used quadratic function for this purpose is:

$$\hat{g}(\mathbf{x}) = c_0 + \sum_{i=1}^{N} c_i x_i + \sum_{i=1}^{N} c_{ii} x_i^2 + \sum_{i=1}^{N} \sum_{j=1, j\neq i}^{N} c_{ij} x_i x_j = \mathbf{V}^T \cdot \mathbf{c} \tag{B.1}$$

where $\mathbf{c}^T = \{c_0, c_i, c_{ii}, c_{ij}\}$ is the vector of coefficients that can be determined with the least squares method and $\mathbf{V}^T = \{1, x_i, x_i^2, x_i x_j\}$. A number of M fitting points $\{x_k, k = 1...M\}$ is chosen and the the function is evaluated in these points (e.g. by Finite Element Analysis) obtaining $y_k = g(x_k)$. The error ξ can be expressed as a function of the coefficient vector $\mathbf{c}$

$$\xi(\mathbf{c}) = \sum_{k=1}^{M} [y_k - \mathbf{V}^T(x_k) \cdot \mathbf{c}]^2 \tag{B.2}$$

and has to be minimized. The solution can be obtained by

$$\mathbf{c} = (\boldsymbol{\nu}^T \boldsymbol{\nu})^{-1} \boldsymbol{\nu}^T \mathbf{y} \tag{B.3}$$

where $\boldsymbol{\nu}$ is a matrix whose rows are the vectors $\mathbf{V}^T(x_k)$ and $\mathbf{y}$ is a vector containing the supports y_k.

There are, of course, more possible formulations of response surfaces that are e.g. of higher order or splines or including/excluding cross-terms. Here the intention is only to present the basic idea. There are several possibilities two implement the idea of response surfaces in probabilistic calculation techniques:

- Build the RS and carry out the complete probabilistic analysis using the RS.
- Use the RS for (analytical) integration techniques.
- Use the RS as decision support for detecting important regions (as in DARS).

Appendix C

Expected Number of Calculations for Crude Monte Carlo

For the use of Crude Monte Carlo in a reliability problem we can make an estimate of the expected number of calculations given a certain acceptable error.

The basic idea of Monte Carlo is that a failure probability P_f can be estimated by the following ratio:

Let N be the number of realizations of the random vector $\mathbf{X}$ that is carried out in the Monte Carlo analysis. N_f is the number of realization where the evaluation of $\mathbf{X}$ in the limit state function $Z(\mathbf{X})$ leads to failure, thus $Z(\mathbf{X}) \leq 0$.

Then the ratio

$$P_f \approx \frac{N_f}{N} \tag{C.1}$$

is an estimate of the probability of failure P_f.

The error in this approximation can be written as

$$\epsilon = \frac{N_f}{N \cdot P_f} - 1 \tag{C.2}$$

Its expectation is $E[\epsilon] = 0$ and the standard deviation can be written as

$$\sigma(\epsilon) = \sqrt{\frac{1 - P_f}{N \cdot P_f}} \tag{C.3}$$

Due to the *Central Limit Theorem* ϵ is normally distributed for sufficiently large N. We require the error ϵ to be smaller than the acceptable error E with a certain reliability/confidence. As the expectation is $E[\epsilon] = 0$, the requirement can be written as

$$k \cdot \sigma(\epsilon) \leq E \tag{C.4}$$

Then we can estimate the minimum necessary number of calculations as

$$N > \frac{k^2}{E^2}\left(\frac{1}{P_f} - 1\right) \tag{C.5}$$

This also implies that the number of calculations required is independent of the number of random variables.

Example

If a 95%-confidence interval ($k = 2$) is required with an acceptable error of 10% ($E = 0.1$), the necessary number of realizations can be estimated using the expected failure probability by

$$N > 400\left(\frac{1}{P_f} - 1\right) \tag{C.6}$$

Appendix D

System Failure Probability using FORM (Hohenbichler)

The method FORM itself is not capable of coping with system reliability aspects. It can only be used to determine respectively approximate the failure probability of single limit states. The method described in this section can be applied to combine FORM outcomes in order to determine the common reliability of several failure mechanisms, i.e. the system reliability.

We will start with a method developed by Hohenbichler [20] that allows us to approximate the failure probability of a parallel system for two mechanisms. Subsequently a series system of two elements and also n elements are treated using the Hochenbichler concept.

D.1 Parallel System with Two Components (Hohenbichler)

Assume, we have a parallel system of two elements with failure probability

$$P_f = P(Z_1 < 0 \cap Z_2 < 0) \tag{D.1}$$

whose failure domain in Z-space is illustrated in figure D.1.

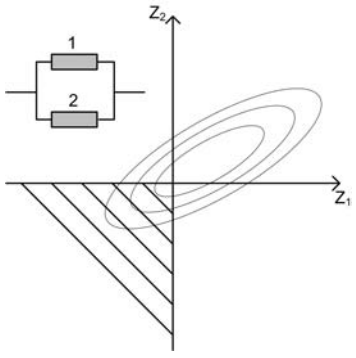

Figure D.1: Failure Domain of a Serial System with 2 Elements

The failure probability can be written as:

$$P_f = P(Z_1 < 0)P(Z_2 < 0|Z_1 < 0) \tag{D.2}$$

Hohenbichler's method serves for determining the part of the conditional probability. It supposes that the reliability indices β_i (number of elements: $i = 1, 2$) and the influence factors α_{ij} (number of random variables x_j: $j = 1, ..., n$) are known as results of a FORM-analysis. The correlation coefficient between the element failures can be obtained from the influence factors:

$$\rho = \sum_{j=1}^{n} \alpha_{1j}\alpha_{2j} \tag{D.3}$$

For the following derivation we assume $\beta_1 > \beta_2$ and we rewrite the limit states as functions of the standard normal variables u and v:

$$Z_1 = \beta_1 - u \quad and \quad Z_2 = \beta_2 - v \tag{D.4}$$

Since the β_i are constant, u and v are correlated in the same way as the limit states:

$$\rho(u, v) = \rho(Z_1, Z_2) = \rho \tag{D.5}$$

We switch from the dependent variables u and v to the independent variables u and w (w is standard normal and independent of u). Z_1 is not affected by this change whereas Z_2 can be expressed as:

$$Z_2 = \beta_2 - \rho u - w\sqrt{1 - \rho^2} \tag{D.6}$$

The correctness of equation D.6 is proven by the following three expressions:

$$expectation: \ \mu(Z_2) = \beta_2 - 0 - 0 = 0 \tag{D.7}$$

$$variance: \ \sigma^2(Z_2) = \left(\frac{\partial Z_2}{\partial u}\right)^2 \sigma_u^2 + \left(\frac{\partial Z_2}{\partial w}\right)^2 \sigma_w^2 = \rho^2 + (1 - \rho^2) = 1 \tag{D.8}$$

$$correlation: \ cov(Z_1 Z_2) = E[(Z_1 - \mu(Z_1))(Z_2 - \mu(Z_2))] \tag{D.9}$$

$$\rho(Z_1 Z_2) = \frac{cov(Z_1 Z_2)}{\sigma(Z_1)\sigma(Z_2)} = \rho \tag{D.10}$$

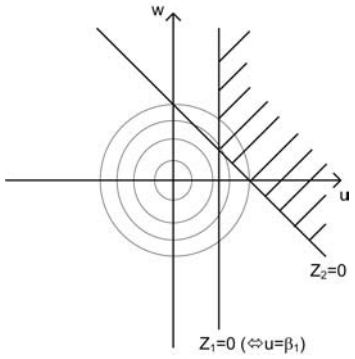

Figure D.2: Representation of Z_1 and Z_2 in the u-w-plane

We can represent the two new formulations for Z_1 (eq. D.4) and Z_2 (eq. D.6) in the *u-w-plane* as in figure D.2 and rewrite the conditional probability from equation D.2 as:

$$P(Z_2 < 0 | Z_1 < 0) = P(\beta_2 - \rho u - w\sqrt{1 - \rho^2} < 0 | \beta_1 - u < 0) \tag{D.11}$$

The idea of Hohenbichler was to replace u by a new variable u' in such a way that this conditional probability can be rewritten as an unconditional one. For that purpose he used a truncated normal distribution that is conditioned on $u > \beta_1$ (all values below β_1 are zero and the area under the standard normal distribution for values larger than β_1 is scaled up to 1):

$$u' = \Phi^{-1}(1 - p \cdot \Phi(u)) \quad with \quad p = P(u > \beta_1) \tag{D.12}$$

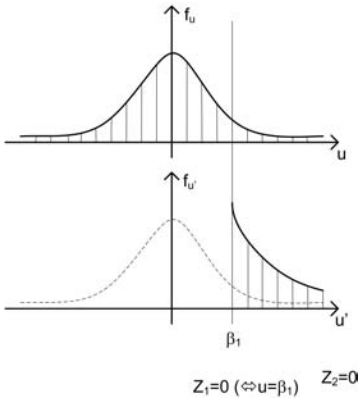

Figure D.3: Transformation $u \rightarrow u'$ by Truncating Normal Distribution

With this new variable the conditional expectation becomes:

$$P(Z_2 < 0 | Z_1 < 0) = P(Z^e < 0) = P(\beta_2 - \rho u' - w\sqrt{1 - \rho^2} < 0) \tag{D.13}$$

and the new limit state can be written as:

$$\Phi^{-1}(1 - p \cdot \Phi(u)) - w\sqrt{1 - \rho^2} \tag{D.14}$$

A FORM-analysis leads us to the desired $P(Z^e < 0)$.

D.2 Serial System with Two Components

The failure probability of a serial system with two elements respectively mechanisms can be written as:

$$P_f = P(Z_1 < 0 \cup Z_2 < 0) = P(Z_1 < 0) + P(Z_2 < 0) - P(Z_1 < 0 \cap Z_2 < 0) \tag{D.15}$$

where the last term was solved in the previous section.

D.3 Equivalent α for a Serial System with 2 Components

After carrying out FORM analyses for the limit states $Z_i(X_1, ..., X_n) < 0$ with the basic random variables X_j $(j = 1, ..., n)$ the reliability indices β_i and the influence coefficients α_{ij} are obtained as well as the joint failure probability $P_f = P(Z_1 < 0 \cap Z_2 < 0)$. The limit state functions can now be rewritten in standard format:

$$\begin{aligned} Z_1 &= \beta_1 + \alpha_{11}u_{11} + \alpha_{12}u_{12} + ... + \alpha_{1n}u_{1n} \\ Z_2 &= \beta_2 + \alpha_{21}u_{21} + \alpha_{22}u_{22} + ... + \alpha_{2n}u_{2n} \end{aligned} \tag{D.16}$$

As before the correlation between the limit states is determined by:

$$\rho = \sum_{j=1}^{n} \alpha_{1j}\alpha_{2j} \tag{D.17}$$

where is implicitly assumed that the variables X_j are fully correlated between the different limit states. For the problems contemplated, this is sufficient. If e.g. a dike ring is split into several sections there might also be a correlation coefficient ρ_{ijk} between the X_j necessary.

The aim is to find the coefficients of the equivalent limit state

$$Z^e = \beta^e + \alpha_1^e u_1 + \alpha_2^e u_2 + ... + \alpha_n^e u_n \tag{D.18}$$

that belongs to

$$P(Z^e < 0) = P(Z_1 < 0 \cap Z_2 < 0) \tag{D.19}$$

The equivalent β is already known via the joint failure probability and the α-values can be determined by a perturbation with ϵ_j:

$$\alpha_j^e = \frac{\beta^e(\epsilon_j) - \beta^e(0)}{\epsilon_j} \tag{D.20}$$

where $\beta^e(\epsilon_j)$ is

$$\beta^e(\epsilon_j) = \Phi^{-1}[P(Z^e < 0)] \quad with \quad \mu(u_j) = \epsilon_j \tag{D.21}$$

and thus

$$\beta^e(\epsilon_j) = \Phi^{-1}[P(Z_1 < -\alpha_{1j}\epsilon_j \cap Z_2 < -\alpha_{2j}\epsilon_j)] \tag{D.22}$$

If required the α_j^e can be normalized on $\sum(\alpha_j^e)^2 = 1$.

D.4 Serial System with Arbitrary Number of Components

In order to calculate the failure probability of an arbitrary serial system $P(Z_1 < 0 \cap Z_2 < 0) \cap ... \cap Z_N < 0)$ the previously described procedure can be repeated $N - 1$ times. Since the determination of the equivalent influence factors is an approximation, the whole procedure is an approximation as well. By experience the best performance is achieved, if always the two most correlated of the remaining limit states are combined first.

Appendix E

Ditlevsen Bounds

In appendix D an approximation method for the failure probability of a serial system was presented. A method for obtaining bounds of this probability was presented by Ditlevsen in 1979 [10].

The failure probability of a serial system is described as:

$$P_f = P(Z_1 < 0 \cup Z_2 < 0) = P(Z_1 < 0) + P(Z_2 < 0) - P(Z_1 < 0 \cap Z_2 < 0) \tag{E.1}$$

The last term $P(Z_1 < 0 \cap Z_2 < 0)$ is to be determined on basis of correlation information between the two limit states (see also appendix D).

$$\rho(Z_1, Z_2) = \sum_{j=1}^{n} \alpha_{1j}\alpha_{2j} \tag{E.2}$$

where α_{ij} are the influence coefficients for stochastic variable X_j in limit state $i = [1, 2]$.

According to the derivation of Ditlevsen (see [10]), the lower bounds of the failure probability for 'parallel system' are:

$$P(Z_1 < 0 \cap Z_2 < 0) \geq \Phi(-\beta_1)\Phi(-\beta_2^*) \tag{E.3}$$

$$P(Z_1 < 0 \cap Z_2 < 0) \geq \Phi(-\beta_1^*)\Phi(-\beta_2) \tag{E.4}$$

where β_2^* is

$$\beta_2^* = \frac{\beta_2 - \rho\beta_1}{\sqrt{1-\rho^2}} \tag{E.5}$$

(β_1^* is determined accordingly)
The upper bound is determined by the sum of the lower bounds:

$$P(Z_1 < 0 \cap Z_2 < 0) \leq \Phi(-\beta_1)\Phi(-\beta_2^*) + \Phi(-\beta_1^*)\Phi(-\beta_2) \tag{E.6}$$

Appendix F

Constitutive Model Choice and Relevant FEM-Features

F.1 Constitutive Models

In this section an overview of the constitutive models that are potentially suitable for retaining structure modelling is given. The main features and properties of these models are explained, upon which they are evaluated for applicability in the presented reliability analysis framework. In principle the model choice is problem dependent and has to be carried out for each specific case. Only general features[1] of the described models can be treated here.

Finite Element Modelling, as all kinds of modelling by definition, is developed for simulating and predicting the real world behavior of a material respectively a structure as exactly as possible. The constitutive models describing the material behavior differ significantly in degree of sophistication. On the one hand there are relatively simple models like linear elasticity that resemble the real world behavior reasonably for some materials like e.g. steel within a certain range of stresses and strains. Simple models usually require only a small number of parameters. For soils, however, elasticity theory reaches its limits quite quickly because plastic deformations play an important role and the behavior is often strongly non-linear. To this end more sophisticated constitutive models have been developed like elasto-plastic or hypo-plastic models. These can include hardening or softening of the material, which is also observed in nature. A drawback of these models can be the high number of parameters, which automatically involves a large amount of sample tests in order to determine these parameters.

F.1.1 Comparison of Available Constitutive Models

In the following a number of models that are in general suitable for standard excavation and retaining structure analysis is presented. Other models could be applicable for special situations, like the Soft Soil Creep Model in order to take time-dependent secondary compression into account, but are not treated here.

[1] The descriptions and analyses are restricted to drained behavior.

Linear Elasticity

For most of the potential applications in soils linear elasticity is insufficient for approximating the stress-strain behavior. Especially when relatively large deformations are involved, irreversible deformations and the strength properties of the soil play an important role. Linear elastic models, however, only include stiffness properties of the soil.

An example is Hooke's law (in incremental form) with:

$$d\boldsymbol{\sigma} = \mathbf{D} d\boldsymbol{\epsilon} \tag{F.1}$$

where $\mathbf{D}$ is the material stiffness matrix:

$$\mathbf{D} = \frac{E}{(1+\nu)(1-2\nu)} \begin{pmatrix} 1-\nu & \nu & \nu & 0 & 0 & 0 \\ \nu & 1-\nu & \nu & 0 & 0 & 0 \\ \nu & \nu & 1-\nu & 0 & 0 & 0 \\ 0 & 0 & 0 & 1/2-\nu & 0 & 0 \\ 0 & 0 & 0 & 0 & 1/2-\nu & 0 \\ 0 & 0 & 0 & 0 & 0 & 1/2-\nu \end{pmatrix} \tag{F.2}$$

which includes the *Young's modulus* E and the *Poisson ratio* ν as stiffness parameters.

Even though no use will be made of this model for soil, the behavior of steel can be approximated by linear elasticity reasonably well and the model will be applied for sheet pile walls and tie-back anchors as well as for struts or walings for the contemplated problems.

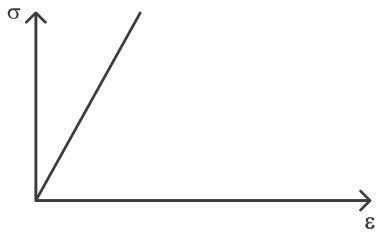

Figure F.1: Stress-Strain Curve for Linear Elasticity

Elasto-Plasticity

If we need to continue the calculations beyond the limits of the regions where the material behavior can be reasonable approximated by linear elasticity, one possibility is the to use elastic perfectly plastic models.

There are many formulations for yield criteria (limit between elastic and plastic behavior) like von Mises (max. deviatoric stress) or Tresca (max. shear stress). These criteria are suitable for materials like steel, where the isotropic stress state has negligible influence on the yield criterion, i.e. the failure surface is parallel to the space diagonal in 3D-stress space.

For soils this approximation does not perform well. One essential property of frictional materials is that their strength increases with increasing mean stress.

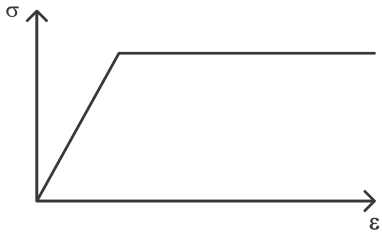

Figure F.2: Stress-Strain Curve for Elastic Perfectly Plastic Models

Elastic - Plastic Model with Mohr-Coulomb Failure Criterion

The Mohr-Coulomb criterion takes several effects into account that are essential for the description of soil behavior. Basically soil has only a limited amount of tensile strength that is due to cohesion. The shear strength increases under increasing mean stress. Thus the total shear strength is composed by a part due to the frictional properties and another cohesive part (refer also to chapter 7.5.3). Strictly speaking, this model also belongs to the previous described family of elastic-perfectly plastic models.

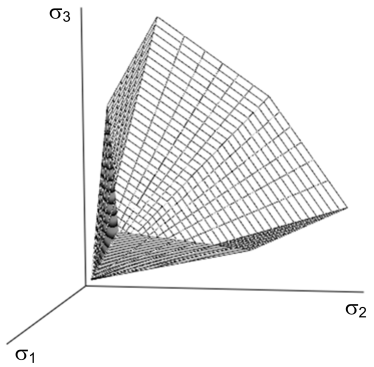

Figure F.3: Mohr-Coulomb Yield Criterion in Principal Stress Space

This model uses 5 input parameters:

- Stiffness parameters: E and ν (as in linear elasticity)
- Strength respectively plasticity parameters: c (cohesion) and ϕ (friction angle)
- Dilative Behavior: ψ (dilation angle)

In the 'Mohr-Coulomb Model' (MC), as implemented in Plaxis, the average stiffness values are used, i.e. the stiffness is stress-independent. For application in excavation problems there is general consensus that this model gives conservative results for the loads on the retaining wall and thus in general also for the generated moments, the deflections and the anchor forces. It is not suitable for deformation analysis of settlements next to or heave inside the excavation. The approximation of the strength of the whole system (failure mechanisms in the soil) is reasonably good.

Hardening Soil Model

The Hardening Soil Model (HS) is an advanced critical state theory model that is based on a hyperbolic stress-strain relationship in triaxial compression including shear and compaction hardening. By combining these two types of hardening it is suitable for hard and soft soils. As implemented in Plaxis it also accounts for stress-dependency of the stiffness. Another important feature is that it takes the loading history into account (memory of pre-consolidation stress) and makes a difference for the stiffness between primary loading and un-/re-loading.

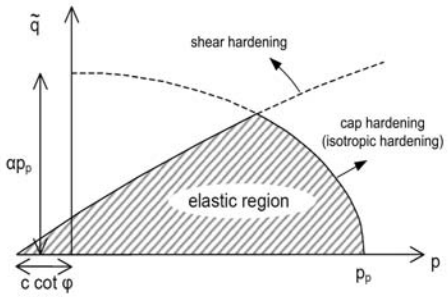

Figure F.4: Hardening Soil Model Hardening Criteria in p-q-Plane (based on Plaxis Material Models Manual v8.2)

This model uses 7 standard[2] input parameters:

- Stiffness parameters: E_{50}^{ref} (secant stiffness in standard triaxial test), E_{oed}^{ref} (tangent stiffness for primary oedometer loading), E_{ur}^{ref} (un-/reloading stiffness) and m (power of stress dependency of stiffness)
- Strength respectively plasticity parameters: c (cohesion) and ϕ (friction angle)
- Dilative Behavior: ψ (dilation angle)

The ultimate failure criterion is also in this model described by the Mohr-Coulomb Criterion. Due to the shear hardening and the stress-dependent stiffness it is well suited for sand, gravel and stiff clays, whereas the compaction hardening also makes it suitable for soft soils, such as normally consolidated clay and peat[3].

Specifically for retaining structures it can be stated that, if applied for the suitable soil types, the deformations of the wall as well as the settlements next to the wall and the bending moments are estimated more accurately with the HS-model than with Mohr-Coulomb. For the shear failure mechanisms in drained soil no substantial difference should be observed. The general performance is thus better, but the investment in terms of a larger number of parameters is to be considered.

[2]Other advanced parameters can be used, but are preferably maintained at standard settings, like e.g. un-/reloading Poisson ratio ν_{ur} or the cohesion increment c_{incr}. See also [31].

[3]This opinion is confirmed by the instructions in the CUR 166.

Hypo-Plasticity

The concept of Hypo-Plasticity was developed by searching for a mathematical formulation that would satisfy a number of properties that are typical for soil behavior like:

- incremental non-linearity (stress-dependency of stiffness)
- homogeneity in stress
- critical state limits etc.

These features are similar to the capabilities of the Hardening Soil model, but the mathematical formulation is different. An important aspect is that the soil behavior is density-dependent. Strength and stiffness are formulated as functions of the void ratio. Currently there is no Hypoplastic Model available in the commercial version of Plaxis[4]. It is recommended to follow the developments in the relatively young field of Hypo-Plasticity and investigate the possibilities of its application.

F.1.2 Conclusions

For deterministic analysis of deep excavations the CUR 166 [8] gives recommendations on the use of constitutive models, which are mainly based on investigation[5] for the North-South Line (metro) in Amsterdam. Basically it can be concluded that the Hardening Soil Model is best suited for realistic estimates of the deformations and occurring bending moments, even though for small structures Mohr-Coulomb is a simple and efficient alternative giving safe lower respectively upper bounds. Only where long-term creep behavior of very soft soils is involved, the use of the Soft Soil Creep Model should be considered.

[4]There are user-defined hypo-plastic models.

[5]The report is an internal report of the Adviesbureau Noord-Zuid Lijn by Vermeer et al. The report itself was not available and it is referred to the information given in the CUR 166.

F.2 Relevant FEM-Features

In reliability analysis the number of calculations is usually too high to check the outcomes of every single limit state evaluation manually. Hence the aim is to create an FE-model including the calculation configuration that is as stable as possible. Usually this requirement is conflictive with the also desirable properties of low calculation times and high accuracy.

Another topic in reliability analysis is the incapability of FEM methods to deliver results when the failure domain is reached because equilibrium would be needed in order to obtain these results. There are methods to determine 'the distance to failure (no equilibrium)', of course only in the non-failure domain. One of these is the 'ϕ-c-reduction technique' implemented in Plaxis.

The 'ϕ-c-Reduction Technique'

The 'ϕ-c-reduction'[6] is a tool that is included in Plaxis and allows us to calculate a kind of safety factor regarding to failure in the soil elements. The construction stage whose 'stability' is to be checked is modelled and calculated in the normal way and used as starting point for the procedure. From this equilibrium situation the ϕ-c-reduction lowers the strength parameters of the soil by dividing them stepwise by an increasing common factor (MSf) until the FEM-model is on the edge of equilibrium and non-equlibrium:

$$\sum MSf = \frac{tan\phi}{tan\phi_{reduced}} = \frac{c}{c_{reduced}} \tag{F.3}$$

The appropriateness and stability of this procedure in combination with reliability analysis will be investigated by means of example calculations. In principle the intention is to use the method for limit state formulations that describe failure mechanisms in the soil. Of course, it can only deliver values in the non-failure domain.

Interface Strength

For a more realistic soil-structure interaction, in most FEM-packages there are interface elements available. In Plaxis these interfaces obtain properties from the adjacent soil, whilst the strength properties are reduced by the factor:

$$c_{inter} = R_{inter} \cdot c_{soil} \tag{F.4}$$

$$\phi_{inter} = arctan(R_{inter} \cdot tan\phi_{soil}) \tag{F.5}$$

The dilatancy angle of the interfaces is set to $\psi_{inter} = 0$.

The yield limit of the interfaces is defined according to the Coulomb criterion. In the elastic region two phenomena are likely to occur:

1. Slipping (relative movement parallel to the interface):

$$u_{slip} = \frac{\tau}{K_{\parallel}} = \frac{\tau \cdot t_{inter}}{G_{inter}} \tag{F.6}$$

[6]For detailed information refer to Brinkgreve and Bakker (1991) [5].

2. Gapping (relative movement perpendicular to the interface):

$$u_{gap} = \frac{\sigma}{K_\perp} = \frac{\sigma \cdot t_{inter}}{E_{oed,inter}} \tag{F.7}$$

where t_{inter} is the virtual interface thickness[7], $K_\parallel$ and $K_\perp$ are the interface shear and normal stiffness, and $E_{oed,inter}$ and G_{inter} are the interface compression and shear moduli determined by:

$$G_{inter} = R_{inter}^2 \cdot G_{soil} \tag{F.8}$$

$$E_{oed,inter} = 2G_{inter}\frac{1-\nu_{inter}}{1-2\nu_{inter}} \quad with\ \nu_{inter} = 0.45 \tag{F.9}$$

Considering these relations there might be a considerable influence of this parameter depending on the problem that is analyzed. The recommendation by Brinkgreve et al [6] is to use a value for R_{inter} in the order of 2/3. Other authors, according to the CUR 166 gives recommendations for higher values in the case of sheet pile walls like 0.9. It should be stated, especially in the framework of this thesis, that there are no test procedures available and that this parameter is uncertain. Even though there is a lack of data, this uncertainty should be taken into account unless it can be proven that the sensitivity to this parameter is negligible. For the analysis in this work a Beta distribution with parameters $R_{inter} \sim Beta(0.6/0.1/0.0/1.0)$ will be used for most of the applications.

Updated Mesh Analysis

For large deformations (as in the case of road embankments or dike bodies on soft soils) the simple plastic calculations might lead to inaccurate results, since the limits are reached where large deformation theory is required. In Plaxis this can be achieved by carrying out an *updated mesh analysis*. With this option the node and integration point positions are updated according to the calculated displacements. Furthermore, an objective stress measure is handled that accounts for the rotations of stresses.

This analysis type will be adopted in this thesis, whenever initial deterministic calculations show considerable differences between simple plastic analysis and updated mesh analysis. It should be noted that it will not be applied for the generation of initial stresses by means of *gravity loading*. The displacements in the gravity loading procedure are physically meaningless and usually reset to zero in the subsequent calculation phase, which is not possible in updated mesh analysis.

Initial Stress Generation

If the surface level and the layer boundaries are horizontal, the initial stress state can be generated using the K_0-procedure in deterministic analysis. K_0 is the ratio between horizontal and vertical effective stresses:

$$K_0 = \frac{\sigma'_{xx}}{\sigma'_{yy}} \tag{F.10}$$

[7] t_{inter} is determined automatically in Plaxis.

For normally consolidated soil, the expression $K_0 = 1 - sin\phi$ by Jaky is usually applied, whereas for overconsolidated soils the value is higher.

In principle this method is also applicable for reliability analysis. With Plaxis, however there are practical reasons impeding this. As explained in chapter 6, for the automated calculation process, only the Plaxis calculation module is used. The initial stress generation is part if the input module and therefore not available. It is therefore recommended to always use *gravity loading*[8] for the generation of the appropriate initial stress state according to each parameter realization as first calculation step. That means also the the initial calculation phase (before gravity loading) must be generated with zero effective stresses.

It is important to note that with gravity loading the initial stress state is highly sensitive to the Poisson's ratio ν. For elastic[9] one dimensional compression the relation between Poisson's ratio and the generated K_0 is:

$$\nu = \frac{K_0}{1 + K_0} \tag{F.11}$$

Thus one should restrict the possible values for ν (possibly by an appropriate distribution type) to a range that leads to realistic initial stress states. Otherwise plasticity might occur during the generation of the initial stresses. E.g. for cohesionless soils this occurs[10] for:

$$\frac{1 - sin\phi}{1 + sin\phi} > \frac{\nu}{1 - \nu} \tag{F.12}$$

The Limit Equilibrium

The '*limit equilibrium*' is defined as a state where the FEM-calculation is between reaching equilibrium and not reaching equilibrium, i.e. still encountering unbalanced nodal forces. In fact the limit equilibrium can also be interpreted as the set of parameter combinations that lead to the preceding definition. In several situations this state is applied as criterion for defining failure.

In the ϕ-c-reduction the distance to 'failure' is expressed in the factor MSf (for definition see section F.2) whose magnitude is defined by the input parameters and the parameters that represent the limit equilibrium.

Also in the CUR 166 this definition is implicitly accepted as failure criterion. In chapter 4.3 of part 1 it is stated that the embedment depth of the sheet pile is sufficient, if equilibrium is reached in all calculation phases using design values.

This suggests that this criterion may also be used for reliability methods. For detecting after a calculation, if equilibrium was reached, several information sources are available. The calculation log files give information over the state that the calculation finally reached. Furthermore, the multiplier $\sum MStage$ is 1, when the equilibrium was achieved and else smaller than 1. Note that this holds only for calculation phases in staged construction calculations as applied in this thesis.

[8] First calculation phase with the gravity multiplier $\sum Mweight$ set to 1. The displacements in the next phase are set to zero.

[9] Thus only applicable for linear-elasticity and Mohr-Coulomb!

[10] Only using Mohr-Coulomb.

Appendix G

Calculation Results PEM (Zhou-Nowak)

Example 1: Beam On Two Supports - P and E stochastic (LSF variant 1)

RANDOM VARIABLES

Number	Name	Type (1/2)*	mean	std	par1	par2
1	P	1	100	20	1.0E+02	2.000E+01
2	E	1	30000000	3000000	3.0E+07	3.000E+06

* 1=Gaussian 2=Lognormal

INTEGRATION POINT VALUES IN U-SPACE

z1 = 0.000 z2 = 2.000 z3 = 1.414

Z-function: L[=20]/100 - P*L[=20]^3/(48*E*I[=0.00572])

PERMUTATIONS			in u-space		in x-space		Uy	maxUy	Z-value (Z)	weight w	w*Z	Z^2	w*Z^2	w*Uycalc	Uycalc^2	w*Uycalc^2
1	0	0	0.000	0.000	100.00	30000000.0	0.0971		0.10287	0.5	0.051437	0.010583	0.005291623	0.0485625	0.0094333	0.00471664
2	0	+z2	0.000	2.000	100.00	36000000.0	0.0809		0.11906	0.0625	0.007441	0.014176	0.000885991	0.0050586	0.0065509	0.00040943
3	0	-z2	0.000	-2.000	100.00	24000000.0	0.1214		0.07859	0.0625	0.004912	0.006177	0.00038606	0.0075879	0.0147395	0.00092122
4	+z2	0	2.000	0.000	140.00	30000000.0	0.1360		0.06402	0.0625	0.004002	0.004099	0.000256199	0.0084984	0.0184892	0.00115558
5	-z2	0	-2.000	0.000	60.00	30000000.0	0.0583	0.2	0.14172	0.0625	0.008858	0.020086	0.001255372	0.0036422	0.003396	0.00021225
6	+z3	+z3	1.414	1.414	128.28	34242640.7	0.1092		0.09084	0.0625	0.005678	0.008252	0.000515757	0.0068224	0.0119157	0.00074473
7	+z3	-z3	1.414	-1.414	128.28	25757359.3	0.1451		0.05488	0.0625	0.00343	0.003012	0.000188244	0.0090699	0.0210596	0.00131622
8	-z3	+z3	-1.414	1.414	71.72	34242640.7	0.0610		0.13898	0.0625	0.008686	0.019314	0.001207147	0.003814	0.0037239	0.00023274
9	-z3	-z3	-1.414	-1.414	71.72	25757359.3	0.0811		0.11887	0.0625	0.00743	0.014131	0.000883173	0.0050704	0.0065816	0.00041135
										1.0000	0.10		0.01	0.10		0.01

RESULTS

via Z-function distribution:

mean = 0.10187
var = 0.00049
std = 0.02217

normallly dsitributed response:

P(Z<0) = 2.155E-06
beta = 4.596E+00

lognormallly dsitributed Z-function:

(cannot be smaller than zero)

via response distribution (using critical value):

mean = 0.09813 -3.834056
var = 0.00049
std = 0.02217 1.739286

normallly dsitributed response:

P(Z<0) = 2.155E-06
beta = 4.596E+00

lognormallly dsitributed response:

P(Z<0) = 1.004E-01
beta = 1.279E+00

Example 1: Beam On Two Supports - P and E stochastic (LSF variant 2)

RANDOM VARIABLES

Number	Name	Type (1/2)*	mean	std	par1	par2
1	P	1	100	20	1.0E+02	2.000E+01
2	E	1	30000000	3000000	3.0E+07	3.000E+06

* 1=Gaussian 2=Lognormal

Z-function: 0.48*E^I[=0.00572] - P^L[=20]^2

INTEGRATION POINT VALUES IN U-SPACE

z1 = 0.000 z2 = 2.000 z3 = 1.414

PERMUTATIONS			in u-space		in x-space		Z-value (Z)	weight w	w*Z	Z^2	w*Z^2
1	0	0	0.000	0.000	100.00	30000000.0	42368.0	0.5	21184	1.795E+09	897523712
2	0	+z2	0.000	2.000	100.00	36000000.0	58841.6	0.0625	3677.6	3.462E+09	216395868.2
3	0	-z2	0.000	-2.000	100.00	24000000.0	25894.4	0.0625	1618.4	670519951	41907496.96
4	+z2	0	2.000	0.000	140.00	30000000.0	26368.0	0.0625	1648	695271424	43454464
5	-z2	0	-2.000	0.000	60.00	30000000.0	58368.0	0.0625	3648	3.407E+09	212926464
6	+z3	+z3	1.414	1.414	128.28	34242640.7	42702.9	0.0625	2668.9304	1.824E+09	113971028.3
7	+z3	-z3	1.414	-1.414	128.28	25757359.3	19405.7	0.0625	1212.8561	376581085	23536317.81
8	-z3	+z3	-1.414	1.414	71.72	34242640.7	65330.3	0.0625	4083.1439	4.268E+09	266753028.7
9	-z3	-z3	-1.414	-1.414	71.72	25757359.3	42033.1	0.0625	2627.0696	1.767E+09	110423918.2
								1.0000	42368.00		1926892298

RESULTS

via Z-function distribution:

mean = 42368.0
var = 131844874.2
std = 11482.4

normallly dsitributed response:

P(Z<0) = 1.122E-04
beta = 3.690E+00

Example 1: Beam On Two Supports - P stochastic (LSF variant 1)

RANDOM VARIABLES

Number	Name	Type (1/2)*	mean	std	par1	par2	* 1=Gaussian 2=Lognormal
1	P	1	100	20	1.0E+02	2.000E+01	

Z-function: L[=20]/100 - P*L[=20]^3/(48*E[=3E+7]*I[=0.00572])

INTEGRATION POINT VALUES IN U-SPACE

z1 = 0.000 z2 = 1.732 z3 = 1.225

PERMUTATIONS		u-space	x-space	Uy	maxUy	Z-value (Z)	weight w	w*Z	Z^2	w*Z^2	w*Uycalc	Uycalc^2	w*Uycalc^2
1	0	0.000	100.00	0.0971		0.10287	0.66666667	0.068583	0.0105832	0.0070555	0.06475	0.009433	0.006288856
2	+z2	1.732	134.64	0.1308	0.2	0.06923	0.16666667	0.011538	0.0047928	0.0007988	0.021795	0.017101	0.002850142
3	-z2	-1.732	65.36	0.0635		0.13652	0.16666667	0.022753	0.0186377	0.0031063	0.01058	0.00403	0.000671618
							1.0000	0.10		0.01	0.10		0.01

RESULTS

via Z-function distribution:		via response distribution (using critical value):		
mean =	0.10287	mean =	0.09713	-3.960804
var =	0.00038	var =	0.00038	
std =	0.01943	std =	0.01943	1.80502
normallly dsitributed response:		**normallly dsitributed response:**		
P(Z<0) =	5.918E-08	P(Z<0) =	5.918E-08	
beta =	5.296E+00	beta =	5.296E+00	
lognormallly dsitributed Z-function:		**lognormallly dsitributed response:**		
(cannot be smaller than zero)		P(Z<0) =	#NUM!	
		beta =	#NUM!	

Example 1: Beam On Two Supports - P stochastic (LSF variant 2)

RANDOM VARIABLES

Number	Name	Type (1/2)*	mean	std	par1	par2
1	P	1	100	20	1.0E+02	2.000E+01

* 1=Gaussian 2=Lognormal

INTEGRATION POINT VALUES IN U-SPACE

z1 = 0.000 z2 = 1.732 z3 = 1.225

Z-function: 0.48*E[=3E+7]*I[=0.00572] - P*L[=20]^2

PERMUTATIONS		u-space	x-space	Z-value (Z)	weight w	w*Z	Z^2	w*Z^2
1	0	0.000	100.00	42368.0	0.66666667	28245.3333	1795047424	1196698283
2	+z2	1.732	134.64	28511.6	0.16666667	4751.93226	812910966	135485161
3	-z2	-1.732	65.36	56224.4	0.16666667	9370.73441	3161183882	526863980.3
					1.0000	42368.00		1859047424.0

RESULTS

via Z-function distribution:

mean = 42368.0
var = 64000000.0
std = 8000.0

normallly dsitributed response:

P(Z<0) = 5.918E-08
beta = 5.296E+00

Example 1: Beam On Two Supports - E stochastic (LSF variant 1)

RANDOM VARIABLES

Number	Name	Type (1/2)*	mean	std	par1	par2
1	E	1	30000000	3000000	3.0E+07	3.000E+06

* 1=Gaussian 2=Lognormal

INTEGRATION POINT VALUES IN U-SPACE

z1 = 0.000 z2 = 1.732 z3 = 1.225

Z-function: L[=20]/100 - P*L[=20]^3/(48*E[=3E+7]*I[=0.00572])

PERMUTATIONS		u-space	x-space	Uy	maxUy	Z-value (Z)	weight w	w*Z	Z^2	w*Z^2	w*Uycalc	Uycalc^2	w*Uycalc^2
1	0	0.000	30000000	0.0971		0.10287	0.66666667	0.068583	0.0105832	0.0070555	0.06475	0.009433	0.006288856
2	+z2	1.732	35196152	0.0828	0.2	0.11721	0.16666667	0.019536	0.0137391	0.0022898	0.013798	0.006854	0.001142257
3	-z2	-1.732	24803848	0.1175		0.08253	0.16666667	0.013755	0.0068109	0.0011352	0.019579	0.0138	0.002299938
							1.0000	0.10		0.01	0.10		0.01

RESULTS

via Z-function distribution:		via response distribution (using critical value):		
mean =	0.10187	mean =	0.09813	-4.599262
var =	0.00010	var =	0.00010	
std =	0.01011	std =	0.01011	2.134368
normallly dsitributed response:		normallly dsitributed response:		
P(Z<0) =	3.600E-24	P(Z<0) =	0.000E+00	
beta =	1.007E+01	beta =	#NUM!	

Example 1: Beam On Two Supports - E stochastic (LSF variant 2)

RANDOM VARIABLES

Number	Name	Type (1/2)*	mean	std	par1	par2	* 1=Gaussian 2=Lognormal
1	E	1	30000000	3000000	3.0E+07	3.000E+06	

INTEGRATION POINT VALUES IN U-SPACE

z1 = 0.000 z2 = 1.732 z3 = 1.225

Z-function: 0.48*E[=3E+7]*I[=0.00572] - P*L[=20]^2

PERMUTATIONS		u-space	x-space	Z-value (Z)	weight w	w*Z	Z^2	w*Z^2
1	0	0.000	30000000.00	42368	0.66666667	28245.3333	1795047424	1196698283
2	+z2	1.732	35196152.42	56635	0.16666667	9439.09268	3207472944	534578824
3	-z2	-1.732	24803847.58	28101	0.16666667	4683.57398	789691150	131615191.6
					1.0000	42368.00		1862892298.2

RESULTS

via Z-function distribution:

mean = 42368.0
var = 67844874.2
std = 8236.8

normallly dsitributed response:

P(Z<0) = 1.347E-07
beta = 5.14E+00

Appendix H

ProBox Results Format

The results in *ProBox* are presented in a standard format on the application screen. In this thesis the results are presented in result tables in the same format. The format is explained in figure H.1.

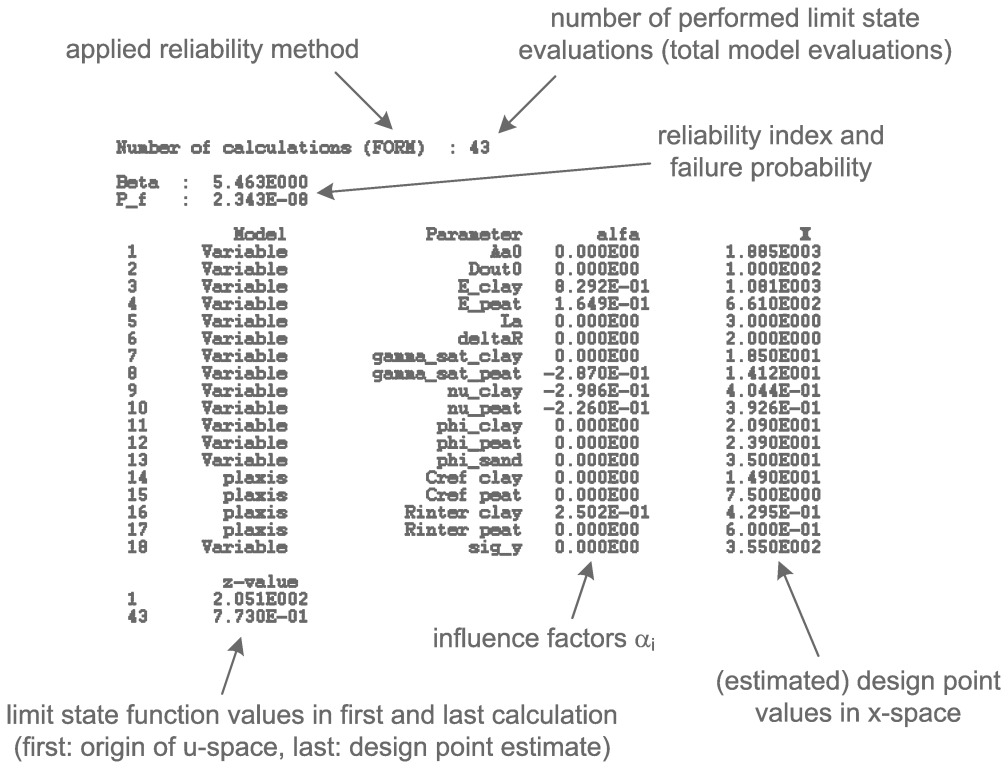

Figure H.1: ProBox Results Format

Remark: Usually the information about the LSF-values of the first and last calculation are omitted in the result tables.

Appendix I

NEN 6740 - Table 1

The next page contains *table 1* from the Dutch code *NEN 6740* with the characteristic values for soil types that are typical in the Netherlands.

NEN 6740 - Table 1

type of soil		representative mean value of the soil parameters												
name	admixture	consistency[1]	γ[2] [kN/m^3]	γ_{sat} [kN/m^3]	q_c[3)6)] [MPa]	C'_p	C'_s	C_c	C_a[5)]	C_{sw}	E[6)] [MPa]	ϕ' [°]	c' [kPa]	f_{undr} [kPa]
gravel	little silty	loose	17	19	15	500	–	0.008	0	0.003	75	32.5	–	–
		medium	18	20	25	1,000	–	0.004	0	0.002	125	35		
		dense	19 or 20	21 or 22	30	1,200 or 1,400	–	0.003 or 0.002	0	0.001 or 0	150 or 200	37.5 or 40		
	very silty	loose	18	20	10	400	–	0.009	0	0.003	50	30	–	–
		medium	19	21	15	600	–	0.006	0	0.002	75	32.5		
		dense	20 or 21	22 or 22.5	25	1,000 or 1,500	–	0.003 or 0.002	0	0.001 or 0	125 or 150	35 or 40		
sand	clean	loose	17	19	5	200	–	0.021	0	0.007	25	30	–	–
		medium	18	20	15	600	–	0.006	0	0.003	75	32.5		
		dense	19 or 20	21 or 22	25	1,000 or 1,500	–	0.003 or 0.002	0	0.001 or 0	125 or 150	35 or 40		
	little silty/clayey		18 or 19	20 or 21	12	450 or 650	–	0.008 or 0.005	0	0.003 or 0.001	25 or 35	27 or 32.5	–	–
	very silty/clayey		18 or 19	20 or 21	8	200 or 400	–	0.019 or 0.009	0	0.006 or 0.001	20 or 30	25 or 30		
silt[4)]	little sandy	soft	19	19	1	25	650	0.168	0.004	0.056	2	27.5 or 30	0	50
		medium	20	20	2	45	1,300	0.084	0.002	0.028	5	27.5 or 32.5	2	100
		stiff	21 or 22	21 or 22	3	70 or 100	1,900 or 2,500	0.049 or 0.030	0.001	0.017 or 0.005	10 or 20	27.5 or 35	5 or 7.5	200 or 300
	very sandy		19 or 20	19 or 20	2	45 or 70	1,300 or 2,000	0.092 or 0.055	0.002	0.031 or 0.005	5 or 10	27.5 or 35	0 or 2	50 or 100
clay	clean	soft	14	14	0.5	7	80	1.357	0.013	0.452	1	17.5	0	25
		medium	17	17	1.0	15	160	0.362	0.006	0.121	2	17.5	10	50
		stiff	19 or 20	19 or 20	2.0	25 or 30	320 or 500	0.168 or 0.126	0.004	0.056 or 0.042	4 or 10	17.5 or 25	25 or 30	100 or 200
	little sandy	soft	15	15	0.7	10	110	0.759	0.009	0.253	1.5	22.5	0	40
		medium	18	18	1.5	20	240	0.237	0.005	0.079	3	22.5	10	80
		stiff	20 or 21	20 or 21	2.5	30 or 50	400 or 600	0.126 or 0.069	0.003	0.042 or 0.014	5 or 10	22.5 or 27.5	25 or 30	120 or 170
	very sandy		18 or 20	18 or 20	1.0	25 or 140	320 or 1,680	0.190 or 0.027	0.004	0.063 or 0.025	2 or 5	27.5 or 32.5	0 or 2	0 or 10
	organic	soft	13	13	0.2	7.5	30	1.690	0.015	0.550	0.5	15	0 or 2	10
		medium	15 or 16	15 or 16	0.5	10 or 15	40 or 60	0.760 or 0.420	0.012	0.250 or 0.140	1.0 or 2.0	15	0 or 2	25 or 30
peat	not preloaded	soft	10 or 12	10 or 12	0.1	5 or 7.5	20 or 30	7.590 or 1.810	0.023	2.530 or 0.600	0.2 or 0.5	15	2 or 5	10 or 20
	medium preloaded	medium	12 or 13	12 or 13	0.2	7.5 or 10	30 or 40	1.810 or 0.900	0.016	0.600 or 0.300	0.5 or 1.0	15	5 or 10	20 or 30
variation coefficient			0.05		–	0.25						0.10	0.20	

The table gives the low representative value of means of the concerned soil type. Within an area, defined by the row of the admixture and the column of the parameter (a 'box'), it applies:

- for γ, γ_{sat}, C'_p, C'_s, E', ϕ', c' and f_{undr}: if raising the value leads to an unfavorable situation (larger/bigger dimensions of the foundation), then the right-value in the same row has to be used, or, if there is no right-value mentioned, the value of the row below;
- for C_c, C_a and C_{sw}: if lowering the value leads to an unfavorable situation, then the right-value of the same row has to be used, or, if there is no right-value mentioned, the value of the row below.

1) loose: $0 < R_n < 0.33$
medium: $0.33 \leq R_n \leq 0.67$
dense: $0.67 \leq R_n \leq 1.00$

2) for a natural moisture content

3) the here mentioned values of q_c (cone resistance) have to be used as entry to the table and are not allowed be used in calculations

4) saturated silt/loam

5) values of C_a are valid for an increase of stresses of 100 % as a maximum

6) q_c and E are standardized on an effective vertical stress of 100 kPa. To get a right entry into the table via q_c, the measured values of q_c have to be converted to a level of effective vertical stresses of 100 kPa. The factor of conversion C_N has to be determined with the graph in figure 2A (NEN 6740). Doing so, one finds the E-modulus for a vertical effective stress level of 100 kPa. For other stress levels the E has to be converted to that specific stress level. "E" has to be interpreted as $E'_{50;rep}$

Appendix J

Soil Properties (JCSS)

The following tables were taken from the JCSS Probabilistic Model Code [23]:

Non cohesive Soil type	Density	Dry Unit Weight [kN/m^3]	Saturated Unit Weight [kN/m^3]	Internal Friction tan(φ')	Stiffness [MN/m^2]
Coarse gravel, Boulders	loose medium dense	15-17 17-18 18-20	19-20 20-21 21-23	0.65-0.73 0.70-0.83 0.78-0.90	150-300 150-300 250-350
Sand, gravel Uniform grain Size	loose medium dense	15-16 17-18 18-19	19-20 20-21 21-22	0.58-0.65 0.65-0.73 0.70-0.83	30-100 50-150 100-200
Sand, gravel Non-uniform Grain size	loose medium dense	17-19 18-20 20-21	20-22 21-23 22-24	0.57-0.70 0.62-0.75 0.70-0.85	30-100 50-150 150-250
Sand Slightly Silty Silty		 18-20 18-20	 20-21.5 19.5-20.5	 0.50-0.65 0.45-0.60	 25-50 20-40

Cohesive Soil type	Consis-tency	Saturated Unit Weight [kN/m^3]	Internal friction tan(φ') (drained)	Cohesion (drained) [kN/m^2]	Undrained Shearing Strength [kN/m^2]	Stiffness (normally consolida-ted) [MN/m^2]
Inorganic cohesive soils, Plastic	soft stiff very stiff	16-18 17-19 20-22	0.27-0.36 0.27-0.36 0.27-0.36	0-5 5-15 15-30	10-20 20-50 50-100	1-2 2-4 4-10
Inorganic cohesive soils, Medium plastic	soft stiff very stiff	17-19 18-20 19-21	0.35-0.42 0.35-0.42 0.35-0.42	0-5 5-10 10-20	0-10 15-30 40-100	1-2 2-4 4-10
Inorganic cohesive soils, Weakly plastic		18-20	0.40-0.60	0-5	0-10	2-5
Boulder clay		20-24	0.52-0.64	20-30	-	200-700
Organic cohesive soils, Silt	soft stiff	13-18 14-19	0.24-0.28 0.24-0.28	0-5 5-10	5-20 15-30	0.2-0.5 0.5-1

Table J.1: Indicative Soil Properties of Non-Cohesive and Cohesive Soils (Mean-Values)

Soil property	Standard deviation [% of expected mean value]
Unit weight [kN/m^3]	5 – 10 %
Internal Friction tan(φ') (drained)	10 – 20 %
Drained Cohesion [kN/m^2]	10 – 50 %
Undrained Shearing Strength [kN/m^2]	10 – 40 %
Stiffness [MN/m^2]	20 – 100 %

Table J.2: Indicative Variation Coefficients Soil Properties

Appendix K

Central Moments of Normal Distribution for given 95%-Characteristic Values and Variation Coefficient

If a quantile $q_{\hat{p}}$, i.e. the value that is not exceeded with a probability of $\hat{p}$ percent, and the variation coefficient $COV(X)$ of the variable X are given, we can recalculate the central moments of a variable with Normal Distribution using the following considerations.

The probability the a realization of X is smaller than $q_{\hat{p}}$ can be expressed as:

$$P(X \leq q_{\hat{p}}) = \Phi\left\{\frac{q_{\hat{p}} - \mu_x}{\sigma_x}\right\} \tag{K.1}$$

Using the definition of the variation coefficient $COV(X) = \frac{\sigma_x}{\mu_x}$ we obtain:

$$P(X \leq q_{\hat{p}}) = \Phi\left\{\frac{q_{\hat{p}} - \mu_x}{COV(X)\mu_x}\right\} \tag{K.2}$$

$$\Leftrightarrow \quad \Phi^{-1}\{P(X \leq q_{\hat{p}})\} \cdot COV(X)\mu_x = q_{\hat{p}} - \mu_x \tag{K.3}$$

Thus we obtain:

$$\mu_x = \frac{q_{\hat{p}}}{1 + \Phi^{-1}\{P(X \leq q_{\hat{p}})\} \cdot COV(X)} \tag{K.4}$$

$$\sigma_x = COV(X)\mu_x \tag{K.5}$$

Appendix L

DARS-Results Case 1

The applicability of FORM for the limit states sheet pile failure and anchor failure was confirmed by the following results obtained by DARS (level III).

Number of calculations (DARS) : 655

Beta : 4.281E000
P_f : 9.303E-006

	Model	Parameter	alfa	X
1	Variable	Asp	0.000E00	1.500E002
2	Variable	E_clay	8.931E-01	1.256E003
3	Variable	E_peat	1.124E-01	7.320E002
4	Variable	Isp	0.000E00	3.420E004
5	Variable	Wel	0.000E00	1.800E003
6	Variable	gamma_sat_clay	-3.901E-02	1.885E001
7	Variable	gamma_sat_peat	-1.521E-01	1.312E001
8	Variable	nu_clay	-3.001E-01	3.865E-01
9	Variable	nu_peat	9.750E-02	3.402E-01
10	Variable	phi_clay	3.855E-02	2.102E001
11	Variable	phi_peat	-4.102E-03	2.354E001
12	Variable	phi_sand	8.223E-02	3.356E001
13	plaxis	Cref clay	8.002E-02	1.325E001
14	plaxis	Cref peat	-1.886E-03	7.366E000
15	plaxis	Rinter clay	2.598E-01	4.546E-01
16	plaxis	Rinter peat	-9.421E-02	6.024E-01
17	Variable	sig_y	0.000E00	2.400E002

Table L.1: Reliability Results Sheet Pile Failure with DARS

Number of calculations (FORM) : 99

Beta : 5.962E000
P_f : 1.246E-09

	Model	Parameter	alfa	X
1	Variable	Aa	0.000E00	4.200E002
2	Variable	E_clay	8.501E-01	9.920E002
3	Variable	E_peat	1.451E-01	6.759E002
4	Variable	La	0.000E00	3.000E000
5	Variable	gamma_sat_clay	-3.201E-02	1.812E001
6	Variable	gamma_sat_peat	-2.981E-01	1.359E001
7	Variable	nu_clay	-2.902E-01	4.152E-01
8	Variable	nu_peat	-2.625E-01	4.001E-01
9	Variable	phi_clay	1.889E-02	2.014E001
10	Variable	phi_peat	-7.480E-05	2.351E001
11	Variable	phi_sand	5.890E-02	3.452E001
12	plaxis	Cref clay	6.659E-02	1.399E001
13	plaxis	Cref peat	-8.421E-02	7.335E000
14	plaxis	Rinter clay	2.452E-01	4.201E-01
15	plaxis	Rinter peat	4.254E-03	5.885E-01
16	Variable	sig_y	0.000E00	1.570E003

Table L.2: Reliability Results Anchor Failure with DARS

Appendix M

Equivalent Rectangular Cross Section

In the Plaxis file-structure the parameters for a plate/beam-element are stored in terms of the *shear modulus* G [GPa], the *Poisson's ratio* ν [-] and the *thickness* d [m] of the beam, as if it was a rectangular cross-section.

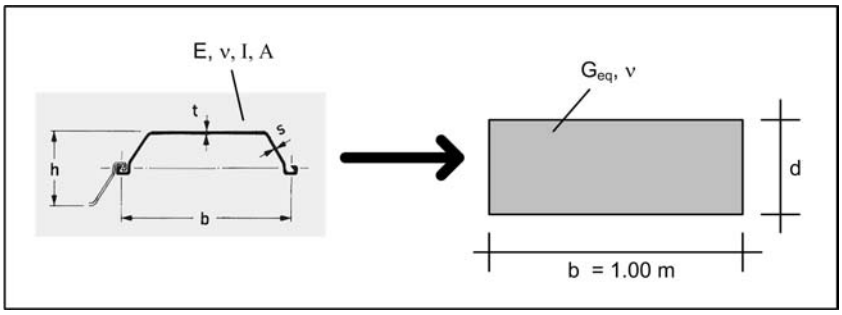

Figure M.1: Rectangular Cross Section Equivalent To Sheet Pile in Bending and Compression

For the variation of input values it is more convenient to use values that are available in tables and that are handled in the common practice, like the *moment of inertia* around the y-axis I_y [cm4/m] and the *cross section* A [cm2/m], which are usually given per m retaining wall. The *Young's modulus* E of steel is considered a material constant as well as the *Poisson's ratio* ν. In the following the conversion rules to obtain the properties of an equivalent rectangular cross-section from given sheet pile properties are summarized.

M.1 Steel Properties

The following material properties are assumed as constants for steel:

- Young's modulus: $E = 210\ [GPa]$
- Poisson's ratio: $\nu = 0.28\ [-]$

From these two properties the shear modulus is obtained by the following relation:

$$G = \frac{E}{2(1+\nu)} = \frac{210}{2(1+0.28)} \approx 82\ GPa \tag{M.1}$$

M.2 Equivalent Behavior in Bending and Compression

The idea of the conversion is to work with the properties of a simpler rectangular cross section that behaves equally to the sheet pile in bending and compression/extension. Therefore the following two relations must hold:

$$EI = E_{eq}\frac{bd^3}{12} \tag{M.2}$$

$$EA = E_{eq}bd \tag{M.3}$$

M.3 Equivalent Thickness

The equivalence of the rectangle to the sheet pile shape has to hold for bending *and* compression/extension. The same thickness d is used for the bending stiffness $EI = Ebd^3/12$ and the compression stiffness $EA = Ebd$ and therefore the following holds:

$$d = 12EI/(Ebd^2) = EA/(Eb) = d \tag{M.4}$$

it follows that

$$d = \sqrt{12\frac{I}{A}} \tag{M.5}$$

M.4 Equivalent Young's Modulus

By amending this geometrical property, also the Young's modulus has to obtain an equivalent value. Since the ratio of $I/A = h^2/12$ is constant, it doesn't matter whether we choose for EI or EA for obtaining E_{eq} and for sake of simplicity we choose EA:

$$EA = E_{eq}bd \tag{M.6}$$

it follows that

$$E_{eq} = \frac{EA}{bd} = \frac{EA}{\sqrt{12\frac{I}{A}}} = \frac{EA}{d} \tag{M.7}$$

where $b = 1m$, since we consider a plane-strain situation and all magnitudes are per m in y-direction (out of plane). The reducing factor for E to E_{eq} is consequently the factor A/d.

M.5 Expressed in Parameters Used by Plaxis

As mentioned earlier, we assume the *moment of inertia* around I_y [cm4/m] and the *cross section* A [cm2/m] to be given besides the material constants of steel. The user-interface of Plaxis is fed by EA, EI and ν. If I and A are considered as stochastic variables we have to apply the following relations in ProBox:

1. $d = \sqrt{12\frac{I}{A}}$
2. $G_{eq} = \frac{E_{eq}}{2(1+\nu)} = \frac{EA}{2d(1+\nu)}$

Note that, if d is used in the second equation, it has to be calculated first from I and A!

Appendix N

Parameter Correlations AZ-Profiles

For AZ sheet pile profiles, there are almost linear relations between the *cross-sectional area* A and the *moment of inertia* I respectively the elastic section modulus W_{el}. In the following linear fit relations between these quantities are derived. By expressing the quantities as dependent of each other, on can carry out parametric studies on e.g. the sheet pile type or the section modulus in an automatized way.

It is observed that for the same class of profile (e.g. AZ, excluding special profiles), there is a nearly linear relationship between I, A and Wel. As example consider the following list (table N.1, source: website Arbed) of AZ-profiles, where all special profiles were excluded.

Type	b	h	e	a	A	m (pile)	m (m2)	W	I
	mm	mm	mm	mm	cm²/m	kg/m	kg/m²	cm³/m	cm⁴/m
AZ 12	670	302	8.5	8.5	126	66.1	99	1200	18140
AZ 13	670	303	9.5	9.5	137	72	107	1300	19700
AZ 14	670	304	10.5	10.5	149	78.3	117	1400	21300
AZ 17	630	379	8.5	8.5	138	68.4	109	1665	31580
AZ 18	630	380	9.5	9.5	150	74.4	118	1800	34200
AZ 19	630	381	10.5	10.5	164	81	129	1940	36980
AZ 25	630	426	12	11.2	185	91.5	145	2455	52250
AZ 26	630	427	13	12.2	198	97.8	155	2600	55510
AZ 28	630	428	14	13.2	211	104.4	166	2755	58940
AZ 34	630	459	17	13	234	115.5	183	3430	78700
AZ 36	630	460	18	14	247	122.2	194	3600	82800
AZ 38	630	461	19	15	261	129.1	205	3780	87080
AZ 46	580	481	18	14	291	132.6	229	4595	110450
AZ 48	580	482	19	15	307	139.6	241	4800	115670
AZ 50	580	483	20	16	322	146.7	253	5015	121060

Table N.1: Standard AZ-Profile Dimensions (without special sizes)

Plotting A against I we obtain figure N.1:

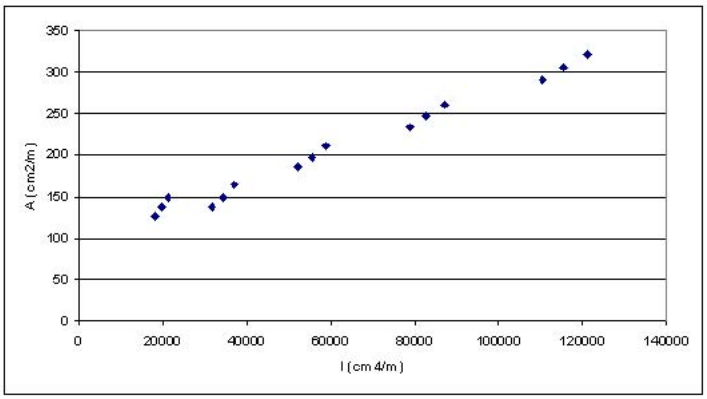

Figure N.1: Plot A Against I for AZ-Profiles

As fit-procedure the least-squares method is applied. The quantity to be minimized was, however, chosen to be the sum of the differences of the original ratios I/A and the fitted ratios I/A_{fit}:

$$\sum_i \left(\frac{I_i}{A_i} - \frac{I_i}{A_{i,fit}} \right)^2 \tag{N.1}$$

The best fit results for:

$$A_{fit} = 93.93 + \frac{I}{542.17} \; [cm^2/m] \tag{N.2}$$

where I must be inserted in $[cm4/m]$.
The resulting fit is shown in figure N.2:

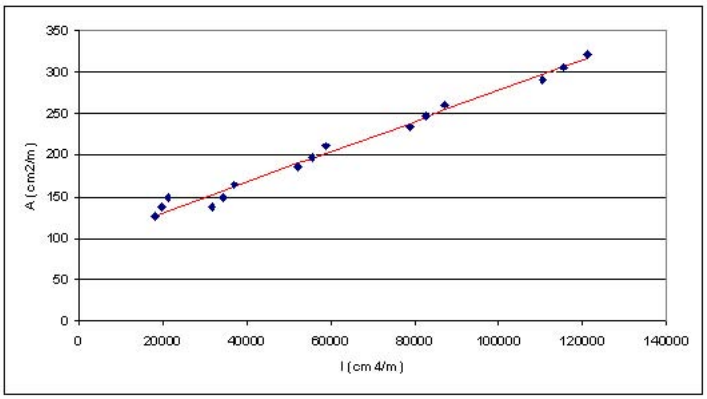

Figure N.2: Plot A_{fit} and A Against I for AZ-Profiles

Similarly the moment of inertia I can be fit to the elastic section modulus W_{el} by:

$$I_{fit} = 25.4 \cdot W_{el} - 15,000 \ [cm^4/m] \tag{N.3}$$

where W_{el} must be inserted in $[cm3/m]$.

The resulting fit is shown in figure N.3:

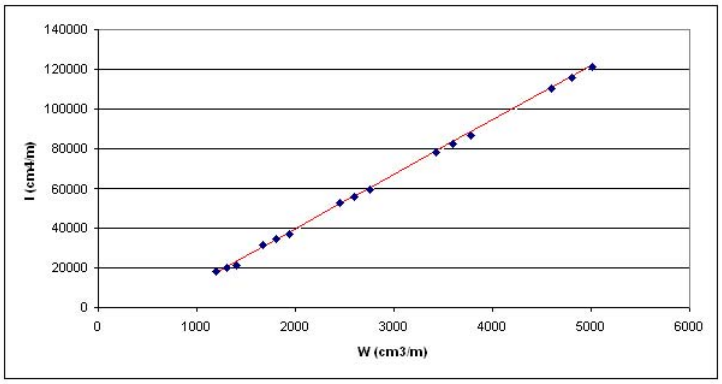

Figure N.3: Plot I_{fit} and I Against W_{el} for AZ-Profiles

This least-squares fit-procedure is easily reproducible for other types of sheet piles in a simple spreadsheet. The steps for e.g. A and I are:

1. Insert the columns of A and I.
2. Calculate the ratio of the original values I/A.
3. Create a cell with an arbitrary value for the intersection of the fit with the y-axis b. This is the first fit parameter.
4. Calculate $a = I/(A - b)$ and create a cell with the summation of these terms. This is the second fit parameter.
5. Calculate $A_{fit} = aI + b$.
6. Build the ratio I/A_{fit}.
7. Calculate the square differences of the original I/A and the fitted I/A_{fit}.
8. Create a cell with the sum of these squared differences $\sum_i \left(\frac{I_i}{A_i} - \frac{I_i}{A_{i,fit}}\right)^2$.
9. Use the *solver* to minimize this cell's value by changing b. The new a and b are the fit parameters.

Appendix O

The Variance of $sin\phi$ compared to the Variance of ϕ or $tan\phi$

The FEM code Plaxis applied in this thesis stores and works with $sin(\phi)$ instead of the friction angle itself. In order to take the variability of ϕ properly into account, the following formulae and graphs can be used. Also the use of $tan(\phi)$ is discussed.

O.1 General Procedure to Estimate Mean and Variance of a Function

For an arbitrary one-parameter function G, which is a function of a one-parameter estimator $G(\hat{\theta})$, the *expected value* can in general be approximated (Taylor-expansion) by:

$$E[G(\theta)] = G(\hat{\theta}) + O\left(\frac{1}{n}\right) \tag{O.1}$$

where $G(q)$ is some function of q and q is the population parameter where $E(\theta) = q$ as $n \to \infty$ (n is the sample size). Thus for large n the expected value $E[G(\theta)]$ converges to the mean m.

For the same one-parameter distribution the *variance* can be estimated by [1]:

$$Var(G(\theta)) = \left(\frac{\partial G}{\partial \theta}\right)^2_{\theta=\hat{\theta}} Var(\theta) + O\left(\frac{1}{n^{\frac{3}{2}}}\right) \tag{O.2}$$

For the present problem we can neglect the error terms, since we assume the mean and variance of the variable to be known.

[1] see http://www.weibull.com: Approximate Estimates Of The Mean And Variance Of A Function

O.2 From a given variance of ϕ to the variance of $sin(\phi)$

The transformation function and its derivative are:

$$\begin{aligned} f(\phi) &= sin(\phi) \\ f'(\phi) &= cos(\phi) \end{aligned} \tag{O.3}$$

Therefore the variance and the standard deviation of the function can be written as:

$$Var(sin\phi) = \left(\frac{\partial sin\phi}{\partial \phi}\right)^2_{\phi=\hat{\phi}} Var(\phi) = cos^2\phi|_{\phi=\hat{\phi}}\, Var(\phi) \tag{O.4}$$

Taking the square root gives the standard deviation:

$$\sigma_{sin\phi} = |cos\hat{\phi}|\ \sigma_\phi \tag{O.5}$$

Expressed in coefficients of variation:

$$COV(sin\phi) = \frac{|cos\phi|}{\mu_{sin\phi}}\ COV(\phi)\ \mu_\phi = \frac{COV(\phi)\ \hat{\phi}}{tan(\hat{\phi})} \tag{O.6}$$

Figures O.1 and O.2 show the standard deviation and the variation coefficient of $sin\phi$ as function of ϕ and its variation coefficient.

O.3 From a given variance of ϕ to the variance of $tan(\phi)$

The transformation function and its derivative are:

$$\begin{aligned} f(\phi) &= tan(\phi) \\ f'(\phi) &= 1/cos^2(\phi) \end{aligned} \tag{O.7}$$

Similar to the previous section the standard deviation results in:

$$\sigma_{tan\phi} = \frac{1}{cos^2\hat{\phi}}\ \sigma_\phi \tag{O.8}$$

Expressed in coefficients of variation:

$$COV(tan\phi) = \frac{cos\hat{\phi}}{cos^2\hat{\phi}\ sin\hat{\phi}}\ COV(\phi)\ \hat{\phi} = \frac{1}{cos\hat{\phi}\ sin\hat{\phi}}\ COV(\phi)\ \hat{\phi} \tag{O.9}$$

Figures O.3 and O.4 show the standard deviation and the variation coefficient of $tan\phi$ as function of ϕ and its variation coefficient:

O.4 From a given variance of $tan\phi$ to the variance of $sin(\phi)$

The transformation function and its derivative are:

$$\begin{aligned} f(\phi) &= sin(\phi) \\ f'(\phi) &= cos(\phi) \end{aligned} \tag{O.10}$$

Similar to the previous sections the standard deviation results in:

$$\sigma_{sin\phi} = \sigma_{\phi}\, cos\hat{\phi} \tag{O.11}$$

The standard deviation of $tan\phi$ can be transformed to:

$$\sigma_{\phi} = \sigma_{tan\phi}\, cos^2\hat{\phi} \tag{O.12}$$

Combining the last two equations leads to.

$$\sigma_{\phi} = \sigma_{tan\phi}\, cos^3\hat{\phi} \tag{O.13}$$

Expressed in coefficients of variation:

$$COV(sin\phi) = |cos^3\hat{\phi}|\frac{COV(tan\hat{\phi})\ \mu_{tan\phi}}{\mu_{sin\phi}} = cos^2\hat{\phi}\, COV(tan\hat{\phi}) \tag{O.14}$$

Figures O.5 shows the variation coefficient of $sin\phi$ as function of ϕ and the variation coefficient of tan ϕ.

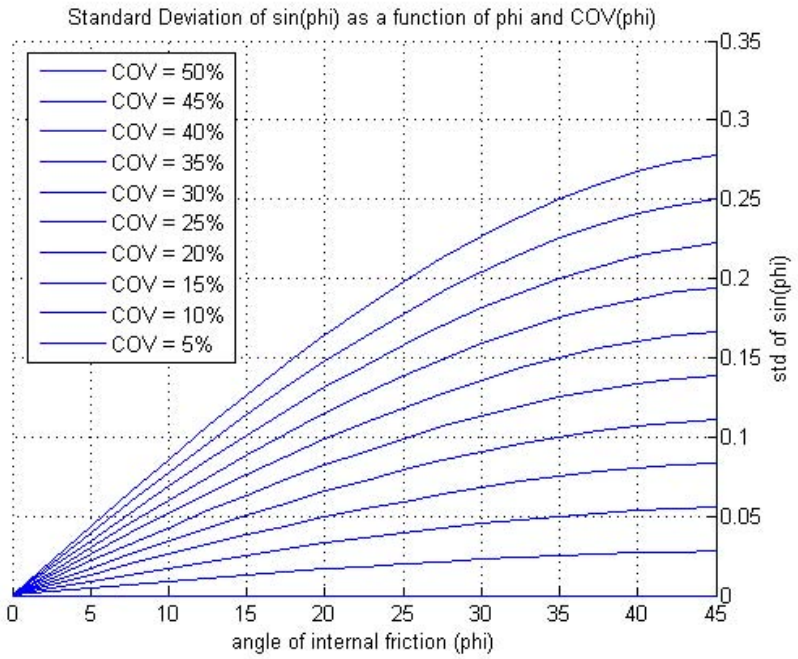

Figure O.1: Standard Deviation of sin ϕ as function of phi and COV(ϕ)

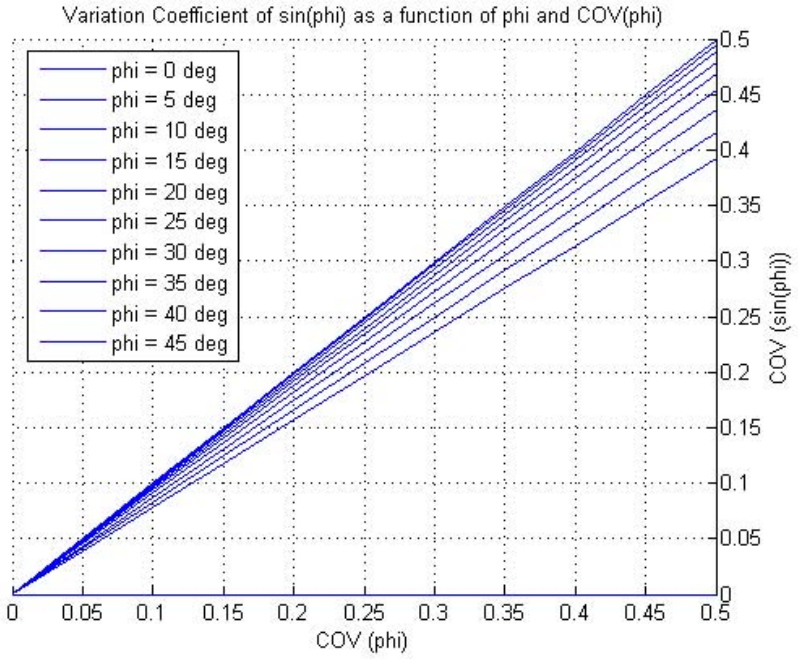

Figure O.2: Variation Coefficient of sin ϕ as function of phi and COV(ϕ)

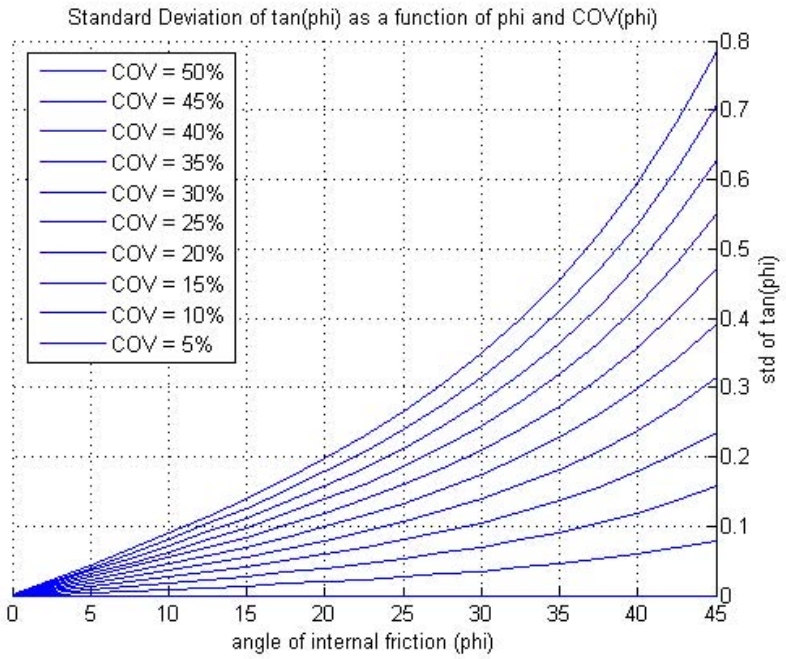

Figure O.3: Standard Deviation of tan ϕ as function of phi and COV(ϕ)

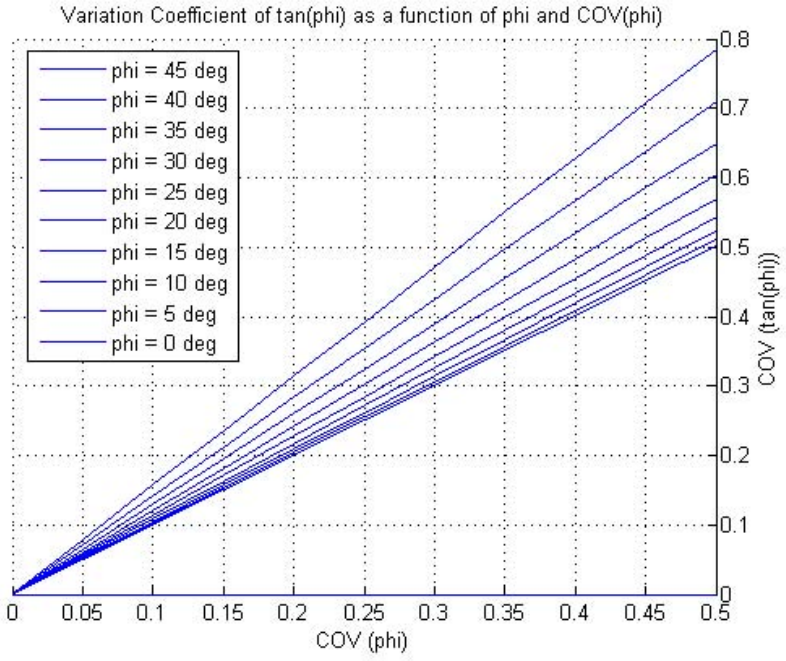

Figure O.4: Variation Coefficient of tan ϕ as function of phi and COV(ϕ)

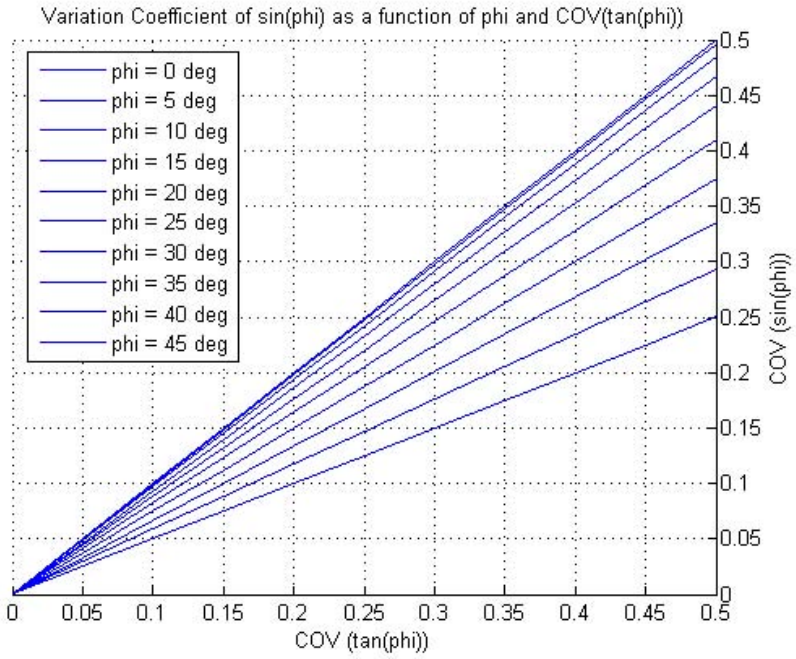

Figure O.5: Variation Coefficient of sin ϕ as function of phi and COV(tan ϕ)